Low Complexity Space-Time coding for MIMO systems.

Amr Ismail

N° d'ordre : 2011-20-TH

THÈSE DE DOCTORAT

SPECIALITE : PHYSIQUE

Ecole Doctorale « Sciences et Technologies de l'Information des Télécommunications et des Systèmes »

Présentée par :

Amr ISMAIL

Sujet :

Codes Espace-Temps à Faible Complexité pour Systèmes MIMO

Soutenue le **24 Novembre 2011** devant les membres du jury :

Prof. Jean-Claude BELFIORE	Telecom ParisTech	Rapporteur
Prof. Luc VANDENDORPE	Université catholique de Louvain	Rapporteur
Prof. Ezio BIGLIERI	Universitat Pompeu Fabra University of California Los Angeles	Examinateur
Prof. Pierre DUHAMEL	Directeur de Recherches CNRS	Examinateur
Prof. David GESBERT	Institut Eurecom	Examinateur
Prof. Hikmet SARI	SUPELEC	Directeur de thèse
Prof associé. Jocelyn FIORINA	SUPELEC	Co-encadrant

To my family.

Remerciements

Je tiens à remercier mon directeur de thèse le professeur Hikmet Sari, chef du Département Télécommunications à Supélec, pour ses précieux conseils et ses proposition de sujets de recherche sans lesquelles ce travail n'aurait pas été possible. Je voudrais également remercier le professeur associé Jocelyn Fiorina mon co-encadrant, pour les nombreuses discussions et ses conseils qui m'ont aidé à améliorer la qualité de mon travail.

Des remerciements particuliers sont dus à mes collégues, Ayaz Ahmad, Joffrey Villard, et Najett Neji pour l'environnement chaleureux qu'ils ont crée lors de mon séjour à Supélec, je voudrais également exprimer ma gratitude aux membre de l'administration du Département des télécommunications, Mme Catherine Magnet, Huu Hung Vuong et José Fonseca pour leur coopération.

Acknowledgements

I would like to thank my thesis supervisor Professor Hikmet Sari, Head of the Telecommunications Department at Supélec, for his valuable guidance and proposal of research topics without which this work would not have been possible. I would like also to thank Associate professor Jocelyn Fiorina my co-advisor, for the many fruitful discussions and his advices that helped me improve the quality of my work.

Special thanks are due to my colleagues, Ayaz Ahmad, Joffrey Villard, and Najett Neji for the warm environment they created during my stay at Supélec, I would like also to express my gratitude to the administrative staff of the Telecommunications Department, Mme Catherine Magnet, Huu Hung Vuong and José Fonseca for their cooperation.

Résumé

Les dernières années ont témoigné une augmentation spectaculaire de la demande sur les communications sans fil fiables à haut-débit en raison de l'incorporation de l'accès à l'Internet et les services multimédias exigeantes tels que le *streaming* audio et vidéo en haute définition aux appareils sans fil modernes. Afin de répondre à ces nouvelles exigences, le recours aux techniques *Multiple-Input Multiple-Output* (MIMO) était inévitable, car ils sont capables d'offrir des communications sans fil fiables à haut-débit sans l'allocation de bande passante supplémentaire.

Dans le cas des systèmes à boucle ouverte où l'émetteur ne dispose pas d'information sur l'état du canal, les techniques de codage spatio-temporel se sont avérés d'exploiter efficacement les degrés de liberté du canal MIMO tout en profitant du gain de diversité maximal. Comme son nom l'indique, un code espace-temps (*Space-Time Codes*(STC)) consiste à coder les symboles d'information en deux dimensions (le temps et l'espace). D'autre part, la complexité de décodage ML du STC généralement augmente exponentiellement avec le taux ce qui impose un défi important à l'incorporation des STC dans les normes de communications récentes en raison des restrictions de consommation de puissance.

Dans cette thèse, nous nous concentrons sur les codes espace-temps en bloc (*Space-Time Block Codes* (STBC)) où la matrice du code est une combinaison linéaire des symboles réels transmis. Plusieurs familles de STBC qui admettent un décodage ML à complexité réduite de décodage ont été proposées, notamment les codes *g-group decodable, fast decodable et fast-group decodable*.

Les STBC *g-group decodable* sont des codes où la métriques ML peut être exprimée comme une somme de g termes en fonction des ensembles

disjoints des symboles transmis permettant ainsi de détecter ces groupes de symboles séparément ce qui réduit considérablement la complexité de détection. Si le nombre de symboles réels dans chaque groupe est limité à 1, les codes *g-group decodable* coïncident avec les codes orthogonaux bien connus. Cependant, pour q'un STBC soit *g-group decodable*, un certain nombre de conditions doivent être satisfaites ce qui limite les taux atteignables. Par ailleurs, les méthodes de construction proposées pour les codes *g group decodable* sont basées sur conditions suffisantes mais pas nécessaires qui pourraient réduire davantage les taux atteignables. Dans le chapitre 4, nous étudions le taux maximal des STBC *g-group decodable* pour un type spécifique de matrices de code qui inclut la majorité des STBC proposés dans la littérature. Nous proposer une nouvelle approche numérique basée sur des conditions nécessaires et suffisantes des codes *g-group decodable* et nous fournissons le taux maximal du code symétrique $g = 2$ et le code non-symétrique $g = 3$ dans le cas de quatre antennes d'émission.

Afin de remédier la limitation du taux des codes *g-group decodable*, une autre famille de codes a été proposée, les codes *Fast Decodable* (FD). Un code FD est conditionnellement *g-group decodable* ce qui permet d'utiliser l'approche de détection conditionnelle pour décoder les symboles transmis en deux étapes. La première étape consiste à évaluer les estimations ML conditionnelles des symboles appartenant au code *g-group decodable*. Dans la deuxième étape, le décodeur n'a que décoder le reste des symboles. Dans le chapitre 5, nous nous concentrons sur le multiplexage de deux codes orthogonaux dans le cas de quatre antennes d'émission par le biais d'une matrice unitaire. Nous dérivons une limite supérieure sur le taux du code lorsque la propriété de mise en forme cubique est satisfaite et nous fournissons un nouvel code FD.

Les codes *Fast-Group Decodable* (FGD) sont *g-group decodable* tels que chaque groupe de symbole est FD. Dans le chapitre 6, nous proposons une approche systématique pour obtenir un code FGD de taux 1 pour un nombre d'antennes d'émission quelconque. En appliquant

la méthode proposée dans le cas de quatre antennes d'émission, nous obtenons un nouveau code FGD de taux 1 qui (notre connaissance) a la moindre complexité de décodage (pire cas) parmi les codes comparables dans la littérature. Le taux est ensuite augmenté par le multiplexage de deux codes de taux 1 donnant une naissance à un nouveau FD code de taux 2 qui a également la moindre complexité de décodage.

Abstract

The last few years witnessed a dramatic increase in the demand on high-rate reliable wireless communications due to the incorporation of broadband internet access and demanding multimedia services such as high-definition audio and video streaming to modern wireless devices. In order to meet these new requirements, resorting to Multiple-Input Multiple-Output (MIMO) techniques was inevitable as they may offer high-rate reliable wireless communications without any additional bandwidth.

In the open loop case where the transmitter does not have any prior knowledge about the channel state information, space-time coding techniques have proved to efficiently exploit the MIMO channel degrees of freedom while taking advantage of the maximum diversity gain. As indicated by its name, a Space-Time Code (STC) refers to the coding of the information symbols over two dimensions namely time and space. On the other hand, the ML decoding complexity of STCs generally increases exponentially with the rate which imposes an important challenge to the incorporation of STCs in recent communications standards due to power consumption restrictions.

In the present thesis, we focus on Space-Time Block Codes (STBCs) where the code matrix is expressed as a linear combination of the transmitted real symbols. Several families of STBCs that admit a reduced ML decoding complexity have been proposed in the literature, namely the g-group-decodable, fast-decodable and fast-group-decodable codes. The g-group decodable STBCs are codes where the ML metric may be expressed as a sum of g terms depending on disjoint sets of the transmitted symbols thus enabling separate detection of these disjoint sets and

significantly reducing the detection complexity. If the number of real symbols in each group is restricted to be one, the g-group-decodable codes coincide with the well-known orthogonal codes. However, for a STBC to be g-group decodable, a certain number of conditions must be satisfied which reduces the achievable rates. Moreover, the proposed construction methods for the g-group-decodable codes are based on sufficient but not necessary conditions which may reduce further the attainable rates. In Chapter 4, we investigate the maximal achievable rates of g-group-decodable STBCs for a specific type of code matrices that subsumes the majority of the STBCs proposed in the literature. We propose a new numerical approach based on necessary and sufficient conditions for g-group-decodable codes and present the maximal-rate symmetric $g = 2$ code and $g = 3$ code in the case of four transmit antennas.

In order to remedy the rate limitation of the g-group-decodable codes, another family of codes has been proposed, namely the fast decodable codes. A fast-decodable STBC encloses a g-group-decodable code and makes use of the conditional detection approach to decode the transmitted symbols in two steps. The first step consists of evaluating the conditional ML estimation of the symbols belonging to the g-group-decodable code. In the second step, the decoder has only to decode the rest of the symbols. In Chapter 5, we focus on the multiplexing of two orthogonal STBCs in the case of four transmit antennas by the means of a unitary matrix. We derive an upper bound for the rate of the proposed code structure in order to satisfy the cubic shaping property and then we prove that this rate is indeed achievable.

Fast-group-decodable STBCs are g-group-decodable codes such that each group of symbol is fast-decodable. In Chapter 6, we propose a systematic approach to obtain fast-group-decodable rate-1 STBCs for an arbitrary number of transmit antennas. Applying the proposed method in the case of four transmit antennas, we obtain a new rate-1 fast-group-decodable STBC that has to the best of our knowledge the least worst-

case decoding complexity among comparable STBCs in the literature. The rate is then increased through multiplexing two rate-1 codes giving rise to a new fast-decodable rate-2 STBC that has the least worst-case decoding complexity.

Contents

List of Figures

List of Tables

Mathematical Notations

x	Scalar x (small letters)
$\mathbf{x}$	Vector $\mathbf{x}$ (bold small letters)
$\mathbf{X}$	Matrix $\mathbf{X}$ (bold capital letters)
$\mathbf{I}$	The identity matrix
$\mathbf{X}^T$	Transpose of $\mathbf{X}$
$\mathbf{X}^H$	Hermitian of $\mathbf{X}$
$\det(\mathbf{X})$	Determinant of $\mathbf{X}$
$\text{tr}(\mathbf{X})$	Trace of $\mathbf{X}$
$\|\mathbf{X}\|_F$	Frobenius norm of $\mathbf{X}$
$vec(\mathbf{X})$	Transforms the $m \times n$ matrix $\mathbf{X}$ into the $mn \times 1$ vector through vertical concatenation of the columns of $\mathbf{X}$
$\tilde{\mathbf{x}}$	Concatenates vertically the real and imaginary parts of its vector input
$\tilde{\mathbf{X}}$	Concatenates vertically the real and imaginary parts of its matrix input
$\mathcal{A}$	finite set $\mathcal{A}$ (calligraphic letters)
$\|\mathcal{A}\|$	The cardinality of $\mathcal{A}$
$\otimes$	Kronecker product
δ_{kj}	Kronecker delta
$x \sim \mathcal{CN}(\mu, \sigma)$	x is a circular symmetric Gaussian random variable with mean μ and variance σ
$\text{sign}(x)$	returns 1 if $x \geq 0$ and -1 otherwise
$\text{round}(x)$	rounds x to the nearest integer
$\text{diag}(\mathbf{x})$	returns a diagonal matrix with $\mathbf{x}$ on its main diagonal
$\Re(.)$	Real part of its argument
$\Im(.)$	Imaginary part of its argument
$\mathcal{M}_n$	The set of complex $n \times n$ matrices
$\mathbb{Z}$	The set of integers
$\mathbb{Q}$	The set of rational numbers
$\mathbb{R}$	The set of real numbers
$\mathbb{C}$	The set of complex numbers
$a \equiv b \,(\text{mod } n)$	$a - b$ is a multiple of n where $a, b, n \in \mathbb{Z}$
$(m)_n$	m modulo n

Acronyms

CIOD	Coordinate Interleaved Orthogonal Design
CSI	Channel State Information
CTC	Convolutional Turbo Code
CUW	Clifford Unitary Weight
DAST	Diagonal Algebraic Space-Time
EPTD	Equal Power Transmit Diversity
FD	Fast-Decodable
FEC	Forward Error Correction Code
FGD	Fast-Group Decodable
HPA	High Power Amplifier
ISI	Inter-Symbol Interference
LLR	Log-Likelihood Ratio
ML	Maximum Likelihood
MISO	Multiple-Input Single-Output
MIMO	Multiple-Input Multiple-Output
MRC	Maximum Ratio Combining
NVD	Non Vanishing Determinant
OFDM	Orthogonal Frequency Division Multiplexing
OTD	Optimum Transmit Diversity
PAPR	Peak-to Average Power Ratio
PED	Partial Euclidean Distance
QAM	Quadrature Amplitude Modulation
QOD	Quasi-Orthogonal Design
QPSK	Quadrature Phase Shift Modulation
SD	Sphere Decoder
SIMO	Single-Input Multiple-Output
SISO	Single-Input Single-Output
SSD	Single-Symbol Decodable
STBC	Space-Time Block Code
STC	Space-Time Code
STD	Switching Transmit Diversity
STTC	Space-Time Trellis Code
TAST	Threaded Algebraic Space-Time

Première partie

Français

Chapitre 1

Introduction

En raison des imperfections intrinsèques à l'environnement (notamment l'atténuation du signal et la propagation par trajets multiples), la transmission fiable de données constitue un défi technologique. L'atténuation du signal transmis est le résultat de plusieurs facteurs tels que la perte de propagation, le rayonnement imparfait des antennes, et l'effet de *shadowing*. Celle-ci rend le signal transmis plus vulnérable aux erreurs. La propagation par trajets multiples correspond au fait que les signaux transmis dans l'environnement sans fil suivent plusieurs chemins avant d'atteindre leur destination. Le signal reçu est alors un mélange de répliques retardées du signal d'origine, chacune transmise à travers un canal distinct. Cet effet de propagation par trajets multiples créé des interférences entre symboles (*Inter-Symbol Interference* (ISI)) en raison de l'étalement des retards de canal et créé des évanouissements profonds (*deep fades*) à cause de la superposition destructive des signaux au niveau du récepteur. Alors que les égaliseurs et les techniques d'*Orthogonal Frequency Division Multiplexing* (OFDM) ont été proposées afin de réduire l'effet de ISI, les techniques de diversité se sont avérées efficaces dans le traitement du phénomène d'évanouissements profonds.

De manière générale, les techniques de diversité consistent à répliquer les données de sorte que chaque réplique soit transmise par un canal indépendant, assurant donc une haute probabilité de bonne détection au récepteur. Cette redondance peut être mise en œuvre dans plusieurs domaines. Dans le domaine temporel, les répliques du signal sont envoyées sur plusieurs créneaux, espacés d'un temps supérieur au temps de cohérence du canal. Cela peut être réalisé grâce à la combinaison d'un code correcteur d'erreurs et d'un entrelaceur. Dans le domaine

fréquentiel, les répliques sont envoyées sur plusieurs sous-porteuses, dont l'écart est supérieure à la bande de cohérence du canal. Toutefois, les deux techniques ci-dessus ont besoin d'une bande passante supplémentaire pour atteindre le degré de diversité souhaité.

La diversité spatiale est une technique efficace pouvant offrir une bonne protection contre les évanouissement profonds sans allouer de bande passante supplémentaire. Elle peut être implémentée au récepteur, à l'émetteur, ou aux deux à la fois. Dans un système qui exploite la diversité de réception, le signal est envoyé à partir d'une seule antenne et reçu sur plusieurs antennes ; système *Single-Input Multiple-Output* (SIMO). Dans un système qui exploite la diversité de transmission, les répliques du signal sont envoyées à partir de plusieurs antennes et reçus sur une seule antenne ; système *Multiple-Input Single-Output* (MISO). Un système est dit *Multiple-Input Multiple-Output* (MIMO) s'il exploite la diversité des deux côtés, c'est-à-dire les répliques sont envoyées à partir de plusieurs antennes et reçues sur plusieurs antennes. Afin de garantir l'indépendance entre les multiples canaux ainsi créés, les antennes doivent être espacées d'au moins une moitié de longueur d'onde de fonctionnement [2]. Notons que pour des systèmes avec des contraintes d'espace, la diversité de polarisation peut être employée en utilisant des antennes à double polarisation au lieu des antennes espacées uni-polarisées, au détriment d'une certaine perte de performance [3].

Les trois configurations SIMO $1 \times N_r$ 1.1(a), MISO $N_t \times 1$ 1.1(b) et MIMO $N_t \times N_r$ 1.1(c) sont représentées à la figure 1.1. Dans la configuration SIMO (resp. MISO), le gain de diversité est majoré par le nombre maximal de canaux indépendants entre l'émetteur et le récepteur soit N_r (resp.N_t). Un système MIMO quant à lui, peut offrir un degrés de diversité égal à $N_t.N_r$. Par ailleurs, la configuration MIMO peut offrir plus de degrés de liberté. Les degrés de liberté du canal correspondent au nombre maximal de canaux parallèles équivalents [4]. Comme il sera présenté dans la suite, les configurations SIMO et MISO offrent un degré liberté égale à 1, alors que la configuration MIMO peut offrir jusqu'à min $\{N_t, N_r\}$ degrés de liberté. En résumé, le système MIMO permet d'obtenir de meilleures performances (en raison de son gain de diversité supérieur) et un taux plus élevé (en raison de ses degrés de liberté).

(a) Configuration SIMO

(b) Configuration MISO

(c) Configuration MIMO

FIGURE 1.1 – Configurations différentes

Alors que le gain de diversité maximal peut être réalisé dans un système SIMO (resp. MISO) par *Maximum Ratio Combining* (MRC) (resp. *optimal beamforming*), les techniques de codage spatio-temporel où les symboles d'information sont codés sur deux dimensions (l'espace et le temps) sont capables d'exploiter efficacement les canaux MIMO. En fait, les codes espace-temps (*Space-Time Codes* (STC)) peuvent exploiter conjointement l'ensemble des degrés de liberté et de la diversité maximale tout en ne nécessitant aucune connaissance préalable de l'état du canal à l'émetteur. Par conséquent, ils ont été adoptés dans les systèmes à boucle ouverte dans les normes de communication sans fil [5, 6] et dans la prochaine norme LTE

3GPP. Le défi principal dans la mise en œuvre des STC est leur complexité de décodage, qui augmente généralement de manière exponentielle avec le taux du code.

Les premiers STC proposés dans la littérature, notamment les *Space-Time Trellis Codes* (STTC) [7], peuvent fournir des performances élevées au détriment d'une complexité de décodage accrue (le nombre d'états dans le décodeur de Viterbi croît exponentiellement avec le taux et le nombre d'antennes d'émission). Afin d'y remédier, une famille des STC linéaires *Space-Time Block Codes* (STBC) a été proposée [8]. La matrice du code est alors une combinaison linéaire des symboles d'information. Cette linéarité inhérente à la matrice du STBC permet l'utilisation d'algorithmes de *closest lattice point search* (généralement connus sous le nom des algorithmes de décodage sphérique [9, 10]) ainsi que d'algorithmes sous-optimaux tels que *successive nulling and cancelling* [11], et *augmented lattice reduction* [12] récemment proposé.

Cependant, alors que les décodeurs sphériques réduisent considérablement la complexité moyenne de décodage (définie comme le nombre moyen de nœuds visités sur l'arbre de recherche [13]), il n'ont aucun impact sur la complexité de décodage (pire cas) qui généralement augmente exponentiellement avec le taux du STBC. La complexité de décodage correspond au nombre minimal d'évaluations de la métrique ML nécessaire à un décodeur à recherche exhaustive pour déterminer de façon optimale le mot de code transmit [14, 15]. Pour une matrice de STBC $\mathbf{X}$ qui code K symboles complexes tirés d'une constellation de M points, la complexité de décodage est de l'ordre de M^K. Dans ce contexte, le STBC $\mathbf{X}$ admet un décodage à faible complexité si et seulement si l'ordre de sa complexité de décodage est inférieur à M^K.

Les codes *g-group decodable* [16] constituent une composante de base pour la construction des codes à faible complexité de décodage. Dans un code *g-group decodable*, au lieu de décoder conjointement tous les symboles transmis, ceci peuvent être découplés en groupes qui peuvent être décodés séparément sans aucune perte de performance. Par exemple, si un code $\mathbf{X}$ qui encode $2K$ symboles réels est *g-group decodable*, la complexité de décodage peut être considérablement réduite de M^K à $\sum_{i=1}^{g} \sqrt{M}^{n_i}$ où $\sum_{i=1}^{g} n_i = 2K$ où n_i désigne le nombre de symboles réels dans le groupe i. Cependant, cette réduction de complexité de décodage impose un cer-

tain nombre de restrictions sur la matrice du STBC, ce qui limite considérablement le taux atteignable. Afin de contourner la limitation sur le taux des codes *g-group decodable*, mais au détriment d'une hausse de complexité de décodage, une autre famille de codes notamment les codes dit *Fast-Decodable* (FD) a été proposée. Ces codes permettent des taux considérablement plus élevés que ceux les codes *g-group decodable* par la relaxation des conditions de *g-group decodability* tout en conservant un niveau raisonnable de complexité de décodage. Un code FD est conditionnellement *g-group decodable* ce qui permet la mise en œuvre de la détection conditionnelle. Une construction simple de codes FD est obtenue grâce au multiplexage de plusieurs codes *g-group decodable* [14, 17]. Une famille de codes dite *Fast-Group Decodable* (FGD) qui combine les deux familles ci-dessus a été récemment proposée [18]. Ces codes FGD sont des codes *g-group decodable* tels que chaque groupe de symboles est FD.

Cette thèse porte sur la conception de nouveaux STBC à faible complexité.

1.1 Contributions

Les contributions de cette thèse sont résumées ci-dessous :

- Les méthodes de construction proposées pour les codes *g-group decodable* [16, 19] sont basées sur des conditions suffisantes mais pas nécessaires, qui peuvent réduire les taux atteignables. Dans le chapitre 4, nous étudions le taux réalisable des codes *g-group decodable* pour un type spécifique de matrices de code qui inclut la majorité des STBC proposés dans la littérature. Nous proposons une nouvelle approche numérique basée sur les conditions nécessaires et suffisantes des codes *g-group decodable* et nous montrons que, pour le type de matrices de code considéré, cette méthode est considérablement simplifiée. Nous nous concentrons sur le cas de quatre antennes d'émission et nous fournissons les taux maximaux du code 2-*group decodable* symétrique et du code 3-*group decodable* non-symétrique. Les résultats de ce chapitre ont été présentée à IEEE Global Telecommunications (GLOBECOM'10), à Miami, (Floride, Etats-Unis), en 2010 [15] et dans un article soumis à IEEE Transactions on Communications ($2^{\text{ème}}$ tour de révision en cours).

- Dans le contexte des codes FD, nous nous concentrons dans le chapitre 5 sur le multiplexage de deux STBC orthogonaux dans le cas de quatre antennes d'émission. Tout d'abord, nous démontrons une borne supérieure pour le taux du code proposé lorsque la propriété de mise en forme cubique est satisfaite. Ensuite, nous montrons que le code proposé conserve le gain de codage du code orthogonal taux 3/4 indépendamment de l'ordre de la constellation QAM non-normalisée. Autrement dit, le code proposé est donc *NonVanishing Determinant* (NVD)[20]. Les résultats de simulation montrent que, non seulement le code proposé présente de meilleures performances que les STBC existants, mais il peut être décodé avec une complexité moyenne inférieure et offre un meilleur *Peak to Average Power Ratio*(PAPR). Les résultats de ce chapitre ont été publié dans la revue IEEE Transactions on Wireless Communications [21] et sera présenté prochainement à IEEE Global Telecommunications Conference (GLOBECOM'11), à Houston, (Texas, USA), en 2011 [22].

- Dans le chapitre 6, nous proposons une approche systématique pour la construction des codes FGD de taux 1 pour $2^a,\ a \in \mathbb{N}$ antennes d'émission. Si le nombre d'antennes d'émission n'est pas une puissance de deux, il suffit de supprimer le nombre approprié de colonnes du code FGD correspondant à la puissance de deux directement supérieure, par exemple, le code FGD pour trois antennes de transmission est obtenu en supprimant 1 colonne du code FGD à 4 antennes. Nous appliquons la méthode proposée dans le cas de quatre antennes d'émission et nous obtenons un nouveau code de taux 1 dont la complexité de décodage (pire cas) est(à notre connaissance la plus faible. Le gain de codage est optimisé par l'étirement de constellation *constellation stretching* plutôt que par rotation de constellation pour préserver la structure FGD et minimiser le PAPR. Nous montrons que le code proposé est NVD grâce au choix judicieux du coefficient d'étirement de constellation. Ensuite, le taux est augmenté par multiplexage de deux codes de taux 1 par le biais d'une matrice unitaire, donnant naissance à un nouveau code FD de taux 2 qui a également à notre connaissance la complexité de décodage (pire cas) la plus faible. La matrice unitaire est numériquement optimisée dans le cas de

la constellation QPSK. Un nouveau code de taux 3/2 est obtenu par poinçonnage du code de taux 2. Les résultats de simulation montrent que les codes de taux 1 et 3/2 ont une faible complexité moyenne de décodage, alors que le code de taux 2 a une faible complexité de décodage dans la région des faibles SNR. A ce sujet, deux articles ont été soumis à IEEE International Conference on Communications (ICC'12), Ottawa, Canada, 2012 [23] et à IEEE Transactions on Wireless Communications [24].

- Dans l'annexe D, nous considérons le cas où un feedback à débit limité est disponible à l'émetteur et proposons un nouvel schéma quasi-optimal de diversité d'émission où la puissance moyenne transmise est également répartie entre les deux antennes d'émission. Ces résultats ont été présenté lors de IEEE International Symposium on Personal, Indoor and Mobile Radio Communications (PIMRC'10) [25] et publié dans IEEE Communications Letters [26].

1.2 Organisation de la thèse

Cette thèse est organisé de la manière suivante : dans le chapitre 2, nous étudions les critères de conception des STBC, les définitions de base et quelques-unes des familles importantes de STBC. Dans le chapitre 3, nous considérons trois familles de codes à faible complexité de décodage : les codes *g-group decodable*, les codes FD, et les codes FGD. La nouvelle méthode de construction des codes *g-group decodable* est présentée dans le chapitre 4 ainsi que les codes obtenus dans le cas de quatre antennes d'émission.

Dans le chapitre 5, une structure de multiplexage de deux codes orthogonaux est fournie, ainsi qu'une limite supérieure sur le taux lorsque la propriété de mis en forme cubique est satisfaite. Nous présentons ensuite notre code FD . Dans le chapitre 6, nous proposons une approche systématique pour la construction de code FGD de taux 1 pour un nombre arbitraire d'antennes d'émission. Nous étudions le cas de quatre antennes d'émission et obtenons un nouvelle famille de STBC à faible complexité du décodage dont le taux varie de 1 à 2 symboles complexes par utilisation de canal. Les conclusions ainsi que les directions de recherche potentielles

sont fournies dans le chapitre 7.

Chapitre 2

Codes espace-temps en bloc

Les codes espace-temps en bloc *Space-Time Block Codes* (STBC) ont été initialement proposés comme une alternative à faible complexité aux *Space-Time Trellis Codes* (STTC) qui souffrent d'une complexité élevée de décodage. Les STBC sont caractérisés par leur linéarité sur le corps des nombres réels puisque la matrice du code est une combinaison linéaire des symboles d'information réels. Cette linéarité sous-jacente dans les STBC transforme le problème de décodage au sens du maximum de vraisemblance en un problème de *closest lattice search* qui peut être efficacement résolu par les algorithmes de décodage sphérique. De plus, les STBC se sont avérés d'exploiter efficacement les degrés de liberté de canal MIMO et sa diversité.

Le premier STBC proposé est un schéma de diversité de transmission pour deux antennes connu sous le nom de *code d'Alamouti* [27]. Il peut être décodé de manière optimale avec une complexité qui croît linéairement avec la taille de la constellation. De plus, dans le cas des constellations rectangulaires telles que 4,16,64-QAM, il peut être efficacement décodé avec une complexité constante indépendamment de la taille de la constellation utilisée. D'autre part, le code d'Alamouti satisfait le critère du NVD [20], propriété qui peut être exploitée par l'utilisation d'une modulation adaptative à taux de transmission variable (à travers le choix de l'ordre de modulation) en fonction de la qualité du canal. Par ailleurs, si l'on considère la configuration spéciale 2×1, le code d'Alamouti est de taux maximal et n'engendre aucune perte d'information.

Dans le but de généraliser le schéma d'Alamouti à un nombre d'antennes d'émission supérieur à deux, la famille bien connue des STBC orthogonaux a été proposée. Malheureusement, le taux des codes orthogonaux décroît exponentiellement

avec le nombre d'antennes d'émission ce qui les rend plus adaptés aux communications à taux faible. Afin de pallier la perte de taux des STBC orthogonaux, plusieurs familles de codes ont été proposées, parmi lesquelles nous mentionnons les codes *Diagonal Algebraic Space-Time* (DAST) [28], les codes *Threaded Algebraic Space-Time* (TAST) [29] et les codes parfaits [30]. Ces familles de codes fournissent un taux de transmission considérablement supérieur aux codes orthogonaux, au détriment d'une hausse de complexité de décodage. Les codes DAST peuvent atteindre un taux de transmission d'un symbole complexe par utilisation de canal pour un nombre arbitraire d'antennes d'émission alors que les code TAST et les codes parfaits ont l'avantage de fournir le taux maximal pour n'importe quelle configuration de canal MIMO.

Dans ce chapitre, nous commençons par présenter le modèle de canal MIMO adopté tout au long de cette thèse, le modèle quasi-statique de Rayleigh à évanouissements plats *flat quasi-static Rayleigh fading*. Le décodage optimal des STBC ainsi que les différentes mesures de complexité sont ensuite présentés. Enfin, nous discutons les critères de la conception des STBC.

2.1 Modèle

Lors de l'étude des STBC, le modèle en canal bande de base adopté est le modèle du canal quasi-statique de Rayleigh à évanouissements plats. Comme son nom l'indique, la réponse fréquentielle du canal est considérée plate sur la bande de fréquence d'intérêt et les coefficients du canal sont modélisés par des variables aléatoires distribuées selon la loi de Rayleigh, supposées constants sur la période de signalisation, et qui varient indépendamment d'un mot de code à un autre. Les échantillons de bruit sont supposés décorrélés spatialement et temporellement et, pour des antennes suffisamment espacées, les coefficients du canal sont supposés spatialement décorrélés. Mathématiquement, le modèle du canal MIMO en bande de base peut être décrit par l'équation suivante :

$$\underset{T\times N_r}{\mathbf{Y}} = \underset{T\times N_t}{\mathbf{X}}\underset{N_t\times N_r}{\mathbf{H}} + \underset{T\times N_r}{\mathbf{W}} \tag{2.1}$$

où T est la période de signalisation d'un mot de code, N_r est le nombre d'antennes de réception, N_t est le nombre d'antennes d'émission, $\mathbf{Y}$ est la matrice du signal

reçu, $\mathbf{X}$ est la matrice du code, $\mathbf{H}$ est la matrice des coefficients du canal avec les entrées $h_{kl} \sim \mathcal{CN}(0,1)$, et $\mathbf{W}$ est la matrice de bruit avec les entrées $w_{ij} \sim \mathcal{CN}(0, N_0)$. Selon le modèle ci-dessus, la $t^{\text{ème}}$ ligne de la matrice $\mathbf{X}$ contient les symboles transmis à travers les N_t antennes lors de la $t^{\text{ème}}$ utilisation du canal, tandis que la $n^{\text{ème}}$ colonne contient les symboles transmis à travers la $n^{\text{ème}}$ antenne d'émission pendant la période de signalisation T d'un mot de code. Il est à noter que même si le modèle ci-dessus suppose un canal plat entre l'émetteur et le récepteur, il reste applicable dans le scénario de canaux sélectifs en fréquence. En effet, l'utilisation de l'Orthogonal Frequency Division Multiplexing (OFDM) transforme tout canal sélectif en multiples canaux à évanouissement plat. Dans un tel scénario, notons N_c le nombre de sous-porteuses le modèle système (2.1) peut être réécrit de la manière suivante [31] :

$$\mathbf{Y}(p) = \mathbf{X}(p)\,\mathbf{H}(p) + \mathbf{W}(p)\,,\ \forall p = 0, \ldots, N_c - 1 \tag{2.2}$$

où $\mathbf{Y}(p)$, $\mathbf{X}(p)$ désignent la matrice du signal reçu, et la matrice STBC à la sous-porteuse p, respectivement. L'entrée $h_{kl}(p)$ de la matrice $\mathbf{H}(p)$ correspond à la transformée de Fourier rapide à N_c points de la réponse impulsionnelle du canal entre l'antenne d'émission k et l'antenne de réception l évaluée à la sous-porteuse p. L'entrée $w_{ij}(p) \sim \mathcal{CN}(0, N_0)$ de la matrice de bruit $\mathbf{W}(p)$ est la transformée de Fourier rapide à N_c points du bruit additif gaussien à la $j^{\text{ème}}$ antenne de réception lors du $i^{\text{ème}}$ intervalle symbole OFDM évaluée à la sous-porteuse p.

Une matrice de code espace-temps en bloc qui encode $2K$ symboles réels est une combinaison linéaire des symboles transmis [8] :

$$\mathbf{X} = \sum_{k=1}^{2K} \mathbf{A}_k x_k \tag{2.3}$$

avec $\forall k \in \{1, \ldots, 2K\}$, $x_k \in \mathbb{R}$ et $\mathbf{A}_k \in \mathbb{C}^{T \times N_t}$ sont des matrices appelées matrices de dispersion linéairement indépendantes sur $\mathbb{R}$. Par ailleurs, un STBC est dit unitaire si l'ensemble de ses matrices de dispersion sont unitaires.

Définition 2.1 *Un STBC qui encode $2K$ symboles réels sur une période de signalisation T présente un taux de K/T symboles complexes par utilisation de canal.*

Remplaçant $\mathbf{X}$ dans (2.1) par son expression dans (2.3), on obtient :

$$\mathbf{Y} = \sum_{k=1}^{2K} (\mathbf{A}_k \mathbf{H})\, x_k + \mathbf{W}. \tag{2.4}$$

Par l'application de l'opérateur vec$(.)$ sur l'équation ci-dessus, nous obtenons :

$$\text{vec}(\mathbf{Y}) = \sum_{k=1}^{2K} (\mathbf{I}_{N_r} \otimes \mathbf{A}_k)\, \text{vec}\,(\mathbf{H})\, x_k + \text{vec}(\mathbf{W}). \tag{2.5}$$

où $\mathbf{I}_{N_r}$ est la matrice identité de taille $N_r \times N_r$.
Si $\mathbf{y}_i$, $\mathbf{h}_i$ et $\mathbf{w}_i$ désignent les colonnes i des matrices $\mathbf{Y}$, $\mathbf{H}$ et $\mathbf{W}$, respectivement, alors l'équation (2.5) peut être écrite sous forme matricielle :

$$\underbrace{\begin{bmatrix} \mathbf{y}_1 \\ \vdots \\ \mathbf{y}_{N_r} \end{bmatrix}}_{\mathbf{y}} = \underbrace{\begin{bmatrix} \mathbf{A}_1\mathbf{h}_1 & \dots & \mathbf{A}_{2K}\mathbf{h}_1 \\ \vdots & \vdots & \vdots \\ \mathbf{A}_1\mathbf{h}_{N_r} & \dots & \mathbf{A}_{2K}\mathbf{h}_{N_r} \end{bmatrix}}_{\boldsymbol{\mathcal{H}}} \underbrace{\begin{bmatrix} x_1 \\ \vdots \\ x_{2K} \end{bmatrix}}_{\mathbf{s}} + \underbrace{\begin{bmatrix} \mathbf{w}_1 \\ \vdots \\ \mathbf{w}_{N_r} \end{bmatrix}}_{\mathbf{w}}. \tag{2.6}$$

Un système d'équations réels peut être obtenu en séparant les parties réelle et imaginaire de l'équation ci-dessus :

$$\tilde{\mathbf{y}} = \tilde{\boldsymbol{\mathcal{H}}}\mathbf{s} + \tilde{\mathbf{w}} \tag{2.7}$$

où $\tilde{\mathbf{y}}, \tilde{\mathbf{w}} \in \mathbb{R}^{2N_rT \times 1}$ et $\tilde{\boldsymbol{\mathcal{H}}} \in \mathbb{R}^{2N_rT \times} 2K$. Notons que le système ci-dessus n'est pas sous-déterminé (le nombre d'équations est inférieur au nombre de variables) si $N_rT \geq K$, en supposant que les $\{\mathbf{A}_k : k = 1, \dots 2K\}$ sont linéairement indépendantes sur $\mathbb{R}$. L'avantage d'un système d'équations linéaires bien conditionné est que l'estimation ML peut être obtenue grâce à un décodeur sphérique dont la complexité de calcul attendue croît avec K^3 [8]. Si le système d'équations linéaires est sous-déterminé, la complexité de calcul attendue du décodeur sphérique croît de manière exponentielle avec $K - N_rT$ [8].

2.2 Décodage

En supposant que l'état du canal est parfaitement connu au niveau du récepteur, le décodeur optimal est celui qui décide en faveur du vecteur d'information s qui minimise la distance euclidienne entre le vecteur de données reçues et les possibles sorties du canal non-bruité :

$$\mathbf{s}^{\text{ML}} = \arg \min_{\hat{\mathbf{s}} \in \mathcal{C}} \|\tilde{\mathbf{y}} - \tilde{\boldsymbol{\mathcal{H}}}\hat{\mathbf{s}}\|^2 \tag{2.8}$$

où $\mathcal{C}$ représente l'espace vectoriel de s.
Une mise en œuvre directe de l'estimateur ML ci-dessus serait un décodeur à recherche exhaustive, qui évalue la métrique ML pour tous les vecteurs possibles s et en choisit finalement un avec la métriques ML minimale. Ce décodeur n'est pas utilisé dans les systèmes de communication pratiques en raison de sa complexité de calcul élevée : il nécessite $|\mathcal{C}|$ évaluations de la métrique ML et $|\mathcal{C}| - 1$ comparaisons. Cela conduit à la définition suivante de complexité de décodage (pire cas).

Définition 2.2 *La complexité décodage (pire cas) est définie comme le nombre minimal d'évaluations de la métrique ML nécessaire à un décodeur à recherche exhaustive pour estimer de façon optimale le mot de code transmit [14].*

2.2.1 Décodeur sphérique

Une implémentation plus pratique du décodeur ML peut être obtenue en interprétant (2.8) comme un problème *bounded closest lattice point search* qui peut être effectivement réalisé par un décodeur sphérique. En fait, le décodeur sphérique transforme (2.8) en un problème de recherche sur un arbre réel en appliquant la décomposition QR à $\tilde{\boldsymbol{\mathcal{H}}}$. Le problème se transforme alors en la détermination du chemin avec la plus petite métrique. En supposant que $N_r T \geq$ K, par la décomposition QR de $\tilde{\boldsymbol{\mathcal{H}}}$ on obtient :

$$\tilde{\boldsymbol{\mathcal{H}}} = \begin{bmatrix} \mathbf{Q}_1 & \mathbf{Q}_2 \end{bmatrix} \begin{bmatrix} \mathbf{R} \\ \mathbf{0} \end{bmatrix} \tag{2.9}$$

où $\mathbf{Q}_1 \in \mathbb{R}^{2N_r T \times 2K}$, $\mathbf{Q}_2 \in \mathbb{R}^{2N_r T \times (2N_r T - 2K)}$, $\mathbf{Q}_i^T \mathbf{Q}_i = \mathbf{I},\ i \in \{1, 2\}$, $\mathbf{R}$ est une matrice réelle triangulaire supérieure de taille $2K \times 2K$ et $\mathbf{0}$ est la matrice nulle de taille $(2N_r T - 2K) \times 2K$. Par conséquent, l'estimation ML s'écrit :

$$\mathbf{s}^{\mathrm{ML}} = \arg \min_{\hat{\mathbf{s}} \in \mathcal{C}} \|\tilde{\mathbf{y}} - \mathbf{Q}_1 \mathbf{R} \hat{\mathbf{s}}\|^2, \tag{2.10}$$

soit, puisque que la matrice $\mathbf{Q}_1$ est unitaire :

$$\mathbf{s}^{\mathrm{ML}} = \arg \min_{\hat{\mathbf{s}} \in \mathcal{C}} \|\mathbf{y}' - \mathbf{R} \hat{\mathbf{s}}\|^2 \tag{2.11}$$

où $\mathbf{y}' = \mathbf{Q}_1^T \tilde{\mathbf{y}}$.

Grâce à la structure triangulaire supérieure de $\mathbf{R}$, nous avons :

$$\begin{aligned}\mathbf{s}^{\mathrm{ML}} =& \arg \min_{\hat{\mathbf{s}} \in \mathcal{A}^{2K}} \sum_{i=1}^{2K} \left| y'_i - \sum_{j=i}^{2K} r_{i,j} \hat{x}_j \right|^2 \\ =& \arg \min_{\hat{\mathbf{s}} \in \mathcal{A}^{2K}} \left\{ \underbrace{\left| y'_1 - \sum_{j=1}^{2K} r_{1,j} \hat{x}_j \right|^2}_{W_{2K}} + \underbrace{\left| y'_2 - \sum_{j=2}^{2K} r_{2,j} \hat{x}_j \right|^2}_{W_{2K-1}} + \ldots \underbrace{\left| y'_{2K} - r_{2K,2K} \hat{x}_{2K} \right|^2}_{W_1} \right\}.\end{aligned} \tag{2.12}$$

Minimiser la quantité ci-dessus revient à trouver le chemin le plus court dans un arbre réel à $2K$ niveaux, où chaque chemin de la racine aux feuilles correspond à un choix particulier de symboles d'information, et où la métrique associée à la branche au niveau i est la métrique partielle W_i. Un arbre réel binaire (cas de transmission BPSK) à quatre niveaux est représenté dans la figure 2.1. Un choix possible de l'estimation ML $\{1, -1, 1, -1\}$ est marqué en gras.

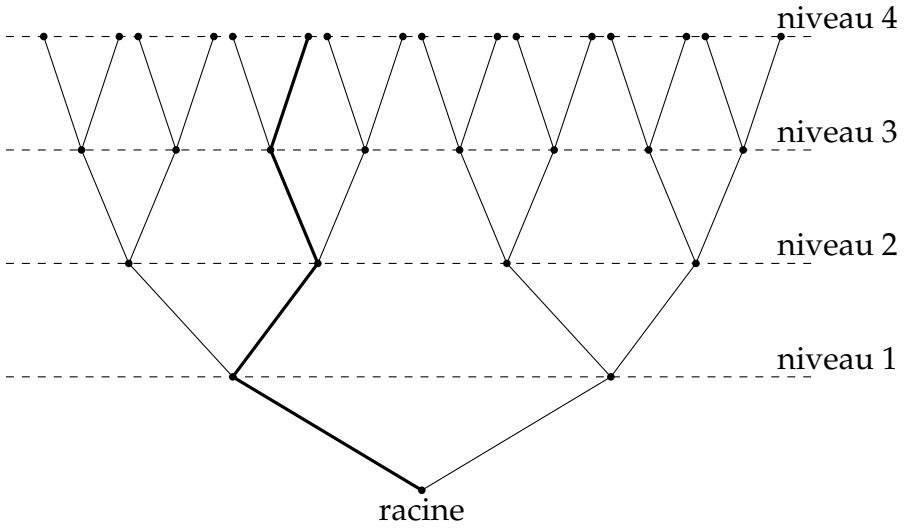

FIGURE 2.1 – Arbre réel à quatre niveaux

Au début, le rayon de la sphère est initialisé à l'infini et le décodeur sphérique commence à parcourir l'arbre par la racine en remontant jusqu'aux feuilles. Les nœuds frères sont visités selon l'énumération de Schnorr-Euchner [32] qui les trie par métrique de branche croissante. Chaque fois qu'un nœud feuille est atteint, sa métrique accumulée est comparée à la valeur actuelle du rayon de la sphère.

Si cette métrique est inférieure au rayon actuel de la sphère, ce dernier est mis à jour et le chemin est déclaré comme un candidat valable de l'estimation ML. Sinon le chemin est rejeté : il est considéré en dehors de la sphère actuelle. Les nœuds feuilles ne doivent pas être triés car, pour une valeur donnée de $(x_2, \ldots, x_{2k})$, l'estimation ML conditionnelle de x_1 notée $x_1^{\mathrm{ML}}|\,(\hat{x}_2, \ldots, \hat{x}_{2K})$, peut être obtenue directement par un détecteur à seuil. Pour une constellation QAM carrée non normalisée avec M points, cette opération est décrite par :

$$x_1^{\mathrm{ML}}|\,(\hat{x}_2, \ldots, \hat{x}_{2K}) = \mathrm{sign}\,(z_1) \times \min\Big[\Big|2\ \mathrm{round}\Big(\,(z_1 - 1)\,/2\Big) + 1\Big|, \sqrt{M} - 1\Big] \quad (2.13)$$

où $z_1 = \Big(y_1' - \sum_2^{2k} j = r_{1,j}\hat{x}_j\Big)\,/r_{1,1}$. Ceci est équivalent à la l'élagage du dernier niveau de l'arbre réel. Par conséquent, la complexité de décodage est divisée par $\sqrt{M}$.

En fait, d'après (2.12) la métrique associée à un chemin croît avec les niveaux de l'arbre. Supposant que la métrique accumulée jusqu'au nœud (a) au niveau i est supérieure ou égale au rayon actuel de la sphère. Tous les nœuds enfants issus de (a) peuvent alors être supprimés (puisque leur métrique accumulée sera strictement supérieure au rayon actuel de la sphère). Par ailleurs, grâce à la stratégie d'énumération de Schnorr-Euchner, on peut aussi éliminer les nœuds frères de (a). Par conséquent, le décodeur sphérique devra descendre au niveau $i-1$ et commencer à envisager les nœuds frères du nœud parent de (a).

Cet élagage de l'arbre résulte en une réduction significative du nombre de nœuds visités, facteur déterminant dans la rapidité de convergence du décodeur sphérique. Cela nous amène à définir une autre mesure de complexité : la complexité moyenne de décodage.

Définition 2.3 *La complexité moyenne de décodage est définie comme le nombre moyen de nœuds de l'arbre de recherche visités par un décodeur sphérique afin d'estimer de façon optimale le mot de code transmit [13].*

Il est à noter que, dans le cas des symboles réels, le classement de Schnorr-Euchner des nœuds frères au niveau i pour un trajet donné jusqu'au niveau $i-1$ peut être obtenu directement, sans évaluation explicite des PED. Plus explicitement on a :

$$S_i = \begin{cases} (x_i^{\mathrm{nc}}, x_i^{\mathrm{nc}} + 1, x_i^{\mathrm{nc}} - 1, x_i^{\mathrm{nc}} + 2, x_i^{\mathrm{nc}} - 2, \ldots) & \text{si } z_i \geq x_i^{\mathrm{nc}} \\ (x_i^{\mathrm{nc}}, x_i^{\mathrm{nc}} - 1, x_i^{\mathrm{nc}} + 1, x_i^{\mathrm{nc}} - 2, x_i^{\mathrm{nc}} + 2, \ldots) & \text{sinon} \end{cases} \quad (2.14)$$

où S_i désigne l'ordre dans lequel les nœuds au niveau i sont visités, et x_i^{nc} désigne le *nulling and cancelling point* [11] et qui est obtenu en remplaçant z_1 par $z_i = \left(y_i' - \sum_{j=i+1}^{2K} r_{i,j}\hat{x}_j\right)/r_{i,i}$ dans (2.13). Un pseudo-code du décodeur sphérique appliqué à un arbre réel de quatre niveaux est illustré dans la page suivante. La fonction `sort` renvoi l'ordre dans lequel les points réels de la constellation PAM $\mathcal{A}$ sont visités selon la procédure simplifiée d'énumération de Schnorr-Euchner [32].

2.3 Critères de conceptions des STBC

L'objectif principal dans la conception d'un STBC est d'obtenir de bonnes performances tout en conservant un niveau raisonnable de complexité au niveau du récepteur. Dans ce qui suit, les différents critères de conception des STBC pour des canaux quasi-statiques de Rayleigh à évanouissements plats sur la bande de fréquence d'intérêt sont passés en revue. La discussion des critères de conception de STBC à faible complexité est reportée au chapitre 3. En supposant que le récepteur dispose d'une connaissance parfaite du canal, l'estimation ML dans le modèle (2.1) est obtenue par :

$$\mathbf{X}^{\text{ML}} = \arg\min_{\hat{\mathbf{X}}\in\mathcal{C}} \|\mathbf{Y} - \hat{\mathbf{X}}\mathbf{H}\|_F \tag{2.15}$$

Grâce à la borne de l'union, la probabilité d'un décodage erroné vérifie l'inégalité suivante :

$$P_e \leq \sum_{\mathbf{X}\in\mathcal{C}} P(\mathbf{X}) \sum_{\substack{\mathbf{X}'\neq\mathbf{X} \\ \mathbf{X}'\in\mathcal{C}}} P(\mathbf{X}\to\mathbf{X}') \tag{2.16}$$

où $P(\mathbf{X})$ désigne la probabilité que $\mathbf{X}$ soit envoyée, et $P(\mathbf{X}\to\mathbf{X}')$ est la *Pairwise Error Probability* (PEP), la probabilité moyenne que le décodeur décide en faveur de $\mathbf{X}'$ alors que $\mathbf{X}$ a été envoyée (en supposant que le dictionnaire $\mathcal{C}$ ne contient que $\mathbf{X}$ et $\mathbf{X}'$). En supposant que les mots de code sont équiprobables, l'inégalité ci-dessus se réduit à :

$$P_e \leq \frac{1}{|\mathcal{C}|} \sum_{\mathbf{X}\in\mathcal{C}} \sum_{\substack{\mathbf{X}'\neq\mathbf{X} \\ \mathbf{X}'\in\mathcal{C}}} P(\mathbf{X}\to\mathbf{X}') \tag{2.17}$$

En raison de la symétrie du code, on a :

$$P_e \leq \sum_{\substack{\mathbf{X}'\neq\mathbf{X} \\ \mathbf{X}'\in\mathcal{C}}} P(\mathbf{X}\to\mathbf{X}') \tag{2.18}$$

Algorithm I: Décodeur sphérique pour un arbre réel à quatre niveaux et une constellation QAM à M points

$C = \infty$
$z_4 = y'_4 / r_{4,4}$
$x_4^{\mathsf{nc}} = \mathtt{sign}\left(z_4\right) \times \mathtt{min}\left[\left|2\ \mathtt{round}\left(\left(z_4 - 1\right)/2\right) + 1\right|, \sqrt{M} - 1\right]$
$\Xi_4 = \mathtt{sort}(z_4, x_4^{\mathsf{nc}})$
$k_4 = 1$
while $k_4 \leq \sqrt{M}$ **and** $\left(y'_4 - r_{4,4}\mathcal{A}\left(\Xi_4\left(k_4\right)\right)\right)^2 < C$ **do**
  $x_4 = \mathcal{A}\left(\Xi_4\left(k_4\right)\right)$
  $W_4 = \left(y'_4 - r_{4,4}x_4\right)^2$
  $z_3 = \left(y'_3 - r_{3,4}x_4\right)/r_{3,3}$
  $x_3^{\mathsf{nc}} = \mathtt{sign}\left(z_3\right) \times \mathtt{min}\left[\left|2\ \mathtt{round}\left(\left(z_3 - 1\right)/2\right) + 1\right|, \sqrt{M} - 1\right]$
  $\Xi_3 = \mathtt{sort}(z_3, x_3^{\mathsf{nc}})$
  $k_3 = 1$
  while $k_3 \leq \sqrt{M}$ **and** $\left(y'_3 - r_{3,3}\mathcal{A}\left(\Xi_3\left(k_3\right)\right) - r_{3,4}x_4\right)^2 + W_4 < C$ **do**
    $x_3 = \mathcal{A}\left(\Xi_3\left(k_3\right)\right)$
    $W_3 = \left(y'_3 - \sum_{j=3}^{4} r_{3,j}x_j\right)^2$
    $z_2 = \left(y'_2 - \sum_{j=3}^{4} r_{2,j}x_j\right)/r_{2,2}$
    $x_2^{\mathsf{nc}} = \mathtt{sign}\left(z_2\right) \times \mathtt{min}\left[\left|2\ \mathtt{round}\left(\left(z_2 - 1\right)/2\right) + 1\right|, \sqrt{M} - 1\right]$
    $\Xi_2 = \mathtt{sort}(z_2, x_2^{\mathsf{nc}})$
    $k_2 = 1$
    while $k_2 \leq \sqrt{M}$ **and** $\left(y'_2 - r_{2,2}\mathcal{A}\left(\Xi_2\left(k_2\right)\right) - \sum_{j=3}^{4} r_{2,j}x_j\right)^2 + \sum_{i=3}^{4} W_i < C$ **do**
      $x_2 = \mathcal{A}\left(\Xi_2\left(k_2\right)\right)$
      $W_2 = \left(y'_2 - \sum_{j=2}^{4} r_{2,j}x_j\right)^2$
      $z_1 = \left(y'_1 - \sum_{j=2}^{4} r_{1,j}x_j\right)/r_{1,1}$
      $x_1 = \mathtt{sign}\left(z_1\right) \times \mathtt{min}\left[\left|2\ \mathtt{round}\left(\left(z_1 - 1\right)/2\right) + 1\right|, \sqrt{M} - 1\right]$
      $W_1 = \left(y'_1 - r_{1,1}x_1 - \sum_{j=2}^{4} r_{1,j}x_j\right)^2$
      $P = \sum_{i=1}^{4} W_i$
      if $P < C$ **then**
        $C = P$
        $\hat{\mathbf{s}} = \mathbf{x}$
      end
      $k_2 = k_2 + 1$
    end
    $k_3 = k_3 + 1$
  end
  $k_4 = k_4 + 1$
end

Mais, d'après (2.15) :

$$P\left(\mathbf{X} \to \mathbf{X}'|\mathbf{H}\right) = Q\left(\sqrt{\frac{\gamma}{2}}\|\left(\mathbf{X}-\mathbf{X}'\right)\mathbf{H}\|_F\right) \tag{2.19}$$

où $\gamma = 1/N_0$ et $Q\left(x\right)$ est la fonction d'erreur complémentaire. Par application de la borne de Chernoff et évaluation de la moyenne sur les réalisations du canal, une limite supérieure sur la probabilité de confondre $\mathbf{X}$ et $\mathbf{X}'$ peut être obtenue :

$$P\left(\mathbf{X} \to \mathbf{X}'\right) \leq \frac{4^{rN_r}}{\left(\prod_{n=1}^{r}\lambda_n\right)^{N_r}\gamma^{rN_r}} \tag{2.20}$$

où r désigne le rang de la matrice $\left(\mathbf{X}-\mathbf{X}'\right)$ et $\{\lambda_n, n = 1\ldots, r\}$ désignent l'ensemble des r valeurs propres non-nulle de $\left(\mathbf{X}-\mathbf{X}'\right)^H\left(\mathbf{X}-\mathbf{X}'\right)$. D'après (2.18) et (2.20), on peut garantir de bonnes performances, en particulier dans la région SNR élevés par les deux critères suivantes :

2.3.1 Critère du rang

Un STBC est dit être de diversité pleine, si le rang de toutes les différences possibles des mots de code non-nulle est maximisée, c'est à dire si :

$$G_d = \min_{\substack{\mathbf{X}\neq\mathbf{X}'\\ \mathbf{X},\mathbf{X}'\in\mathcal{C}}} \text{rank}\left(\mathbf{X}-\mathbf{X}'\right) = N_t \tag{2.21}$$

2.3.2 Critère du déterminant

Pour améliorer davantage les performances d'un code à diversité pleine, il est souhaitable de maximiser son gain de codage, défini par :

$$\delta_{\mathbf{X}} = \min_{\substack{\mathbf{X}\neq\mathbf{X}'\\ \mathbf{X},\mathbf{X}'\in\mathcal{C}}} \det\left(\left(\mathbf{X}-\mathbf{X}'\right)^H\left(\mathbf{X}-\mathbf{X}'\right)\right) = \prod_{n=1}^{r}\lambda_n \tag{2.22}$$

Un STBC ayant un degré de diversité plus élevé aura une courbe de probabilité d'erreur en fonction de SNR plus raide dans l'échelle logarithmique, alors qu'un STBC avec un gain de codage plus élevé aura une courbe de probabilité d'erreur décalée vers la gauche. D'après (2.22), on peut se rendre compte que le gain de codage est une fonction décroissante de la taille de la constellation. Autrement dit, si $\mathcal{C}_1 \subset \mathcal{C}_2$:

$$\min_{\substack{\mathbf{X}\neq\mathbf{X}'\\ \mathbf{X},\mathbf{X}'\in\mathcal{C}_2}} \det\left(\left(\mathbf{X}-\mathbf{X}'\right)^H\left(\mathbf{X}-\mathbf{X}'\right)\right) \leq \min_{\substack{\mathbf{X}\neq\mathbf{X}'\\ \mathbf{X},\mathbf{X}'\in\mathcal{C}_1}} \det\left(\left(\mathbf{X}-\mathbf{X}'\right)^H\left(\mathbf{X}-\mathbf{X}'\right)\right) \tag{2.23}$$

Cela conduit à la définition suivante.

Définition 2.4 *Un STBC* $\mathbf{X}$ *est NonVanishing Determinant (NVD) si son gain de codage pour les constellations non-normalisées est majoré par une constante non-nulle indépendante de la taille de la constellation [20] :*

$$\delta_{\mathbf{X}} \geq \psi > 0 \tag{2.24}$$

où ψ *est une constante.*

La propriété NVD est souhaitable car elle peut être exploitée par l'utilisation d'une modulation adaptative dont le taux de transmission varie (à travers le choix de l'ordre de modulation) en fonction de la qualité du canal sans fil. Par ailleurs, il a été montré [33] q'un STBC NVD à taux plein (voir **Définition 2.5**) atteint le compromis de multiplexage-diversité (*Diversity-Multiplexing Trade-off*[4] (DMT)) pour un nombre d'antennes quelconque de réception.

2.3.3 Critère d'information mutuelle maximale

Les critères précédents tendent à optimiser les performances des STBC, en particulier dans la région des SNR élevés, en minimisant la limite asymptotique supérieure sur le PEP (2.20). On peut également optimiser les STBC du point de vue de la théorie de l'information et choisir les paramètres du code qui maximisent l'information mutuelle entre le vecteur de données transmises et le vecteur de données reçues [8]. La relation entrées-sorties d'un canal MIMO qui a N_t antennes d'émission et N_r antennes de réception peut être exprimée par :

$$\mathbf{y} = \sqrt{\frac{\rho}{N_t}}\mathbf{H}\mathbf{s} + \mathbf{n} \tag{2.25}$$

où $\mathbf{y} \in \mathbb{C}^{N_r}$, $\mathbf{H} \in \mathbb{C}^{N_r \times N_t}$ avec des entrées $h_{i,j} \sim \mathcal{CN}(0,1)$, $\mathbf{s} \in \mathbb{C}^{N_t}$ avec des entrées s_i telles que $\mathbb{E}|s_i|^2 = 1$, $\mathbf{n} \in \mathbb{C}^{N_r}$ avec des entrées $n_i \sim \mathcal{CN}(0,1)$ et ρ est le rapport signal-bruit par antenne de réception. Par conséquent, la capacité ergodique est donnée par [34] :

$$C(N_t, N_r, \rho) = \mathbb{E}\log_2 \det\left(\mathbf{I}_{N_r} + \frac{\rho}{N_t}\mathbf{H}\mathbf{H}^H\right). \tag{2.26}$$

De ce point de vue, un bon STBC est celui qui ne limite pas la capacité du canal MIMO. Si un système MIMO emploie un STBC qui encode $2K$ symboles réels soumis à la contrainte de puissance

$$\sum_{k=1}^{2K} \text{tr}\left(\mathbf{A}_k^H \mathbf{A}_k\right) = 2TK \tag{2.27}$$

son modèle d'entrée/sortie peut être exprimé par :

$$\mathbf{y} = \sqrt{\frac{\rho}{K}}\boldsymbol{\mathcal{H}}\mathbf{s} + \mathbf{w} \tag{2.28}$$

où ρ désigne le SNR moyen par antenne de réception. Par conséquent, la capacité ergodique du système ci-dessus est égale à :

$$C_{\text{STBC}}(\rho) = \frac{1}{T}\mathbb{E}\log_2 \det\left(\mathbf{I}_{2K} + \frac{\rho}{K}\boldsymbol{\mathcal{H}}^H\boldsymbol{\mathcal{H}}\right). \tag{2.29}$$

où le terme $1/T$ est ajouté pour compenser le temps de signalisation T nécessaire à la transmission du vecteur d'information $\mathbf{s}$, contrairement à (2.26) où à chaque instant, N_t symboles complexes sont transmis. Ainsi, un STBC employant N_t antennes d'émission et N_r antennes de réception est dit *information lossless* si la condition suivante est satisfaite :

$$C_{\text{STBC}}(\rho) = C(N_t, N_r, \rho) \tag{2.30}$$

2.3.4 Taux élevé

À SNR élevé, la capacité du canal MIMO (2.26) s'écrit comme [4] :

$$C(N_t, N_r, \rho \gg 1) \approx \min\{N_t, N_r\}\log\frac{\rho}{N_t} + \sum_{k=|N_t-N_r|+1}^{\min\{N_t,N_r\}} \mathbb{E}\{\log_2 \chi_k\} \tag{2.31}$$

où χ_k est une variable aléatoire qui suit la loi du chi-deux à $2k$ degrés de liberté. Par rapport à un canal *Single Input Single Output* (SISO) où la capacité croît linéairement avec $\log\rho$, la capacité d'un canal MIMO $N_t \times N_r$ croît linéairement avec $\min\{N_t, N_r\}\log\rho$ asymptotiquement, ce qui est équivalent à $\min\{N_t, N_r\}$ canaux SISO parallèles. En d'autres termes, un canal MIMO possède $\min\{N_t, N_r\}$ degrés de liberté. Cette interprétation est importante car elle nous indique le nombre maximal de flux de données indépendants qu'une configuration MIMO peut supporter pour une communication fiable. Ceci conduit à la définition suivante :

Définition 2.5 *Un STBC est dit à taux plein s'il exploite tous les degrés de liberté disponibles dans le canal MIMO, c'est à dire, si son taux est égal à min* $\{N_t, N_r\}$ *symboles complexes par utilisation de canal [2].*

2.3.5 Mise en forme cubique

Pour une constellation multidimensionnelle donnée, il est souhaitable de maximiser son efficacité de SNR, c'est-à-dire de maximiser la distance Euclidienne minimale pour une puissance moyenne donnée. Ainsi, il est utile d'exprimer la matrice de code $\mathbf{X}$ comme :

$$\widetilde{\text{vec}\,(\mathbf{X})} = \mathbb{G}\mathbf{s}. \tag{2.32}$$

Cette représentation signifie que la matrice de code engendre donc un sous-ensemble d'un réseau de points *lattice* réel multidimensionnel Λ, de matrice génératrice $\mathbb{G}$. Un paramètre-clé pour déterminer l'efficacité de SNR pour une constellation multidimensionnelle est son gain de mise en forme *shaping gain* γ_s [35], déterminé par la région $\mathcal{R}$ délimitant le réseau de points.

Il a été montré [35] que la région $\mathcal{R}$ qui maximise le gain de mise en forme est une hypersphère, et que le gain de mise en forme correspondant est approximativement égale à 1.53 dB quand le nombre de dimensions de l'hypersphère tend vers l'infini. Malheureusement, en raison de la complexité de mise en œuvre d'un réseau délimité par une région sphérique, il est nécessaire de recourir à un réseau de point cubique [1] facilement mis en œuvre et ne présentant pas de perte de mise en forme ($\gamma_s = 0$ dB). Un STBC qui encode $2K$ symboles réels est dit de mise en forme cubique (*cubic shaping*) si sa matrice génératrice réelle $\mathbb{G}$ est telle que [14] :

$$\mathbb{G}^T\mathbb{G} = \alpha\mathbf{I}_{2K} \tag{2.33}$$

où $\alpha = \text{tr}\left(\mathbf{A}_k^H\mathbf{A}_k\right),\ k = 1, \ldots, 2K$. D'après (2.32), la propriété de mise en forme cubique préserve la puissance moyenne transmise. La condition (2.33) peut être écrite en termes de matrice génératrice complexe $\mathbf{G}$:

$$\Re\left\{\mathbf{G}^H\mathbf{G}\right\} = \alpha\mathbf{I}_{2K} \tag{2.34}$$

où $\mathbb{G} = \tilde{\mathbf{G}}$.

[1] Le terme cubique dans ce contexte réfère généralement à un hypercube pas nécessairement en trois dimensions

Chapitre 3

Codes espace-temps en bloc de faible complexité de décodage

Nous avons décrit au chapitre précédent les principaux critères de conception d'un STBC afin de fournir de bonnes performances pour les canaux de Rayleigh quasi-statiques à évanouissements plats. Toutefois, pour des considérations pratiques, il est souhaitable de prendre en compte d'autres critères, principalement la faible complexité de décodage, que nous pouvons définir de la manière suivante :

Définition 3.1 *Un STBC encodant $2K$ symboles réels tirés d'une constellation complexe de taille M est dit de faible complexité de décodage si et seulement si sa complexité de décodage est inférieure à M^K.*

La nécessité de STBC à faible complexité de décodage semble être inévitable dans le cas de débits élevés des communications dans les systèmes MIMO employant un nombre d'antennes supérieur à deux. En effet, malgré leur faible complexité de décodage (en croissance linéaire avec la taille de la constellation utilisée), les STBC orthogonaux souffrent d'une limitation stricte de débit pour plus de deux antennes. D'autre part, les alternatives à débit plein, notamment les codes TAST et les codes parfaits, ont généralement un niveau élevé de complexité de décodage (pire cas), et de complexité moyenne si un décodeur sphérique est utilisé.

Sans doute, le premier STBC de faible complexité de taux 1 code pour le cas de quatre antennes d'émission est le STBC quasi-orthogonal (QO) initialement proposé par H. Jafarkhani [36], puis optimisé par la rotation de constellation assurant un gain de diversité maximal [37, 38]. Le STBC QO relâche partiellement les conditions d'orthogonalité en permettant la détection conjointe de deux symboles

complexes. Les codes QO de taux 1 et à diversité pleine ont été ultérieurement proposés pour un nombre arbitraire d'antennes d'émission, le code QO d'origine en étant un cas particulier [39]. Dans ce contexte général, la *quasi-orthogonalité* signifie le découplage des symboles émis en deux groupes de même taille.

Cependant, des STBC de complexité de décodage inférieure peuvent être obtenus grâce au principe de g*-group decodability* établi par S. Karmakar *et al.* [19, 16]. En effet, la g*-group decodability* généralise la quasi-orthogonalité en permettant le découplage des symboles émis en plus de deux groupes, pas nécessairement de même taille. Par ailleurs, il est possible d'obtenir des STBC 4*-group decodable* de taux 1 et à diversité pleine pour un nombre quelconque d'antennes d'émission [40].

Une autre approche permettant la conception de STBC à faible complexité consiste en la détection conditionnelle [41], où la détection ML est réalisée en deux étapes. Lors de la première étape, l'estimation ML d'un sous-ensemble des symboles émis $(x_1, x_2, \ldots, x_k)$ est évaluée conditionnellement par une valeur donnée du reste des symboles $(\hat{x}_{k+1}, \hat{x}_{k+2}, \ldots, \hat{x}_{2k})$ et que l'on peut noter par $\left(x_1^{\text{ML}}, x_2^{\text{ML}}, \ldots, x_k^{\text{ML}} | \hat{x}_{k+1}, \hat{x}_{k+2}, \ldots, \hat{x}_{2K}\right)$. Dans la deuxième étape, le récepteur minimise la métrique ML sur les valeurs possibles de $(x_{k+1}, x_{k+2}, \ldots, x_{2k})$ seulement. Cette procédure n'a généralement aucun effet sur la complexité du décodage à moins que les symboles $(x_1, x_2, \ldots, x_k)$ admettent un décodage à complexité allégée. Dans ce cas, la complexité de décodage peut être considérablement réduite. Cette technique de réduction est connue sous le nom de décodage rapide (*fast decoding*). Les codes qui admettent un décodage rapide sont dit *Fast Decodable* (FD).

Plus récemment, des STBC combinant les deux familles de codes (g*-group decodable* et *fast decodable*, les code *Fast-Group Decodable* (FGD) ont été proposées dans [18]. Ces codes sont g*-group decodable* de manière à ce que chaque groupe de symboles soit FD.

Ce chapitre est dédié à l'étude détaillée des trois familles de codes à faible complexité ainsi que leurs complexités de décodage.

3.1 Codes *g-group decodable*

Les STBC *g-group decodable* sont conçus de manière que la métrique ML est exprimée sous la forme d'une somme de g termes en fonctions des groupes disjoints de symboles, ce qui réduit considérablement la complexité de décodage, en permettant la détection de ces groupes disjoints de symboles sans perte de performance :

Définition 3.2 *Un STBC encodant $2K$ symboles réels est dit g-group decodable si et seulement si sa métrique ML peut être exprimée comme une somme de g termes en fonctions des sous-ensembles disjoints des symboles émis [16, 19].*

Afin qu'il soit *g-group decodable*, les conditions à satisfaire par les matrices de dispersion d'un STBC [19, 16] sont dérivées ici pour autonomie à partir de la décision ML du modèle du système (2.1). En supposant que le récepteur dispose d'une connaissance parfaite du canal, l'estimation ML du mot de code est donnée par :

$$\begin{aligned}\mathbf{X}^{\mathrm{ML}} &= \arg\min_{\mathbf{X}\in\mathcal{C}} \|\mathbf{Y}-\mathbf{X}\mathbf{H}\|_F^2 \\ &= \arg\min_{\mathbf{X}\in\mathcal{C}} \mathrm{tr}\left[(\mathbf{Y}-\mathbf{X}\mathbf{H})^H(\mathbf{Y}-\mathbf{X}\mathbf{H})\right]\end{aligned} \tag{3.1}$$

Si $\mathbf{X}$ peut être exprimée comme une somme de sous-codes $\mathbf{X}_i,\ i=1,\dots g$ tels que :

$$\mathbf{X}=\sum_{i=1}^{g}\mathbf{X}_i,\ \mathbf{X}_i^H\mathbf{X}_j+\mathbf{X}_j^H\mathbf{X}_i=\mathbf{0},\ 1\le i\neq j\le g \tag{3.2}$$

Alors, (3.1) s'écrit sous la forme suivante :

$$\begin{aligned}\mathbf{X}^{\mathrm{ML}} &= \arg\min_{\mathbf{X}\in\mathcal{C}} \mathrm{tr}\left[\mathbf{Y}^H\mathbf{Y}-\sum_{i=1}^{g}\mathbf{Y}^H\mathbf{X}_i\mathbf{H}-\mathbf{H}^H\mathbf{X}_i^H\mathbf{Y}+\mathbf{H}^H\mathbf{X}_i^H\mathbf{X}_i\mathbf{H}\right] \\ &= \sum_{i=1}^{g}\arg\min_{\mathbf{X}_i\in\mathcal{C}_i} \mathrm{tr}\left[\mathbf{Y}^H\mathbf{Y}-\mathbf{Y}^H\mathbf{X}_i\mathbf{H}-\mathbf{H}^H\mathbf{X}_i^H\mathbf{Y}+\mathbf{H}^H\mathbf{X}_i^H\mathbf{X}_i\mathbf{H}\right]-\sum_{i=1}^{g-1}\mathrm{tr}\left[\mathbf{Y}^H\mathbf{Y}\right]\end{aligned} \tag{3.3}$$

où $\mathcal{C}_i$ dénote le dictionnaire du sous-code i. En sachant que le dernier terme de l'équation ci-dessus est constant pour une matrice donnée de signal reçu, l'estimation ML peut donc être exprimée sous la forme :

$$\mathbf{X}^{\mathrm{ML}}=\sum_{i=1}^{g}\arg\min_{\mathbf{X}_i\in\mathcal{C}_i}\|\mathbf{Y}-\mathbf{X}_i\mathbf{H}\|_F^2. \tag{3.4}$$

En termes de matrices de dispersion, les conditions dans (3.2) sont équivalentes à :

$$\mathbf{A}_k^H\mathbf{A}_l+\mathbf{A}_l^H\mathbf{A}_k=\mathbf{0},\ \forall\mathbf{A}_k\in\mathcal{G}_i,\ \mathbf{A}_l\in\mathcal{G}_j,\ 1\le i\neq j\le g,\ |\mathcal{G}_i|=n_i,\sum_{i=1}^{g}n_i=2K. \tag{3.5}$$

avec $\mathcal{G}_i$ désigne l'ensemble des matrices de dispersion associées au groupe i de symboles. Par exemple, si un STBC encodant $2K$ symboles réels est *g-group decodable*, sa complexité de décodage peut être réduite de $\sqrt{M}^{2K-1}$ à $\sum_{i=1}^{g}\sqrt{M}^{n_i-1}$ où M est la taille de la constellation QAM carrée utilisée. Si un décodeur sphérique réel est utilisé en conjonction avec un détecteur à seuil, la *g-group decodability* divise l'arbre réel original à $(2K-1)$ niveaux en g petits arbres ayant chacun (n_i-1) niveaux. Dans le cas particulier des STBC orthogonaux, la complexité de décodage est $\mathcal{O}(1)$, puisque les détecteurs à seuil (2.13) nécessitent un nombre fixe d'opérations arithmétiques indépendamment de la taille de constellation QAM carrée utilisée. La matrice réelle triangulaire supérieure $\mathbf{R}$ correspondante est une matrice diagonale en bloc :

$$\mathbf{R} = \begin{bmatrix} \mathbf{R}_1 & \mathbf{0} & \dots & \mathbf{0} \\ \mathbf{0} & \mathbf{R}_2 & \dots & \mathbf{0} \\ \vdots & \vdots & \ddots & \vdots \\ \mathbf{0} & \mathbf{0} & \dots & \mathbf{R}_g \end{bmatrix} \tag{3.6}$$

où $\mathbf{R}_i$ est une matrice triangulaire supérieure de taille $n_i \times n_i$.

Outre sa réduction significative de la complexité de décodage, la structure de *g-group decodability* permet une optimisation simplifiée du gain de codage puisque le problème d'optimisation de ce gain se réduit en l'optimisation du gain de codage individuel de chaque sous-code. Comme l'on peut constater dans la proposition suivante :

Proposition 3.1 *Si un STBC* $\mathbf{X}$ *est g-group decodable de sorte que :*

$$\mathbf{X} = \sum_{i=1}^{g} \mathbf{X}_i,\ \mathbf{X}_i^H \mathbf{X}_j + \mathbf{X}_j^H \mathbf{X}_i = \mathbf{0},\ 1 \leq i \neq j \leq g \tag{3.7}$$

son gain de codage $\delta_{\mathbf{X}}$ *peut être exprimé comme :*

$$\delta_{\mathbf{X}} = min\left\{\delta_{\mathbf{X}_1}, \delta_{\mathbf{X}_2}, \dots, \delta_{\mathbf{X}_g}\right\} \tag{3.8}$$

La preuve découle directement de (3.5) et de l'inégalité du déterminant de Minkowski [42].

Démonstration. D'après la définition du gain de codage (2.22), on a :

$$\delta_{\mathbf{X}} = \min_{\substack{\mathbf{X}\neq\mathbf{X}' \\ \mathbf{x},\mathbf{x}'\in\mathcal{C}}} \det\left[(\mathbf{X}-\mathbf{X}')^H(\mathbf{X}-\mathbf{X}')\right] = \min_{\Delta\mathbf{X}\in\Delta\mathcal{C}/\{\mathbf{0}\}} \det\left[(\Delta\mathbf{X})^H(\Delta\mathbf{X})\right] \tag{3.9}$$

Grâce à (3.5), l'équation ci-dessus s'écrit sous la forme suivante :

$$\delta_{\mathbf{X}} = \min_{\Delta\mathbf{X}\in\Delta\mathcal{C}/\{\mathbf{0}\}} \det\left[\sum_{i=1}^{g}\Delta\mathbf{X}_i^H\Delta\mathbf{X}_i\right] \tag{3.10}$$

D'autre part, d'après l'inégalité du déterminant de Minkowski [42] :

$$\left(\det\left[\mathbf{A}+\mathbf{B}\right]\right)^{1/n} \geq \left(\det\left[\mathbf{A}\right]\right)^{1/n} + \left(\det\left[\mathbf{B}\right]\right)^{1/n} \tag{3.11}$$

où $\mathbf{A}, \mathbf{B} \in \mathcal{M}_n$ sont des matrices définies positives. Par conséquent on obtient :

$$\begin{aligned}\det\left[\sum_{i=1}^{g}\Delta\mathbf{X}_i^H\Delta\mathbf{X}_i\right] &\geq \left(\sum_{i=1}^{g}\left(\det\left[\Delta\mathbf{X}_i^H\Delta\mathbf{X}_i\right]\right)^{1/n}\right)^n \\ &= \sum_{i=1}^{g}\det\left[\Delta\mathbf{X}_i^H\Delta\mathbf{X}_i\right] + C \\ &\geq \sum_{i=1}^{g}\det\left[\Delta\mathbf{X}_i^H\Delta\mathbf{X}_i\right]\end{aligned} \tag{3.12}$$

où la dernière inégalité est justifiée par le fait que $C \geq 0$. L'égalité est obtenue pour le cas trivial $\Delta\mathbf{X} = \mathbf{0}$ ou pour le cas $\Delta\mathbf{X} = \Delta\mathbf{X}_k$ et $\Delta\mathbf{X}_i = \mathbf{0}\ \forall 1 \leq i \neq k \leq g$. Ainsi on a :

$$\begin{aligned}\delta_{\mathbf{X}} =& \min\left\{\min_{\Delta\mathbf{X}_1\in\Delta\mathcal{C}_1/\{\mathbf{0}\}}\det\left[\Delta\mathbf{X}_1^H\Delta\mathbf{X}_1\right], \ldots, \min_{\Delta\mathbf{X}_g\in\Delta\mathcal{C}_g/\{\mathbf{0}\}}\det\left[\Delta\mathbf{X}_g^H\Delta\mathbf{X}_g\right]\right\} \\ =& \min\left\{\delta_{\mathbf{X}_1}, \delta_{\mathbf{X}_2}, \ldots, \delta_{\mathbf{X}_g}\right\}\end{aligned} \tag{3.13}$$

ce qui termine la preuve. □

Un exemple de STBC *g-group decodable* est le code 4-*group decodable* de taux 1 pour $2^a,\ a \in \mathbb{N}$ [17]. Pour le cas de quatre antennes d'émission, la matrice du code 4-*group decodable* de taux 1 est exprimée comme suit :

$$\begin{bmatrix} x_1 - x_2 + ix_3 - ix_4 & x_5 - x_6 + ix_7 - ix_8 & 0 & 0 \\ -x_5 + x_6 + ix_7 - ix_8 & x_1 - x_2 - ix_3 + ix_4 & 0 & 0 \\ 0 & 0 & x_1 + x_2 - ix_3 - ix_4 & x_5 + x_6 + ix_7 + ix_8 \\ 0 & 0 & -x_5 - x_6 + ix_7 + ix_8 & x_1 + x_2 + ix_3 + ix_4 \end{bmatrix}$$

Les 4 groupes de symboles sont : $\{x_1, x_2\}, \{x_3, x_4\}, \{x_5, x_6\}, \{x_7, x_8\}$. En conséquence, la complexité de décodage est égale à $4\sqrt{M}$ pour les constellations QAM carrées et $4M$ pour les constellations quelconques.

3.2 Codes *fast decodable*

On définit un STBC *fast decodable* comme étant un code conditionnellement *g-group decodable*, c'est à dire dont la matrice de code s'écrit :

$$\mathbf{X}(\mathbf{s}) = \mathbf{X}_1(\mathbf{s}_1) + \mathbf{X}_2(\mathbf{s}_2) \tag{3.14}$$

où $\mathbf{X}_1(\mathbf{s}_1)$ est un code *g-group decodable* :

Définition 3.3 *un STBC encodant $2K$ symboles réels est dit fast decodable si et seulement si ses matrices de dispersion satisfont aux conditions :*

$$\mathbf{A}_k^H \mathbf{A}_l + \mathbf{A}_l^H \mathbf{A}_k = \mathbf{0},\ \forall \mathbf{A}_k \in \mathcal{G}_i,\ \mathbf{A}_l \in \mathcal{G}_j,\ 1 \leq i \neq j \leq g,\ |\mathcal{G}_i| = n_i, \sum_{i=1}^{g} n_i = \kappa < 2K. \tag{3.15}$$

La définition ci-dessus généralise légèrement la définition de codes FD dans [14] où un code FD est restreint à être conditionnellement orthogonal, (i.e. $n_1 = n_2 \ldots = n_g = 1$. L'avantage de codes FD est qu'on peut faire appel à la détection conditionnelle pour réduire la complexité de décodage. La première étape consiste à évaluer l'estimation ML conditionnée de s_1 à une valeur donnée de s_2 que nous notons $\mathrm{s}_1^{\mathrm{ML}}|\hat{\mathrm{s}}_2$. Lors de la deuxième étape, le décodeur devra minimiser la métrique ML sur toutes les valeurs possibles de s_2 seulement. Par exemple, si un STBC encodant $2K$ symboles réels est FD, sa complexité de décodage pour les constellations QAM carrées est réduite de $\sqrt{M}^{2K-1}$ à $\sqrt{M}^{2K-\kappa} \times \sum_{i=1}^{g} \sqrt{M}^{n_i-1}$. Si le code *g-group decodable* est orthogonal, la complexité de décodage est réduite à $\sqrt{M}^{2k-\kappa}$. Cette approche est équivalente à la division des derniers κ niveaux de l'arbre réel en g arbres, chacun doté de $n_i - 1,\ i = 1, \ldots, g$ niveaux. Dans le cas particulier où $n_i = 1,\ \forall i = 1, \ldots, g$ (autrement dit, le code FD est conditionnellement orthogonal), le *fast decoding* se réduit à la suppression des derniers κ niveaux de l'arbre à valeurs réelles. La matrice triangulaire supérieure $\mathbf{R}$ correspondante peut s'écrire sous la forme :

$$\mathbf{R} = \begin{bmatrix} \mathbf{A} & \mathbf{B} \\ \mathbf{0} & \mathbf{C} \end{bmatrix}$$

où $\mathbf{B}$ n'a pas de structure spéciale, $\mathbf{C}$ est un matrice triangulaire supérieure $(2K-\kappa)\times(2K-\kappa)$, et $\mathbf{A}$ est une matrice bloc-diagonale $\kappa \times \kappa$:

$$\mathbf{A} = \begin{bmatrix} \mathbf{R}_1 & \mathbf{0} & \dots & \mathbf{0} \\ \mathbf{0} & \mathbf{R}_2 & \dots & \mathbf{0} \\ \vdots & \vdots & \ddots & \vdots \\ \mathbf{0} & \mathbf{0} & \dots & \mathbf{R}_g \end{bmatrix}$$

avec $\mathbf{R}_i$ une matrice triangulaire supérieure de taille $n_i \times n_i$.
Parmi les exemples des codes FD, on peut citer le code Sezginer-Sari [43] dont la matrice de code est donnée par (3.16) et le *silver code* [44, 45] dont la matrice de code est donnée par (3.17).

$$\mathbf{X} = \frac{1}{\sqrt{2}} \begin{bmatrix} as_1 + bs_3 & -cs_2^* - ds_4^* \\ as_2 + bs_4 & cs_1^* + ds_3^* \end{bmatrix} \tag{3.16}$$

avec $a = c = 1$, $b = \frac{1-\sqrt{7}+i\left(1+\sqrt{7}\right)}{4}$, et $d = -jb$, ce qui donne un gain de codage de 2 indépendamment de la constellation QAM non-normalisée utilisée.

$$\mathbf{X} = \frac{1}{\sqrt{2}} \begin{bmatrix} s_1 & -s_2^* \\ s_2 & s_1^* \end{bmatrix} + \begin{bmatrix} 1 & 0 \\ 0 & -1 \end{bmatrix} \begin{bmatrix} z_1 & -z_2^* \\ z_2 & z_1^* \end{bmatrix} \tag{3.17}$$

$(z_1, z_2)^T = \mathbf{U}\,(s_3, s_4)^T$, et $\mathbf{U}$ est donnée par :

$$\mathbf{U} = \frac{1}{\sqrt{7}} \begin{bmatrix} 1+j & -1+2j \\ 1+2j & 1-j \end{bmatrix}$$

ce qui correspond à un gain de codage 16/7 indépendamment de la constellation QAM non-normalisée utilisée.

Les deux codes 2×2 ci-dessus peuvent être écrits comme une somme de deux codes d'Alamouti donnant lieu à une complexité de décodage de M^2 pour les constellations QAM carrées et $2M^3$ pour des constellations arbitraires. Un example des codes FD dans le cas de quatre antennes d'émission est le code 4×4 de taux 2 [46] décrit par la matrice de code (3.18).

$$\mathbf{X} = \begin{bmatrix} s_{1I} + js_{3Q} & -s_{2I} + js_{4Q} & e^{j\pi/4}(s_{5I} + js_{7Q}) & e^{j\pi/4}(-s_{6I} + js_{8Q}) \\ s_{2I} + js_{4Q} & s_{1I} - js_{3Q} & e^{j\pi/4}(s_{6I} + js_{8Q}) & e^{j\pi/4}(s_{5I} - js_{7Q}) \\ e^{j\pi/4}(s_{7I} + js_{5Q}) & e^{j\pi/4}(-s_{8I} + js_{6Q}) & s_{3I} + js_{1Q} & -s_{4I} + js_{2Q} \\ e^{j\pi/4}(s_{8I} + js_{6Q}) & e^{j\pi/4}(s_{7I} - js_{5Q}) & s_{4I} + js_{2Q} & s_{3I} - js_{1Q} \end{bmatrix} \tag{3.18}$$

où $(s_{iI}, s_{iQ}) \in e^{j\theta_g}\mathcal{A}$, $\theta_g = \frac{1}{2}\arctan(2)$ et $\mathcal{A}$ désigne la constellation QAM conventionnelle. Le code ci-dessus peut s'exprimer sous la forme de deux codes 4-*group*

decodable ce qui donne lieu à une complexité de décodage de l'ordre de $4M^{4.5}$ pour les constellations QAM conventionnelles carrées et $4M^5$ pour des constellations QAM arbitraires.

3.3 Code *Fast-Group Decodable*

Un STBC est dit *fast-group decodable* s'il est g-*group decodable* avec $g > 1$ de manière à ce que chaque sous-code soit FD.

Définition 3.4 *Un STBC encodant $2K$ symboles réels est dit fast-group decodable si et seulement si :*

$$\mathbf{A}_k^H \mathbf{A}_l + \mathbf{A}_l^H \mathbf{A}_k = \mathbf{0},\ \forall \mathbf{A}_k \in \mathcal{G}_i,\ \mathbf{A}_l \in \mathcal{G}_j,\ 1 \leq i \neq j \leq g,\ |\mathcal{G}_i| = n_i, \sum_{i=1}^{g} n_i = 2K$$

tel que les matrices de dispersion de chaque sous-code satisfont aux conditions :

$$\mathbf{A}_k^H \mathbf{A}_l + \mathbf{A}_l^H \mathbf{A}_k = \mathbf{0},\ \forall \mathbf{A}_k \in \mathcal{G}_{i,m},\ \mathbf{A}_l \in \mathcal{G}_{i,n},\ 1 \leq m \neq n \leq g_i,$$
$$|\mathcal{G}_{i,j}| = n_{i,j},\ \sum_{j=1}^{g_i} n_{i,j} = \kappa_i < n_i.$$

$\mathcal{G}_{i,m}$ (resp. g_i) désigne l'ensemble des matrices de dispersion constituants le groupe m (resp. le nombre de groupes internes) du groupe i des symboles $\mathcal{G}_i$. Par exemple, si un STBC encodant $2K$ symboles réels est FGD, l'ordre de sa complexité de décodage pour les constellations QAM carrées est réduite de $\sqrt{M}^{2K-1}$ à $\sum_{i=1}^{g} \sqrt{M}^{n_i-\kappa_i} \times \sum_{j=1}^{g_i} \sqrt{M}^{n_{i,j}-1}$. De manière similaire, si le code g-*group-decodable* de chaque groupe est orthogonal, l'ordre de la complexité de décodage est égale à $\sum_{i=1}^{g} \sqrt{M}^{n_i-\kappa_i}$. Au cas où un décodeur sphérique est utilisé, la propriété de *fast-group decodability* se réduit à diviser l'arbre réel original avec à $(2K-1)$ niveaux en g petits arbres ayant chacun n_i niveaux, et à diviser les derniers κ_i niveaux de l'arbre i en g_i arbres à $(n_{i,j}-1)$ niveaux. La structure de la matrice triangulaire supérieure $\mathbf{R}$ prend la forme suivante

$$\mathbf{R} = \begin{bmatrix} \mathbf{R}_1 & \mathbf{0} & \dots & \mathbf{0} \\ \mathbf{0} & \mathbf{R}_2 & \dots & \mathbf{0} \\ \vdots & \vdots & \ddots & \vdots \\ \mathbf{0} & \mathbf{0} & \dots & \mathbf{R}_g \end{bmatrix} \tag{3.19}$$

dans laquelle on a pour $1 \leq i \leq g$:

$$\mathbf{R}_i = \begin{bmatrix} \mathbf{A}_i & \mathbf{B}_i \\ \mathbf{0} & \mathbf{C}_i \end{bmatrix} \tag{3.20}$$

$\mathbf{B}_i$ n'a pas de structure spéciale, $\mathbf{C}_i$ est une matrice triangulaire supérieure $(n_i - \kappa_i)\times(n_i - \kappa_i)$, et $\mathbf{A}_i$ est une matrice $\kappa_i \times \kappa_i$ diagonale par bloc :

$$\mathbf{A}_i = \begin{bmatrix} \mathbf{R}_{i,1} & \mathbf{0} & \dots & \mathbf{0} \\ \mathbf{0} & \mathbf{R}_{i,2} & \dots & \mathbf{0} \\ \vdots & \vdots & \ddots & \vdots \\ \mathbf{0} & \mathbf{0} & \dots & \mathbf{R}_{i,g_i} \end{bmatrix} \tag{3.21}$$

$\mathbf{R}_{i,j}$ est une matrice triangulaire supérieure de taille $n_{i,j} \times n_{i,j}$. Un example de codes FGD dans le cas de deux antennes d'émission est le code 2×2 de taux 5/4 décrit par sa matrice de code (3.22) [47] :

$$\mathbf{X} = \begin{bmatrix} x_1 - x_2 + jx_3 + jx_4 + jx_5 & x_1 + x_2 - jx_3 + jx_4 + jx_5 \\ x_1 + x_2 + jx_3 - jx_4 + jx_5 & -x_1 + x_2 + jx_3 + jx_4 - jx_5 \end{bmatrix} \tag{3.22}$$

Dans le cas de quatre antennes d'émission, un exemple de codes FGD est le code 4×4 de taux 17/8 décrit par sa matrice de code (3.23)[47] :

$$\mathbf{X} = \begin{bmatrix} \mathbf{A} & \mathbf{B} \\ \mathbf{C} & \mathbf{D} \end{bmatrix} \tag{3.23}$$

où :

$$\begin{aligned}
\mathbf{A} &= \begin{bmatrix} x_1 + jx_6 + jx_9 + jx_{12} + jx_{17} & x_7 + jx_8 + x_{14} + jx_{15} \\ -x_7 + jx_8 - x_{14} + jx_{15} & x_1 + jx_6 + jx_9 - jx_{12} - jx_{17} \end{bmatrix} \\
\mathbf{B} &= \begin{bmatrix} -x_2 + jx_3 + x_{10} + jx_{11} & x_4 + jx_5 + x_{13} + jx_{16} \\ -x_4 + jx_5 + x_{13} - jx_{16} & -x_2 - jx_3 - x_{10} + jx_{11} \end{bmatrix} \\
\mathbf{C} &= \begin{bmatrix} x_2 + jx_3 - x_{10} + jx_{11} & x_4 + jx_5 - x_{13} - jx_{16} \\ -x_4 + jx_5 - x_{13} + jx_{16} & x_2 - jx_3 + x_{10} + jx_{11} \end{bmatrix} \\
\mathbf{D} &= \begin{bmatrix} x_1 - jx_6 + jx_9 - jx_{12} + jx_{17} & x_7 - jx_8 - x_{14} + jx_{15} \\ -x_7 - jx_8 + x_{14} + jx_{15} & x_1 - jx_6 + jx_9 + jx_{12} - jx_{17} \end{bmatrix}
\end{aligned}$$

Pour deux antennes d'émission, nous avons $g = 2, n_1 = 1, n_2 = 4$ et $g_1 = 1, g_2 = 3$ avec $n_{2,j} = 1,\ j = 1, 2, 3$, ce qui donne lieu à une complexité de décodage de l'ordre de $\sqrt{M}$. Pour le cas de quatre antennes d'émission, nous avons $g = 2, n_1 = 1, n_2 = 16$ et $g_1 = 1, g_2 = 5$, avec $n_{2,j} = 1,\ j = 1, 2, 3, 4, 5$, et l'ordre de la complexité de décodage est alors égal à $M^{5,5}$.

Chapitre 4

Approche numérique pour la construction des codes *g-group decodable*

L'approche adoptée pour la construction des codes *g-symbol decodable* (resp. *g-group decodable*) notamment les codes *Clifford Unitary-Weight* (CUW)-*g-symbol decodable* [19](resp. *g-group decodable* [16]) est basée sur des conditions suffisantes mais pas nécessaires, pouvant limiter le taux atteignable pour n'importe quel nombre de groupes orthogonaux. Dans [48], les auteurs ont déterminé le taux maximal pour les codes *Clifford Unitary Weight (CUW)-λ-symbol decodable* mais seulement pour le cas où le nombre de symboles λ dans chaque groupe est de la forme $2^a,\ a \in \mathbb{N}$. Dans [49], les auteurs ont prouvé que le taux d'un STBC $2^a \times 2^a$ *UW-single-symbol decodable* est majoré par $\frac{a}{2^{a-1}}$. La question sur le taux atteignable maximal pour un nombre arbitraire de groupes orthogonaux reste alors ouverte.

Ce chapitre traite le cas particulier des codes *UW-g-group decodable* pour 2^a antennes d'émission où les matrices de dispersion sont limitées aux matrices unitaires *single thread* dont les entrées non-nulles appartiennent à l'ensemble $\{\pm 1, \pm j\}$. L'objectif de ce chapitre est de trouver le taux atteignable maximal pour n'importe quel nombre de groupes orthogonaux dans ce cas précis. Ce type spécial de matrices de dispersion garantit une diversité-par-symbole pleine *symbol-wise diversity* [50] et inclut la grande majorité des codes existants dans la littérature (une liste non exhaustive comprend [16, 19, 39, 51, 40]). Dans ce contexte, nous proposons une extension de l'approche proposée dans [15] pour construire des codes *UW-2-group decodable* basée sur des conditions nécessaires et suffisantes pour le cas des

codes *UW-g-group decodable* de manière récursive.

Contrairement à l'approche adoptée dans [52] où les matrices de dispersions $\mathbf{A}_k$ et $\mathbf{B}_l$ sont directement cherchées , nous traitons les matrices $\boldsymbol{\lambda}_{kl}$ où $\boldsymbol{\lambda}_{kl} = \mathbf{A}_k^H \mathbf{B}_l$. Ainsi, le nombre de matrices $\boldsymbol{\lambda}_{kl}$ candidates pouvant être utilisées pour la construction de codes *UW-g-group decodable* est réduit étant donnée que telles matrices doivent satisfaire des contraintes supplémentaires. La représentation dans l'espace vectoriel est ensuite utilisée pour construire les matrices $\boldsymbol{\lambda}_{kl}$ dont nous montrons que le nombre est limité (voir l'annexe A). Une routine de recherche peut être appliquée pour trouver les codes *UW-g-group decodable* existants à des taux donnés, ce qui nous permet de déterminer le taux atteignable maximal pour un nombre arbitraire de groupes orthogonaux. Les codes *UW-g-group decodable* pour un nombre d'antennes d'émission autre qu'une puissance de deux pouvant être facilement obtenus par l'élimination du nombre approprié de colonnes de la matrice de code correspondant au nombre supérieur d'antennes d'émission s'écrivant comme une puissance de deux.

4.1 Résultats

Dans cette partie, nous illustrons des exemples d'application de la méthode proposée pour trouver le taux atteignable maximal des codes 4×4 *UW-g-group decodable* où les matrices de dispersion sont limitées aux matrices *single thread* dont les entrées non-nulles appartiennent à l'ensemble $\{\pm1, \pm j\}$. Les matrices de dispersion ont été déterminées par recherche exhaustive.

Pour le code *UW-2-group decodable* symétrique, nous avons constaté que le taux atteignable maximal est limité à $5/4$ symboles complexes par utilisation de canal (voir Tableau 4.1). Cependant, si la restriction de symétrie est relâchée, on peut aisément obtenir des codes *UW-2-group decodable* ayant des taux de $\frac{n^2+1}{2n}$ pour n antennes d'émission [47] donnant lieu à un code *UW-2-group decodable* de taux $17/8$ pour les quatre antennes d'émission.

Pour le code *UW-3-group decodable*, nous avons remarqué que le taux atteignable maximal est limité à 1 symbole complexe par utilisation de canal (voir Tableau 4.2). Pour les codes *4-group decodable*, il est connu que le taux atteignable maximal est

de 1 symbole complexe par utilisation de canal [49]. Des exemples de ces codes peuvent être retrouvés dans [16, 19, 40, 53].

Tableau 4.1 – Matrices de dispersion du code UW-2-*group decodable* de taux 5/4

$\mathbf{A}_1 = \begin{bmatrix} 0 & 0 & 0 & 1 \\ 0 & 1 & 0 & 0 \\ 1 & 0 & 0 & 0 \\ 0 & 0 & 1 & 0 \end{bmatrix}$	$\mathbf{B}_1 = \begin{bmatrix} 0 & 0 & 0 & -j \\ 0 & j & 0 & 0 \\ j & 0 & 0 & 0 \\ 0 & 0 & -j & 0 \end{bmatrix}$
$\mathbf{A}_2 = \begin{bmatrix} 0 & 0 & 0 & 1 \\ 0 & 1 & 0 & 0 \\ -1 & 0 & 0 & 0 \\ 0 & 0 & -1 & 0 \end{bmatrix}$	$\mathbf{B}_2 = \begin{bmatrix} 0 & 0 & 0 & -j \\ 0 & j & 0 & 0 \\ -j & 0 & 0 & 0 \\ 0 & 0 & j & 0 \end{bmatrix}$
$\mathbf{A}_3 = \begin{bmatrix} 0 & 0 & 0 & 1 \\ 0 & 1 & 0 & 0 \\ -1 & 0 & 0 & 0 \\ 0 & 0 & 1 & 0 \end{bmatrix}$	$\mathbf{B}_3 = \begin{bmatrix} 0 & 0 & 0 & -j \\ 0 & -j & 0 & 0 \\ j & 0 & 0 & 0 \\ 0 & 0 & -j & 0 \end{bmatrix}$
$\mathbf{A}_4 = \begin{bmatrix} 0 & 0 & 0 & 1 \\ 0 & 1 & 0 & 0 \\ 0 & 0 & -j & 0 \\ -j & 0 & 0 & 0 \end{bmatrix}$	$\mathbf{B}_4 = \begin{bmatrix} 0 & -1 & 0 & 0 \\ 0 & 0 & 0 & 1 \\ j & 0 & 0 & 0 \\ 0 & 0 & -j & 0 \end{bmatrix}$
$\mathbf{A}_5 = \begin{bmatrix} 0 & 0 & 0 & 1 \\ 0 & 1 & 0 & 0 \\ 0 & 0 & 1 & 0 \\ -1 & 0 & 0 & 0 \end{bmatrix}$	$\mathbf{B}_5 = \begin{bmatrix} 0 & -j & 0 & 0 \\ 0 & 0 & 0 & -j \\ j & 0 & 0 & 0 \\ 0 & 0 & -j & 0 \end{bmatrix}$

Tableau 4.2 – Matrices de dispersion du code UW-3-*group decodable* de taux 1

$\mathbf{A}_1 = \begin{bmatrix} -j & 0 & 0 & 0 \\ 0 & j & 0 & 0 \\ 0 & 0 & -1 & 0 \\ 0 & 0 & 0 & 1 \end{bmatrix}$	$\mathbf{C}_1 = \begin{bmatrix} 1 & 0 & 0 & 0 \\ 0 & 1 & 0 & 0 \\ 0 & 0 & 0 & 1 \\ 0 & 0 & 1 & 0 \end{bmatrix}$
$\mathbf{A}_2 = \begin{bmatrix} -j & 0 & 0 & 0 \\ 0 & j & 0 & 0 \\ 0 & 0 & 1 & 0 \\ 0 & 0 & 0 & -1 \end{bmatrix}$	$\mathbf{C}_2 = \begin{bmatrix} 0 & j & 0 & 0 \\ j & 0 & 0 & 0 \\ 0 & 0 & 0 & 1 \\ 0 & 0 & 1 & 0 \end{bmatrix}$
$\mathbf{B}_1 = \begin{bmatrix} 0 & -1 & 0 & 0 \\ 1 & 0 & 0 & 0 \\ 0 & 0 & 0 & j \\ 0 & 0 & -j & 0 \end{bmatrix}$	$\mathbf{C}_3 = \begin{bmatrix} 0 & -j & 0 & 0 \\ -j & 0 & 0 & 0 \\ 0 & 0 & 0 & 1 \\ 0 & 0 & 1 & 0 \end{bmatrix}$
$\mathbf{B}_2 = \begin{bmatrix} 0 & -1 & 0 & 0 \\ 1 & 0 & 0 & 0 \\ 0 & 0 & 0 & -j \\ 0 & 0 & j & 0 \end{bmatrix}$	$\mathbf{C}_4 = \begin{bmatrix} 1 & 0 & 0 & 0 \\ 0 & 1 & 0 & 0 \\ 0 & 0 & -j & 0 \\ 0 & 0 & 0 & -j \end{bmatrix}$

Pour le code 2-*group decodable* de taux 5/4, $g = 2, n_1 = n_2 = 5$. Il s'en suit que la complexité de décodage (pire cas) pour les constellations QAM carrées est de l'ordre de $\sum_{i=1}^{2} \sqrt{M}^{n_i-1} = 2M^2$. Pour le cas de constellations QAM non-rectangulaires, le code de taux $5/4$ n'est plus 2-*group decodable* en raison de l'enchevêtrement des parties réelles et imaginaires des symboles complexes émis. Dans ce cas, nous pouvons utiliser la détection conditionnelle [41] pour évaluer l'estimation ML de $(x_1, \ldots, x_4)$ et $(x_5, \ldots, x_8)$ séparément (grâce à la structure quasi-orthogonale) pour une valeur donnée de (x_9, x_{10}). Par conséquent, la complexité de décodage est de l'ordre de $2M^3$.

Pour le code 3-*group decodable* de taux 1, on a $g = 3, n_1 = n_2 = 2, n_3 = 4$. La complexité de décodage des constellations QAM carrées est alors de l'ordre de $\sum_{i=1}^{3} \sqrt{M}^{n_i-1} = 2\sqrt{M}+M^{1.5}$. Pour le cas des constellations QAM non-rectangulaires, le code 3-*group decodable* de taux 1 maintient sa structure, mais avec une augmentation de l'ordre de complexité de décodage à $\sum_{i=1}^{3} M^{n_i/2} = 2M + M^2$.

Ces résultats sont résumés au le tableau 4.3. Il est à noter que le gain de codage

Tableau 4.3 – Sommaire des résultats

Nombre de groupes	Taux maximal	Ordre de complexité	
		QAM carrées	QAM non-rectangulaires
2	5/4	$2M^2$	$2M^3$
3	1	$2\sqrt{M} + M^{1.5}$	$2M + M^2$
4	1	$4\sqrt{M}$	$4M$

des codes proposés est égal à zéro, mais la diversité pleine peut encore être assurée en appliquant une rotation de constellation pour chaque groupe de symboles. Ceci n'affecte pas la structure 3-*group decodable*, et par conséquent la complexité de décodage reste inchangée.

Chapitre 5

Multiplexage des codes orthogonaux

Rappelant la définition de STBC *fast decodable* au chapitre 3, un STBC encodant $2K$ symboles réels est dit *fast decodable* si et seulement s'il est conditionnellement g-*group decodable*. Dans le cas particulier où le code de faible complexité est un code orthogonal encodant κ symboles réels, l'ordre de la complexité de décodage pour les constellations QAM carrés avec M points est réduit de $\sqrt{M}^{2K-1}$ à $\sqrt{M}^{2k-\kappa}$ grâce à la technique de détection conditionnelle.

Ce chapitre est consacré à l'étude du multiplexage de deux codes orthogonaux à l'aide d'une matrice unitaire dans le cas de quatre antennes. La matrice unitaire est choisie de telle sorte que le code résultant conserve la propriété de mise en forme cubique [20] des STBC orthogonaux qui le constituent. Toutefois, la propriété de mise en forme cubique est atteinte au détriment d'une limitation de taux de la structure proposée. Nous déterminons une limite supérieure du taux réalisable de $5/4$ symboles complexes par utilisation de canal et nous proposons plusieurs codes permettant d'atteindre cette limite. Nous reprenons une des réalisations du code minimisant le PAPR et nous prouvons analytiquement (voir l'annexe B) que le code proposé conserve le gain de codage de ses codes orthogonaux constituants et que le gain de codage reste constant quelle que soit la constellation QAM non-normalisée utilisée. En d'autres termes, le code proposé est NVD [20].

5.1 Structure FD

Les tentatives précédentes de construire des STBC FD consistaient à multiplexer deux codes ou plus de faible complexité de décodage par le biais d'une matrice

(généralement unitaire) dont les entrées sont déterminées par optimisation numérique du gain de codage [14, 46, 54, 55, 56, 57]. Dans ce contexte, le problème de la construction d'un code FD pour quatre antennes d'émission par le multiplexage de deux STBC orthogonaux a été étudié dans [58, 59] où le code FD est exprimé comme suit :

$$\mathbf{X}_{3/2} = \mathbf{X}_{3/4}(x_1, \ldots, x_6) + \mathbf{U}\mathbf{X}_{3/4}(x_7, \ldots, x_{12}). \tag{5.1}$$

$\mathbf{X}_{3/4}$ désigne la matrice de code orthogonale pour quatre antennes de taux $3/4$ [60] et $\mathbf{U}$ est choisie de sorte à maximiser le gain de codage. Dans [58], la matrice $\mathbf{U}$ a été limitée à des matrices diagonales unitaires, pour fournir un PAPR faible puisque cette structure empêche la combinaison de plus de deux symboles. En fait, $\mathbf{U}$ est exprimée de la manière suivante :

$$\mathbf{U} = \begin{bmatrix} e^{j\theta_1} & 0 & 0 & 0 \\ 0 & e^{j\theta_2} & 0 & 0 \\ 0 & 0 & e^{j\theta_3} & 0 \\ 0 & 0 & 0 & e^{j\theta_4} \end{bmatrix}$$

où les phases $\theta_1, \theta_2, \theta_3, \theta_4$ sont optimisées numériquement pour obtenir un gain de codage élevé pour la modulation QPSK. Ces valeurs numériques des phases sont égales à $3\pi/10, 3\pi/10, 3\pi/10, -2\pi/3$ respectivement [58]. Par contre, dans [59], la matrice de $\mathbf{U}$ n'est plus unitaire :

$$\mathbf{U} = \frac{1}{\sqrt{5}} \begin{bmatrix} 1 & 1+j & 1+j & 1+j \\ -1+j & 1 & 1-j & 1+j \\ -1-j & 1+j & 1 & 1+j \\ 1-j & -1-j & -1+j & 1 \end{bmatrix} \tag{5.2}$$

La structure FD proposée s'écrit selon l'équation suivante :

$$\mathbf{X}_{\text{new}} = \mathbf{X}_{3/4}(x_1, \ldots, x_6) + e^{j\phi}\mathbf{X}_{3/4}(x_7, \ldots, x_{12})\mathbf{U}. \tag{5.3}$$

$\mathbf{U}$ est une matrice unitaire choisie pour garantir la propriété de mise en forme cubique (voir partie 2.3.5) par ailleurs, ϕ est choisie pour maximiser le gain de codage. Toutefois, comme l'indique la proposition suivante, la satisfaction de la propriété de mise en forme cubique de la structure du code proposé (5.3) pour ϕ arbitraire impose une limitation sur le taux. D'autre part, nous démontrons que le code proposé répondant à la mise en forme cubique est NVD [20], ainsi évitant l'inconvénient majeur des constructions antérieures [58, 59] qui reposent sur

l'optimisation numérique, irréalisable pour les constellations de grande taille (par exemple 64-QAM et au-delà).

Proposition 5.1 *Pour le code FD proposé, la propriété de mise en forme cubique est atteignable pour ϕ quelconque si son taux est inférieur ou égal à 5/4.*

A partir de la **Proposition 5.1**, nous proposons un nouveau code FD de taux 5/4 satisfaisant la mise en forme cubique et qui est NVD grâce au choix judicieux de ϕ. Le code proposé, notée $\mathbf{X}_{5/4}$ s'exprime par :

$$\mathbf{X}_{5/4}(\mathbf{s}) = \mathbf{X}_{3/4}(x_1, \ldots, x_6) + e^{j\phi} \left(\mathbf{R}_2 x_7 + \mathbf{R}_3 x_8 + \mathbf{R}_1 x_9 + \mathbf{R}_5 x_{10}\right) \mathbf{R}_4 \tag{5.4}$$

où $\mathbf{s} = [\mathbf{s}_1, \mathbf{s}_2]$, $\mathbf{s}_1 = [x_1, \ldots, x_6]$, $\mathbf{s}_2 = [x_7, \ldots, x_{10}]$, $\mathbf{R}_i,\ i \in \{1, 5\}$ et la matrice d'identité de taille 4×4 sont les matrices de dispersion de $\mathbf{X}_{3/4}$ et ϕ est choisie pour maximiser le gain de codage. La matrice du code proposé prend la forme ci-dessous [22] :

$$\mathbf{X}_{5/4} = \begin{bmatrix} x_1 + jx_2 - jx_{10}e^{j\phi} & x_3 + jx_4 & x_5 + jx_6 + jx_9 e^{j\phi} & -e^{j\phi}(x_7 + jx_8) \\ -x_3 + jx_4 & x_1 - jx_2 - jx_{10}e^{j\phi} & e^{j\phi}(-x_7 + jx_8) & -x_5 - jx_6 + jx_9 e^{j\phi} \\ -x_5 + jx_6 + jx_9 e^{j\phi} & e^{j\phi}(x_7 + jx_8) & x_1 - jx_2 + jx_{10}e^{j\phi} & x_3 + jx_4 \\ -e^{j\phi}(-x_7 + jx_8) & x_5 - jx_6 + jx_9 e^{j\phi} & -x_3 + jx_4 & x_1 + jx_2 + jx_{10}e^{j\phi} \end{bmatrix} \tag{5.5}$$

Par une recherche exhaustive, nous avons découvert qu'en choisissant $\phi = \frac{1}{2}\cos^{-1}(1/5)$ le gain de codage est maximal et celui-ci reste constant jusqu'à la constellations 64-QAM non-normalisée. Toutefois, un résultat plus fort est indiqué dans la proposition suivante :

Proposition 5.2 *Le choix de $\phi = \frac{1}{2}\cos^{-1}(1/5)$ garantie que le code proposé est NVD avec le gain de codage maximal.*

Démonstration. voir l'annexe B. □

5.2 Simulation et résultats numériques

Le codes sont comparés en termes de complexité de décodage pour les constellations QAM carrées, de déterminant minimum (Min det) [1] et de PAPR. Le déterminant minimal est défini comme suit :

$$\text{Min det} = \min_{\Delta\mathbf{s} \in \Delta\mathcal{C} \setminus \{\mathbf{0}\}} |\det\left((\mathbf{X}(\Delta\mathbf{s}))\right)| = \sqrt{\delta} \tag{5.6}$$

[1] Pour raison de cohérence, le déterminant minimal est évalué à puissance moyenne émise identique par utilisation de canaux pour tous les codes

où $\Delta \mathbf{s} = \mathbf{s} - \mathbf{s}'$, $\Delta\mathcal{C}$ est l'espace vectoriel engendré par $\Delta \mathbf{s}$, et δ est le gain de codage. D'autre part, le PAPR est défini comme suit :

$$\text{PAPR}_n = \frac{\max\limits_t |\mathbf{X}(t,n)|^2}{T^{-1}\sum\limits_t \mathbb{E}\{|\mathbf{X}(t,n)|^2\}} \tag{5.7}$$

avec $t \in \{1, \dots T\}$ et $n \in \{1, \dots N_t\}$. En raison de la symétrie entre les antennes d'émission, l'indice n sera omis. Dans un premier temps, nous comparons une version de taux 1 poinçonnée du code de (5.4) en supprimant x_9 et x_{10} [21] à l'état de l'art. La comparaison est résumée au Tableau 5.1.

Tableau 5.1 – Comparaison en terme de complexité, de Min det et de PAPR

Code	Complexité de décodage (QAM carrée)	Min det QAM	PAPR (dB)		
			QPSK	16QAM	64QAM
Code poinçonné de taux 1	M	16	0	2.5	3.7
Code de N.Sharma-C.B.Papadias[37]	$2M$	16	0	2.5	3.7
Code de M.Sinnokrot-J.Barry[61]	$4\sqrt{M}$	7.11	0	2.5	3.7
Code de S.Karmakar-S.Rajan[16, 40]	$4\sqrt{M}$	12.8	1.6	4.2	5.3
Code de Md.Khan-S.Rajan[62]	$4\sqrt{M}$	12.8	5.8	8.3	9.5

On peut remarquer plusieurs phénomènes, Le code proposé atteint le gain de codage le plus élevé par rapport aux STBC de faible complexité de décodage taux 1 et de diversité pleine 4×4 existants. On peut alors s'attendre à ce que ce code offre de meilleures performances dans la région de SNR élevé. Le code proposé et les codes de [37, 61] ont le PAPR le plus faible, qui est celui de la constellation utilisée. D'autre part, notre code souffre d'une légère augmentation dans la complexité de décodage par rapport aux codes de [61, 16, 40, 62], mais cela ne pénalisera le code proposé que pour les constellations QAM d'ordre élevé (plus précisément pour $M \geq 64$).

Dans un deuxième temps, nous comparons notre code de taux 5/4 à la version poinçonnée de taux 5/4 du code [46] et la version poinçonnée de taux 5/4 du code [59]. La comparaison est résumée au le Tableau 5.2. La version poinçonnée des codes dans [59] et [46] est obtenue en éliminant le nombre approprié de symboles tels que la complexité de décodage reste minimale. Pour le code de taux 3/2 (S. Sirianunpiboon *et al.* [59]), la version poinçonnée de taux 5/4 est obtenue

Tableau 5.2 – Comparaison en terme de complexité, de Min det et de PAPR

Code	Complexité de décodage (QAM carrée)	Min det QAM	PAPR (dB)		
			QPSK	16QAM	64QAM
Code proposé de taux 5/4	M^2	16	3.6	6.2	7.3
Code de S.Sirianunpiboon de taux 5/4[59]	M^2	N/A	4.8	7.3	8.5
Code de P.Srinath-S.Rajan de taux 5/4 [46]	$4M^{1.5}$	12.8	4.8	7.3	8.5

en supprimant x_6, alors que pour le code de taux 2 (P. Srinath-S.Rajan [46]) la version poinçonnée de taux 5/4 est obtenue en éliminant $s_{6I}, s_{6Q}, \ldots, s_{8I}, s_{8Q}$. Nous constatons que le code proposé a un gain de codage plus élevé, un PAPR plus faible au détriment d'une légère augmentation de la complexité de détection, pénalisant notre code pour les constellation 64-QAM ou au-delà.

Chapitre 6

Nouvelle famille de codes à faible complexité de décodage pour quatre antennes

Ce chapitre propose d'abord un schéma de construction de nouveaux codes FGD de taux 1 pour 2^a antennes d'émission. Les codes de taux 1 pour un nombre d'antennes autre qu'une puissance de deux est aisément obtenu en supprimant le nombre approprié de colonnes de la matrice du code correspondante au nombre supérieur d'antennes puissance de deux. Par exemple, le code de taux 1 pour le cas de trois antennes d'émission est obtenu en supprimant une colonne de la matrice de code de taux 1 pour quatre antennes d'émission. Nous nous focalisons sur le cas de quatre antennes d'émission et nous prouvons que la complexité de décodage du code proposé est inférieure à celles des codes de faible complexité existants. Le gain de codage du code est ensuite optimisé tout en gardant le PAPR à son minimum (celui de la constellation utilisée). Nous démontrons que le gain de codage est constant indépendamment de la constellation QAM utilisée non-normalisée. Donc le code est NVD.

En deuxième étape, nous proposons deux codes de taux élevés grâce au multiplexage et l'optimisation numérique donnant lieu à deux nouveaux codes FD de taux 3/2 et 2 symboles complexes par utilisation du canal. Les codes proposés sont comparés aux codes existants. La complexité de décodage des codes proposés est inférieure à celles des codes similaires existants. En outre, la complexité moyenne de décodage de nos codes de taux 1 et le taux 3/2 est inférieure alors que notre code de taux 2 maintient l'infériorité de sa complexité moyenne pour les faibles

valeurs du SNR.

6.1 Approche systématique de construction des codes FGD

Proposition 6.1 *Pour 2^a antennes d'émission, les deux ensembles de matrices :$\mathcal{G}_1 = \{\mathbf{I}, \mathbf{R}_1, \ldots, \mathbf{R}_a\} \cup \mathcal{A}$ et $\mathcal{G}_2 = \{\mathbf{R}_{a+1}, \ldots, \mathbf{R}_{2a+1}\} \cup \mathcal{B}$ satisfont* (3.5) *où $\mathcal{A}$ et $\mathcal{B}$ sont donnés respectivement par les Tableaux 6.1 et 6.2, [24].*

Tableau 6.1 – Différents cas de $\mathcal{A}$

a	$\mathcal{A}$
$4n$	$\left\{j \prod_{i=a+1}^{2a+1} \mathbf{R}_i\right\} \bigcup_{m=1}^{a-2} \left\{j^{\delta_{\mathcal{A}}(m)} \prod_{i=a+1}^{2a+1} \mathbf{R}_i \prod_{i=1}^{m} \mathbf{R}_{k_i} : 1 \leq k_1 < \ldots < k_m \leq a\right\}$
$4n+1$	$\left\{\prod_{i=a+1}^{2a+1} \mathbf{R}_i\right\} \bigcup_{m=1}^{a-2} \left\{j^{\delta_{\mathcal{A}}(m)} \prod_{i=a+1}^{2a+1} \mathbf{R}_i \prod_{i=1}^{m} \mathbf{R}_{k_i} : 1 \leq k_1 < \ldots < k_m \leq a\right\}$
$4n+2$	$\left\{\prod_{i=a+1}^{2a+1} \mathbf{R}_i\right\} \bigcup_{m=1}^{a-2} \left\{j^{\delta_{\mathcal{A}}(m)} \prod_{i=a+1}^{2a+1} \mathbf{R}_i \prod_{i=1}^{m} \mathbf{R}_{k_i} : 1 \leq k_1 < \ldots < k_m \leq a\right\}$
$4n+3$	$\left\{j \prod_{i=a+1}^{2a+1} \mathbf{R}_i\right\} \bigcup_{m=1}^{a-2} \left\{j^{\delta_{\mathcal{A}}(m)} \prod_{i=a+1}^{2a+1} \mathbf{R}_i \prod_{i=1}^{m} \mathbf{R}_{k_i} : 1 \leq k_1 < \ldots < k_m \leq a\right\}$

Tableau 6.2 – Différents cas de $\mathcal{B}$

a	$\mathcal{B}$
$4n$	$\{j \prod_{i=1}^{a} \mathbf{R}_i\} \bigcup_{m=2,4}^{a-2} \left\{j^{\delta_{\mathcal{B}}(m)} \prod_{i=1}^{a} \mathbf{R}_i \prod_{i=1}^{m} \mathbf{R}_{k_i} : a+1 \leq k_1 < \ldots < k_m \leq 2a+1\right\}$
$4n+1$	$\bigcup_{m=1,3}^{a-2} \left\{j^{\delta_{\mathcal{B}}(m)} \prod_{i=1}^{a} \mathbf{R}_i \prod_{i=1}^{m} \mathbf{R}_{k_i} : a+1 \leq k_1 < \ldots < k_m \leq 2a+1\right\}$
$4n+2$	$\{\prod_{i=1}^{a} \mathbf{R}_i\} \bigcup_{m=2,4}^{a-2} \left\{j^{\delta_{\mathcal{B}}(m)} \prod_{i=1}^{a} \mathbf{R}_i \prod_{i=1}^{m} \mathbf{R}_{k_i} : a+1 \leq k_1 < \ldots < k_m \leq 2a+1\right\}$
$4n+3$	$\bigcup_{m=1,3}^{a-2} \left\{j^{\delta_{\mathcal{B}}(m)} \prod_{i=1}^{a} \mathbf{R}_i \prod_{i=1}^{m} \mathbf{R}_{k_i} : a+1 \leq k_1 < \ldots < k_m \leq 2a+1\right\}$

$\delta_{\mathcal{A}}(m), \delta_{\mathcal{B}}(m)$ sont donnés par le Tableau 6.3 :

Tableau 6.3 – Différents cas de δ

a	$\delta_{\mathcal{A}}(m)$	$\delta_{\mathcal{B}}(m)$
$4n$	$\frac{\left((m)_4-1\right)\left((m)_4-2\right)}{2}$	$\frac{2-(m)_4}{2}$
$4n+1$	$\frac{\left(\left((m)_4\right)\left((m)_4-1\right)\right)_4}{2}$	$\frac{(m)_4-1}{2}$
$4n+2$	$\frac{\left(\left((m)_4\right)\left((m)_4-3\right)\right)_4}{2}$	$\frac{(m)_4}{2}$
$4n+3$	$\frac{\left((m)_4-2\right)\left((m)_4-3\right)}{2}$	$\frac{3-(m)_4}{2}$

et $\mathbf{R}_i,\ i \in \{1,\ldots,2a+1\}$ avec la matrice d'identité de taille $2^a \times 2^a$ sont les matrices de dispersion correspondantes au STBC orthogonal dans le cas de 2^a antennes d'émission.

Des exemples de codes FGD de taux 1 pour 4,8 and 16 antennes d'émissions sont donnés dans au Tableau 6.4. Nous nous intéressons particulièrement dans

Tableau 6.4 – Exemples de codes FGD de taux 1

Tx	$\mathcal{G}_1$	$\mathcal{G}_2$
4	$\mathbf{I}, \mathbf{R}_2, \mathbf{R}_4, \mathbf{R}_1\mathbf{R}_3\mathbf{R}_5$	$\mathbf{R}_1, \mathbf{R}_3, \mathbf{R}_5, \mathbf{R}_2\mathbf{R}_4$
8	$\mathbf{I}, \mathbf{R}_2, \mathbf{R}_4, \mathbf{R}_6$	$\mathbf{R}_1, \mathbf{R}_3, \mathbf{R}_5, \mathbf{R}_7$
	$j\mathbf{R}_1\mathbf{R}_3\mathbf{R}_5\mathbf{R}_7$	$j\mathbf{R}_2\mathbf{R}_4\mathbf{R}_6\mathbf{R}_1$
	$j\mathbf{R}_1\mathbf{R}_3\mathbf{R}_5\mathbf{R}_7\mathbf{R}_2$	$j\mathbf{R}_2\mathbf{R}_4\mathbf{R}_6\mathbf{R}_3$
	$j\mathbf{R}_1\mathbf{R}_3\mathbf{R}_5\mathbf{R}_7\mathbf{R}_4$	$j\mathbf{R}_2\mathbf{R}_4\mathbf{R}_6\mathbf{R}_5$
	$j\mathbf{R}_1\mathbf{R}_3\mathbf{R}_5\mathbf{R}_7\mathbf{R}_6$	$j\mathbf{R}_2\mathbf{R}_4\mathbf{R}_6\mathbf{R}_7$
16	$\mathbf{I}, \mathbf{R}_2, \mathbf{R}_4, \mathbf{R}_6, \mathbf{R}_8$	$\mathbf{R}_1, \mathbf{R}_3, \mathbf{R}_5, \mathbf{R}_7, \mathbf{R}_9$
	$j\mathbf{R}_1\mathbf{R}_3\mathbf{R}_5\mathbf{R}_7\mathbf{R}_9$	$j\mathbf{R}_2\mathbf{R}_4\mathbf{R}_6\mathbf{R}_8$
	$\mathbf{R}_1\mathbf{R}_3\mathbf{R}_5\mathbf{R}_7\mathbf{R}_9\mathbf{R}_2$	$\mathbf{R}_2\mathbf{R}_4\mathbf{R}_6\mathbf{R}_8\mathbf{R}_1\mathbf{R}_3$
	$\mathbf{R}_1\mathbf{R}_3\mathbf{R}_5\mathbf{R}_7\mathbf{R}_9\mathbf{R}_4$	$\mathbf{R}_2\mathbf{R}_4\mathbf{R}_6\mathbf{R}_8\mathbf{R}_1\mathbf{R}_5$
	$\mathbf{R}_1\mathbf{R}_3\mathbf{R}_5\mathbf{R}_7\mathbf{R}_9\mathbf{R}_6$	$\mathbf{R}_2\mathbf{R}_4\mathbf{R}_6\mathbf{R}_8\mathbf{R}_1\mathbf{R}_7$
	$\mathbf{R}_1\mathbf{R}_3\mathbf{R}_5\mathbf{R}_7\mathbf{R}_9\mathbf{R}_8$	$\mathbf{R}_2\mathbf{R}_4\mathbf{R}_6\mathbf{R}_8\mathbf{R}_1\mathbf{R}_9$
	$\mathbf{R}_1\mathbf{R}_3\mathbf{R}_5\mathbf{R}_7\mathbf{R}_9\mathbf{R}_2\mathbf{R}_4$	$\mathbf{R}_2\mathbf{R}_4\mathbf{R}_6\mathbf{R}_8\mathbf{R}_3\mathbf{R}_5$
	$\mathbf{R}_1\mathbf{R}_3\mathbf{R}_5\mathbf{R}_7\mathbf{R}_9\mathbf{R}_2\mathbf{R}_6,$	$\mathbf{R}_2\mathbf{R}_4\mathbf{R}_6\mathbf{R}_8\mathbf{R}_3\mathbf{R}_7$
	$\mathbf{R}_1\mathbf{R}_3\mathbf{R}_5\mathbf{R}_7\mathbf{R}_9\mathbf{R}_2\mathbf{R}_8$	$\mathbf{R}_2\mathbf{R}_4\mathbf{R}_6\mathbf{R}_8\mathbf{R}_3\mathbf{R}_9$
	$\mathbf{R}_1\mathbf{R}_3\mathbf{R}_5\mathbf{R}_7\mathbf{R}_9\mathbf{R}_4\mathbf{R}_6,$	$\mathbf{R}_2\mathbf{R}_4\mathbf{R}_6\mathbf{R}_8\mathbf{R}_5\mathbf{R}_7$
	$\mathbf{R}_1\mathbf{R}_3\mathbf{R}_5\mathbf{R}_7\mathbf{R}_9\mathbf{R}_4\mathbf{R}_8$	$\mathbf{R}_2\mathbf{R}_4\mathbf{R}_6\mathbf{R}_8\mathbf{R}_5\mathbf{R}_9$
	$\mathbf{R}_1\mathbf{R}_3\mathbf{R}_5\mathbf{R}_7\mathbf{R}_9\mathbf{R}_6\mathbf{R}_8$	$\mathbf{R}_2\mathbf{R}_4\mathbf{R}_6\mathbf{R}_8\mathbf{R}_7\mathbf{R}_9$

cette partie au cas spécial de quatre antennes d'émission. Le code FGD de taux 1 proposé est le résultat de l'application directe de la **Proposition 6.1** pour le cas de quatre antennes d'émission. Posons $a = 2$, nous avons $\mathcal{G}_1 = \{\mathbf{I}, \mathbf{R}_2, \mathbf{R}_4, \mathbf{R}_1\mathbf{R}_3\mathbf{R}_5\}$ et $\mathcal{G}_2 = \{\mathbf{R}_1, \mathbf{R}_3, \mathbf{R}_5, \mathbf{R}_2\mathbf{R}_4\}$. Remarquons que le choix des matrices de dispersion ci-dessus garantit une puissance moyenne émise fixe quel que soit l'antenne d'émission ou l'instant de signalisation. Le code proposé de taux 1, dénoté par $\mathbf{X}_1$, est exprimé de la manière suivante :

$$\mathbf{X}_1(\mathbf{s}) = \mathbf{I}x_1 + \mathbf{R}_2x_2 + \mathbf{R}_4x_3 + \mathbf{R}_1\mathbf{R}_3\mathbf{R}_5x_4 + \mathbf{R}_1x_5 + \mathbf{R}_3x_6 + \mathbf{R}_5x_7 + \mathbf{R}_2\mathbf{R}_4x_8. \quad (6.1)$$

Le code proposé $\mathbf{X}_1$ est FGD avec $g = 2, n_1 = n_2 = 4$ et $g_1 = g_2 = 3$ tel que $n_{i,j} = 1,\ i = 1,2,\ j = 1,2,3 \Rightarrow \kappa_1 = \kappa_2 = 3$. Par conséquent, la complexité de

décodage est égale à $\sum_{i=1}^{g} \sqrt{M}^{n_i-\kappa_i} = 2\sqrt{M}$. Toutefois, le gain de codage de $\mathbf{X}_1$ est égal à zéro. Afin d'atteindre la diversité pleine, nous avons fait appel à la technique d'étirement de constellation [63, 61] plutôt que la technique de rotation de constellation. En effet, si cette dernière est utilisée, les symboles orthogonaux à l'intérieur de chaque groupe seront enchevêtrés, ce qui détruira la structure FGD du code et provoquera une augmentation significative de la complexité de décodage.

La matrice de code de diversité pleine prend la forme indiquée en (6.2) où $\mathbf{s} = [x_1, \ldots, x_8]$ et k est choisi pour fournir un gain de codage élevé. Le terme $\sqrt{\frac{2}{1+k^2}}$ est ajouté pour normaliser la puissance moyenne émise par antenne et par instant de signalisation.

$$\mathbf{X}_1(\mathbf{s}) = \sqrt{\frac{2}{1+k^2}} \begin{bmatrix} x_1 + ikx_5 & x_2 + ikx_6 & x_3 + ikx_7 & -ikx_4 - x_8 \\ -x_2 + ikx_6 & x_1 - ikx_5 & -ikx_4 - x_8 & -x_3 - ikx_7 \\ -x_3 + ikx_7 & ikx_4 + x_8 & x_1 - ikx_5 & x_2 + ikx_6 \\ ikx_4 + x_8 & x_3 - ikx_7 & -x_2 + ikx_6 & x_1 + ikx_5 \end{bmatrix} \tag{6.2}$$

Proposition 6.2 *En prenant $k = \sqrt{\frac{3}{5}}$, le code proposé est NVD avec un gain de codage égal à 1 [24].*

Dans l'intérêt d'illustration, une comparaison entre la constellation 16-QAM régulière et la constellation 16-QAM étirée est représentée à la figure 6.1 où les points noirs sont les points de la constellation 16-QAM régulière alors que les points rouges sont les points la constellation 16-QAM étirée avec le coefficient d'étirement $k = \sqrt{\frac{3}{5}}$. Le code proposé de taux 2, dénoté par $\mathbf{X}_2$, est simplement obtenu par multiplexage de deux codes de taux 1 par le biais d'une matrice unitaire. Le code de taux 2 est mathématiquement exprimé par :

$$\mathbf{X}_2\left(x_1, \ldots, x_{16}\right) = \mathbf{X}_1\left(x_1, \ldots, x_8\right) + e^{j\phi}\mathbf{X}_1\left(x_9, \ldots, x_{16}\right)\mathbf{U} \tag{6.3}$$

où $\mathbf{U}$ et ϕ sont choisies tel que le gain de codage est maximisé. Il a été numériquement vérifié que choisir $\mathbf{U} = j\mathbf{R}_1$ et $\phi = \tan^{-1}\left(\frac{1}{2}\right)$ maximise le gain de codage pour la constellation QPSK et que ce gain est égal à 1.

6.2 Résultats numériques et simulation

Nous comparons dans cette partie nos codes proposés à faible complexité avec les codes comparables existants en termes de complexité de décodage, de PAPR, et

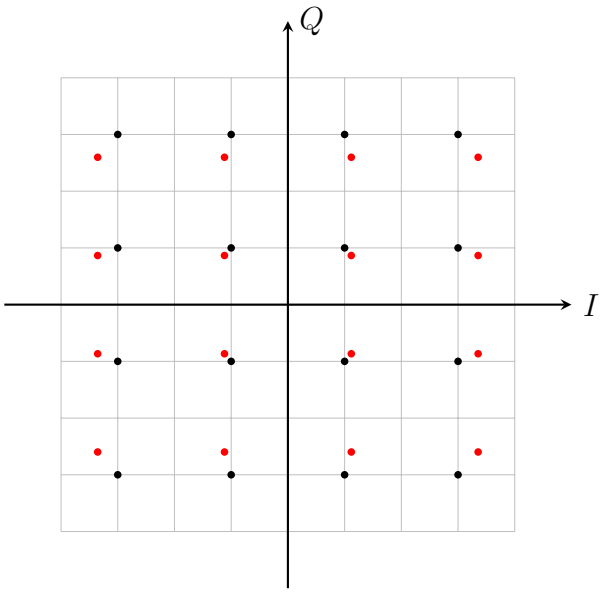

FIGURE 6.1 – Points de la constellation 16-QAM régulière vs. points de la constellation 16-QAM étirée

de la complexité moyenne de décodage. A partir du Tableau 6.5 nous constatons que la complexité de décodage du code de taux 1 proposé est la moitié de celle de [62] et [61]. La complexité de décodage du code proposé de taux 3/2 est la moitié de celle du code poinçonné de taux 3/2 [46] et est réduite d'un facteur $\sqrt{M}/2$ par rapport au code de taux 3/2 [59].

Tableau 6.5 – Comparaison en termes de complexité de décodage et de PAPR

Code	complexité de décodage de QAM carré	PAPR (dB)		
		QPSK	16QAM	64QAM
Le code de taux 1 proposé	$2\sqrt{M}$	0	2.5	3.7
Code de M.Sinnokrot-J.Barry [61]	$4\sqrt{M}$	0	2.5	3.7
Code de Md.Khan-S.Rajan[62]	$4\sqrt{M}$	5.8	8.3	9.5
Le code de taux 3/2 proposé	$2M^{2.5}$	3	5.6	6.7
Code de S.Sirianunpiboon *et al.*[59]	M^3	5.4	8	8.4
Code de P.Srinath-S.Rajan rate-3/2[46]	$4M^{2.5}$	4	6.5	7.7
Le code de taux 2 proposé	$2M^{4.5}$	2.8	5.3	6.5
Code de P.Srinath-S.Rajan[46]	$4M^{4.5}$	2.8	5.3	6.5

Chapitre 7

Conclusions et perspectives

Pendant cette thèse, nous avons abordé la construction de codes à faible complexité avec une focalisation particulière sur le cas de quatre antennes d'émission, en raison de son importance pratique dans les normes de communication actuelles et future. Nous résumons ci-après les contributions de la thèse et nous fournissons certains axes de recherche futur potentiels.

7.1 Contributions

Nous avons abordé la question de trouver le taux maximal réalisable des codes *g-group decodable* pour un type spécifique de matrices de dispersion incluant la majorité des codes existants. Dans ce contexte, nous avons fourni une méthode de construction par recherche exhaustive basée sur des conditions nécessaires et suffisantes pour les codes *g-group decodable*. Nous avons prouvé que pour le type considéré des matrices de dispersion, la méthode proposée est considérablement simplifiée. Nous nous sommes concentrés sur le cas de quatre antennes d'émission et nous avons déterminé le taux maximal des codes *2-group decodable* symétriques et les codes *3-group decodable* non-symétriques.

Nous avons ensuite proposé un nouveau code FD 4×4 par multiplexage de deux codes orthogonaux en utilisant une matrice unitaire. Nous avons démontré que, afin de préserver la propriété de mise en forme cubique, le taux du nouveau code ne peut pas dépasser $5/4$ symboles complexes par utilisation du canal. Le gain de codage a été optimisé et nous avons démontré que ce gain est indépendant de la constellation QAM non-normalisée employée. Les résultats de simulation

ont montré que d'une part la performance du code proposé surpasse les codes existants, et d'autre part notre code peut être décodé avec une complexité moyenne de décodage inférieure et il fournit le PAPR minimal.

Nous avons proposé une approche systématique pour la construction des codes FGD de taux 1 pour un nombre arbitraire d'antennes d'émission. Dans le cas de quatre antennes d'émission, la complexité de décodage du nouveau code FGD de taux 1 est inférieure à celles des codes existants. Le gain de codage du code a été optimisé grâce à l'étirement de la constellation plutôt que la rotation de la constellation pour préserver la structure FGD et minimiser le PAPR, qui est celui de la constellation utilisée.

Nous avons aussi fourni une preuve analytique que le code proposé est en effet NVD par le choix judicieux du coefficient d'étirement. Le taux a été augmenté par multiplexage de deux codes de taux 1 par le biais d'une matrice unitaire donnant naissance à un nouveau code FGD de taux 2 associé à complexité de décodage minimale. La matrice unitaire était numériquement optimisée pour le cas de la constellation QPSK. Un nouveau code de taux $3/2$ a été obtenu par le poinçonnage du code de taux 2. Les résultats de simulation ont montré que les codes proposés de taux 1 et $3/2$ ont une faible complexité moyenne de décodage alors que le code de taux 2 a une faible complexité moyenne de décodage dans la région de faibles SNR.

Nous avons également étudié le cas dans lequel un *feedback* limitée est disponible à l'émetteur et nous avons proposé un nouveau schéma de diversité quasi-optimal à puissance d'émission identique.

7.2 Perspectives

Une problématique intéressante à poursuivre est l'augmentation du taux des codes à faible complexité à travers le relâchement de certaines contraintes imposées dans cette thèse et dans la littérature. Dans ce contexte, il serait intéressant d'étudier les taux maximaux de codes rectangulaires *g-group decodable* (i.e. $T > N_t$). Dans [47], les auteurs ont abordé la construction de codes *2-group decodable* de forme rectangulaire et carrée et ont prouvé que pour la forme rectangulaire, les codes sont asymptotiquement du taux plein, c'est-à-dire que pour $T \gg N_t$, le taux de

code approche N_t. Cette augmentation du taux de code est évidemment obtenue au détriment d'un retard accru, celà impose un compromis entre le taux et le retard prenant en considération la tolérance de délai du système. Une voie possible serait de développer une extension du travail établi dans [47] dans le contexte plus général des codes *g-group decodable*.

Parmi les perspectives potentielles de cette thèse, il serait également intéressant de trouver des codes *g-group decodable* avec des matrices de dispersion non-unitaires *Non Unitary weight* (NUW) de taux maximal (au cours de cette thèse, les matrices de dispersion ont été limitées à des matrices unitaires). Seuls quelques exemples de codes *NUW-g-group decodable* ont été proposés dans la littérature. Par exemple, dans [64], les auteurs se sont concentrés sur les codes NUW *Single Symbol Decodable* (SSD) comportant les *Coordinate Interleaved Orthogonal Design* (CIOD) [62]. Néanmoins, la construction des codes *NUW-g-group decodable* dans le cadre général n'a pas été abordée de manière approfondie en laissant la question sur les taux atteignable maximaux de codes *NUW-g-group decodable* encore ouverte.

Part II

English

Chapter 1

Introduction

Achieving reliable communications over wireless channels has always been considered as a challenging problem. This is mainly due the inherent impairments in the wireless environment, namely the signal attenuation and the multipath propagation. The transmitted signal attenuation is the result of several factors such as the propagation loss, the antennas loss, and the shadowing effect, which render the transmitted signal more vulnerable to errors. The multipath propagation as indicated by its name reflects the fact that the signals transmitted in the wireless media follow multiple paths before reaching their destination causing the received signal to be a mixture of delayed replicas of the original signal, each experiencing a distinct channel. The effect of multipath propagation may be summarized in the Inter-Symbol Interference (ISI) due to the channel delay spread and the deep fades due to destructive signal superposition at the receiver. While equalizers and Orthogonal Frequency Division Multiplexing (OFDM) techniques have been proposed in order to mitigate the channel delay spread effect, the so called diversity techniques have proved to be effective when dealing with the multipath fading phenomena.

Generally speaking, the diversity techniques can be seen as replicating the data such that each replica experiences an independent fade thus alleviating the fading effect by assuring a high probability of reliable detection at the receiver side. This redundancy may be implemented in several domains, for instance in the time domain where the signal replicas are sent over several time slots that are spaced by more than the channel coherence time (this may be realized through combining Forward Error Correcting (FEC) codes with bit interleaving) or in the frequency

domain where the signal replicas are sent over several sub-carriers that are spaced by more than the channel coherence bandwidth. However, both of the above techniques need the allocation of an additional bandwidth to achieve the required diversity degree and thus are bandwidth deficient.

An efficient technique which can offer a high protection to the transmitted signal against deep fades while requiring no additional bandwidth is space diversity. Space diversity can be employed at the receiver side, transmitter side, or both. In a system that employs receive diversity, the signal is sent from a single antenna and received at multiple antennas and this configuration is referred to as a Single-Input Multiple-Output (SIMO) system, whereas in a system that employs transmit diversity, the signal replicas are sent from multiple antennas and received at at single antenna and this configuration is referred to as a Multiple-Input Single-Output (MISO) system. In a system that exploits diversity at both ends, namely a Multiple-Input Multiple-Output (MIMO) system, the signal replicas are sent from multiple antennas and received at multiple antennas. In order to preserve the independence between the multiple transmitter-receiver channels, the antennas must be spaced by at least half of the wavelength of the operating frequency [2]. However for systems with space limitations, the polarization diversity can be employed by using dual-polarized antennas instead of spaced uni-polarized antennas at the expense of some performance loss [3].

In order to realize the advantages of MIMO over SIMO and MISO systems, consider the following three configurations, a $1 \times N_r$ SIMO system Fig 1.1(a), a $N_t \times 1$ MISO system Fig 1.1(b) and a $N_t \times N_r$ MIMO system Fig 1.1(c). In the SIMO (resp. MISO) configuration, the diversity gain is upper bounded by N_r (resp. N_t) which is the maximum number of independent channels between the transmitter and the receiver sides whereas the $N_t \times N_r$ MIMO system can offer a degree of diversity equal to $N_t N_r$. Moreover, the MIMO configuration may offer higher degrees of freedom than the SIMO and MISO configurations. The channel degrees of freedom is defined as the maximum provided number of parallel spatial channels [4]. As it will be presented in the sequel, the SIMO and MISO configurations cannot offer a degree of freedom grater than one whereas the MIMO configuration can offer up to $\min\{N_t, N_r\}$ degrees of freedom. To recapitulate, a MIMO system can provide

better performance (due to its higher diversity gain) and higher rate (due its higher channel degrees of freedom) than both SIMO and MISO systems.

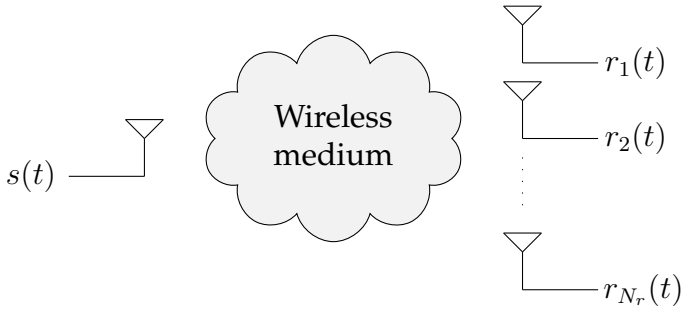

(a) SIMO configuration

(b) MISO configuration

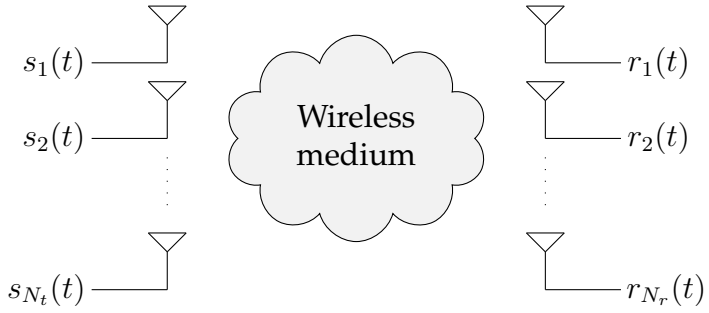

(c) MIMO configuration

Figure 1.1: Different configurations

While the maximum diversity gain may be achieved in a SIMO (resp. MISO) system through Maximum Ratio Combining (MRC) (resp. optimum beamforming), space-time coding techniques where the information symbols are coded over two dimensions, namely space and time have proved to exploit efficiently the MIMO channels. Actually, Space-time coding can jointly exploit all of the available degrees of freedom and diversity while requiring no prior knowledge of Channel State Information (CSI) at the transmitter. Therefore, they have been incorpo-

rated as open-loop techniques in recent wireless communications standards (e.g. [5, 6]) and in the upcoming 3GPP LTE. The main challenge in implementing STCs is their complexity of decoding which generally increases exponentially with the code rate.

The first STCs proposed in the literature, namely the Space-Time Trellis Codes (STTCs) [7] can provide high performance at the expense of a prohibitively high decoding complexity as the number of states in the Viterbi decoder grows exponentially with the rate and the number of transmit antennas. In order to address the high-complexity drawback of the implementation of STTCs in practical MIMO systems, a linear family counterpart of STCs has been proposed namely the Space-Time Block Codes (STBCs) [8], where the transmitted code matrix can be expressed as a weighted linear combination of information symbols. This inherent linearity in the STBC matrix allows the use of *closest lattice point* searching algorithms generally known as sphere decoding algorithms [9, 10] as well as simple sub-optimum decoding algorithms such as successive nulling and cancelling [11], and the recently proposed augmented lattice reduction [12] algorithm.

However, despite that the use of sphere decoders significantly reduces the average decoding complexity defined as the average number of visited nodes by a tree search decoder in order to optimally estimate the transmitted symbols codeword [13], it has no impact on the worst-case decoding complexity that generally increases exponentially with the rate of the STBC. By worst-case decoding complexity order, we mean the minimum number of times an exhaustive search decoder has to compute the Maximum Likelihood (ML) metric to optimally estimate the transmitted symbols codeword [14, 15], so for a STBC matrix $\mathbf{X}$ that encodes K complex symbols drawn from a constellation with M points, the worst-case decoding complexity order is equal to M^K. In that sense, the STBC $\mathbf{X}$ is said to be low-complexity decodable iff its worst-case decoding complexity order is less than M^K.

Arguably, the main family of low-complexity STBCs are the g-Group Decodable (g-GD) STBCs [16]. A g-GD STBC is designed such that instead of jointly decoding all of the transmitted symbols codeword, symbols may be decoupled into disjoint groups that can be decoded separately without any loss of perfor-

mance. For instance, if the STBC $\mathbf{X}$ that encodes $2K$ real symbols is g-group decodable, the worst-case decoding complexity can be significantly reduced from M^K to $\sum_{i=1}^{g} \sqrt{M}^{n_i}$ where $\sum_{i=1}^{g} n_i = 2K$ and n_i denotes the number of real symbols in the i'th group. However, the multi-group decodability imposes a number of strict conditions on the STBC matrix which in turn limits greatly the achievable rates. In order to address this rate-complexity trade-off, a family of STBCs namely the Fast-Decodable (FD) STBCs has been proposed. FD codes enable substantially higher rates than g-group decodable codes by relaxing the multi-group decodability conditions while maintaining an affordable level of worst-case decoding complexity. A FD STBC strictly encloses a g-group-decodable code which enables the use of the conditional detection approach to decode the transmitted symbols in two steps. The first step consists of evaluating the conditional ML estimation of the symbols belonging to the g-group-decodable code and the second step consists of decoding the rest of the symbols. A straight forward construction of FD STBCs is obtained through multiplexing multiple g-GD STBCs [14, 17]. Recently, a family of codes that combines both approaches namely Fast-Group Decodable (FGD) STBCs has been proposed [18]. FGD STBCs are g-group-decodable codes such that each group of symbols is fast-decodable.

Recognizing the importance of the low-complexity criterion in STBC design for practical considerations, this thesis focuses on the design of new low-complexity STBCs.

1.1 Contributions

The contributions of the thesis are summarized in the following:

- The proposed construction methods for the g-group-decodable codes [16, 19] are based on sufficient but not necessary conditions which may reduce further the attainable rates. In Chapter 4, we investigate the maximal achievable rates of g-group-decodable STBCs for a specific type of code matrices that subsumes the majority of the proposed STBCs in the literature. We propose a new numerical approach based on necessary and sufficient conditions for g-group-decodable codes and prove that for the considered special type of code

matrices, the proposed method is considerably simplified. We focus on the case of four transmit antennas and provide the maximal-rate of symmetric 2-group decodable and 3-group decodable codes. The material of this chapter was partially presented at the IEEE Global Telecommunications Conference (GLOBECOM'10), Miami, Florida, USA, 2010 [15] and in a submitted paper to IEEE Transactions on Communications (under 2nd round revision).

- In the context of FD codes, we focus in Chapter 5 on the multiplexing of two orthogonal STBCs in the case of four transmit antennas by the means of a unitary matrix. First, we derive an upper bound for the rate of the proposed code structure in order to satisfy the cubic shaping property. Then, we prove that the proposed code retains the coding gain of the rate-3/4 orthogonal STBC regardless of the underlying QAM constellation prior to normalization, i.e., that the proposed code achieves the NonVanishing Determinant (NVD) property [20]. Simulation results show that not only the proposed code outperforms existing STBCs in the literature, but it can be decoded at a lower average decoding complexity and provides a better Peak-to-Average Power Ratio (PAPR). The material of this chapter was partially published in the IEEE Transactions on Wireless Communications [21] and will be presented at the upcoming IEEE Global Telecommunications Conference (GLOBECOM'11), Houston, Texas, USA, 2011 [22].

- In Chapter 6, we propose a systematic approach to obtain FGD rate-1 STBCs for 2^a transmit antennas. If the number of transmit antennas is not a power of two, the corresponding FGD code can be obtained by deleting the appropriate number of columns of the FGD of the nearest greater number of antennas that is a power of two, e.g., the FGD code for three transmit antennas is obtained by removing one column from the 4×4 FGD. We apply the proposed method to the case of four transmit antennas and obtain a new rate-1 FGD STBC that has to the best of our knowledge the smallest worst-case decoding complexity among comparable STBCs in the literature. The coding gain of the proposed code in then optimized through constellation stretching rather than the constellation rotation to preserve the FGD structure and to minimize the PAPR which is that of the underlying constellation. We provide an

analytical proof that the NVD property is indeed achievable through proper choice of the constellation stretching factor. Subsequently, the rate is then increased through multiplexing two rate-1 codes by means of a unitary matrix giving rise to a new fast-decodable rate-2 STBC that has the least worst-case decoding complexity. The unitary matrix is numerically optimized for the case of QPSK constellation. A new rate-3/2 STBC is obtained through puncturing the rate-2 code. Simulation results show that the proposed rate-1 and 3/2 codes have a lower average decoding complexity, while the rate-2 code has a lower decoding complexity in the low SNR regime. The material of this chapter is partially presented in a paper submitted to the IEEE International Conference on Communications (ICC'12), Ottawa, Canada, 2012 [23] and submitted to the IEEE Transactions on Wireless Communications [24].

- In Appendix D, we consider the case where a limited feedback is available at the transmitter and propose a new near-optimum equal-power transmit diversity scheme. The material of this appendix was presented at the IEEE International Symposium on Personal, Indoor and Mobile Radio Communications (PIMRC'10) [25] and published in part at the IEEE Communications Letters [26].

1.2 Organization of the thesis

The rest of the thesis is organized as follows: in Chapter 2, we thoroughly review the code design criteria, basic definitions and some of the significant STBC families. In Chapter 3, we review the three families of low-complexity STBCs namely the g-group-decodable codes, the fast decodable codes, and the fast-group-decodable codes. The new g-group decodable codes construction method is provided in Chapter 4 with the obtained codes for the case of four transmit antennas.

In Chapter 5, the proposed orthogonal designs multiplexing structure is provided, where we derive an upper bound of the rate to preserve the cubic shaping property and present the fast-decodable code that achieves this bound. In Chapter 6, we propose a systematic approach for the construction of rate-1 fast-group-decodable codes for an arbitrary number of transmit antennas. We then focus on

the case of four transmit antennas and propose a new family of STBCs with the smallest worst-case decoding complexity whose rate ranges from one to two complex symbols per channel use. The thesis conclusions and perspective work are provided in Chapter 7.

Chapter 2

Space-Time Block Codes

Space-Time Block Codes (STBCs) were originally proposed as a low-complexity alternative to Space-Time Trellis Codes (STTCs) which suffered from a prohibitively high decoding complexity. The STBCs are characterized by their linearity over the field of real numbers as the transmitted code matrix can be expressed as a linear weighted combination of real information symbols. This inherent linearity in the STBCs turns Maximum Likelihood (ML) decoding into a closest lattice search problem which can be effectively solved via the well known sphere decoding algorithms. Moreover, STBCs have proved to efficiently exploit the MIMO channel degrees of freedom and diversity.

The first proposed STBC was unquestionably the elegant two transmit antennas diversity scheme known afterwards as *the Alamouti code* [27]. In fact, the Alamouti code can be optimally decoded with a complexity that only grows linearly with the underlying constellation's size for general constellations, and furthermore, if we consider the case of rectangular Quadrature Amplitude (QAM) constellations such as 4,16,64-QAM, the Alamouti code can be effectively decoded at a constant complexity irrespectively of the underlying constellation's size. Besides its low-complexity decoding, the Alamouti's code has the NVD property [20], a property that can be exploited through the use of adaptive modulation which varies the transmission rate (through the choice of the modulation order) according to the wireless channel quality. Moreover, if we consider the special 2×1 configuration, the Alamouti code is full-rate and information lossless.

In the attempt to generalize Alamouti's low-complexity scheme for a number of transmit antennas greater than two, the well known family of low-complexity

codes namely orthogonal STBCs has been proposed. Unfortunately, the rate of square orthogonal STBCs decay exponentially with the number of transmit antennas which makes them more suitable to low-rate communications. In order to address the rate loss of orthogonal STBCs, several families of codes have been proposed, among them we mention the Diagonal Algebraic Space-Time (DAST) codes [28], the Threaded Algebraic Space-Time (TAST) codes [29] and the perfect STBCs [30]. These families of codes provide high-rate transmission through the relaxation of the orthogonality constraints. The DAST codes can achieve a rate-one transmission for arbitrary number of transmit antennas while TAST and perfect codes have the advantage of being full-rate STBCs in the sense that they can attain the maximal achievable rate for any MIMO channel configuration.

In this chapter, we begin by presenting the MIMO channel model adopted throughout this thesis, namely the flat quasi-static Rayleigh fading model. The optimal decoding of STBCs and related issues namely the decoding complexity measures are then discussed. We elaborate the important STBC design criteria, and then some of the well known STBC families are reviewed and compared in terms of these criteria.

2.1 System model

When dealing with STBCs, a useful baseband channel model is the flat quasi-static Rayleigh fading channel model. As indicated by its name, the channel frequency response is considered to be flat over the frequency band of interest and the path fading coefficient are modelled through Rayleigh distributed random variables that are assumed to remain constant over the codeword signalling period and vary independently from codeword to codeword. The noise samples are assumed to be spatially and temporally uncorrelated, and for sufficiently spaced antennas, the channel coefficients are assumed to be spatially uncorrelated. Mathematically speaking, the baseband MIMO channel input-output relation may be described by:

$$\underset{T\times N_r}{\mathbf{Y}} = \underset{T\times N_t}{\mathbf{X}}\underset{N_t\times N_r}{\mathbf{H}} + \underset{T\times N_r}{\mathbf{W}} \tag{2.1}$$

where T is the codeword signalling period, N_r is the number of receive antennas, N_t is the number of transmit antennas, $\mathbf{Y}$ is the received signal matrix, $\mathbf{X}$ is the

code matrix, $\mathbf{H}$ is the channel coefficients matrix with entries $h_{kl} \sim \mathcal{CN}(0,1)$, and $\mathbf{W}$ is the noise matrix with entries $w_{ij} \sim \mathcal{CN}(0, N_0)$. According to the above model, the t'th row of $\mathbf{X}$ denotes the symbols transmitted through the N_t transmit antennas during the t'th channel use while the n'th column denotes the symbols transmitted through the n'th transmit antenna during the codeword signalling period T. It is worth noting that even if the above model assumes a flat fading channel between the transmitter and receiver sides, it remains applicable for the selective fading channels scenario. This is because in such channels, the use of Orthogonal Frequency Division Multiplexing (OFDM) simply transforms the selective fading channel into multiple flat fading channels. In such a scenario, the system model (2.1) can be rewritten as in [31]:

$$\mathbf{Y}(p) = \mathbf{X}(p)\,\mathbf{H}(p) + \mathbf{W}(p)\,,\ \forall p = 0, \ldots, N_c - 1 \tag{2.2}$$

where $\mathbf{Y}(p)$, $\mathbf{X}(p)$ denote the received signal matrix, and the STBC matrix at the p'th subcarrier, respectively. The entries $h_{kl}(p)$ of the matrix $\mathbf{H}(p)$ denote the N_c points FFT of the channel impulse response between the k'th transmit antenna and the l'th receive antenna evaluated at the p'th subcarrier, the entries $w_{ij}(p) \sim \mathcal{CN}(0, N_0)$ of the noise matrix $\mathbf{W}(p)$ denote the N_c points FFT of the AWGN at the j'th antenna during the i'th OFDM symbol interval evaluated at the p'th subcarrier and N_c denotes the number of sub-carriers.

Generally speaking, a STBC matrix that encodes $2K$ real symbols can expressed as a linear combination of the transmitted symbols as [8]:

$$\mathbf{X} = \sum_{k=1}^{2K} \mathbf{A}_k x_k \tag{2.3}$$

with $x_k \in \mathbb{R}$ and the $\mathbf{A}_k, k = 1, ..., 2K$ are $T \times N_t$ complex matrices called dispersion or weight matrices that are required to be linearly independent over $\mathbb{R}$ as will be justified shortly. Moreover, a STBC is said to be unitary iff all of its weight matrices are unitary.

Definition 2.1 *A STBC that encodes $2K$ real symbols over T signalling periods is said to have a rate of K/T complex symbols per channel use.*

A useful manner to express the system model can be directly obtained by replacing $\mathbf{X}$ in (2.1) by its expression in (2.3):

$$\mathbf{Y} = \sum_{k=1}^{2K} (\mathbf{A}_k \mathbf{H})\, x_k + \mathbf{W}. \tag{2.4}$$

Applying the vec$(.)$ operator to the R.H.S and the L.H.S we obtain:

$$\text{vec}(\mathbf{Y}) = \sum_{k=1}^{2K} (\mathbf{I}_{N_r} \otimes \mathbf{A}_k)\, \text{vec}\,(\mathbf{H})\, x_k + \text{vec}(\mathbf{W}). \tag{2.5}$$

where $\mathbf{I}_{N_r}$ is the $N_r \times N_r$ identity matrix.
If $\mathbf{y}_i$, $\mathbf{h}_i$ and $\mathbf{w}_i$ designate the i'th columns of the received signal matrix $\mathbf{Y}$, the channel matrix $\mathbf{H}$ and the noise matrix $\mathbf{W}$ respectively, then equation (2.5) can be written in matrix form as:

$$\underbrace{\begin{bmatrix} \mathbf{y}_1 \\ \vdots \\ \mathbf{y}_{N_r} \end{bmatrix}}_{\mathbf{y}} = \underbrace{\begin{bmatrix} \mathbf{A}_1\mathbf{h}_1 & \dots & \mathbf{A}_{2K}\mathbf{h}_1 \\ \vdots & \vdots & \vdots \\ \mathbf{A}_1\mathbf{h}_{N_r} & \dots & \mathbf{A}_{2K}\mathbf{h}_{N_r} \end{bmatrix}}_{\boldsymbol{\mathcal{H}}} \underbrace{\begin{bmatrix} x_1 \\ \vdots \\ x_{2K} \end{bmatrix}}_{\mathbf{s}} + \underbrace{\begin{bmatrix} \mathbf{w}_1 \\ \vdots \\ \mathbf{w}_{N_r} \end{bmatrix}}_{\mathbf{w}}. \tag{2.6}$$

A real system of equations can be obtained by separating the real and imaginary parts of the above to obtain:

$$\tilde{\mathbf{y}} = \tilde{\boldsymbol{\mathcal{H}}}\mathbf{s} + \tilde{\mathbf{w}} \tag{2.7}$$

where $\tilde{\mathbf{y}}, \tilde{\mathbf{w}} \in \mathbb{R}^{2N_rT \times 1}$, and $\tilde{\boldsymbol{\mathcal{H}}} \in \mathbb{R}^{2N_rT \times 2K}$. It is worth noting that the above real system of linear equations is not under-determined if $N_rT \geq K$, assuming that the set $\{\mathbf{A}_k : k = 1, \dots 2K\}$ is linearly independent over $\mathbb{R}$. The advantage of having a well conditioned system of linear equations is that the ML estimate may be obtained through a sphere decoder whose expected computational complexity growth is roughly cubic in K [8]. If the system of linear equations is underdetermined, the expected computational complexity of the sphere decoder grows exponentially with $K - N_rT$.

2.2 STBC decoding

Assuming that perfect Channel State Information (CSI) is available at the receiver, the optimal decoder namely the ML decoder is the one which decides in favor

of the real information symbol vector s that minimizes the Euclidean distance between the received data vector and all possible noiseless channel outputs. Mathematically:

$$\mathbf{s}^{\mathrm{ML}} = \arg \min_{\hat{\mathbf{s}} \in \mathcal{C}} \|\tilde{\mathbf{y}} - \tilde{\boldsymbol{\mathcal{H}}}\hat{\mathbf{s}}\|^2 \tag{2.8}$$

where $\mathcal{C}$ denotes the vector space spanned by s.
A straightforward implementation of the ML estimator above would be the exhaustive search decoder, which evaluates the ML metric for all possible data vectors s and finally chooses the one with the minimum ML metric. Typically, this decoder is not used in practical communication systems due to its high computational complexity which involves the evaluation of the ML metric $|\mathcal{C}|$ times and $|\mathcal{C}| - 1$ comparisons. This leads to the definition of a useful complexity measure namely the worst-case decoding complexity.

Definition 2.2 *The worst-case decoding complexity is defined as the minimum number of times an exhaustive search decoder has to compute the ML metric to optimally estimate the transmitted codeword [14]*

2.2.1 Introducing the Sphere Decoder

A more practical implementation of the ML decoder can be obtained by interpreting (2.8) as a bounded closest lattice point search problem which can be effectively done through the well known sphere decoder. Actually the sphere decoder transforms (2.8) into a real-valued tree search based problem by applying the QR decomposition to $\tilde{\boldsymbol{\mathcal{H}}}$. The problem then turns into finding the path with the smallest accumulated Partial Euclidean Distance (PED). Assuming that $N_r T \geq K$, the QR decomposition of $\tilde{\boldsymbol{\mathcal{H}}}$ yields:

$$\tilde{\boldsymbol{\mathcal{H}}} = \begin{bmatrix} \mathbf{Q}_1 & \mathbf{Q}_2 \end{bmatrix} \begin{bmatrix} \mathbf{R} \\ \mathbf{0} \end{bmatrix} \tag{2.9}$$

where $\mathbf{Q}_1 \in \mathbb{R}^{2N_rT \times 2K}$,$\mathbf{Q}_2 \in \mathbb{R}^{2N_rT \times (2N_rT-2K)}$, $\mathbf{Q}_i^T\mathbf{Q}_i = \mathbf{I},\ i = 1, 2$, $\mathbf{R}$ is a $2K \times 2K$ real upper triangular matrix and $\mathbf{0}$ is a $(2N_rT - 2K) \times 2K$ null matrix. Accordingly, the ML estimate may be expressed as:

$$\mathbf{s}^{\mathrm{ML}} = \arg \min_{\hat{\mathbf{s}} \in \mathcal{C}} \|\tilde{\mathbf{y}} - \mathbf{Q}_1\mathbf{R}\hat{\mathbf{s}}\|^2 \tag{2.10}$$

Noting that the multiplication of a column vector by a orthogonal matrix does not alter its norm, the above reduces to:

$$\mathbf{s}^{\mathrm{ML}} = \arg\min_{\hat{\mathbf{s}}\in\mathcal{C}} \|\mathbf{y}' - \mathbf{R}\hat{\mathbf{s}}\|^2 \tag{2.11}$$

where $\mathbf{y}' = \mathbf{Q}_1^T\tilde{\mathbf{y}}$.

Thanks to the upper triangular structure of $\mathbf{R}$ we have:

$$\begin{aligned}\mathbf{s}^{\mathrm{ML}} =& \arg\min_{\hat{\mathbf{s}}\in\mathcal{A}^{2K}} \sum_{i=1}^{2K}\left|y_i' - \sum_{j=i}^{2K} r_{i,j}\hat{x}_j\right|^2 \\ =& \arg\min_{\hat{\mathbf{s}}\in\mathcal{A}^{2K}} \left\{ \underbrace{\left|y_1' - \sum_{j=1}^{2K} r_{1,j}\hat{x}_j\right|^2}_{W_{2K}} + \underbrace{\left|y_2' - \sum_{j=2}^{2K} r_{2,j}\hat{x}_j\right|^2}_{W_{2K-1}} + \ldots \underbrace{\left|y_{2K}' - r_{2K,2K}\hat{x}_{2K}\right|^2}_{W_1} \right\}.\end{aligned} \tag{2.12}$$

Equation (2.12) can be graphically interpreted as finding the shortest path in a $2K$-levels real valued tree, where each path from the root to the leaf nodes corresponds to a particular choice of real information symbols, and the branch metric at the i'th level is the corresponding PED W_i. For the sake of illustration, a four levels real-valued binary tree (e.g. for BPSK signalling) is depicted in Fig 2.1. A possible ML estimation path $\{1, -1, 1, -1\}$ is marked by thick lines.

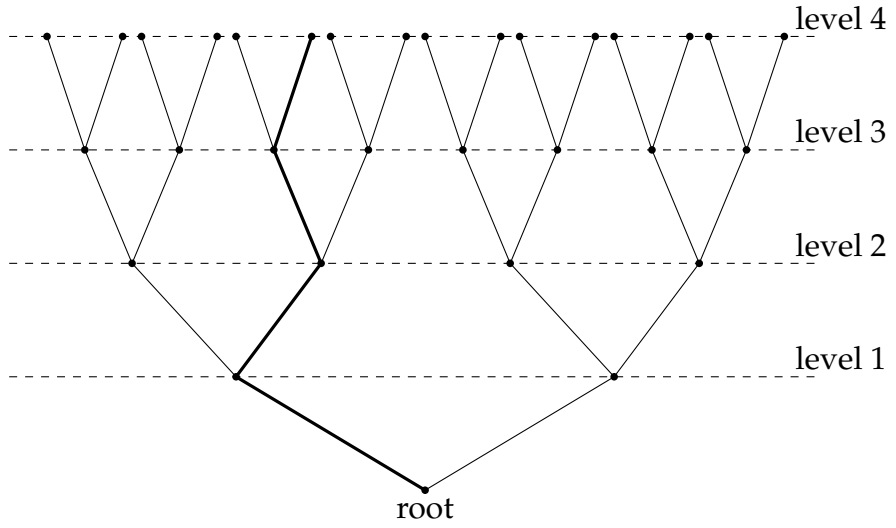

Figure 2.1: A four level real valued tree with BPSK constellation

At the beginning, the sphere radius is initialized to infinity and the sphere decoder starts scanning the tree from its root ascending to the leaf nodes in a depth-first traversal manner. The sibling nodes are visited according to the Schnorr-Euchner enumeration [32] which sorts the sibling nodes in ascending order of their branch metric. Whenever a leaf node is reached, its accumulated path metric is compared to the current value of the sphere radius. If the accumulated path metric is less than the current sphere radius, the sphere radius is updated to the path's metric and the path is considered as valid ML estimation candidate; otherwise the path is discarded as it will be considered to be out of the current sphere. Indeed, the leaf nodes need not to be sorted, because for a given value of $(x_2, \ldots, x_{2K})$, the ML estimate of x_1 that we denote $x_1^{\mathrm{ML}}|\,(\hat{x}_2, \ldots, \hat{x}_{2K})$ can be directly obtained through a hard slicer. For a square unnormalized QAM constellation with M points, this may be mathematically expressed as:

$$x_1^{\mathrm{ML}}|\,(\hat{x}_2, \ldots, \hat{x}_{2K}) = \mathrm{sign}\,(z_1) \times \min\Big[\Big|2\,\mathrm{round}\Big(\,(z_1 - 1)\,/2\Big) + 1\Big|, \sqrt{M} - 1\Big] \quad (2.13)$$

where $z_1 = \Big(y_1' - \sum_{j=2}^{2K} r_{1,j}\hat{x}_j\Big)\,/r_{1,1}$ which is equivalent to the pruning of the last level of the real valued tree and consequently the worst-case complexity is divided by $\sqrt{M}$.

A closer look at (2.12) reveals that the accumulated path metric is a non-decreasing function with the ascending tree's levels. This suggests that if the accumulated path metric to the node (a) at level i is greater than or equal to the current sphere radius, all child nodes stemming from (a) can be safely removed as their accumulated path metric will be strictly greater than the sphere radius. Moreover, thanks to the Schnorr-Euchner enumeration strategy one may also discard (a)'s sibling nodes as their branch metrics are strictly greater than that of (a). Therefore, the sphere decoder has to descend to the level $i - 1$ and start considering the sibling nodes of (a)'s parent node. This *pruning* of the tree results in a significant reduction in the number of visited nodes which is the major factor in determining how fast the sphere decoder will converge to the ML estimate of the transmitted codeword. This leads us to define another important complexity measure namely the average decoding complexity.

Definition 2.3 *The average decoding complexity is defined to be the average number of visited nodes by a tree search decoder in order to optimally estimate the transmitted codeword [13].*

It is worth noting that for real valued information symbols, the Schnorr-Euchner sorting of the nodes at level i for a given path to level $i-1$ can be directly obtained without explicit evaluation of PEDs. More explicitly one has:

$$S_i = \begin{cases} (x_i^{\text{nc}}, x_i^{\text{nc}}+1, x_i^{\text{nc}}-1, x_i^{\text{nc}}+2, x_i^{\text{nc}}-2, \ldots) & \text{if } z_i \geq x_i^{\text{nc}} \\ (x_i^{\text{nc}}, x_i^{\text{nc}}-1, x_i^{\text{nc}}+1, x_i^{\text{nc}}-2, x_i^{\text{nc}}+2, \ldots) & \text{otherwise} \end{cases} \tag{2.14}$$

where S_i denotes the order in which the nodes at level i are visited, and x_i^{nc} refers to the nulling and cancelling point [11] and is obtained exactly as in (2.13) with the only difference that z_1 will be replaced by $z_i = \left(y_i' - \sum_{j=i+1}^{2K} r_{i,j}\hat{x}_j\right)/r_{i,i}$. A pseudo-code of the sphere decoder for a four level real-valued tree is illustrated in the next page. The `sort` function returns the order in which the real PAM constellation points $\mathcal{A}$ are visited according to the simplified Schnorr-Euchner enumeration [32] whereas the `round` and `sign` functions implement the round and sign operators, respectively.

2.2.2 Soft decoding

In practical communication systems, space-time codes may be concatenated with an outer FEC, typically turbo codes, with interleaving to further enhance the BER performance [65]. In this case, the receiver will have to evaluate the Log-Likelihood Ratios (LLR) that will be fed to the turbo decoder. For this purpose, let $\mathbf{b}$ denote the binary information vector of length Kq where $q = \log_2(M)$. The log-likelihood ratio for the l'th bit of $\mathbf{b}$ namely b_l is given by:

$$\Lambda(b_l) = \log \frac{\Pr\left[b_l = 1|\tilde{\mathbf{y}}\right]}{\Pr\left[b_l = 0|\tilde{\mathbf{y}}\right]}$$

thanks to Bayes rule the above simplifies to:

$$\Lambda(b_l) = \log_2 \frac{\Pr\left[b_l = 1; \tilde{\mathbf{y}}\right]}{\Pr\left[b_l = 0; \tilde{\mathbf{y}}\right]} = \log \frac{\sum\limits_{\mathbf{b}|b_l=1} \Pr\left[\mathbf{b}; \tilde{\mathbf{y}}\right]}{\sum\limits_{\mathbf{b}|b_l=0} \Pr\left[\mathbf{b}; \tilde{\mathbf{y}}\right]} = \log \frac{\sum\limits_{\mathbf{s}|b_l=1} \Pr\left[\mathbf{s}; \tilde{\mathbf{y}}\right]}{\sum\limits_{\mathbf{s}|b_l=0} \Pr\left[\mathbf{s}; \tilde{\mathbf{y}}\right]}.$$

Algorithm I: The SD for four level real-valued tree and square QAM of size M

$C = \infty$
$z_4 = y'_4 / r_{4,4}$
$x_4^{\mathsf{nc}} = \mathtt{sign}\left(z_4\right) \times \mathtt{min}\left[\left|2\ \mathtt{round}(\left(z_4 - 1\right)/2) + 1\right|, \sqrt{M} - 1\right]$
$\Xi_4 = \mathtt{sort}(z_4, x_4^{\mathsf{nc}})$
$k_4 = 1$
while $k_4 \leq \sqrt{M}$ **and** $\left(y'_4 - r_{4,4}\mathcal{A}\left(\Xi_4\left(k_4\right)\right)\right)^2 < C$ **do**
  $x_4 = \mathcal{A}\left(\Xi_4\left(k_4\right)\right)$
  $W_4 = \left(y'_4 - r_{4,4}x_4\right)^2$
  $z_3 = \left(y'_3 - r_{3,4}x_4\right)/r_{3,3}$
  $x_3^{\mathsf{nc}} = \mathtt{sign}\left(z_3\right) \times \mathtt{min}\left[\left|2\ \mathtt{round}(\left(z_3 - 1\right)/2) + 1\right|, \sqrt{M} - 1\right]$
  $\Xi_3 = \mathtt{sort}(z_3, x_3^{\mathsf{nc}})$
  $k_3 = 1$
  while $k_3 \leq \sqrt{M}$ **and** $\left(y'_3 - r_{3,3}\mathcal{A}\left(\Xi_3\left(k_3\right)\right) - r_{3,4}x_4\right)^2 + W_4 < C$ **do**
    $x_3 = \mathcal{A}\left(\Xi_3\left(k_3\right)\right)$
    $W_3 = \left(y'_3 - \sum_{j=3}^{4} r_{3,j}x_j\right)^2$
    $z_2 = \left(y'_2 - \sum_{j=3}^{4} r_{2,j}x_j\right)/r_{2,2}$
    $x_2^{\mathsf{nc}} = \mathtt{sign}\left(z_2\right) \times \mathtt{min}\left[\left|2\ \mathtt{round}(\left(z_2 - 1\right)/2) + 1\right|, \sqrt{M} - 1\right]$
    $\Xi_2 = \mathtt{sort}(z_2, x_2^{\mathsf{nc}})$
    $k_2 = 1$
    while $k_2 \leq \sqrt{M}$ **and** $\left(y'_2 - r_{2,2}\mathcal{A}\left(\Xi_2\left(k_2\right)\right) - \sum_{j=3}^{4} r_{2,j}x_j\right)^2 + \sum_{i=3}^{4} W_i < C$ **do**
      $x_2 = \mathcal{A}\left(\Xi_2\left(k_2\right)\right)$
      $W_2 = \left(y'_2 - \sum_{j=2}^{4} r_{2,j}x_j\right)^2$
      $z_1 = \left(y'_1 - \sum_{j=2}^{4} r_{1,j}x_j\right)/r_{1,1}$
      $x_1 = \mathtt{sign}\left(z_1\right) \times \mathtt{min}\left[\left|2\ \mathtt{round}(\left(z_1 - 1\right)/2) + 1\right|, \sqrt{M} - 1\right]$
      $W_1 = \left(y'_1 - r_{1,1}x_1 - \sum_{j=2}^{4} r_{1,j}x_j\right)^2$
      $P = \sum_{i=1}^{4} W_i$
      if $P < C$ **then**
        $C = P$
        $\hat{\mathbf{s}} = \mathbf{x}$
      end
      $k_2 = k_2 + 1$
    end
    $k_3 = k_3 + 1$
  end
  $k_4 = k_4 + 1$
end

Assuming that the information vectors s are equally likely, one has:

$$\Lambda(b_l) = \log \frac{\sum\limits_{\mathbf{s}|b_l=1} \Pr\left[\tilde{\mathbf{y}}|\mathbf{s}\right]}{\sum\limits_{\mathbf{s}|b_l=0} \Pr\left[\tilde{\mathbf{y}}|\mathbf{s}\right]} = \log \frac{\sum\limits_{\mathbf{s}|b_l=1} e^{-\frac{\|\tilde{\mathbf{y}}-\tilde{\boldsymbol{\mathcal{H}}}\mathbf{s}\|^2}{N_0}}}{\sum\limits_{\mathbf{s}|b_l=0} e^{-\frac{\|\tilde{\mathbf{y}}-\tilde{\boldsymbol{\mathcal{H}}}\mathbf{s}\|^2}{N_0}}}. \tag{2.15}$$

It is worth noting that the log likelihood computation can be simplified using the following approximation:

$$\log\left(\sum_i e^{x_i}\right) \approx \max_i \log\left(e^{x_i}\right) \tag{2.16}$$

Thus we may approximate the log-likelihood ratio as:

$$\begin{aligned} \Lambda(b_l) &\approx \max_{\mathbf{s}|b_l=1} \log\{e^{-\frac{\|\tilde{\mathbf{y}}-\tilde{\boldsymbol{\mathcal{H}}}\mathbf{s}\|^2}{N_0}}\} - \max_{\mathbf{s}|b_l=0} \log\{e^{-\frac{\|\tilde{\mathbf{y}}-\tilde{\boldsymbol{\mathcal{H}}}\mathbf{s}\|^2}{N_0}}\} \\ &= \left(\min_{\mathbf{s}|b_l=1}\{\|\tilde{\mathbf{y}}-\tilde{\boldsymbol{\mathcal{H}}}\mathbf{s}\|^2\} - \min_{\mathbf{s}|b_l=0}\{\|\tilde{\mathbf{y}}-\tilde{\boldsymbol{\mathcal{H}}}\mathbf{s}\|^2\}\right)/N_0. \end{aligned} \tag{2.17}$$

Thanks to the similarity between the above equation and (2.8), all of the STBCs that enjoy a low worst-case decoding complexity in the sense of hard decoding evenly enjoy a reduced computational complexity in the evaluation of the LLR values. Moreover, one may resort to the sphere decoder previously described to efficiently evaluate (2.17).

2.3 STBC design criteria

The main goal in the design of any STBC is to provide good performance while being decodable at a reasonable level of complexity at the receiver. In what follows, the design criteria of STBCs over quasi static flat fading Rayleigh channels are reviewed. The discussion of the design criteria of low-complexity STBC is deferred to the next chapter. Assuming that perfect CSI is available at the receiver, the ML decision rule of model (2.1) is the following:

$$\mathbf{X}^{\mathrm{ML}} = \arg\min_{\hat{\mathbf{X}}\in\mathcal{C}} \|\mathbf{Y} - \hat{\mathbf{X}}\mathbf{H}\|_F \tag{2.18}$$

Thanks to the union bound, the probability of an erroneous decoding may be bounded as:

$$P_e \leq \sum_{\mathbf{X}\in\mathcal{C}} P\left(\mathbf{X}\right) \sum_{\substack{\mathbf{X}'\neq\mathbf{X} \\ \mathbf{X}'\in\mathcal{C}}} P\left(\mathbf{X}\rightarrow\mathbf{X}'\right) \tag{2.19}$$

where $P(\mathbf{X})$ denotes the probability that $\mathbf{X}$ is sent, and $P(\mathbf{X} \to \mathbf{X}')$ is the Pairwise Error Probability (PEP) which denotes the average probability that the decoder decides in favor of $\mathbf{X}'$ given that $\mathbf{X}$ was sent assuming that the codebook $\mathcal{C}$ contains only $\mathbf{X}$ and $\mathbf{X}'$. Assuming equiprobable codewords, the above reduces to:

$$P_e \leq \frac{1}{|\mathcal{C}|} \sum_{\mathbf{X} \in \mathcal{C}} \sum_{\substack{\mathbf{X}' \neq \mathbf{X} \\ \mathbf{x}' \in \mathcal{C}}} P(\mathbf{X} \to \mathbf{X}') \tag{2.20}$$

and due to the symmetry of the code, one has:

$$P_e \leq \sum_{\substack{\mathbf{X}' \neq \mathbf{X} \\ \mathbf{x}' \in \mathcal{C}}} P(\mathbf{X} \to \mathbf{X}') \tag{2.21}$$

But from (2.18) we have:

$$P(\mathbf{X} \to \mathbf{X}'|\mathbf{H}) = Q\left(\sqrt{\frac{\gamma}{2}} \| (\mathbf{X} - \mathbf{X}')\mathbf{H} \|_F\right) \tag{2.22}$$

where $\gamma = 1/N_0$ and $Q(x)$ is the well known Gaussian tail function. Applying the Chernoff bound and averaging over channel realizations, the probability of confusing $\mathbf{X}$ and $\mathbf{X}'$ can be asymptotically upper bounded as:

$$P(\mathbf{X} \to \mathbf{X}') \leq \frac{4^{rN_r}}{\left(\prod_{n=1}^{r} \lambda_n\right)^{N_r} \gamma^{rN_r}} \tag{2.23}$$

where r denotes the rank of $(\mathbf{X} - \mathbf{X}')$ and $\lambda_n,\ n = 1 \ldots, r$ denote the r non-zero eigen values of $(\mathbf{X} - \mathbf{X}')^H (\mathbf{X} - \mathbf{X}')$. From (2.21) and (2.23), one can guarantee good performance, especially in the high SNR region through the follwoing two criteria:

2.3.1 Rank criterion

A STBC is said to be full-diversity if the rank of all possible non-zero codewords differences is maximized, that is:

$$G_d = \min_{\substack{\mathbf{X} \neq \mathbf{X}' \\ \mathbf{x}, \mathbf{x}' \in \mathcal{C}}} \text{rank}(\mathbf{X} - \mathbf{X}') = N_t \tag{2.24}$$

2.3.2 Determinant criterion

For further performance improvement of a full diversity code, it is desirable to maximize its coding gain defined by:

$$\delta_{\mathbf{X}} = \min_{\substack{\mathbf{X}\neq\mathbf{X}' \\ \mathbf{X},\mathbf{X}'\in\mathcal{C}}} \det\left(\left(\mathbf{X}-\mathbf{X}'\right)^{H}\left(\mathbf{X}-\mathbf{X}'\right)\right) = \prod_{n=1}^{r}\lambda_n \tag{2.25}$$

Roughly speaking, a STBC with higher diversity gain will have a steeper error probability curve versus SNR in the logarithmic scale, while a STBC with higher coding gain will have a shifted error probability curve to the left. From (2.25), one can realize that the coding gain is a non-increasing function in the size of the underlying constellation. That is, if $\mathcal{C}_1 \subset \mathcal{C}_2$ one strictly has:

$$\min_{\substack{\mathbf{X}\neq\mathbf{X}' \\ \mathbf{X},\mathbf{X}'\in\mathcal{C}_2}} \det\left(\left(\mathbf{X}-\mathbf{X}'\right)^{H}\left(\mathbf{X}-\mathbf{X}'\right)\right) \leq \min_{\substack{\mathbf{X}\neq\mathbf{X}' \\ \mathbf{X},\mathbf{X}'\in\mathcal{C}_1}} \det\left(\left(\mathbf{X}-\mathbf{X}'\right)^{H}\left(\mathbf{X}-\mathbf{X}'\right)\right) \tag{2.26}$$

This leads us to the following useful definition:

Definition 2.4 *A STBC* $\mathbf{X}$ *is said to have NonVanishing Determinant (NVD) if its coding gain prior to constellation normalization is upper bounded by a non-zero constant that does not depend on the constellation size [20] or mathematically:*

$$\delta_{\mathbf{X}} \geq \psi > 0 \tag{2.27}$$

where ψ *is constant.*

The NVD is a highly desirable property as it may be exploited through the use of adaptive modulation which varies the transmission rate (through the choice of the modulation order) according to the wireless channel quality. Moreover, it has been shown in [33] that full-rate (see **Definition 2.5**) NVD STBC achieves the Diversity-Multiplexing trade-off [4] for any number of receive antennas.

2.3.3 Maximum mutual information criterion

The previous criteria tend to optimize the performance of the STBC especially in the high SNR region by minimizing the asymptotic upper limit on the PEP. One can design the STBC from an information theoretic perspective and choose the code parameters that maximize the mutual information between the transmitted and

the received vectors [8]. Recall that for a MIMO channel that employs N_t transmit antennas and N_r receive antennas whose input-output relation can be expressed as:

$$\mathbf{y} = \sqrt{\frac{\rho}{N_t}}\mathbf{H}\mathbf{s} + \mathbf{n} \tag{2.28}$$

where $\mathbf{y} \in \mathbb{C}^{N_r}$, $\mathbf{H} \in \mathbb{C}^{N_r \times N_t}$ with entries $h_{i,j} \sim \mathcal{CN}(0,1)$, $\mathbf{s} \in \mathbb{C}^{N_t}$ with entries $\mathbb{E}|s_i|^2 = 1$, $\mathbf{n} \in \mathbb{C}^{N_r}$ with entries $n_i \sim \mathcal{CN}(0,1)$, and ρ denotes the signal to noise ratio per receive antenna. Therefore the ergodic capacity is given by [34]:

$$C(N_t, N_r, \rho) = \mathbb{E}\log_2 \det\left(\mathbf{I}_{N_r} + \frac{\rho}{N_t}\mathbf{H}\mathbf{H}^H\right). \tag{2.29}$$

From this standpoint, a good STBC is the one that does not limit the capacity of the MIMO channel. If a MIMO system employs a STBC that encodes $2K$ real symbols subject to the power constraint:

$$\sum_{k=1}^{2K} \text{tr}\left(\mathbf{A}_k^H \mathbf{A}_k\right) = 2TK \tag{2.30}$$

its input/output model may be expressed as:

$$\mathbf{y} = \sqrt{\frac{\rho}{K}}\boldsymbol{\mathcal{H}}\mathbf{s} + \mathbf{w} \tag{2.31}$$

where ρ denotes the average SNR per receive antenna. Therefore, the ergodic capacity of the above system equals to:

$$C_{\text{STBC}}(\rho) = \frac{1}{T}\mathbb{E}\log_2 \det\left(\mathbf{I}_{2K} + \frac{\rho}{K}\boldsymbol{\mathcal{H}}^H\boldsymbol{\mathcal{H}}\right). \tag{2.32}$$

where the term $1/T$ is added to compensate for the T time period spanned for transmitting the information vector $\mathbf{s}$ in contrary to (2.29) where at each time slot N_t complex symbols are transmitted. Therefore, for a STBC employing N_t transmit antennas and N_r receive antennas to be information lossless, the following condition must be satisfied:

$$C_{\text{STBC}}(\rho) = C(N_t, N_r, \rho) \tag{2.33}$$

2.3.4 High-rate

At high SNR, the MIMO channel capacity (2.29) may be expressed as [4]:

$$C(N_t, N_r, \rho \gg 1) \approx \min\{N_t, N_r\}\log\frac{\rho}{N_t} + \sum_{k=|N_t-N_r|+1}^{\min\{N_t,N_r\}} \mathbb{E}\{\log_2 \chi_k\} \tag{2.34}$$

where χ_k is a chi-square random variable with $2k$ degrees of freedom. Compared to the Single-Input Single-Output (SISO) case where the capacity grows linearly with $\log \rho$, the capacity of a $N_t \times N_r$ MIMO channel asymptotically grows linearly with $\min\{N_t, N_r\} \log \rho$ which is equivalent to $\min\{N_t, N_r\}$ parallel SISO channels. In other words one can state that the available degrees of freedom of a given MIMO channel is equal to $\min\{N_t, N_r\}$. This interpretation is substantial as it tells us the maximum number of independent data streams that a given MIMO configuration can support for reliable communication, which leads us to the following definition:

Definition 2.5 *A STBC is said to be full-rate if it exploits all the available MIMO channel degrees of freedom, that is, its rate is equal to min* $\{N_t, N_r\}$ *complex symbols per channel use [2].*

2.3.5 Cubic shaping

For a given multidimensional constellation, it is highly desirable to maximize its SNR efficiency that is to maximize its minimum squared *euclidean distance* for a given constellation average power, or inversely, to minimize its average power for a given minimum squared euclidean distance. For this purpose, it is useful to express the code matrix $\mathbf{X}$ as:

$$\widetilde{\mathrm{vec}\,(\mathbf{X})} = \mathbb{G}\mathbf{s}. \tag{2.35}$$

The code matrix may then be seen to span a subset of a multi-dimensional real lattice Λ whose generator matrix is $\mathbb{G}$. A key parameter to determine the SNR efficiency of a given multi-dimensional constellation is its constellation shaping gain γ_s [35] which is completely determined by the lattice bounding region $\mathcal{R}$.

It has been shown in [35] that the lattice bounding region $\mathcal{R}$ that maximizes the shaping gain is a hyper-sphere and that the corresponding shaping gain approaches 1.53 dB as the number of dimensions of the hypersphere tends to infiniti. Unfortunately, due the prohibitively high implementation complexity of the lattice with spherical bounding region, one needs to resort to the *cubic* lattice [1] which is easily implemented and exhibits no shaping loss $\gamma_s = 0$ dB. A STBC that encodes

[1]The term cubic in this context refers generally to a hypercube not necessary in three dimensions

$2K$ real symbols is said to have the cubic shaping property if its real generator matrix $\mathbb{G}$ is such that[14]:

$$\mathbb{G}^T\mathbb{G} = \alpha\mathbf{I}_{2K} \tag{2.36}$$

where $\alpha = \text{tr}\left(\mathbf{A}_k^H\mathbf{A}_k\right),\ k = 1,\ldots,2K$. From (2.35), it is easily noticed that the cubic shaping property preserves the average transmitted power. The condition in (2.36) may be written in terms of the complex generator matrix $\mathbf{G}$ as:

$$\Re\left\{\mathbf{G}^H\mathbf{G}\right\} = \alpha\mathbf{I}_{2K} \tag{2.37}$$

where $\mathbb{G} = \tilde{\mathbf{G}}$.

2.4 Known families of STBCs

In this section we review some of the important code constructions, beginning by the orthogonal STBCs.

2.4.1 Orthogonal STBCs

Orthogonal STBCs are characterized by their linear worst-case decoding complexity at the receiver, that is, the transmitted complex symbols can be decoded separately without any loss of performance. Mathematically speaking a unitary STBC that encodes $2K$ real symbols is said to be orthogonal iff its code matrix $\mathbf{X}$ satisfies [66, 60]:

$$\mathbf{X}^H\mathbf{X} = \sum_{i=1}^{2K} x_i^2\mathbf{I}_{N_t}. \tag{2.38}$$

The above condition implies that the code matrix $\mathbf{X}$ is columnwise orthogonal which implies in turns that the real equivalent channel matrix $\tilde{\boldsymbol{\mathcal{H}}}$ is columnwise orthogonal hence the name *orthogonal* STBC. This can be seen from the following: thanks to (2.3), one may re-write (2.38) in terms of the STBC's weight matrices as:

$$\mathbf{A}_i^H\mathbf{A}_j + \mathbf{A}_j^H\mathbf{A}_i = 2\delta_{ij}\mathbf{I}_{N_t},\ i,j = 1,\ldots,2K \tag{2.39}$$

if $\boldsymbol{\hbar}_i$ denotes the i'th column of the equivalent channel matrix $\boldsymbol{\mathcal{H}}$ in (2.6), one has:

$$\begin{aligned}\boldsymbol{\hbar}_k^H\tilde{\mathbf{h}}_l + \boldsymbol{\hbar}_l^H\tilde{\mathbf{h}}_k &= \text{vec}(\mathbf{H})^H\Big[(\mathbf{I}_{N_r}\otimes\mathbf{A}_k)^H(\mathbf{I}_{N_r}\otimes\mathbf{A}_l) + (\mathbf{I}_{N_r}\otimes\mathbf{A}_l)^H(\mathbf{I}_{N_r}\otimes\mathbf{A}_k)\Big]\text{vec}(\mathbf{H})\\ &= \text{vec}(\mathbf{H})^H\left[\mathbf{I}_{N_r}\otimes(\mathbf{A}_k^H\mathbf{A}_l + \mathbf{A}_l^H\mathbf{A}_k)\right]\text{vec}(\mathbf{H})\\ &= 0,\ \forall\, k\neq l\end{aligned}$$

In other words, we have:

$$\Re\left\{\boldsymbol{\hbar}_k^H \boldsymbol{\hbar}_l\right\} = 0 \; \forall \; k \neq l \tag{2.40}$$

In terms of the columns of the real equivalent channel matrix $\tilde{\boldsymbol{\mathcal{H}}}$ (2.7) namely $\tilde{\boldsymbol{\hbar}}$, the above reduces to

$$\tilde{\boldsymbol{\hbar}}_k^T \tilde{\boldsymbol{\hbar}}_l = 0 \; \forall \; k \neq l. \tag{2.41}$$

The orthogonality of the columns of $\tilde{\boldsymbol{\mathcal{H}}}$ implies that the upper triangular matrix $\mathbf{R}$ in (2.11) is diagonal. Therefore the ML metric of an orthogonal STBC that encodes $2K$ real symbols may be expressed as:

$$\begin{aligned}\sum_{i=1}^{2K} |y'_i - \sum_{j=i}^{2K} r_{i,j}\hat{x}_j|^2 =& \sum_{i=1}^{2K} |y'_i - \sum_{i=1}^{2K} r_{i,i}\hat{x}_i|^2 \\ =& |y'_1 - r_{1,1}\hat{x}_1|^2 + |y'_2 - r_{2,2}\hat{x}_2|^2 \ldots |y'_{2K} - r_{2K,2K}\hat{x}_{2K}|^2.\end{aligned} \tag{2.42}$$

Contrary to the first impression from (2.42), the real symbols cannot be decoded separately for general constellations. That is in practical communication systems, the transmitted symbols are drawn from complex constellations and thus the code matrix $\mathbf{X}$ can be seen to encode K complex symbols s_i where x_{2i-1} and x_{2i} are the corresponding real and imaginary parts respectively with $i = 1, \ldots, K$. If the complex symbols s_i are drawn from a general constellation (e.g. PSK or HEX constellations), the corresponding real and imaginary parts have to be jointly decoded and the worst-case decoding complexity is $\mathcal{O}(M)$, with M is the size of the constellation. On the other hand, if the complex symbols s_i are drawn from a rectangular QAM constellations, the ML decoding process of each complex symbol s_i reduces to separate detection of the real and imaginary parts and the orthogonal STBC can be decoded via $2K$ hard PAM slicers as illustrated below:

$$x_i^{\text{ML}} = \text{sign}\left(y'_i / r_{i,i}\right) \times \min\left[\left|2\,\text{round}\Big(\left(y'_i/r_{i,i} - 1\right)/2\Big) + 1\right|, \sqrt{M} - 1\right] \; \forall i = 1, \ldots 2K. \tag{2.43}$$

It is worth noting that the above PAM slicer equations require only a fixed number of simple arithmetic operations, which does not grow with the size of the rectangular QAM constellation. Therefore, according to the definition of the worst-case decoding complexity, they are considered of complexity $\mathcal{O}(1)$. Moreover, from the

definition of the coding gain (2.25) and (2.38) one has:

$$\begin{aligned}\delta_{\mathbf{X}} = \min_{\substack{\mathbf{X}\neq\mathbf{X}' \\ \mathbf{X},\mathbf{X}'\in\mathcal{C}}} \det\left((\mathbf{X}-\mathbf{X}')^H(\mathbf{X}-\mathbf{X}')\right) &= \min_{\Delta\mathbf{X}\in\Delta\mathcal{C}/\{\mathbf{0}\}} \det\left((\Delta\mathbf{X})^H(\Delta\mathbf{X})\right) \\ &= \min_{\Delta\mathbf{s}\in(\Delta\mathcal{A})^{2K}/\{\mathbf{0}\}} \det\left(\sum_{i=1}^{2K}\Delta x_i^2\mathbf{I}_{N_t}\right) \\ &= \min_{\Delta\mathbf{s}\in(\Delta\mathcal{A})^{2K}/\{\mathbf{0}\}} \left(\sum_{i=1}^{2K}\Delta x_i^2\right)^{N_t} \\ &= \min_{\Delta x\in\Delta\mathcal{A}/\{0\}} \left(\Delta x^{2N_t}\right) \\ &= d_{\min}^{2N_t}\end{aligned} \tag{2.44}$$

where $\Delta\mathbf{X} = \mathbf{X} - \mathbf{X}'$, $\Delta\mathcal{C}$ (resp. $\Delta\mathcal{A}^{2K}$) is the code matrix difference codebook (resp. the vector space spanned by the information vector difference) and $d_{\min}$ denotes the minimum distance in the underlying constellation (e.g. Fig 2.2). If one considers unnormalized QAM constellations, $d_{\min}$ is constant and is equal to 2 which means that the orthogonal STBCs have the NVD property. An example of

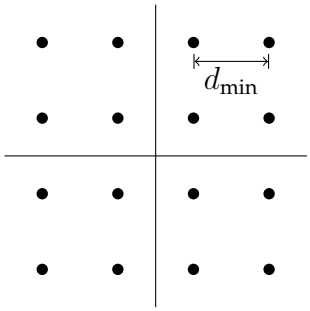

Figure 2.2: $d_{\min}$ for a 16-QAM constellation

orthogonal STBCs is the elegant 2×2 alamouti code whose code matrix takes the form:

$$\mathbf{X} = \begin{bmatrix} s_1 & s_2 \\ -s_2^* & s_1^* \end{bmatrix} \tag{2.45}$$

The question about the existence of orthogonal STBCs for an arbitrary number of transmit antennas has been addressed in the literature from several perspectives, namely the Hurwitz-Radon matrices [66] and the Clifford Algebra [60]. In [66], the authors proposed rate-1/2 orthogonal STBCs for any number of transmit antennas greater than four at the expense of an exponentially growing delay. On the other hand, in [60] the authors restricted themselves to square orthogonal designs

and transformed the problem of finding the maximal-rate orthogonal STBC for N_t transmit antennas into finding the maximum number of $N_t \times N_t$ unitary representation of the Clifford algebra generators. Due to their importance in this thesis, the properties of the Clifford algebra generators matrix representation will be outlined in the following.

The defining relation of the generators of the Clifford algebra over $\mathbb{R}$ is:

$$\gamma_i \gamma_j + \gamma_j \gamma_i = -2\delta_{ij} \mathbb{1} \tag{2.46}$$

The above equation can be split in two equations:

$$\gamma_i^2 = -\mathbb{1} \tag{2.47}$$

$$\gamma_i \gamma_j = -\gamma_j \gamma_i \, \forall i \neq j. \tag{2.48}$$

The link between (2.39) and (2.46) can be easily noticed by introducing a new variable $\boldsymbol{\gamma}_k, \ k = 1, \ldots, 2K$ such that [60]:

$$\boldsymbol{\gamma}_k = \mathbf{A}_1^H \mathbf{A}_k, \ k = 1, \ldots, 2K. \tag{2.49}$$

Consequently, one has:

$$\boldsymbol{\gamma}_1 = \mathbf{I} \tag{2.50}$$

and

$$\boldsymbol{\gamma}_k^H = -\boldsymbol{\gamma}_k, \ k = 2, \ldots, 2K \tag{2.51}$$

$$\boldsymbol{\gamma}_k^2 = -\mathbf{I}, \ k = 2, \ldots, 2K \tag{2.52}$$

$$\boldsymbol{\gamma}_i \boldsymbol{\gamma}_j = -\boldsymbol{\gamma}_j \boldsymbol{\gamma}_i, \ 2 \leq i \neq j \leq 2K. \tag{2.53}$$

The last two conditions are exactly the defining relations of the Clifford algebra generators over $\mathbb{R}$, with the only difference that the new defined matrices $\boldsymbol{\gamma}_k, \ k = 2, \ldots, 2K$ are required to be anti-hermitian, thus unitary. Therefore one can easily determine the maximum achievable rate of square orthogonal STBCs for N_t transmit antennas by finding the maximum number of $N_t \times N_t$ unitary representation of Clifford algebra generators. It has been proved in [60] that for any number of transmit antennas that is a power of two $N_t = 2^a$ there are exactly $2a + 1$ unitary matrix representations of the Clifford algebra generators. For a number of

transmit antennas that is not a power of two, the matrix representations are directly obtained from those of the nearest higher number of transmit antennas that is a power of two by removing the appropriate number of column. For instance, the matrix representations for three transmit antennas are obtained from those for four antennas by simply removing a column. Therefore, for an arbitrary number of transmit antennas N_t, the corresponding rate is equal to:

$$R = \frac{\lceil \log_2 N_t \rceil + 1}{2^{\lceil \log_2 N_t \rceil}}. \tag{2.54}$$

The matrix representations of γ_i denoted $\mathcal{R}(\gamma_i)$ for the $2^a \times 2^a$ case are obtained as [60]:

$$\begin{aligned}
\boldsymbol{\gamma}_2 &= \mathcal{R}(\gamma_1) = \pm j \underbrace{\sigma_3 \otimes \sigma_3 \ldots \otimes \sigma_3}_{a} \\
\boldsymbol{\gamma}_3 &= \mathcal{R}(\gamma_2) = \mathbf{I}_{2^{a-1}} \otimes \sigma_1 \\
\boldsymbol{\gamma}_4 &= \mathcal{R}(\gamma_3) = \mathbf{I}_{2^{a-1}} \otimes \sigma_2 \\
&\vdots \\
\boldsymbol{\gamma}_{2k+1} &= \mathcal{R}(\gamma_{2k}) = \mathbf{I}_{2^{a-k}} \otimes \sigma_1 \underbrace{\otimes \sigma_3 \otimes \sigma_3 \ldots \otimes \sigma_3}_{k-1} \\
\boldsymbol{\gamma}_{2k+2} &= \mathcal{R}(\gamma_{2k+1}) = \mathbf{I}_{2^{a-k}} \otimes \sigma_2 \underbrace{\otimes \sigma_3 \otimes \sigma_3 \ldots \otimes \sigma_3}_{k-1} \\
&\vdots \\
\boldsymbol{\gamma}_{2a+1} &= \mathcal{R}(\gamma_{2a}) = \sigma_1 \otimes \underbrace{\sigma_3 \otimes \sigma_3 \ldots \sigma_3}_{a-1} \\
\boldsymbol{\gamma}_{2a+2} &= \mathcal{R}(\gamma_{2a+1}) = \sigma_2 \otimes \underbrace{\sigma_3 \otimes \sigma_3 \ldots \sigma_3}_{a-1}
\end{aligned} \tag{2.55}$$

where

$$\sigma_1 = \begin{bmatrix} 0 & 1 \\ -1 & 0 \end{bmatrix},\ \sigma_2 = \begin{bmatrix} 0 & j \\ j & 0 \end{bmatrix},\ \sigma_3 = \begin{bmatrix} 1 & 0 \\ 0 & -1 \end{bmatrix} \tag{2.56}$$

The weight matrices are directly obtained from the linear representations of the generators of the Clifford algebra through (2.49). It suffices to choose an arbitrary unitary matrix $\mathbf{A}_1$ and then the rest of the weight matrices can be evaluated as:

$$\mathbf{A}_k = \mathbf{A}_1 \boldsymbol{\gamma}_k,\ k = 1, \ldots, 2a+2 \tag{2.57}$$

For simplicity, one can take $\mathbf{A}_1 = \mathbf{I}$, then the weight matrices of the orthogonal STBC coincide with the linear representations of the Clifford algebra generators. Throughout this thesis, the matrices $\mathbf{R}_0, \mathbf{R}_1, \ldots, \mathbf{R}_{2a+1}$ where $\mathbf{R}_i = \boldsymbol{\gamma}_{i+1},\ i =$

$0, \ldots, 2a+1$ will denote the square weight matrices for the case of 2^a transmit antennas unless otherwise stated. The properties of the matrices $\mathbf{R}_i,\ i = 1, \ldots, 2a+1$ can be summarized as follows:

$$\mathbf{R}_i^H = -\mathbf{R}_i,\ \mathbf{R}_i^2 = -\mathbf{I},\ \forall 1 \leq i \leq 2a+1, \text{ and } \mathbf{R}_i\mathbf{R}_j + \mathbf{R}_j\mathbf{R}_i = \mathbf{0},\ \forall 1 \leq i \neq j \leq 2a+1. \tag{2.58}$$

For the case of four transmit antennas, we obtain the rate-3/4 orthogonal STBC whose code matrix is given by:

$$\mathbf{X}_{3/4} = \begin{bmatrix} s_1 & s_2 & s_3 & 0 \\ -s_2^* & s_1^* & 0 & -s_3 \\ -s_3^* & 0 & s_1^* & s_2 \\ 0 & s_3^* & -s_2^* & s_1 \end{bmatrix} \tag{2.59}$$

and for the case of eight transmit antennas we obtain the rate-1/2 orthogonal STBC whose code matrix is given by:

$$\mathbf{X}_{1/2} = \begin{bmatrix} s_1 & s_2 & s_3 & 0 & s_4 & 0 & 0 & 0 \\ -s_2^* & s_1^* & 0 & -s_3 & 0 & -s_4 & 0 & 0 \\ -s_3^* & 0 & s_1^* & s_2 & 0 & 0 & -s_4 & 0 \\ 0 & s_3^* & -s_2^* & s_1 & 0 & 0 & 0 & s_4 \\ -s_4^* & 0 & 0 & 0 & s_1^* & s_2 & s_3 & 0 \\ 0 & s_4^* & 0 & 0 & -s_2^* & s_1 & 0 & -s_3 \\ 0 & 0 & s_4^* & 0 & -s_3^* & 0 & s_1 & s_2 \\ 0 & 0 & 0 & -s_4^* & 0 & s_3^* & -s_2^* & s_1^* \end{bmatrix} \tag{2.60}$$

In [67], the question about the existence of orthogonal STBCs was addressed in a more general framework where the code matrices are allowed to be rectangular and it has been proven that for a number of transmit antennas $N_t = 2a-1$ and $N_t = 2a$ where $a \in \mathbb{N}$ the maximal possible rate equals $\frac{a+1}{2a}$ whether the code matrix is square or rectangular.

2.4.2 Diagonal Algebraic STBCs

In an attempt to overcome the rate-limitation of orthogonal STBCs through the relaxation of the linear worst-case decoding complexity while retaining the full-diversity property, the so called Diagonal Algebraic Space-Time (DAST) codes were proposed [28]. A DAST code typically sends the information symbols along the diagonal of the code matrix, hence the name *diagonal*, and in order to preserve the full diversity the information symbols are drawn from a rotated constellation

rather than from conventional ones. These full-diversity rotations [68] are obtained through algebraic techniques, hence the name *algebraic*. Mathematically speaking, a DAST code matrix for N_t transmit antennas takes the following form:

$$\mathcal{D}_{N_t} = \text{diag}\left(\mathbf{s}'\right) \tag{2.61}$$

where $\mathbf{s}' = \left(x'_1, \ldots, x'_{N_t}\right)^T$, $\left(x'_1, \ldots, x'_{N_t}\right)^T = \mathbf{U}\left(x_1, \ldots, x_{N_t}\right)^T$, $\mathbf{U}$ is the appropriate $N_t \times N_t$ full-diversity rotation matrix [68] and $\left(x_1, \ldots, x_{N_t}\right)^T$ are drawn from conventional QAM constellations. In the special case where N_t is equal to 1,2 or a multiple of four, the DAST code is expressed as:

$$\mathcal{D}_{N_t} = \boldsymbol{\mathcal{H}}_{N_t}\text{diag}\left(\mathbf{s}'\right) \tag{2.62}$$

where $\boldsymbol{\mathcal{H}}_{N_t}$ denotes the $N_t \times N_t$ Hadamard matrix. The choice of the Hadamard matrices is driven by the fact that for matrices with entries restricted to be $\in \{\pm 1\}$, the Hadamard matrices are the only matrices that maximize the coding gain of the DAST codes[2][28]. The restriction for the linear transformation matrix entries to be $\in \{\pm 1\}$ guarantees that the transmitted power from the different antennas is equal at any time instant. Clearly, The DAST codes can achieve rate-one for an arbitrary number of transmit antennas given that the corresponding rotation matrix exists. The full-diversity property of the DAST codes follows immediately from the fact that the full-diversity rotation matrices are designed to guarantee that all the components of the rotated vectors are unique, in other words, the difference between two rotated vectors cannot have any zero component, which implies that the $\mathbf{X}\left(\Delta\mathbf{s}'\right)$ matrix is always of full-rank $\forall \Delta\mathbf{s} \neq \mathbf{0}$. An important parameter of full diversity rotations is the minimum product distance $d_{\text{p,min}}$ defined as:

$$d_{\text{p,min}} = \min_{\Delta\mathbf{s}' \in (\Delta\mathcal{A})^{N_t} \setminus \{\mathbf{0}\}} \prod_{i=1}^{N_t} |\Delta x'_i|. \tag{2.63}$$

However, from (2.25) one has $G_c = d^2_{\text{p,min}}$, and therefore full-diversity rotation matrices guarantee a high coding gain as they are designed to maximize the minimum

[2]This follows directly from the famous Hadamard determinant inequality which states that for any $n \times n$ matrix $\mathbf{N}$ with entries $\in \{\pm 1\}$ one has:

$$|\det\left(\mathbf{N}\right)| \leq n^{n/2}$$

and that the equality holds only for matrices with orthogonal columns or equivalently Hadamrad matrices of order n.

product distance. Examples of DAST codes for two and four transmit antennas are given below:

$$\mathcal{D}_2 = \begin{bmatrix} x_1' & x_1' \\ x_2' & -x_2' \end{bmatrix} \tag{2.64}$$

where $(x_1', x_2')^T = \mathbf{U}\,(x_1, x_2)^T$ and $\mathbf{U}$ is the optimal 2×2 rotation matrix [68].

$$\mathcal{D}_4 = \begin{bmatrix} x_1' & x_1' & x_1' & x_1' \\ x_2' & -x_2' & x_2' & -x_2' \\ x_3' & x_3' & -x_3' & -x_3' \\ x_4' & -x_4' & -x_4' & x_4' \end{bmatrix} \tag{2.65}$$

where $(x_1', x_2', x_3', x_4')^T = \mathbf{U}\,(x_1, x_2, x_3, x_4)^T$ and $\mathbf{U}$ is the optimal 4×4 rotation matrix [68].

2.4.3 Threaded Algebraic STBCs

The Threaded Algebraic Space-Time (TAST) codes can offer rates as high as the number of transmit antennas by multiplexing L DAST codes such that they occupy disjoint threads giving rise to a new rate-L STBC. A thread in a $n \times n$ matrix corresponds to n entries such that in every column or row there exists only one non-zero entry. An example of different threads in the case of four transmit antennas is depicted is depicted in Fig 2.3 where the 1's mark the entries belonging to the first thread, the 2's mark the entries belonging to the second thread and so on. The rate-L TAST code for N_t transmit antennas may be expressed as:

1	2	3	4
4	1	2	3
3	4	1	2
2	3	4	1

Figure 2.3: $L = 4$ threads

$$\mathcal{T}_{N_t,L} = \sum_{i=1}^{L} \phi_i \text{diag}\,(\mathbf{s}_i')\,\mathbf{J}^{i-1} \tag{2.66}$$

where $\left\{\phi_1 = 1, \phi_2 = \phi^{1/N_t}, \ldots, \phi_L = \phi^{(L-1)/N_t}\right\}$, $\mathbf{s}_i' = \left(x_{i1}', \ldots, x_{iN_t}'\right)^T$, $\mathbf{J} = [\mathbf{e}_{N_t}, \mathbf{e}_1, \ldots, \mathbf{e}_{N_t-1}]$ and $\mathbf{e}_i$ is the i'th column of the $N_t \times N_t$ identity matrix. Thanks to [29],

it can be proved that the coding gain of (2.66) can be represented as a polynomial of degree $L-1$ of ϕ with coefficients belonging to the algebraic number field $\mathbb{Q}(\theta)$ containing the rotation matrix $\mathbf{U}$ elements. Therefore, choosing ϕ to be transcendental or algebraic of degree greater than or equal to L over $\mathbb{Q}(\theta)$ is a sufficient condition to guarantee the full-diversity of the resulting TAST code. However, generally speaking, the TAST codes have an evanescent coding gain as the Diophantine numbers $\left\{1, \phi^1, \ldots, \phi^{L-1}\right\}$ become better approximated when considering larger constellations which prevents the TAST codes from achieving the NVD property [29]. For instance, the full-rate TAST codes for two and three transmit antennas are given by:

$$\mathcal{T}_{2,2} = \begin{bmatrix} x'_{11} & \phi^{1/2} x'_{22} \\ \phi^{1/2} x'_{21} & x'_{12} \end{bmatrix}. \tag{2.67}$$

where $(x'_{i1}, x'_{i2})^T = \mathbf{U}(x_{i1}, x_{i2})^T, i = 1, 2$, $\mathbf{U}$ is the optimal 2×2 rotation matrix in [68] and $\phi = e^{j\pi/6}$.

$$\mathcal{T}_{3,3} = \begin{bmatrix} x'_{11} & \phi^{2/3} x'_{32} & \phi^{1/3} x'_{23} \\ \phi^{1/3} x'_{21} & x'_{12} & \phi^{2/3} x'_{33} \\ \phi^{2/3} x'_{31} & \phi^{1/3} x'_{22} & x'_{13} \end{bmatrix}. \tag{2.68}$$

where $(x'_{i1}, x'_{i2}, x'_{i3})^T = \mathbf{U}(x_{i1}, x_{i2}, x_{i3})^T, i = 1, 2, 3$, $\mathbf{U}$ is the optimal 3×3 rotation matrix in [68] and $\phi = e^{j\pi/12}$.

2.4.4 Perfect STBCs

Perfect STBCs combines several highly desirable properties, namely the full-rate, the NVD, cubic shaping, and the uniformity of the transmitted average energy per antenna . The first proposed 2×2 perfect code was unquestionably the golden code proposed by P. Dayal *et al.* [69], by H. Yao *et al.* [70] and then independently rediscovered by J.-C. Belfiore *et al.* [71] from an algebraic perspective that enabled the extension of golden code in a more general framework for up to six antennas [30] and subsequently to an arbitrary number of transmit antennas [72]. The rate-L perfect STBC matrix $\mathbf{X}$ for N_t transmit antennas may be expressed in a similar form to the TAST codes as:

$$\mathbf{X} = \sum_{i=1}^{L} \mathrm{diag}(\mathbf{M}\mathbf{s}_i)\, \mathbf{J}^{i-1} \tag{2.69}$$

with the difference that $\mathbf{M}$ is the cubic shaping matrix, $\mathbf{s} = (x_1, x_2, x_3, x_4)^T$, $(x_1, \ldots, x_{N_t})^T$ are drawn from conventional QAM or HEX constellations, and $\mathbf{J} = [\gamma \mathbf{e}_{N_t}, \mathbf{e}_1, \ldots, \mathbf{e}_{N_t-1}]$. In the case of two transmit antennas[20]:

$$\mathbf{M} = \begin{bmatrix} 0.4472 - 0.2764i & 0.7236 - 0.4472i \\ 0.7236 + 0.4472i & -0.2764 - 0.4472i \end{bmatrix}, \ \gamma = i \tag{2.70}$$

The corresponding coding gain equals 3.2 for unnormalized QAM constellations. Whereas in the case of four transmit antennas [20]:

$$\mathbf{M} = \begin{bmatrix} 0.258 - 0.312i & 0.346 - 0.418i & -0.418 + 0.505i & -0.214 + 0.258i \\ 0.258 + 0.087i & 0.472 + 0.16i & 0.16 + 0.054i & 0.763 + 0.258i \\ 0.258 + 0.214i & -0.505 - 0.418i & -0.418 - 0.346i & 0.312 + 0.258i \\ 0.258 - 0.763i & -0.054 + 0.16i & 0.16 - 0.472i & -0.087 + 0.258i \end{bmatrix}, \ \gamma = i \tag{2.71}$$

The corresponding coding gain equals 0.2276 for unnormalized QAM constellations

2.4.5 Conclusions

In this chapter we reviewed the system model, the sphere decoder, and the design criteria of the STBCs over Rayleigh quasi-static fading channels. We outlined several families of STBCs namely the orthogonal STBCs, DAST codes, TAST codes, and perfect STBCs. In terms of the design criteria, the orthogonal STBCs achieve the NVD property, satisfy the cubic shaping property at the expense of a limitation of the MIMO channel ergodic capacity and a severe loss of rate with exception of the Alamouti code in the 2×1 MIMO configuration. The DAST codes may achieve the NVD property, the information loss is smaller than that of the orthogonal STBCs and preserve the cubic shaping property while their rate is upper limited by one complex symbol per channel use for an arbitrary number of transmit antennas.

The TAST codes may provide the full diversity, but their coding gain is generally shrinking with the increasing size of the QAM constellation hence the TAST codes do not guarantee the NVD property. On the other hand, the TAST codes may achieve arbitrary rate up to N_t complex symbols per channel use for N_t number of transmit antennas, they preserve the cubic shaping property, and they are information lossless in the case of $L = N_t \leq N_r$.

The perfect STBCs were conceived to guarantee the NVD and the cubic shaping property and they may achieve arbitrary rates up to N_t complex symbol per channel use for N_t transmit antenna. As for the TAST codes, the perfect codes are information lossless in the case of $L = N_t \leq N_r$.

Chapter 3

Low-Complexity STBCs

In the previous chapter, we have outlined the main design criteria for a STBC in order to provide good performance over flat quasi-static Rayleigh fading channels. However, for practical considerations other desirable criteria have to be taken into account, mainly the low-complexity decodability. This leads us to the following definition:

Definition 3.1 *A STBC that encodes $2K$ real symbols drawn from a complex constellation of size M is said to be low-complexity decodable iff its worst-case decoding complexity is lower than M^K.*

The need for low-complexity decodable STBCs seems to be inevitable in the case of high-rate communications over MIMO systems employing a number of antennas higher than two. This is because despite their low worst-case decoding complexity that grows only linearly with the size of the underlying constellation, orthogonal STBCs suffer from a severe rate limitation for more than two antennas. On the other hand, the full-rate alternatives to orthogonal STBCs, namely the TAST and perfect codes have generally a prohibitively high worst-case decoding complexity and high average decoding complexity when employing a sphere decoder.

Arguably, the first proposed low-complexity rate-1 code for the case of four transmit antennas is the Quasi-Orthogonal (QO)STBC originally proposed by H. Jafarkhani [36] and later optimized through constellation rotation to provide full diversity [37, 38]. The QOSTBC partially relaxes the orthogonality conditions by allowing two complex symbols to be jointly detected. Subsequently, rate-one, full-diversity QOSTBCs were proposed for an arbitrary number of transmit antennas

that subsume the original QOSTBC as a special case [39]. In this general framework, the *quasi-orthgonality* stands for decoupling the transmitted symbols into two groups of the same size.

However, STBCs with lower decoding complexity may be obtained through the concept of multi-group decodability principle laid by the S. Karmakar *et al.* in [19, 16]. Indeed, the multi-group decodability generalizes the quasi-orthogonality by allowing the codeword of symbols to be decoupled into more than two groups not necessarily of the same size. Moreover, one can obtain rate-one, full-diversity 4-group decodable STBCs for an arbitrary number of transmit antennas [40].

Another important concept that allows the design of low-complexity STBCs is the conditional detection [41], in which the ML detection is carried out on two steps. The first step consists of evaluating the ML estimation of a subset of the transmitted symbols say $(x_1, x_2, \ldots, x_k)$ conditioned on a given value of the rest of the symbols $(\hat{x}_{k+1}, \hat{x}_{k+2}, \ldots, \hat{x}_{2K})$ that we may note by $\Big(x_1^{\mathrm{ML}}, x_2^{\mathrm{ML}}, \ldots, x_k^{\mathrm{ML}} | \hat{x}_{k+1}, \hat{x}_{k+2}, \ldots, \hat{x}_{2K}\Big)$. In the second step, the receiver minimizes the ML metric only over all the possible values of $(x_{k+1}, x_{k+2}, \ldots, x_{2K})$. Generally, this procedure has no effect on the overall worst-case decoding complexity unless the weight matrices corresponding to the subset $(x_1, x_2, \ldots, x_k)$ enjoy a low-complexity structure. In this case, the overall worst-case decoding complexity may be significantly reduced. This reduction technique refers to fast decoding.

Recently, STBCs that combine the multi-group decodability and the fast decodability, namely the Fast-Group Decodable (FGD) codes, were proposed in [18]. These codes are g-group decodable such that each group of symbols is fast decodable. This chapter is devoted to thoroughly discuss these three families of low-complexity STBCs as well as their corresponding worst-case decoding complexity order.

3.1 Multi-group decodable codes

Multi-group decodable STBCs are designed to significantly reduce the worst-case decoding complexity by allowing separate detection of disjoint groups of symbols

without any loss of performance. This is achieved iff the ML metric can be expressed as a sum of terms depending on disjoint groups of symbols. This suggests the following definition:

Definition 3.2 *A STBC that encodes $2K$ real symbols is said to be g-group decodable iff its ML metric can be expressed as a sum of g terms that depend on disjoint subsets of the transmitted symbols [16, 19].*

The conditions to be satisfied by the weight matrices of a STBC in order to be g-group decodable are derived in [19, 16] from the ML decision rule of the system model (2.1) and are outlined here for self-completeness. Assuming that perfect CSI is available at the receiver side, the ML estimated codeword is given by:

$$\begin{aligned}\mathbf{X}^{\text{ML}} &= \arg\min_{\mathbf{X}\in\mathcal{C}} \|\mathbf{Y}-\mathbf{X}\mathbf{H}\|_F^2 \\ &= \arg\min_{\mathbf{X}\in\mathcal{C}} \text{tr}\left[(\mathbf{Y}-\mathbf{X}\mathbf{H})^H(\mathbf{Y}-\mathbf{X}\mathbf{H})\right]\end{aligned} \tag{3.1}$$

If $\mathbf{X}$ can be expressed as a sum of sub-codes $\mathbf{X}_i,\ i=1,\dots g$ such that:

$$\mathbf{X}=\sum_{i=1}^{g}\mathbf{X}_i,\ \mathbf{X}_i^H\mathbf{X}_j+\mathbf{X}_j^H\mathbf{X}_i=\mathbf{0},\ 1\le i\ne j\le g \tag{3.2}$$

(3.1) reduces to:

$$\begin{aligned}\mathbf{X}^{\text{ML}} &= \arg\min_{\mathbf{X}\in\mathcal{C}} \text{tr}\left[\mathbf{Y}^H\mathbf{Y}-\sum_{i=1}^{g}\mathbf{Y}^H\mathbf{X}_i\mathbf{H}-\mathbf{H}^H\mathbf{X}_i^H\mathbf{Y}+\mathbf{H}^H\mathbf{X}_i^H\mathbf{X}_i\mathbf{H}\right] \\ &= \sum_{i=1}^{g}\arg\min_{\mathbf{X}_i\in\mathcal{C}_i} \text{tr}\left[\mathbf{Y}^H\mathbf{Y}-\mathbf{Y}^H\mathbf{X}_i\mathbf{H}-\mathbf{H}^H\mathbf{X}_i^H\mathbf{Y}+\mathbf{H}^H\mathbf{X}_i^H\mathbf{X}_i\mathbf{H}\right]-\sum_{i=1}^{g-1}\text{tr}\left[\mathbf{Y}^H\mathbf{Y}\right]\end{aligned} \tag{3.3}$$

where $\mathcal{C}_i$ denotes the codebook of the i'th sub-code. Noting that the last term of the above is constant for a given received signal matrix, the ML decision rule may be expressed as:

$$\mathbf{X}^{\text{ML}}=\sum_{i=1}^{g}\arg\min_{\mathbf{X}_i\in\mathcal{C}_i}\|\mathbf{Y}-\mathbf{X}_i\mathbf{H}\|_F^2. \tag{3.4}$$

In terms of weight matrices, it is straightforward to verify that (3.2) is equivalent to:

$$\mathbf{A}_k^H\mathbf{A}_l+\mathbf{A}_l^H\mathbf{A}_k=\mathbf{0},\ \forall\mathbf{A}_k\in\mathcal{G}_i,\ \mathbf{A}_l\in\mathcal{G}_j,\ 1\le i\ne j\le g,\ |\mathcal{G}_i|=n_i,\sum_{i=1}^{g}n_i=2K. \tag{3.5}$$

where $\mathcal{G}_i$ is the set of weight matrices associated to the i'th group of symbols. For instance if a STBC that encodes $2K$ real symbols is g-group decodable, its worst-case decoding complexity order can be reduced from $\sqrt{M}^{2K-1}$ to $\sum_{i=1}^{g}\sqrt{M}^{n_i-1}$ where M is the size of the used square QAM constellation. If a real Sphere Decoder (SD) is used in conjunction with hard PAM slicers, g-group decodability reduces to splitting the original tree with $2K-1$ levels to g smaller trees each with n_i-1 levels. In the special case of orthogonal STBCs, the worst-case decoding complexity is $\mathcal{O}(1)$, as the PAM slicers (2.43) need only a fixed number of arithmetic operations irrespectively of the square QAM constellation size. In order to deduce the structure of the the real upper triangular matrix $\mathbf{R}$ (2.11) in the case of g-group decodable codes, recall from (2.41) that:

$$\mathbf{A}_k^H\mathbf{A}_l+\mathbf{A}_l^H\mathbf{A}_k=\mathbf{0}\;\forall k\neq l\Rightarrow\tilde{\boldsymbol{\hbar}}_k^T\tilde{\boldsymbol{\hbar}}_l=0\;\forall k\neq l \tag{3.6}$$

where $\tilde{\boldsymbol{\hbar}}_k$ denotes the k'th column of the real equivalent channel matrix $\tilde{\boldsymbol{\mathcal{H}}}$ (2.7). Accordingly, in the g-group decodable case (3.5) the above becomes:

$$\tilde{\boldsymbol{\hbar}}_k^T\tilde{\boldsymbol{\hbar}}_l=0\;\forall k\in\Xi_i,\;l\in\Xi_j,\;i\neq j \tag{3.7}$$

here, Ξ_k denotes the set of indexes of the weight matrices corresponding to the k'th group. Applying the QR decomposition on the real equivalent channel matrix $\tilde{\boldsymbol{\mathcal{H}}}$ the above implies:

$$\tilde{\boldsymbol{\hbar}}_k^T\tilde{\boldsymbol{\hbar}}_l=0\Leftrightarrow\mathbf{r}_k^T\mathbf{r}_l=0\;\forall k\in\Xi_i,\;l\in\Xi_j,\;i\neq j \tag{3.8}$$

where $\mathbf{r}_i$ denotes the i'th column of the upper triangular matrix $\mathbf{R}$. Without any loss of generality, suppose that the real symbols are sorted such as $(x_1,\ldots,x_{n_1})$ corresponds to the first group of symbols, $(x_{n_1+1},\ldots,x_{n_1+n_2})$ corresponds to the second group of symbols, and so on. Thanks to the upper triangular nature of $\mathbf{R}$, it is straightforward to verify that $\mathbf{r}_k^T\mathbf{r}_1=0\Rightarrow\mathbf{r}_k(1)=0,\;\forall k\in\Xi_i,i=2,\ldots g$. Consequently, one has that $\mathbf{r}_k^T\mathbf{r}_2=0\Rightarrow\mathbf{r}_k(2)=0,\;\forall k\in\Xi_i,i=2,\ldots g$. Proceeding in the same order, it is easy to verify that $\mathbf{r}_k^T\mathbf{r}_l=0\Rightarrow\mathbf{r}_k(l)=0,\;\forall k\in\Xi_i,l\in\Xi_j,i>j$. In other words, the real upper triangular matrix $\mathbf{R}$ is a block diagonal matrix:

$$\mathbf{R}=\begin{bmatrix}\mathbf{R}_1&\mathbf{0}&\ldots&\mathbf{0}\\\mathbf{0}&\mathbf{R}_2&\ldots&\mathbf{0}\\\vdots&\vdots&\ddots&\vdots\\\mathbf{0}&\mathbf{0}&\ldots&\mathbf{R}_g\end{bmatrix} \tag{3.9}$$

where $\mathbf{R}_i$ is a $n_i \times n_i$ upper triangular matrix.

Besides its induced significant reduction in the worst-case decoding complexity, the multi-group decodability structure enables a simplified coding gain optimization as the global coding gain optimization problem turns into the optimization of the individual coding gain of each sub-code. This is illustrated in the following proposition:

Proposition 3.1 *If a STBC $\mathbf{X}$ is g-group decodable such that:*

$$\mathbf{X} = \sum_{i=1}^{g} \mathbf{X}_i,\ \mathbf{X}_i^H \mathbf{X}_j + \mathbf{X}_j^H \mathbf{X}_i = \mathbf{0},\ 1 \leq i \neq j \leq g \tag{3.10}$$

its coding gain $\delta_{\mathbf{X}}$ is expressed as:

$$\delta_{\mathbf{X}} = \min\left\{\delta_{\mathbf{X}_1}, \delta_{\mathbf{X}_2}, \ldots, \delta_{\mathbf{X}_g}\right\} \tag{3.11}$$

where $\delta_{\mathbf{X}_i}$ denotes the i'th sub-code's coding gain.

The proof follows directly from (3.5) and the Minkowski's determinant inequality [42].

Proof. Recalling the coding gain definition (2.25), one has:

$$\delta_{\mathbf{X}} = \min_{\substack{\mathbf{X} \neq \mathbf{X}' \\ \mathbf{x}, \mathbf{x}' \in \mathcal{C}}} \det\left[(\mathbf{X} - \mathbf{X}')^H (\mathbf{X} - \mathbf{X}')\right] = \min_{\Delta\mathbf{X} \in \Delta\mathcal{C}/\{\mathbf{0}\}} \det\left[(\Delta\mathbf{X})^H (\Delta\mathbf{X})\right] \tag{3.12}$$

Thanks to (3.5), the above reduces to:

$$\delta_{\mathbf{X}} = \min_{\Delta\mathbf{X} \in \Delta\mathcal{C}/\{\mathbf{0}\}} \det\left[\sum_{i=1}^{g} \Delta\mathbf{X}_i^H \Delta\mathbf{X}_i\right] \tag{3.13}$$

But from Minkowski's determinant inequality [42] one has:

$$(\det[\mathbf{A} + \mathbf{B}])^{1/n} \geq (\det[\mathbf{A}])^{1/n} + (\det[\mathbf{B}])^{1/n} \tag{3.14}$$

where $\mathbf{A}, \mathbf{B} \in \mathcal{M}_n$ are positive definite matrices. Therefore we may write:

$$\begin{aligned} \det\left[\sum_{i=1}^{g} \Delta\mathbf{X}_i^H \Delta\mathbf{X}_i\right] &\geq \left(\sum_{i=1}^{g} \left(\det\left[\Delta\mathbf{X}_i^H \Delta\mathbf{X}_i\right]\right)^{1/n}\right)^n \\ &= \sum_{i=1}^{g} \det\left[\Delta\mathbf{X}_i^H \Delta\mathbf{X}_i\right] + C \\ &\geq \sum_{i=1}^{g} \det\left[\Delta\mathbf{X}_i^H \Delta\mathbf{X}_i\right] \end{aligned} \tag{3.15}$$

where the last inequality follows from the fact that $C \geq 0$. Equality holds for the trivial case $\Delta\mathbf{X} = \mathbf{0}$ or $\Delta\mathbf{X} = \Delta\mathbf{X}_k$ and $\Delta\mathbf{X}_i = \mathbf{0}\ \forall 1 \leq i \neq k \leq g$. Thus we have:

$$\begin{aligned}\delta_{\mathbf{X}} =& \min\left\{\min_{\Delta\mathbf{X}_1 \in \Delta\mathcal{C}_1/\{\mathbf{0}\}} \det\left[\Delta\mathbf{X}_1^H \Delta\mathbf{X}_1\right], \ldots, \min_{\Delta\mathbf{X}_g \in \Delta\mathcal{C}_g/\{\mathbf{0}\}} \det\left[\Delta\mathbf{X}_g^H \Delta\mathbf{X}_g\right]\right\} \\ =& \min\left\{\delta_{\mathbf{X}_1}, \delta_{\mathbf{X}_2}, \ldots, \delta_{\mathbf{X}_g}\right\}\end{aligned} \tag{3.16}$$

which concludes the proof. □

An example of multi-group decodable STBCs is the rate-1 UW-4-group decodable codes for $2^a,\ a \in \mathbb{N}$ in [17]. For the case of four transmit antennas, the rate-1 4-group decodable code matrix may be expressed as:

$$\begin{bmatrix} x_1 - x_2 + ix_3 - ix_4 & x_5 - x_6 + ix_7 - ix_8 & 0 & 0 \\ -x_5 + x_6 + ix_7 - ix_8 & x_1 - x_2 - ix_3 + ix_4 & 0 & 0 \\ 0 & 0 & x_1 + x_2 - ix_3 - ix_4 & x_5 + x_6 + ix_7 + ix_8 \\ 0 & 0 & -x_5 - x_6 + ix_7 + ix_8 & x_1 + x_2 + ix_3 + ix_4 \end{bmatrix}$$

The corresponding four groups of symbols are: $\{x_1, x_2\}, \{x_3, x_4\}, \{x_5, x_6\}, \{x_7, x_8\}$. Accordingly, the worst-case decoding complexity is equal to $4\sqrt{M}$ for square QAM constellations and $4M$ for arbitrary constellations.

3.2 Fast-decodable codes

We define a Fast Decodable (FD) code to be a STBC which is conditionally g-group decodable. In other words, the code matrix of a FD STBC can be expressed as:

$$\mathbf{X}(\mathbf{s}) = \mathbf{X}_1(\mathbf{s}_1) + \mathbf{X}_2(\mathbf{s}_2) \tag{3.17}$$

where $\mathbf{X}_1(\mathbf{s}_1)$ is a g-group decodable code. This leads us to the following definition:

Definition 3.3 *A STBC that encodes $2K$ real symbols is said to be fast-decodable if its weight matrices are such that:*

$$\mathbf{A}_k^H \mathbf{A}_l + \mathbf{A}_l^H \mathbf{A}_k = \mathbf{0},\ \forall \mathbf{A}_k \in \mathcal{G}_i,\ \mathbf{A}_l \in \mathcal{G}_j,\ 1 \leq i \neq j \leq g,\ |\mathcal{G}_i| = n_i, \sum_{i=1}^{g} n_i = \kappa < 2K. \tag{3.18}$$

The above definition slightly generalizes the definition of fast-decodable codes in [14] where the where the fast-decodable code is restricted to be conditionally orthogonal, that is $n_1 = n_2 \ldots = n_g = 1$. The advantage of FD STBCs is that one can resort to the conditional detection to significantly reduce the worst-case decoding complexity. The first step consists of evaluating the conditioned ML estimate of s_1 for a given possible value of s_2 which we denote $\mathrm{s}_1^{\mathrm{ML}}|\hat{\mathrm{s}}_2$. In the second step, the decoder will have to minimize the ML metric only over all the possible values of s_2. For instance, if a STBC that encodes $2K$ real symbols is fast decodable, its corresponding worst-case decoding complexity order for square QAM constellations is reduced from $\sqrt{M}^{2K-1}$ to $\sqrt{M}^{2K-\kappa} \times \sum_{i=1}^{g} \sqrt{M}^{n_i-1}$. If the g-group-decodable code is orthogonal, the worst-case decoding complexity order is reduced to $\sqrt{M}^{2K-\kappa}$. The fast decodability reduces to the splitting of the last κ levels of the real SD tree into g smaller trees each with $n_i - 1,\ i = 1, \ldots, g$ levels. In the particular case of $n_i = 1,\ \forall i = 1, \ldots, g$ (i.e. the inner g-group decodable code is in fact an orthogonal STBC), the fast decodability reduces to the removal of the last κ levels of the real valued tree.

Without any loss of generality, we assume that the symbols are sorted such that the first κ real symbols correspond to the g-group decodable code with $(x_1, \ldots, x_{n_1})$ corresponding to the first group of symbols, $(x_{n_1+1}, \ldots, x_{n_1+n_2})$ corresponding to the second group of symbols, and so on. Proceeding in the same way as in the g-group decodable codes case, we obtain $\mathbf{r}_k^T \mathbf{r}_l = 0 \Rightarrow \mathbf{r}_k(l) = 0,\ \forall k \in \Xi_i, l \in \Xi_j, i > j$ with the only difference that $k \leq \kappa$. Consequently, the real upper triangular matrix $\mathbf{R}$ takes the following form:

$$\mathbf{R} = \begin{bmatrix} \mathbf{A} & \mathbf{B} \\ \mathbf{0} & \mathbf{C} \end{bmatrix}$$

where $\mathbf{B}$ has no special structure, $\mathbf{C}$ is an $(2K-\kappa) \times (2K-\kappa)$ upper triangular matrix, and $\mathbf{A}$ is a block diagonal $\kappa \times \kappa$ matrix:

$$\mathbf{A} = \begin{bmatrix} \mathbf{R}_1 & \mathbf{0} & \ldots & \mathbf{0} \\ \mathbf{0} & \mathbf{R}_2 & \ldots & \mathbf{0} \\ \vdots & \vdots & \ddots & \vdots \\ \mathbf{0} & \mathbf{0} & \ldots & \mathbf{R}_g \end{bmatrix}$$

with $\mathbf{R}_i$ being a $n_i \times n_i$ upper triangular matrix.

Examples of FD STBCs include the Sezginer-Sari code [43] described by (3.19) and

the Silver code [44, 45] described by (3.20).

$$\mathbf{X} = \frac{1}{\sqrt{2}} \begin{bmatrix} as_1 + bs_3 & -cs_2^* - ds_4^* \\ as_2 + bs_4 & cs_1^* + ds_3^* \end{bmatrix} \tag{3.19}$$

where $a = c = 1$, $b = \frac{1-\sqrt{7}+j\left(1+\sqrt{7}\right)}{4}$, and $d = -jb$ yielding a coding gain of 2 independently of the underlying QAM constellation prior to normalization.

$$\mathbf{X} = \frac{1}{\sqrt{2}} \begin{bmatrix} s_1 & -s_2^* \\ s_2 & s_1^* \end{bmatrix} + \begin{bmatrix} 1 & 0 \\ 0 & -1 \end{bmatrix} \begin{bmatrix} z_1 & -z_2^* \\ z_2 & z_1^* \end{bmatrix} \tag{3.20}$$

where $(z_1, z_2)^T = \mathbf{U}\,(s_3, s_4)^T$, and $\mathbf{U}$ is given by:

$$\mathbf{U} = \frac{1}{\sqrt{7}} \begin{bmatrix} 1+j & -1+2j \\ 1+2j & 1-j \end{bmatrix}$$

yielding a coding gain $16/7$ regardless of the underlying QAM constellation prior to normalization. Both of the above 2×2 codes can be written as a sum of two Alamouti codewords giving rise to worst-case decoding complexity of order M^2 for square QAM constellations and $2M^3$ for arbitrary constellations. An example of FD STBCs for the case of four transmit antennas is the 4×4 rate-2 [46] shown in (3.21).

$$\mathbf{X} = \begin{bmatrix} s_{1I} + js_{3Q} & -s_{2I} + js_{4Q} & e^{j\pi/4}(s_{5I} + js_{7Q}) & e^{j\pi/4}(-s_{6I} + js_{8Q}) \\ s_{2I} + js_{4Q} & s_{1I} - js_{3Q} & e^{j\pi/4}(s_{6I} + js_{8Q}) & e^{j\pi/4}(s_{5I} - js_{7Q}) \\ e^{j\pi/4}(s_{7I} + js_{5Q}) & e^{j\pi/4}(-s_{8I} + js_{6Q}) & s_{3I} + js_{1Q} & -s_{4I} + js_{2Q} \\ e^{j\pi/4}(s_{8I} + js_{6Q}) & e^{j\pi/4}(s_{7I} - js_{5Q}) & s_{4I} + js_{2Q} & s_{3I} - js_{1Q} \end{bmatrix} \tag{3.21}$$

where $(s_{iI}, s_{iQ}) \in e^{j\theta_g}\mathcal{A}$, $\theta_g = \frac{1}{2}\arctan(2)$ and $\mathcal{A}$ denotes the conventional QAM constellation. The above code can be expressed as a sum of two 4-group decodable codes giving rise to a worst-case complexity order of $4M^{4.5}$ for square QAM constellations and $4M^5$ for arbitrary constellations.

3.3 Fast-group decodable codes

A STBC is said to be Fast-Group-Decodable (FGD) if it is g-group decodable with $g > 1$ such as each sub-code is fast-decodable.

Definition 3.4 *A STBC that encodes $2K$ real symbols is said to be fast-group-decodable iff:*

$$\mathbf{A}_k^H \mathbf{A}_l + \mathbf{A}_l^H \mathbf{A}_k = \mathbf{0},\ \forall \mathbf{A}_k \in \mathcal{G}_i,\ \mathbf{A}_l \in \mathcal{G}_j,\ 1 \leq i \neq j \leq g,\ |\mathcal{G}_i| = n_i, \sum_{i=1}^{g} n_i = 2K$$

and that the weight matrices within each group i are such that:

$$\mathbf{A}_k^H \mathbf{A}_l + \mathbf{A}_l^H \mathbf{A}_k = \mathbf{0},\ \forall \mathbf{A}_k \in \mathcal{G}_{i,m},\ \mathbf{A}_l \in \mathcal{G}_{i,n},\ 1 \leq m \neq n \leq g_i,$$
$$|\mathcal{G}_{i,j}| = n_{i,j},\ \sum_{j=1}^{g_i} n_{i,j} = \kappa_i < n_i.$$

where $\mathcal{G}_{i,m}$ (resp. g_i) denotes the set of weight matrices that constitute the m'th group (resp. the number of inner groups) within the i'th group of symbols $\mathcal{G}_i$. For instance, if a STBC that encodes $2K$ real symbols is fast-group-decodable, its corresponding worst-case decoding complexity order for square QAM constellations is reduced from $\sqrt{M}^{2K-1}$ to $\sum_{i=1}^{g} \sqrt{M}^{n_i-\kappa_i} \times \sum_{j=1}^{g_i} \sqrt{M}^{n_{i,j}-1}$. Similarly, if the g-group-decodable code within each group is orthogonal, the worst-case decoding complexity order is equal to $\sum_{i=1}^{g} \sqrt{M}^{n_i-\kappa_i}$. If a real SD is employed, the fast-group decodability reduces to splitting the original $2K-1$ real valued tree into g smaller trees each with n_i levels, and that for each of these new trees the last κ_i levels are split into g_i smaller trees each with $n_{i,j}-1$ levels. The structure of the corresponding real upper triangular matrix $\mathbf{R}$ follows directly from the case of g-group and fast-decodable codes, or mathematically:

$$\mathbf{R} = \begin{bmatrix} \mathbf{R}_1 & \mathbf{0} & \dots & \mathbf{0} \\ \mathbf{0} & \mathbf{R}_2 & \dots & \mathbf{0} \\ \vdots & \vdots & \ddots & \vdots \\ \mathbf{0} & \mathbf{0} & \dots & \mathbf{R}_g \end{bmatrix} \tag{3.22}$$

such that for $1 \leq i \leq g$, one has:

$$\mathbf{R}_i = \begin{bmatrix} \mathbf{A}_i & \mathbf{B}_i \\ \mathbf{0} & \mathbf{C}_i \end{bmatrix} \tag{3.23}$$

where $\mathbf{B}_i$ has no special structure, $\mathbf{C}_i$ is an $(n_i-\kappa_i) \times (n_i-\kappa_i)$ upper triangular matrices, and $\mathbf{A}_i$ is a $\kappa_i \times \kappa_i$ block diagonal matrix:

$$\mathbf{A}_i = \begin{bmatrix} \mathbf{R}_{i,1} & \mathbf{0} & \dots & \mathbf{0} \\ \mathbf{0} & \mathbf{R}_{i,2} & \dots & \mathbf{0} \\ \vdots & \vdots & \ddots & \vdots \\ \mathbf{0} & \mathbf{0} & \dots & \mathbf{R}_{i,g_i} \end{bmatrix} \tag{3.24}$$

where $\mathbf{R}_{i,j}$ is a $n_{i,j} \times n_{i,j}$ upper triangular matrix. Examples of FGD STBCs include the 2×2 rate-$5/4$ code described by (3.25) [47]:

$$\mathbf{X} = \begin{bmatrix} x_1 - x_2 + jx_3 + jx_4 + jx_5 & x_1 + x_2 - jx_3 + jx_4 + jx_5 \\ x_1 + x_2 + jx_3 - jx_4 + jx_5 & -x_1 + x_2 + jx_3 + jx_4 - jx_5 \end{bmatrix} \tag{3.25}$$

and the 4×4 the rate-$17/8$ described by (3.26)[47]:

$$\mathbf{X} = \begin{bmatrix} \mathbf{A} & \mathbf{B} \\ \mathbf{C} & \mathbf{D} \end{bmatrix} \tag{3.26}$$

where:

$$\begin{aligned}
\mathbf{A} &= \begin{bmatrix} x_1 + jx_6 + jx_9 + jx_{12} + jx_{17} & x_7 + jx_8 + x_{14} + jx_{15} \\ -x_7 + jx_8 - x_{14} + jx_{15} & x_1 + jx_6 + jx_9 - jx_{12} - jx_{17} \end{bmatrix} \\
\mathbf{B} &= \begin{bmatrix} -x_2 + jx_3 + x_{10} + jx_{11} & x_4 + jx_5 + x_{13} + jx_{16} \\ -x_4 + jx_5 + x_{13} - jx_{16} & -x_2 - jx_3 - x_{10} + jx_{11} \end{bmatrix} \\
\mathbf{C} &= \begin{bmatrix} x_2 + jx_3 - x_{10} + jx_{11} & x_4 + jx_5 - x_{13} - jx_{16} \\ -x_4 + jx_5 - x_{13} + jx_{16} & x_2 - jx_3 + x_{10} + jx_{11} \end{bmatrix} \\
\mathbf{D} &= \begin{bmatrix} x_1 - jx_6 + jx_9 - jx_{12} + jx_{17} & x_7 - jx_8 - x_{14} + jx_{15} \\ -x_7 - jx_8 + x_{14} + jx_{15} & x_1 - jx_6 + jx_9 + jx_{12} - jx_{17} \end{bmatrix}
\end{aligned}$$

For the two transmit antennas code we have $g = 2, n_1 = 1, n_2 = 4$ and $g_1 = 1, g_2 = 3$ such as $n_{2,j} = 1,\ j = 1, 2, 3$ yielding a worst-case decoding complexity of order $\sqrt{M}$. For the case of four transmit antennas code we have $g = 2, n_1 = 1, n_2 = 16$ and $g_1 = 1, g_2 = 5$ such as $n_{2,j} = 1,\ j = 1, 2, 3, 4, 5$, and therefore the worst-case decoding complexity order is equal to $M^{5.5}$.

3.4 Conclusions

In this chapter, we focused on the low-complexity design criteria and reviewed the three families of low-complexity STBCs namely, g-group-decodable codes, fast-decodable codes, and fast-group-decodable codes. We determined the structure of the upper triangular matrix $\mathbf{R}$ corresponding to each of these families as well as the worst-case decoding complexity order in terms of the STBC parameters. Therefore, in order to determine the worst-case decoding complexity order and the upper triangular matrix $\mathbf{R}$ structure for any low-complexity STBC, it suffices to fit the code in the appropriate family and determine its structure parameters (e.g. number of disjoint groups of symbols for the g-group-decodable code).

Chapter 4

A Numerical Approach for g-Group Decodable Code Construction

The adopted approach for the construction of the g-symbol (resp. g-group) decodable codes (namely the Clifford Unitary Weight (CUW)-g-symbol [19] (resp. g-group [16]) decodable codes) is based on sufficient but not necessary conditions which may limit the achievable rate for any number of orthogonal groups. In [48] the authors have found the maximal achievable rate for the CUW-λ-symbol decodable codes but only for the case where the number of symbols λ in each group can be expressed as $2^a,\ a \in \mathbb{N}$. In [49] the authors proved that the rate of arbitrary $2^a \times 2^a$ UW-Single-symbol decodable STBCs is upper bounded by $\frac{a}{2^{a-1}}$. Consequently, the question on the maximum achievable rate for an arbitrary number of orthogonal groups remains open.

In this chapter, we limit ourselves to a special case of UW-g-group decodable STBCs for 2^a transmit antennas where the weight matrices are required to be single thread matrices with non-zero entris $\in \{\pm 1, \pm j\}$ and address the problem of finding the highest achievable rate for any number of orthogonal groups. This special type of weight matrices guarantees full symbol-wise diversity [50] and subsumes a wide range of existing codes in the literature (a non-exhaustive list includes [16, 19, 39, 51, 40]). For this purpose we extend the approach proposed in [15] for constructing UW-2-group decodable STBCs based on necessary and sufficient conditions to the case of UW-g-group decodable STBCs in a recursive manner.

The major idea is that contrary to what was done in [52], we are dealing with the $\mathbf{\Lambda}_{kl}$ matrix where $\mathbf{\Lambda}_{kl} = \mathbf{A}_k \mathbf{B}_l^H$ instead of dealing directly with the weight matrices $\mathbf{A}_k$ and $\mathbf{B}_l$. This approach reduced the number of candidate $\mathbf{\Lambda}_{kl}$ matrices that can be used for the construction of the UW-g-group decodable STBCs, as they have to satisfy additional properties over those of the weight matrices. Then, the vector space representation is used to build the $\mathbf{\Lambda}_{kl}$ matrices and we show that the number of candidate $\mathbf{\Lambda}_{kl}$ matrices becomes limited (see Appendix A). A search routine can then be applied to find existing UW-g-group decodable codes at given rates which enables us to determine the maximum achievable rates for an arbitrary number of orthogonal groups. UW-g-group decodable codes for a number of transmit antennas that is not a power of two can be easily obtained by the removal of an appropriate number of columns of the code matrix corresponding to the nearest greater number of transmit antennas that is a power of two.

The chapter is organized as follows: In the next section, we reformulate the g-group decodability conditions in terms of the $\mathbf{\Lambda}$ matrices. Section II addresses the construction of UW-g-group decodable codes. In Section III, we present the results of the exhaustive search of UW-g-group decodable codes for four transmit antennas based on the construction method developed in the former section, and finally we give our conclusion in Section V.

4.1 Necessary and sufficient conditions for g-group decodability

4.1.1 UW-2-group decodability

In order to construct a UW-2-group decodable code which transmits $2K$ real symbols, we must find 2 sets of unitary weight matrices namely $(\mathcal{G}_1, \mathcal{G}_2)$ that are linearly independent over $\mathbb{R}$ such that $n_1 + n_2 = 2K$, and each pair of weight matrices belonging to different sets must satisfy (3.5). In the following, we will reformulate the problem in a way which allows exhaustive search of weight matrices for 2-groups decodable codes. We will call the k'th weight matrix of the first group $\mathbf{A}_k$ and the l'th weight matrix of the second group $\mathbf{B}_l$.

Multiplying (3.5) from the left by $\mathbf{A}_k$ and from the right by $\mathbf{B}_l^H$:

$$\mathbf{A}_k \left(\mathbf{A}_k^H \mathbf{B}_l + \mathbf{B}_l^H \mathbf{A}_k \right) \mathbf{B}_l^H = \mathbf{0} \tag{4.1}$$

which can be written as:

$$(\underbrace{\mathbf{A}_k \mathbf{B}_l^H}_{\mathbf{\Lambda}_{kl}})^2 = -\mathbf{I}_T \tag{4.2}$$

where $\mathbf{I}_T$ is the $T \times T$ identity matrix. Thus $\mathbf{\Lambda}_{kl}$ must be a unitary matrix squaring to $-\mathbf{I}_T$.

$\mathbf{\Lambda}_{kl}$ can be expressed as:

$$\begin{aligned} \mathbf{\Lambda}_{kl} = \mathbf{A}_k \mathbf{B}_l^H &= \mathbf{A}_k \mathbf{B}_1^H \mathbf{B}_1 \mathbf{B}_l^H \\ &= \mathbf{\Lambda}_{k1} \mathbf{B}_1 \mathbf{A}_1^H \mathbf{A}_1 \mathbf{B}_l^H \\ &= \mathbf{\Lambda}_{k1} \mathbf{\Lambda}_{11}^H \mathbf{\Lambda}_{1l} \\ &= -\mathbf{\Lambda}_{k1} \mathbf{\Lambda}_{11} \mathbf{\Lambda}_{1l} \end{aligned} \tag{4.3}$$

In the last step, we used the fact that a unitary matrix that squares to $-\mathbf{I}$ is anti-hermitian.

Proposition 4.1 *A code is said to be UW-2-group decodable code iff:*

1. $\Gamma = \{\mathbf{\Lambda}_{11}, \mathbf{\Lambda}_{k1}, \mathbf{\Lambda}_{1l} : 2 \leq k \leq n_1, 2 \leq l \leq n_2\}$ *is a set of unitary matrices that square to* $-\mathbf{I}$*;*
2. $(\mathbf{\Lambda}_{k1} \mathbf{\Lambda}_{11} \mathbf{\Lambda}_{1l})^2 = -\mathbf{I} \; \forall \; 2 \leq k \leq n_1, \; 2 \leq l \leq n_2$*;*
3. *the set* $\{\mathbf{\Lambda}_{k1}, \mathbf{\Lambda}_{1l} \mathbf{\Lambda}_{11} : 1 \leq k \leq n_1, 1 \leq l \leq n_2\}$ *is linearly independent over* $\mathbb{R}$*.*

where $n_i = |\mathcal{G}_i|$.

Proof. The first and the second conditions are necessary and sufficient in order to satisfy (3.5) and follow directly from (4.2) and (4.3), respectively. The last condition is necessary and sufficient to guarantee that the weight matrices are linear independent over $\mathbb{R}$. We will prove the last condition by proving that if the linear dependence of the weight matrices over $\mathbb{R}$ implies that the set $\{\mathbf{\Lambda}_{k1}, \mathbf{\Lambda}_{1l} \mathbf{\Lambda}_{11} : 1 \leq k \leq n_1, 1 \leq l \leq n_2\}$ is linearly dependent over $\mathbb{R}$ and vice versa. To this end let us suppose that:

$$\sum_{k=1}^{n_1} a_k \mathbf{A}_k + \sum_{l=1}^{n_2} b_l \mathbf{B}_l = \mathbf{0} \tag{4.4}$$

where $\{a_k, b_l : 1 \leq k \leq n_1, 1 \leq l \leq n_2\} \in \mathbb{R}$. Right multiplying the above by $\mathbf{B}_1^H$, we obtain:

$$
\begin{aligned}
(4.4) \quad &\Leftrightarrow \quad \left(\sum_{k=1}^{n_1} a_k \mathbf{A}_k + \sum_{l=1}^{n_2} b_l \mathbf{B}_l\right) \mathbf{B}_1^H = \mathbf{0} && (4.5)\\
&= \quad \sum_{k=1}^{n_1} a_k \mathbf{\Lambda}_{k1} + \sum_{l=1}^{n_2} b_l \mathbf{B}_l \mathbf{B}_1^H = \mathbf{0} && (4.6)\\
&\Leftrightarrow \quad \sum_{k=1}^{n_1} a_k \mathbf{\Lambda}_{k1} + \sum_{l=1}^{n_2} b_l \mathbf{\Lambda}_{1l}^H \mathbf{A}_1 \mathbf{A}_1^H \mathbf{\Lambda}_{11} = \mathbf{0} && (4.7)\\
&= \quad \sum_{k=1}^{n_1} a_k \mathbf{\Lambda}_{k1} - \sum_{l=1}^{n_2} b_l \mathbf{\Lambda}_{1l} \mathbf{\Lambda}_{11} = \mathbf{0} && (4.8)
\end{aligned}
$$

which means that the weight matrices are linearly independent over $\mathbb{R}$ iff the set $\{\mathbf{\Lambda}_{k1}, \mathbf{\Lambda}_{1l}\mathbf{\Lambda}_{11} : 1 \leq k \leq n_1, 1 \leq l \leq n_2\}$ is linearly independent over $\mathbb{R}$. □

In order to construct UW-2-group decodable codes, we will search for matrices satisfying **Proposition 4.1**. Once we have a set Γ that satisfies **Proposition 4.1**, the corresponding UW-2-group decodable code is built as follows, first, we choose an arbitrary unitary matrix $\mathbf{A}_1$ then the STBC weight matrices are obtained according to:

$$
\begin{aligned}
\mathbf{B}_l &= \mathbf{\Lambda}_{1l}^H \mathbf{A}_1;\ 1 \leq l \leq n_2\\
\mathbf{A}_k &= \mathbf{\Lambda}_{k1} \mathbf{B}_1;\ 2 \leq k \leq n_1
\end{aligned}
\tag{4.9}
$$

which means that for a given set Γ the corresponding UW-2-group decodable code is not unique.

4.1.2 UW-g-group decodability

In order to expand the above approach to g-group decodable codes, it is worth noting that any g-group decodable code can be seen as a 2-group decodable code. This means that we can search for g-group decodable codes by iteratively searching for 2-group decodable codes. For instance if we search for a 3-group decodable code, where n_1, n_2 and n_3 are the number of weight matrices (or alternatively real symbols) in the first, second and third group respectively, then we can proceed in two steps as follows:

I- We search for a 2-group decodable code with n_1 and $(n_2 + n_3)$ real symbols in the first and second group, respectively.

II- Among the found second group with (n_2+n_3) weight matrices, we will search for 2-group decodable codes with n_2 and n_3 weight matrices in the first and second group, respectively.

Mathematically speaking, in the first step we search for all the sets:

$$\Gamma = \{\mathbf{\Lambda}_{11}, \mathbf{\Lambda}_{k1}, \mathbf{\Lambda}_{1l} : 2 \leq k \leq n_1, 2 \leq l \leq (n_2 + n_3)\}$$

that satisfy **Proposition 4.1**. In the second step, we will search among the sets $\{\mathbf{\Lambda}_{1l} : 1 \leq l \leq (n_2 + n_3)\}$ for sets that can be divided into two groups of n_2 and n_3 matrices.

Proposition 4.2 *A code is said to be UW-g-group decodable code iff:*

1. $\Gamma = \{\mathbf{\Lambda}_{11}, \mathbf{\Lambda}_{k1}, \mathbf{\Lambda}_{1l} : 2 \leq k \leq n_1, 2 \leq l \leq \sum_{i=2}^{g} n_i\}$ *is a set of unitary matrices squaring to* $-\mathbf{I}$*;*
2. $(\mathbf{\Lambda}_{k1}\mathbf{\Lambda}_{11}\mathbf{\Lambda}_{1l})^2 = -\mathbf{I} \; \forall \; 2 \leq k \leq n_1, \; 2 \leq l \leq \sum_{i=2}^{g} n_i$*;*
3. *The set* $\{\mathbf{\Lambda}_{k1}, \mathbf{\Lambda}_{1l}\mathbf{\Lambda}_{11} : 1 \leq k \leq n_1, 1 \leq l \leq \sum_{i=2}^{g} n_i\}$ *is linearly independent over* $\mathbb{R}$*;*
4. $\mathbf{\Lambda}_{1l}\mathbf{\Lambda}_{1l'} = -\mathbf{\Lambda}_{1l'}\mathbf{\Lambda}_{1l} \; \forall \sum_{i=2}^{L-1} n_i + 1 \leq l \leq \sum_{i=2}^{L} n_i, \sum_{j=2}^{L'-1} n_j + 1 \leq l' \leq \sum_{j=2}^{L'} n_j, \; 2 \leq L \neq L' \leq g.$

where $n_i = |\mathcal{G}_i|$.

Proof. The first three conditions are the same as in **Proposition 4.1**, and therefore we need only to prove the last one. Consider a UW-2-group decodable codes with $\mathcal{G}_1 = \{\mathbf{A}_1, \ldots, \mathbf{A}_{n_1}\}$ and $\bigcup_{m=2}^{g} \mathcal{G}_m = \{\mathbf{B}_1, \ldots, \mathbf{B}_{\sum_{i=2}^{g} n_i}\}$, such that:

$$\mathbf{B}_l^H \mathbf{B}_{l'} + \mathbf{B}_{l'}^H \mathbf{B}_l = \mathbf{0}, \; \forall \; \mathbf{B}_l \in \mathcal{G}_L, \; \mathbf{B}_{l'} \in \mathcal{G}_{L'}, \; 2 \leq L \neq L' \leq g. \tag{4.10}$$

By left and right multiplying the above by $\mathbf{A}_1$ and $\mathbf{A}_1^H$ respectively, we obtain:

$$\mathbf{A}_1 \mathbf{B}_l^H \mathbf{B}_{l'} \mathbf{A}_1^H + \mathbf{A}_1 \mathbf{B}_{l'}^H \mathbf{B}_l \mathbf{A}_1^H = \mathbf{0} \tag{4.11}$$

$$\mathbf{\Lambda}_{1l} \mathbf{\Lambda}_{1l'}^H + \mathbf{\Lambda}_{1l'} \mathbf{\Lambda}_{1l}^H = \mathbf{0} \tag{4.12}$$

$$\mathbf{\Lambda}_{1l} \mathbf{\Lambda}_{1l'} + \mathbf{\Lambda}_{1l'} \mathbf{\Lambda}_{1l} = \mathbf{0}. \tag{4.13}$$

which concludes the proof. □

The weight matrices are obtained as in the UW-2-group decodable code. We first choose an arbitrary unitary matrix $\mathbf{A}_1$ and then:

$$\begin{aligned}\mathbf{B}_l &= \mathbf{\Lambda}_{1l}^H \mathbf{A}_1;\ 1 \leq l \leq \sum_{i=2}^{g} n_i \\ \mathbf{A}_k &= \mathbf{\Lambda}_{k1} \mathbf{B}_1;\ 2 \leq k \leq n_1\end{aligned} \tag{4.14}$$

4.2 Construction of the matrices in Γ

Recall from (2.58) the properties of the $2^a \times 2^a$ matrix representations of the Clifford algebra generators over $\mathbb{R}$:

$$\mathbf{R}_i^H = -\mathbf{R}_i,\ \mathbf{R}_i^2 = -\mathbf{I},\ \forall 1 \leq i \leq 2a+1,\ \text{and}\ \mathbf{R}_i\mathbf{R}_j + \mathbf{R}_j\mathbf{R}_i = \mathbf{0},\ \forall 1 \leq i \neq j \leq 2a+1. \tag{4.15}$$

one has from [73] that if $\{\mathbf{M}_k : k = 1, \ldots, 2a\}$ are pairwise anti-commuting matrices that square to a scalar, then the set:

$$\{\mathbf{I}\} \cup \{\mathbf{M}_k : k = 1, \ldots, 2a\} \bigcup_{m=2}^{2a} \left\{ \prod_{i=2}^{m} \mathbf{M}_{k_i} : 1 \leq k_1 < k_2 \ldots < k_m \leq 2a \right\} \tag{4.16}$$

forms a basis of $\mathcal{M}_{2^a}$ over $\mathbb{C}$. Consequently, thanks to the properties of the matrix representations of Clifford algebra generators (4.15), the set of matrices defined in (4.17) forms a basis of $\mathcal{M}_{2^a}$ over $\mathbb{C}$:

$$\{\mathbf{I}\} \cup \{\mathbf{R}_k : k = 1, \ldots, 2a\} \bigcup_{m=2}^{2a} \left\{ \prod_{i=2}^{m} \mathbf{R}_{k_i} : 1 \leq k_1 < k_2 \ldots < k_m \leq 2a \right\} \tag{4.17}$$

We require that all the basis elements are anti-hermitian in order to facilitate the search of matrices in Γ as will be shown shortly. This may be achieved by replacing $\mathbf{I}$ by $j\mathbf{I}$ and multiplying the basis elements by $j^{\delta(m)}$ where $\delta(m) = \frac{\left((m)_4 - 1\right)\left((m)_4 - 2\right)}{2}$ which does not alter the linear independence over $\mathbb{C}$. Therefore one obtain:

$$\mathcal{B}_{2a} = j\mathbf{I} \cup \{\mathbf{R}_k : k = 1, \ldots, 2a\} \bigcup_{m=2}^{2a} \left\{ j^{\delta(m)} \prod_{i=1}^{m} \mathbf{R}_{k_i} : 1 \leq k_1 < k_2 \ldots < k_m \leq 2a \right\} \tag{4.18}$$

The matrices belonging to the above basis may be easily verified to be anti-hermitian by noting that for $\mathbf{A} = j^{\delta(m)} \prod_{i=1}^{m} \mathbf{R}_{k_i} | k_1 < k_2 \ldots < k_m$, we have:

$$\mathbf{A}^H = (-1)^{\delta(m) + m(m+1)/2} \mathbf{A} \tag{4.19}$$

and it is straightforward to verify that $\delta(m) + m(m+1)/2$ is odd irrespectively of m.

For instance, the basis elements of $\mathcal{M}_4$ over $\mathbb{C}$ denoted by $(\boldsymbol{\alpha}_i : 1 \leq i \leq 16)$ are expressed in Table 4.1.

Table 4.1: The bases of the 4×4 matrices

$\boldsymbol{\alpha}_1 = j\mathbf{I}$	$\boldsymbol{\alpha}_2 = \mathbf{R}_1,$	$\boldsymbol{\alpha}_3 = \mathbf{R}_2$	$\boldsymbol{\alpha}_4 = \mathbf{R}_3$
$\boldsymbol{\alpha}_5 = \mathbf{R}_4$	$\boldsymbol{\alpha}_6 = \mathbf{R}_1\mathbf{R}_2$	$\boldsymbol{\alpha}_7 = \mathbf{R}_1\mathbf{R}_3$	$\boldsymbol{\alpha}_8 = \mathbf{R}_1\mathbf{R}_4$
$\boldsymbol{\alpha}_9 = \mathbf{R}_2\mathbf{R}_3$	$\boldsymbol{\alpha}_{10} = \mathbf{R}_2\mathbf{R}_4$	$\boldsymbol{\alpha}_{11} = \mathbf{R}_3\mathbf{R}_4$	$\boldsymbol{\alpha}_{12} = j\mathbf{R}_1\mathbf{R}_2\mathbf{R}_3$
$\boldsymbol{\alpha}_{13} = j\mathbf{R}_1\mathbf{R}_2\mathbf{R}_4$	$\boldsymbol{\alpha}_{14} = j\mathbf{R}_1\mathbf{R}_3\mathbf{R}_4$	$\boldsymbol{\alpha}_{15} = j\mathbf{R}_2\mathbf{R}_3\mathbf{R}_4$	$\boldsymbol{\alpha}_{16} = j\mathbf{R}_1\mathbf{R}_2\mathbf{R}_3\mathbf{R}_4$

Proposition 4.3 *The properties of the basis elements of $\mathcal{M}_n, n = 2^a$ over $\mathbb{C}$ can be summarized as follows:*

1. $(\boldsymbol{\alpha}_i)^2 = -\mathbf{I},\ \forall 1 \leq i \leq n^2$
2. $\boldsymbol{\alpha}_i^H = -\boldsymbol{\alpha}_i,\ \forall 1 \leq i \leq n^2$
3. $\boldsymbol{\alpha_i}\boldsymbol{\alpha_j} = \pm\boldsymbol{\alpha_j}\boldsymbol{\alpha_i},\ \forall i \neq j$
4. $\boldsymbol{\alpha}_k\boldsymbol{\alpha}_l = \lambda\boldsymbol{\alpha}_m$, *where* $\lambda \in \{\pm 1, \pm j\}\ \forall 1 \leq k \neq l \leq n^2$ *and* $2 \leq m \leq n^2$.

Proof. The first three properties follow directly from (4.15). The latter property can be verified easily from (4.18) and (4.15). It remains only to verify that the product of any pair of distinct basis elements is not proportional to the identity. Let us suppose that $\boldsymbol{\alpha}_k\boldsymbol{\alpha}_l = \lambda\mathbf{I}$ with $k \neq l$, then:

$$\begin{aligned} \boldsymbol{\alpha}_k\boldsymbol{\alpha}_l + \lambda\boldsymbol{\alpha}_k\boldsymbol{\alpha}_k &= \mathbf{0} \\ \boldsymbol{\alpha}_k\left(\boldsymbol{\alpha}_l + \lambda\boldsymbol{\alpha}_k\right) &= \mathbf{0} \end{aligned} \tag{4.20}$$

As all the basis elements are unitary matrices (thus of full rank), the only solution to the above equation is $\boldsymbol{\alpha}_l + \lambda\boldsymbol{\alpha}_k = \mathbf{0}$, which contradicts the linear independence property. □

4.2.1 Necessary conditions for the matrices in Γ

Proposition 4.4 *Let the matrix* $\mathbf{\Lambda}$ *be written as a linear combination of the basis elements in* (4.18) *as below:*

$$\mathbf{\Lambda} = \sum_{i=1}^{n^2} a_i \boldsymbol{\alpha}_i \tag{4.21}$$

Then, $\mathbf{\Lambda}$ *is unitary and squares to* $-\mathbf{I}$ *iff for* $i \in \{1, 2, \ldots, n^2\}$, $a_i \in \mathbb{R}$ *with* $\sum_{i=1}^{n^2} a_i^2 = 1$ *and the sum over the product of commuting pairs of elements of basis equals to* $\mathbf{0}$*.*

Proof. $\mathbf{\Lambda}$ is required to be anti-hermitian and to square to $-\mathbf{I}$:

$$\begin{aligned} \sum_{i=1}^{n^2} a_i \boldsymbol{\alpha}_i + \sum_{i=1}^{n^2} a_i^* \boldsymbol{\alpha}_i^H &= \sum_{i=1}^{n^2} a_i \boldsymbol{\alpha}_i - \sum_{i=1}^{n^2} a_i^* \boldsymbol{\alpha}_i \\ &= \sum_{i=1}^{n^2} \left(a_i - a_i^*\right) \boldsymbol{\alpha}_i = \mathbf{0} \end{aligned} \tag{4.22}$$

From the linear independence property of the basis, the only solution to the above equation is that $a_i = a_i^* \; \forall 1 \leq i \leq n^2$ which proves the first claim of our proposition.

$$\begin{aligned} \left(\sum_{k=1}^{n^2} a_k \boldsymbol{\alpha}_k\right)^2 + \mathbf{I} &= \left(\sum_{k=1}^{n^2} a_k \boldsymbol{\alpha}_k\right)\left(\sum_{l=1}^{n^2} a_l \boldsymbol{\alpha}_l\right) + \mathbf{I} \\ &= \sum_{k=1}^{n^2} a_k^2 \left(\boldsymbol{\alpha}_k\right)^2 + \sum_{\substack{k=1 \\ l \neq k}}^{n^2} a_k a_l \boldsymbol{\alpha}_k \boldsymbol{\alpha}_l + \mathbf{I} \\ &= \left(1 - \sum_{k=1}^{n^2} a_k^2\right) \mathbf{I} + \sum_{\substack{k=1 \\ l \neq k}}^{n^2} a_k a_l \boldsymbol{\alpha}_k \boldsymbol{\alpha}_l \end{aligned}$$

The anticommuting pairs in the second term of the last equation will vanish, and the above equation may be expressed as:

$$\left(1 - \sum_{k=1}^{n^2} a_k^2\right) \mathbf{I} + 2 \sum_{k,l>k} a_k a_l \boldsymbol{\alpha}_k \boldsymbol{\alpha}_l = \mathbf{0} \tag{4.23}$$

where the second summation is held only over commuting pairs of basis elements. From the properties of the basis elements, we know that the product of any pair of distinct basis elements is an element of the basis (with exception of the identity matrix that cannot be expressed as a product of any distinct pair of basis elements according to **Proposition 4.3**). Thus, the only solution for the above equation is:

$$\sum_{k,l>k} a_k a_l \boldsymbol{\alpha}_k \boldsymbol{\alpha}_l = \mathbf{0}; \; \sum_{i=1}^{n^2} a_i^2 = 1 \tag{4.24}$$

which proves **Proposition 4.4**. □

An illustrative example is the following:

$$\mathbf{\Lambda} = \frac{1}{2}\left(\mathbf{R}_1 - \mathbf{R}_3 + \mathbf{R}_1\mathbf{R}_2 + \mathbf{R}_2\mathbf{R}_3\right). \tag{4.25}$$

The above example of $\mathbf{\Lambda}$ satisfies **Proposition 4.4** as the only commuting pairs are $\{\mathbf{R}_1, \mathbf{R}_2\mathbf{R}_3\}$ and $\{-\mathbf{R}_3, \mathbf{R}_1\mathbf{R}_2\}$ and the product of the first pair is the additive inverse of the product of the second pair with $\sum_i a_i^2 = 1$.

Proposition 4.5 *The UW-g-group decodable codes with single thread weight matrices where the non-zero elements $\in \{\pm 1, \pm j\}$ for $n = 2^a$ antennas can exist only for Γ sets where the $\mathbf{\Lambda}$ matrices are expressed as:*

$$\mathbf{\Lambda} = \sum_{k=1}^{n^2} a_k \boldsymbol{\alpha}_k, a_k \in \left\{ \frac{n - 2\kappa}{n} : \kappa \in \mathbb{N} \right\}, \sum_{k=1}^{n^2} a_k^2 = 1$$

Proof. see Appendix A. □

By using **Propositions 4.4**, and **4.5**, we now have the possibility to exhaustively construct all the possible Γ sets that satisfy **Proposition 4.2**.

4.3 Results

In this section we provide examples of the application of the proposed method to find the maximum achievable rate of 4×4 UW-g-group decodable STBCs where the weight matrices are required to be single thread matrices with non-zero entries $\in \{\pm 1, \pm j\}$. The weight matrices were found through exhaustive computer search. For the case of four transmit antennas $(a = 2)$, **Proposition 4.5** reduces to:

$$\mathbf{\Lambda} = \begin{cases} \pm\boldsymbol{\alpha}_k, & k \in \{1, 2, \ldots, 16\} \\ \sum_{i=1}^{4} a_{k_i}\boldsymbol{\alpha}_{k_i}, & a_{k_i} \in \left\{\pm\frac{1}{2}\right\} \end{cases} \tag{4.26}$$

For the symmetric UW-2-group decodable STBCs we found that the maximum achievable rate is limited to $5/4$ complex symbol per channel use (see Table 4.2). However, if the symmetry restriction is relaxed, one can easily obtain rate-$\frac{n^2+1}{2n}$ UW-2-group decodable STBC for n transmit antennas [47] giving rise to a rate-$17/8$ UW-2-group decodable STBC for four transmit antennas.

For UW-3-group decodable codes, we found that the maximum achievable rate is limited to 1 complex symbol per channel use (see Table 4.3). For 4-group decodable codes, it is known that the maximum achievable rate is 1 [49]. Examples of these codes may be found in [16, 19, 40, 53].

Table 4.2: Weight matrices of rate-5/4, UW-2-group decodable code

$\mathbf{A}_1 = \begin{bmatrix} 0 & 0 & 0 & 1 \\ 0 & 1 & 0 & 0 \\ 1 & 0 & 0 & 0 \\ 0 & 0 & 1 & 0 \end{bmatrix}$	$\mathbf{B}_1 = \begin{bmatrix} 0 & 0 & 0 & -j \\ 0 & j & 0 & 0 \\ j & 0 & 0 & 0 \\ 0 & 0 & -j & 0 \end{bmatrix}$
$\mathbf{A}_2 = \begin{bmatrix} 0 & 0 & 0 & 1 \\ 0 & 1 & 0 & 0 \\ -1 & 0 & 0 & 0 \\ 0 & 0 & -1 & 0 \end{bmatrix}$	$\mathbf{B}_2 = \begin{bmatrix} 0 & 0 & 0 & -j \\ 0 & j & 0 & 0 \\ -j & 0 & 0 & 0 \\ 0 & 0 & j & 0 \end{bmatrix}$
$\mathbf{A}_3 = \begin{bmatrix} 0 & 0 & 0 & 1 \\ 0 & 1 & 0 & 0 \\ -1 & 0 & 0 & 0 \\ 0 & 0 & 1 & 0 \end{bmatrix}$	$\mathbf{B}_3 = \begin{bmatrix} 0 & 0 & 0 & -j \\ 0 & -j & 0 & 0 \\ j & 0 & 0 & 0 \\ 0 & 0 & -j & 0 \end{bmatrix}$
$\mathbf{A}_4 = \begin{bmatrix} 0 & 0 & 0 & 1 \\ 0 & 1 & 0 & 0 \\ 0 & 0 & -j & 0 \\ -j & 0 & 0 & 0 \end{bmatrix}$	$\mathbf{B}_4 = \begin{bmatrix} 0 & -1 & 0 & 0 \\ 0 & 0 & 0 & 1 \\ j & 0 & 0 & 0 \\ 0 & 0 & -j & 0 \end{bmatrix}$
$\mathbf{A}_5 = \begin{bmatrix} 0 & 0 & 0 & 1 \\ 0 & 1 & 0 & 0 \\ 0 & 0 & 1 & 0 \\ -1 & 0 & 0 & 0 \end{bmatrix}$	$\mathbf{B}_5 = \begin{bmatrix} 0 & -j & 0 & 0 \\ 0 & 0 & 0 & -j \\ j & 0 & 0 & 0 \\ 0 & 0 & -j & 0 \end{bmatrix}$

For the rate-5/4 2-group decodable code, $g = 2, n_1 = n_2 = 5$ thus the decoding complexity for square QAM constellations is of order $\sum_{i=1}^{2} \sqrt{M}^{n_i - 1} = 2M^2$. For the case of non-rectangular constellations, the rate-5/4 code is no longer 2-group decodable due to the entanglement of the real and imaginary parts of the transmitted complex symbols. In that case, we may use the conditional detection [41] to evaluate the ML estimate of $(x_1, \ldots, x_4)$ and $(x_5, \ldots, x_8)$ separately (thanks to the Quasi-orthogonality structure) for a given value of (x_9, x_{10}). Therefore the decoding complexity is of order $2M^3$.

For the rate-1 3-group decodable code, one has $g = 3, n_1 = n_2 = 2, n_3 = 4$, and therefore the worst-case decoding complexity order of square QAM constellations is $\sum_{i=1}^{3} \sqrt{M}^{n_i - 1} = 2\sqrt{M} + M^{1.5}$. For the case of non-rectangular constellations, the rate-1 3-group decodable code maintains its multi-group decodability structure,

Table 4.3: Weight matrices of rate-1, UW-3-group decodable code

$$\mathbf{A}_1 = \begin{bmatrix} -j & 0 & 0 & 0 \\ 0 & j & 0 & 0 \\ 0 & 0 & -1 & 0 \\ 0 & 0 & 0 & 1 \end{bmatrix} \quad \mathbf{C}_1 = \begin{bmatrix} 1 & 0 & 0 & 0 \\ 0 & 1 & 0 & 0 \\ 0 & 0 & 0 & 1 \\ 0 & 0 & 1 & 0 \end{bmatrix}$$

$$\mathbf{A}_2 = \begin{bmatrix} -j & 0 & 0 & 0 \\ 0 & j & 0 & 0 \\ 0 & 0 & 1 & 0 \\ 0 & 0 & 0 & -1 \end{bmatrix} \quad \mathbf{C}_2 = \begin{bmatrix} 0 & j & 0 & 0 \\ j & 0 & 0 & 0 \\ 0 & 0 & 0 & 1 \\ 0 & 0 & 1 & 0 \end{bmatrix}$$

$$\mathbf{B}_1 = \begin{bmatrix} 0 & -1 & 0 & 0 \\ 1 & 0 & 0 & 0 \\ 0 & 0 & 0 & j \\ 0 & 0 & -j & 0 \end{bmatrix} \quad \mathbf{C}_3 = \begin{bmatrix} 0 & -j & 0 & 0 \\ -j & 0 & 0 & 0 \\ 0 & 0 & 0 & 1 \\ 0 & 0 & 1 & 0 \end{bmatrix}$$

$$\mathbf{B}_2 = \begin{bmatrix} 0 & -1 & 0 & 0 \\ 1 & 0 & 0 & 0 \\ 0 & 0 & 0 & -j \\ 0 & 0 & j & 0 \end{bmatrix} \quad \mathbf{C}_4 = \begin{bmatrix} 1 & 0 & 0 & 0 \\ 0 & 1 & 0 & 0 \\ 0 & 0 & -j & 0 \\ 0 & 0 & 0 & -j \end{bmatrix}$$

but with an increase of decoding complexity order to $\sum_{i=1}^{3} M^{n_i/2} = 2M + M^2$. These results are summarized in Table 4.4. It is worth noting that the coding gain

Table 4.4: summary of results

number of groups	maximum rate	Complexity order of	
		square QAM	non-rectangular QAM
2	5/4	$2M^2$	$2M^3$
3	1	$2\sqrt{M} + M^{1.5}$	$2M + M^2$
4	1	$4\sqrt{M}$	$4M$

of the proposed codes is equal to zero, but the full diversity may still be ensured by applying a constellation rotation to each group of symbols, which does not affect the multi-group decodability structure, and hence the decoding complexity remains unchanged.

4.4 Conclusions

In this paper, we addressed the problem of finding the maximum achievable rates of a special type of UW-g-group decodable STBCs for 2^a transmit antennas. For this purpose, we extended the previously proposed approach of finding UW-2-group decodable codes to search for UW-g-group decodable codes in a recursive fashion.

The new construction method was then applied to the type of weight matrices usually proposed in the literature. It was found that the maximum achievable rate for the symmetric UW-2-group decodable codes is $5/4$ and that the maximum achievable rate for the UW-3-group decodable codes is 1.

Chapter 5

Complex Orthogonal Designs Multiplexing

Recalling the fast-decodable STBC definition in Chapter 3, a STBC that encodes $2K$ real symbols is said to be fast-decodable if it encloses a g-group decodable code of lower rate. In the special case where the low-complexity decodable code is an orthogonal STBC that encodes κ real symbols, the worst case decoding complexity order for square QAM constellations with M points is reduced from $\sqrt{M}^{2K-1}$ to $\sqrt{M}^{2K-\kappa}$ thanks to the conditional detection technique.

In this chapter, the multiplexing of two orthogonal STBCs by means of a unitary matrix in the case of four antennas is investigated. The unitary matrix is chosen such that the resulting code retains the cubic shaping property [20] of its constituent orthogonal STBCs. However, the cubic shaping property comes at the expense of a rate limitation of the proposed structure. We determine an upper bound on the achievable rate that is $5/4$ complex symbol per channel use and propose a multitude of codes that achieve this limit. We pick up one of the code realizations that minimize the PAPR and prove analytically in Appendix B that the the proposed code retains the coding gain of its constituent orthogonal STBCs and that the coding gain remains constant regardless of the underlying QAM constellation prior to normalization, in other words, the proposed code satisfy the NVD [20] property.

5.1 A FD code structure

Prior attempts to construct FD STBCs consist of multiplexing two or more low-complexity decodable codes by means of a matrix (that is typically unitary) whose entries are determined through numerical optimization to provide a large coding gain [14, 46, 54, 55, 56, 57]. In that context, the problem of constructing a FD code for four transmit antennas through multiplexing two orthogonal STBCs has been addressed in [58, 59] where the FD code is expressed as:

$$\mathbf{X}_{3/2} = \mathbf{X}_{3/4}(x_1, \ldots, x_6) + \mathbf{U}\mathbf{X}_{3/4}(x_7, \ldots, x_{12}). \tag{5.1}$$

$\mathbf{X}_{3/4}$ denotes the four antennas rate-3/4 orthogonal STBC code matrix (2.59) and $\mathbf{U}$ is chosen to maximize the coding gain. In [58] the matrix $\mathbf{U}$ was restricted to diagonal unitary matrices in order to provide a low PAPR as it prevents the combination of more than two symbols. Specifically:

$$\mathbf{U} = \begin{bmatrix} e^{j\theta_1} & 0 & 0 & 0 \\ 0 & e^{j\theta_2} & 0 & 0 \\ 0 & 0 & e^{j\theta_3} & 0 \\ 0 & 0 & 0 & e^{j\theta_4} \end{bmatrix}$$

where the phases $\theta_1, \theta_2, \theta_3, \theta_4$ are optimized numerically to provide a large coding gain for QPSK modulation. The numerical values of the phases were found to be equal to $3\pi/10, 3\pi/10, 3\pi/10, -2\pi/3$ respectively. In [59] however, the matrix $\mathbf{U}$ is no longer restricted to be unitary:

$$\mathbf{U} = \frac{1}{\sqrt{5}} \begin{bmatrix} 1 & 1+j & 1+j & 1+j \\ -1+j & 1 & 1-j & 1+j \\ -1-j & 1+j & 1 & 1+j \\ 1-j & -1-j & -1+j & 1 \end{bmatrix} \tag{5.2}$$

The proposed FD STBC structure takes the following from:

$$\mathbf{X}_{\text{new}} = \mathbf{X}_{3/4}(x_1, \ldots, x_6) + e^{j\phi}\mathbf{X}_{3/4}(x_7, \ldots, x_{12})\mathbf{U}. \tag{5.3}$$

where $\mathbf{U}$ is a unitary matrix that is chosen in order to guarantee the cubic shaping property (refer to section 2.3.5) and ϕ is chosen to maximize the coding gain. However, as will be proven in the following proposition satisfying the cubic shaping property of the proposed code structure (5.3) for arbitrary ϕ imposes a rate

limitation. On the other hand, the proposed code that satisfies the cubic shaping is proven to achieve the NVD property [20], thus avoiding the major drawback of prior constructions [58, 59] that rely on numerical optimization which becomes infeasible for large size constellations (e.g. 64-QAM and above).

5.1.1 Cubic shaping

Proposition 5.1 *For the proposed FD STBC, the cubic shaping is attainable for arbitrary ϕ if its rate is less than or equal to 5/4 complex symbol per channel use.*

Proof. The complex generator matrix $\mathbf{G}$ for a STBC may be directly expressed in terms of its weight matrices as:

$$\mathbf{G} = [\text{vec}(\mathbf{A}_1) \dots \text{vec}(\mathbf{A}_{12})] \tag{5.4}$$

As the orthogonal STBC satisfies the cubic shaping property, for the proposed code to satisfy the cubic shaping property (2.36), one must have:

$$\Re\left\{\text{vec}(\mathbf{A}_i)^H \text{vec}(\mathbf{A}_j)\right\} = 0,\ \forall\, 1 \leq i \leq 6,\ 7 \leq j \leq 12. \tag{5.5}$$

In terms of the linear representations of the Clifford Algebra generators (2.55), the above conditions may be expressed as:

$$\Re\left\{e^{j\phi}\text{vec}(\mathbf{R}_i)^H \text{vec}(\mathbf{R}_j\mathbf{U})\right\} = 0,\ \forall\, 0 \leq i,j \leq 5,\ \phi \in [0, 2\pi] \tag{5.6}$$

Therefore, for arbitrary ϕ the above condition reduces to:

$$\text{vec}(\mathbf{R}_i)^H \text{vec}(\mathbf{R}_j\mathbf{U}) = 0,\ \forall\, 0 \leq i,j \leq 5. \tag{5.7}$$

On the other hand, for any complex matrices $\mathbf{A}, \mathbf{B}$ we have:

$$\text{tr}\left(\mathbf{A}^H\mathbf{B}\right) = \text{vec}(\mathbf{A})^H \text{vec}(\mathbf{B}). \tag{5.8}$$

Consequently, the system of equations in (5.7) may be expressed as:

$$\text{tr}\left(\mathbf{R}_i^H\mathbf{R}_j\mathbf{U}\right) = 0,\ \forall\, 0 \leq i,j \leq 5 \tag{5.9}$$

which is again equivalent to:

$$\text{vec}(\mathbf{R}_i\mathbf{R}_j)^H \text{vec}(\mathbf{U}) = 0,\ \forall\, 0 \leq i,j \leq 5. \tag{5.10}$$

Thanks to the fact that the matrices $\mathbf{R}_i, i = 1, \ldots, 5$ square to $-\mathbf{I}$, one may express (5.10) as:

$$\begin{aligned} \operatorname{vec}(\mathbf{I})^H \operatorname{vec}(\mathbf{U}) &= 0 \\ \operatorname{vec}(\mathbf{R}_i\mathbf{R}_j)^H \operatorname{vec}(\mathbf{U}) &= 0,\ \forall\, 0 \leq i \neq j \leq 5. \end{aligned} \tag{5.11}$$

Moreover, it is known that the matrices $\mathbf{R}_i, i = 1, \ldots, 5$ anti-commute pairwise thus reducing the number of distinct linear equations to $\binom{6}{2} + 1 = 16$ which may be expressed in matrix form as:

$$\underbrace{\begin{bmatrix} \operatorname{vec}(\mathbf{I})^H \\ \operatorname{vec}(\mathbf{R}_1)^H \\ \vdots \\ \operatorname{vec}(\mathbf{R}_5)^H \\ \operatorname{vec}(\mathbf{R}_1\mathbf{R}_2)^H \\ \vdots \\ \operatorname{vec}(\mathbf{R}_4\mathbf{R}_5)^H \end{bmatrix}}_{\mathbf{M}} \begin{bmatrix} u_1 \\ \vdots \\ u_{16} \end{bmatrix} = 0 \tag{5.12}$$

It can be easily proved that the set of matrices $\{\mathbf{I}\} \cup \{\mathbf{R}_i\mathbf{R}_j,\ 0 \leq i \neq j \leq 5\}$ is equivalent to the matrix basis of $\mathcal{M}_4$ in Table 4.1, which implies that the matrix $\mathbf{M}$ is full ranked and that the only solution to the above is $u_1 = \ldots u_{16} = 0$.

In order to obtain a non-trivial solution of $\mathbf{U}$, one has to decrease the rate of the new code (5.3). If we remove and arbitrary symbol say $x_k,\ 7 \leq k \leq 12$ of the new code in (5.3) the conditions in (5.11) become:

$$\begin{aligned} \operatorname{vec}(\mathbf{I})^H \operatorname{vec}(\mathbf{U}) &= 0 \\ \operatorname{vec}(\mathbf{R}_i\mathbf{R}_j)^H \operatorname{vec}(\mathbf{U}) &= 0,\ \forall\, 0 \leq i \neq j \leq 5,\ j \neq k \end{aligned} \tag{5.13}$$

Unfortunately, the number of distinct linear equations remains unchanged and equals to $1 + \binom{5}{2} + 5 = 16$. Therefore, one has to decrease further the rate of the new code in order to satisfy the cubic shaping criterion. For instance, if we eliminate $x_l,\ 7 \leq l \leq 12,\ l \neq k$ (5.13) becomes:

$$\begin{aligned} \operatorname{vec}(\mathbf{I})^H \operatorname{vec}(\mathbf{U}) &= 0 \\ \operatorname{vec}(\mathbf{R}_i\mathbf{R}_j)^H \operatorname{vec}(\mathbf{U}) &= 0,\ \forall\, 0 \leq i \neq j \leq 5,\ j \neq k \neq l \end{aligned} \tag{5.14}$$

The number of distinct linear equations is decreased and is equal to $1+\binom{4}{2}+8=15$. A solution to the system of linear equations in (5.14) may be obtained by recalling from (4.17) that the set

$$\{\mathbf{I}\} \cup \{\mathbf{R}_k : k=1,\ldots,4\} \bigcup_{m=2}^{4} \left\{ \prod_{i=2}^{m} \mathbf{R}_{k_i} : 1 \leq k_1 < k_2 \ldots < k_m \leq 4 \right\} \tag{5.15}$$

forms a basis of $\mathcal{M}_4$ over $\mathbb{C}$ and we have from (A.1) (see Appendix A) that:

$$\text{tr}\,(\mathbf{A}) = 0,\ \forall \mathbf{A} \in \mathcal{B}_4 \setminus \{\mathbf{I}\}. \tag{5.16}$$

However, the set $\mathcal{B}_4$ is not unique as it depends on the specific choice of the $\mathbf{R}_{k_i}$ matrices, therefore one has:

$$\text{tr}\,(\mathbf{A}) = 0,\ \forall \mathbf{A} \in \{\mathbf{R}_1,\ldots \mathbf{R}_5\} \bigcup_{m=2}^{4} \left\{ \prod_{i=2}^{m} \mathbf{R}_{k_i} : 1 \leq k_1 < k_2 \leq 5 \right\} \tag{5.17}$$

By recalling the identity (5.8), it is straightforward to verify that choosing $\mathbf{U} = \mathbf{R}_k\mathbf{R}_l$ satisfies (5.14). Consequently, the rate of the proposed code cannot exceed 5/4 which concludes the proof. □

Based of **Proposition 5.1**, we will provide a new rate-5/4 FD STBC that satisfies the cubic shaping property and the NVD [20] property through judicious choice of ϕ.

5.1.2 The proposed code

As clearly seen from the proof of **Proposition 5.1**, one has a multitude of STBCs that satisfy the cubic shaping property depending on the choice of $\mathbf{R}_k$ and $\mathbf{R}_l$. In the following, we will pick up one of the solutions that minimize the PAPR. The proposed code denoted $\mathbf{X}_{5/4}$ arises as a direct application of **Proposition 5.1** by taking $\mathbf{R}_k = \mathbf{I}$ and $\mathbf{R}_l = \mathbf{R}_4$:

$$\mathbf{X}_{5/4}(\mathbf{s}) = \mathbf{X}_{3/4}(x_1,\ldots,x_6) + e^{j\phi}\left(\mathbf{R}_2 x_7 + \mathbf{R}_3 x_8 + \mathbf{R}_1 x_9 + \mathbf{R}_5 x_{10}\right)\mathbf{R}_4 \tag{5.18}$$

with $\mathbf{s} = [\mathbf{s}_1, \mathbf{s}_2]$, $\mathbf{s}_1 = [x_1,\ldots,x_6]$, $\mathbf{s}_2 = [x_7,\ldots,x_{10}]$ and ϕ is chosen to maximize the coding gain. The proposed code matrix takes the form below [22]:

$$\mathbf{X}_{5/4} = \begin{bmatrix} x_1 + jx_2 - jx_{10}e^{j\phi} & x_3 + jx_4 & x_5 + jx_6 + jx_9e^{j\phi} & -e^{j\phi}(x_7 + jx_8) \\ -x_3 + jx_4 & x_1 - jx_2 - jx_{10}e^{j\phi} & e^{j\phi}(-x_7 + jx_8) & -x_5 - jx_6 + jx_9e^{j\phi} \\ -x_5 + jx_6 + jx_9e^{j\phi} & e^{j\phi}(x_7 + jx_8) & x_1 - jx_2 + jx_{10}e^{j\phi} & x_3 + jx_4 \\ -e^{j\phi}(-x_7 + jx_8) & x_5 - jx_6 + jx_9e^{j\phi} & -x_3 + jx_4 & x_1 + jx_2 + jx_{10}e^{j\phi} \end{bmatrix} \tag{5.19}$$

We found through exhaustive search that taking $\phi = \frac{1}{2}\cos^{-1}(1/5)$ maximizes the coding gain and that it remains constant up to 64-QAM unnormalized constellations. However a stronger result is stated in the following proposition:

Proposition 5.2 *Taking $\phi = \frac{1}{2}\cos^{-1}(1/5)$ maximizes the coding gain of the proposed code and that it remains constant irrespectively to the underlying QAM constellations prior to normalization.*

Proof. refer to Appendix B. □

5.2 Decoding

To decode the proposed code, the receiver evaluates the QR decomposition of the real equivalent channel matrix $\tilde{\boldsymbol{\mathcal{H}}}$ (2.7). Thanks to the FD structure (see Section 3.2) of the proposed code with $K = 5, \kappa = 6$ with $g = 6$ such that $n_1 = n_2 \ldots, n_6 = 1$, we deduce that the corresponding upper-triangular matrix $\mathbf{R}$ takes the form:

$$\mathbf{R} = \begin{bmatrix} x & 0 & 0 & 0 & 0 & 0 & x & x & x & x \\ 0 & x & 0 & 0 & 0 & 0 & x & x & x & x \\ 0 & 0 & x & 0 & 0 & 0 & x & x & x & x \\ 0 & 0 & 0 & x & 0 & 0 & x & x & x & x \\ 0 & 0 & 0 & 0 & x & 0 & x & x & x & x \\ 0 & 0 & 0 & 0 & 0 & x & x & x & x & x \\ 0 & 0 & 0 & 0 & 0 & 0 & x & x & x & x \\ 0 & 0 & 0 & 0 & 0 & 0 & 0 & x & x & x \\ 0 & 0 & 0 & 0 & 0 & 0 & 0 & 0 & x & x \\ 0 & 0 & 0 & 0 & 0 & 0 & 0 & 0 & 0 & x \end{bmatrix} \tag{5.20}$$

where x indicates a possible non-zero position. The decoder exploits the structure of the upper triangular matrix $\mathbf{R}$ by computing the ML estimates of the orthogonal symbols $(x_1, \ldots, x_6)$ assuming that a given value of $(x_7, \ldots, x_{10})$ is transmitted. In the case of the square QAM constellations, the ML estimates of the orthogonal symbols $(x_1, \ldots, x_6)$ assuming the knowledge of $(x_7, \ldots, x_{10})$ can be obtained through hard PAM slicers as:

$$x_i^{\mathrm{ML}} | \, (\hat{x}_7, \ldots, \hat{x}_{10}) = \mathrm{sign}\,(z_i) \times \min\Big[\Big|2\,\mathrm{round}\Big(\,(z_i - 1)\,/2\Big) + 1\Big|, \sqrt{M} - 1\Big] \; \forall i = 1, \ldots 6. \tag{5.21}$$

where $z_i = \left(y'_i - \sum_{j=7}^{10} r_{i,j}\hat{x}_j\right)/r_{i,i}\ \forall i = 1, \ldots 6$.

According to the complexity analysis provided in Chapter 3, the worst-case decoding complexity of the proposed code is equal to $\sqrt{M}^{2K-\kappa} = M^2$ as the hard PAM slicers prune the last 6 levels of the original 10 levels real valued search tree. A pseudo code of the sphere decoder of the proposed code is provided below:

Algorithm II: The SD for $\mathbf{X}_{5/4}$ and square QAM of size M

$C = \infty$
$z_{10} = y'_{10}/r_{10,10}$
$x_{10}^{\mathsf{nc}} = \mathtt{sign}\left(z_{10}\right) \times \mathtt{min}\left[\left|2\ \mathtt{round}(\left(z_{10}-1\right)/2) + 1\right|, \sqrt{M}-1\right]$
$\Xi_{10} = \mathtt{sort}(z_{10}, x_{10}^{\mathsf{nc}})$
$k_{10} = 1$
while $k_{10} \leq \sqrt{M}$ **and** $\left(y'_{10} - r_{10,10}\mathcal{A}\left(\Xi_{10}\left(k_{10}\right)\right)\right)^2 < C$ **do**
  $x_{10} = \mathcal{A}\left(\Xi_{10}\left(k_{10}\right)\right)$
  $W_{10} = \left(y'_{10} - r_{10,10}x_{10}\right)^2$
  $\ddots$
  $z_7 = \left(y'_7 - \sum_{i=8}^{10} r_{7,i}x_i\right)/r_{7,7}$
  $x_7^{\mathsf{nc}} = \mathtt{sign}\left(z_7\right) \times \mathtt{min}\left[\left|2\ \mathtt{round}(\left(z_7-1\right)/2) + 1\right|, \sqrt{M}-1\right]$
  $\Xi_7 = \mathtt{sort}(z_7, x_7^{\mathsf{nc}})$
  $k_7 = 1$
  while $k_7 \leq \sqrt{M}$ **and** $\left(y'_7 - r_{7,7}\mathcal{A}\left(\Xi_7\left(k_7\right)\right) - \sum_{j=8}^{10} r_{7,j}x_j\right)^2 + \sum_{i=8}^{10} W_i < C$ **do**
    $x_7 = \mathcal{A}\left(\Xi_7\left(k_7\right)\right)$
    $W_7 = \left(y'_7 - \sum_{j=7}^{10} r_{7,j}x_j\right)^2$
    $z_i = \left(y'_i - \sum_{j=7}^{10} r_{i,j}x_j\right)/r_{i,i},\ i = 1, \ldots, 6$
    $x_i = \mathtt{sign}\left(z_i\right) \times \mathtt{min}\left[\left|2\ \mathtt{round}(\left(z_i-1\right)/2) + 1\right|, \sqrt{M}-1\right],\ i = 1, \ldots, 6$
    $W_i = \left(\left(z_i - x_i\right)r_{i,i}\right)^2,\ i = 1, \ldots, 6$
    $P = \sum_{i=1}^{10} W_i$
    if $P < C$ **then**
      $C = P$
      $\hat{\mathbf{s}} = \mathbf{x}$
    end
    $k_7 = k_7 + 1$
  end
  $\ddots$
  $k_{10} = k_{10} + 1$
end

5.3 Numerical and Simulations Results

The STBCs are compared in terms of square QAM constellations worst-case decoding complexity order, the minimum determinant[1]and the PAPR. The minimum determinant is defined as:

$$\text{Min det} = \min_{\Delta\mathbf{s}\in\Delta\mathcal{C}\setminus\{\mathbf{0}\}} |\det\left((\mathbf{X}(\Delta\mathbf{s}))\right)| = \sqrt{\delta} \tag{5.22}$$

where $\Delta\mathbf{s} = \mathbf{s} - \mathbf{s}'$, $\Delta\mathcal{C}$ is the vector space spanned by $\Delta\mathbf{s}$, δ is the coding gain and the PAPR is defined as:

$$\text{PAPR}_n = \frac{\max\limits_{t} |\mathbf{X}(t,n)|^2}{T^{-1}\sum\limits_{t}\mathbb{E}\{|\mathbf{X}(t,n)|^2\}} \tag{5.23}$$

where $t \in \{1,\dots T\}$ and $n \in \{1,\dots N_t\}$. Due to the symmetry between transmit antennas, the subscript n will be omitted.

Simulations are carried out in a quasi-static Rayleigh fading channel in the presence of AWGN for 4,16, and 64-QAM constellations. ML detection is performed via a depth-first tree traversal with infinite initial radius sphere decoder. The radius is updated whenever a leaf node is reached and sibling nodes are visited according to the simplified Schnorr-Euchner enumeration [32].

Rate-1 code

In a first step, we compare the rate-1 punctured version of the code in (5.18) by removing x_9 and x_{10} [21] to the state-of-art rate-1 low complexity decodable STBCs. The comparison is summarized in Table 5.1. It is worth noting that the complexity of detection of the QOD code in [37] can be reduced from $\mathcal{O}(M^2)$ to $\mathcal{O}(2M)$. Indeed, the QOD in [37] enables separate detection of two groups of complex symbols, namely (s_1, s_3) and (s_2, s_4), giving rise to a worst-case complexity order of $2M^2$. However, by noting that the real and imaginary parts of each symbol are separable, the worst case decoding complexity order may be significantly reduced to $2M$ if we resort to the conditional detection by evaluating the ML estimates of the real and imaginary parts of s_1 assuming that a given value of s_3 is transmitted

[1]For consistency, the minimun determinant is evaluated at fixed average transmitted power per channel use for all codes

Table 5.1: Summary of comparisons in terms of complexity, Min det and PAPR

Code	Square QAM decoding complexity	QAM Min det	PAPR (dB)		
			QPSK	16QAM	64QAM
The proposed rate-1 code	M	16	0	2.5	3.7
N.Sharma-C.B.Papadias code[37]	$2M$	16	0	2.5	3.7
M.Sinnokrot-J.Barry code[61]	$4\sqrt{M}$	7.11	0	2.5	3.7
S.Karmakar-S.Rajan code[16, 40]	$4\sqrt{M}$	12.8	1.6	4.2	5.3
Md.Khan-S.Rajan code[62]	$4\sqrt{M}$	12.8	5.8	8.3	9.5

(i.e. $\Re\{s_1\}^{\mathrm{ML}}|\hat{s}_3$, $\Im\{s_1\}^{\mathrm{ML}}|\hat{s}_3$) and similarly for the real and imaginary parts of s_2 assuming that a given value of s_4 is transmitted which are obtained through hard PAM slicers.

We provide an analytical proof in Appendix C, that taking the rotation angle to be $\pi/6$ or $\pi/3$ maximizes the coding gain and assures the NVD property of the QOD code [37], which may be considered as a complement to the proof of the optimality of $\pi/4$ in [38].

One can notice the following: The proposed code and the achieve the highest coding gain compared to existing low-complexity decodable rate-1 full-diversity 4×4 STBCs in the literature and thus we can expect that they provide better performance in the high SNR regime which can be verified from Figs. 5.1, 5.3, and 5.5. The proposed code along with the codes of [37, 61] have the lowest PAPR which is that of the used constellation. On the other hand, our code suffers from a slight increase in worst-case decoding complexity w.r.t. the codes of [61, 16, 40, 62], but this will only penalize the proposed code for high-order QAM constellations (in fact our code will be more complex to decode only for $M \geq 64$).

In the high SNR region, the initial guess point $\mathbf{s}^{\mathrm{nc}}$ which is the *nulling and cancelling* point (refer to Section 2.2) of the SD becomes closer to the ML estimate, which suggests that the average complexity is asymptotically governed by the number of nodes linking the root to a given leaf node. For the proposed rate-1 code, this number is equal to 2, whereas for the codes in [37, 61, 16, 40, 62] this number equals 4. This interpretation justifies the behaviour of the average decoding complexity curves in the high SNR region in Figs. 5.2, 5.4, and 5.6.

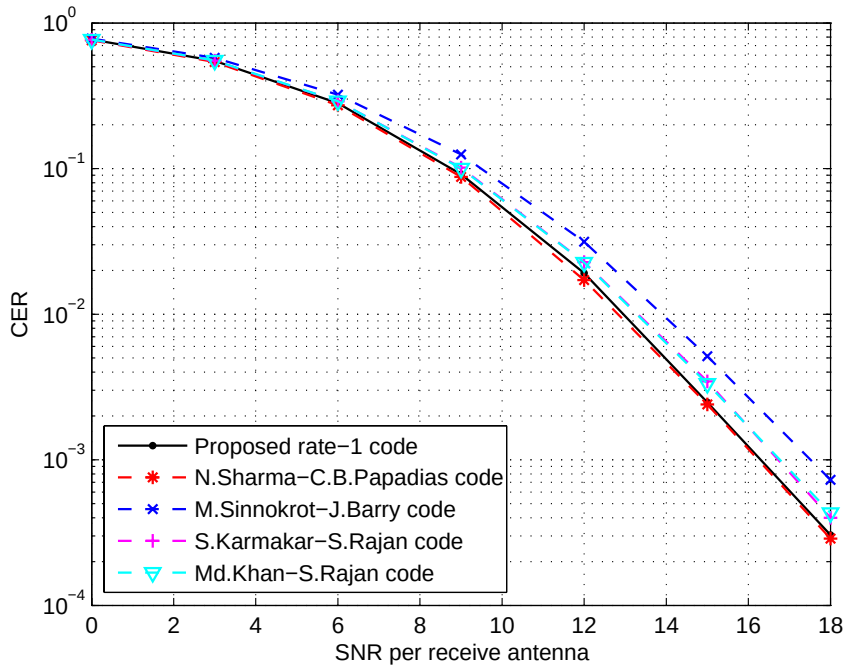

Figure 5.1: CER performance for 4×1 configuration and QPSK

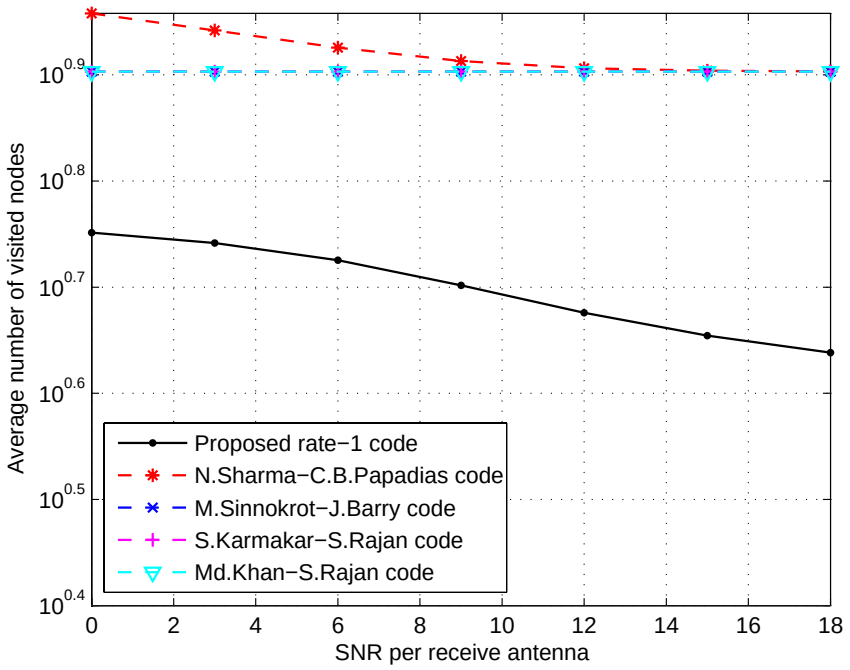

Figure 5.2: Average complexity for 4×1 configuration and QPSK

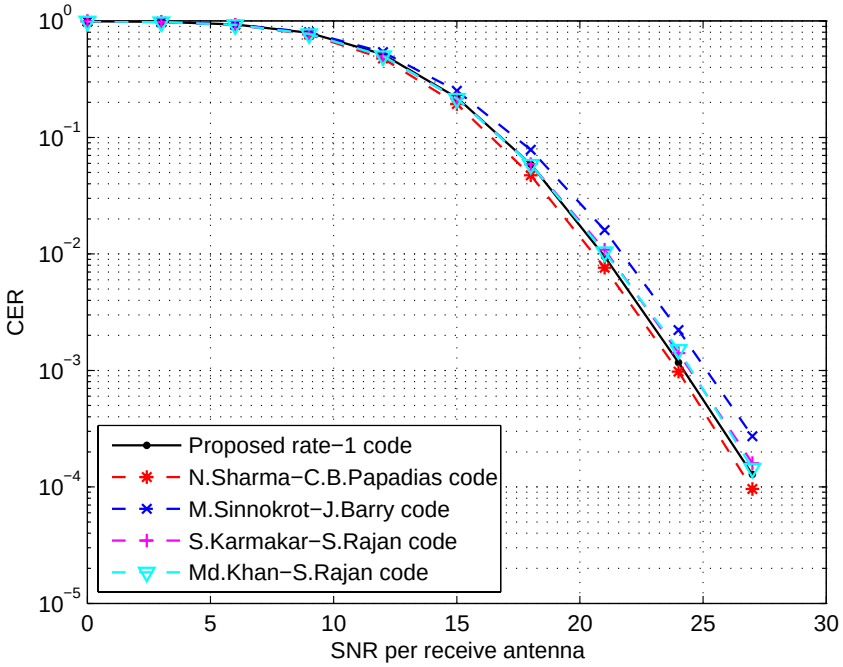

Figure 5.3: CER performance for 4×1 configuration and 16-QAM

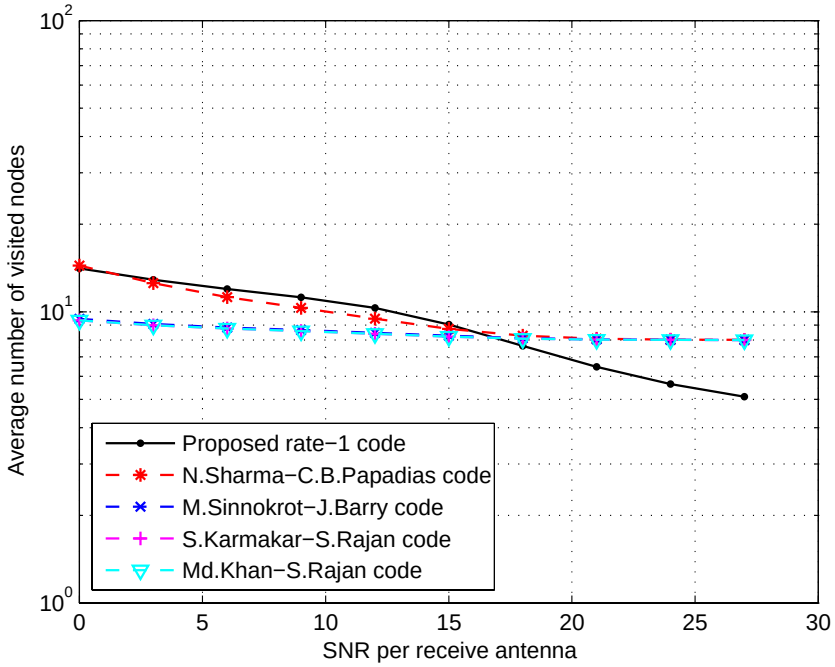

Figure 5.4: Average complexity for 4×1 configuration and 16-QAM

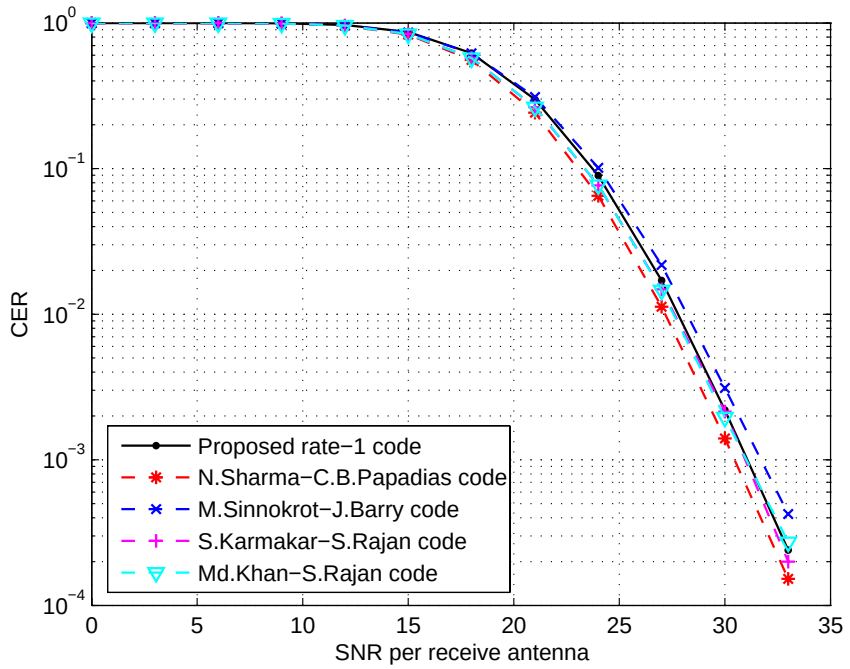

Figure 5.5: CER performance for 4×1 configuration and 64-QAM

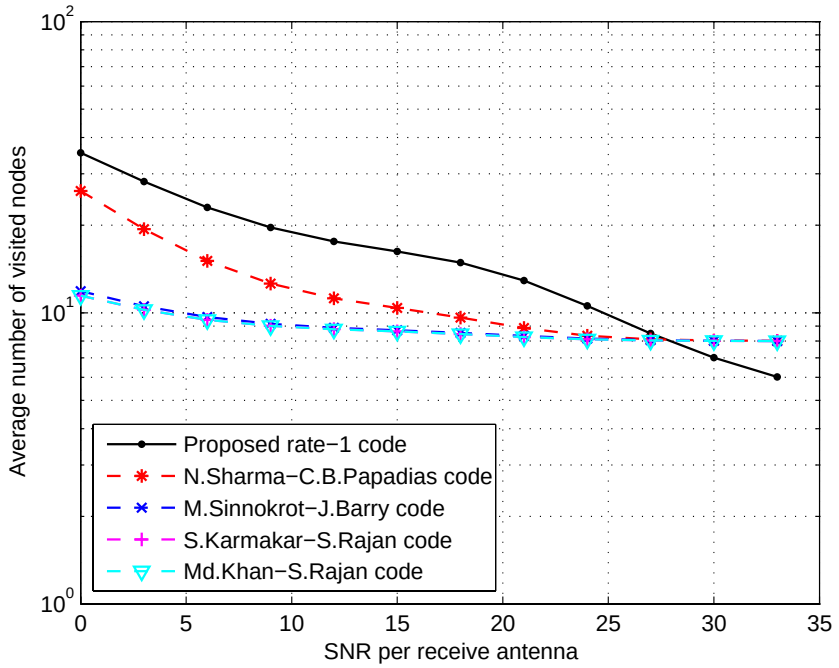

Figure 5.6: Average complexity for 4×1 configuration and 64-QAM

Rate-5/4 code

In a second step, we compare our rate-5/4 code to the rate-5/4 punctured version of the code in [46]and the rate-5/4 punctured version of the code in [59]. The comparison is summarized in Table 5.2.

Table 5.2: Summary of comparisons in terms of complexity, Min det and PAPR

Code	Square QAM decoding complexity	QAM Min det	PAPR (dB)		
			QPSK	16QAM	64QAM
The proposed rate-5/4 code	M^2	16	3.6	6.2	7.3
S.Sirianunpiboon rate-5/4 code[59]	M^2	N/A	4.8	7.3	8.5
P.Srinath-S.Rajan rate-5/4 code[46]	$4M^{1.5}$	12.8	4.8	7.3	8.5

The punctured version of the codes in [59] and [46] is obtained by eliminating the appropriate number of symbols such as to keep the worst-case decoding complexity at its minimum. That is for the rate-3/2 S. Sirianunpiboon *et al.* code in [59] the rate-5/4 punctured version is obtained by removing x_6, whereas for the rate-2 P.Srinath-S.Rajan code in [46], the rate-5/4 punctured version is obtained by removing $s_{6I}, s_{6Q}, \ldots, s_{8I}, s_{8Q}$. One can notice that the proposed code has a higher coding gain, lower PAPR at the expense of a slight increase in worst-case detection complexity that will penalize our code for the 64-QAM constellation and above.

Figs. 5.7,5.9, and 5.11 illustrate the performance comparison in terms of Codeword Error Rate (CER) of the proposed code and the rate-$5/4$ punctured version of the code in [46]. One can notice that the proposed code offers better performance especially at high SNR. This is attributed to the superiority of the coding gain of our code. Furthermore, as can be seen form Figs. 5.8,5.10, and 5.12, our code can be decoded with lower average complexity.

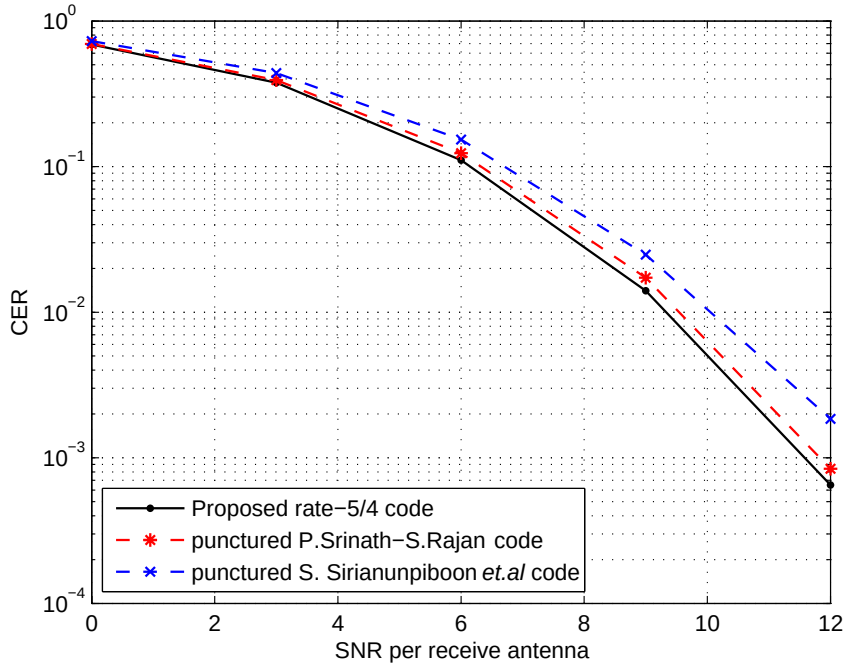

Figure 5.7: CER performance for 4×2 configuration and QPSK

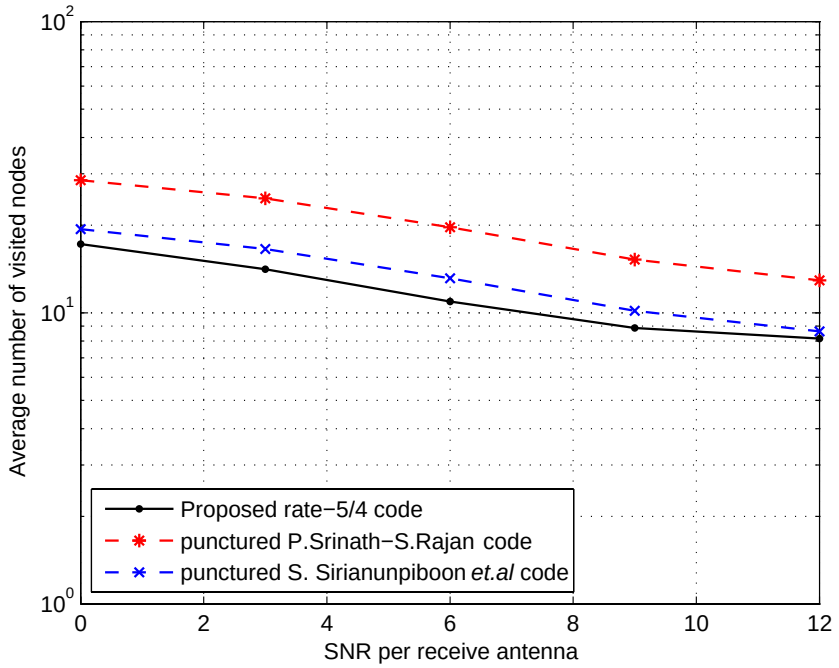

Figure 5.8: Average complexity for 4×2 configuration and QPSK

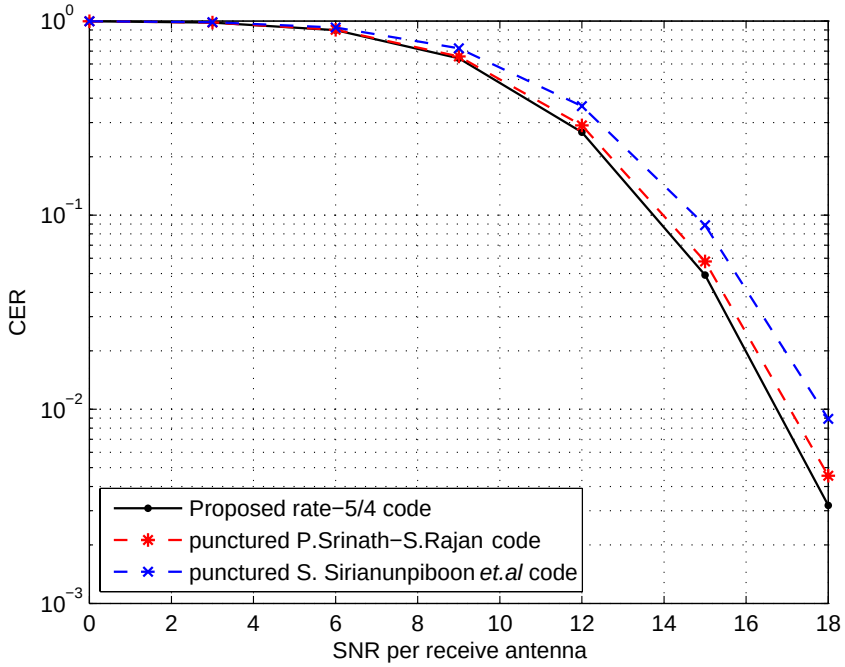

Figure 5.9: CER performance for 4×2 configuration and 16-QAM

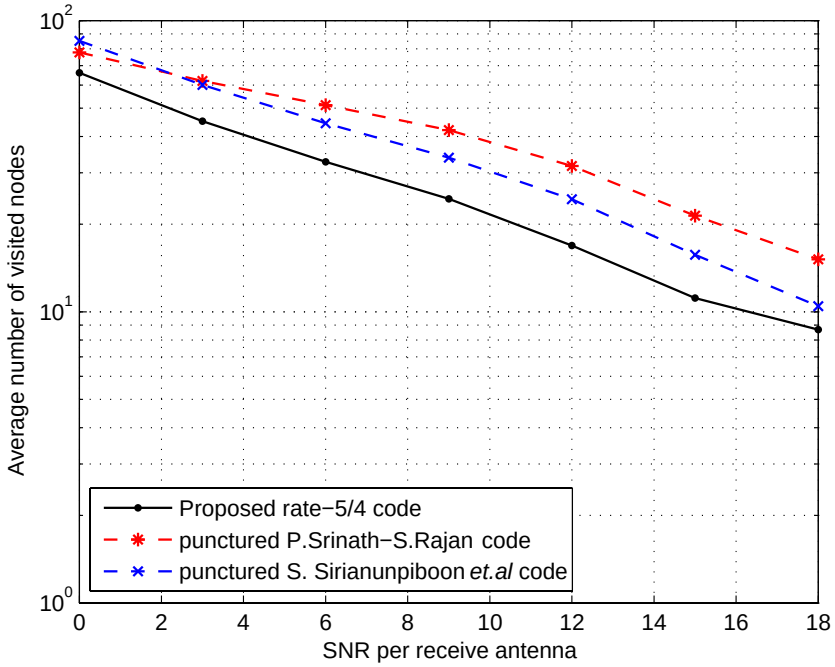

Figure 5.10: Average complexity for 4×2 configuration and 16-QAM

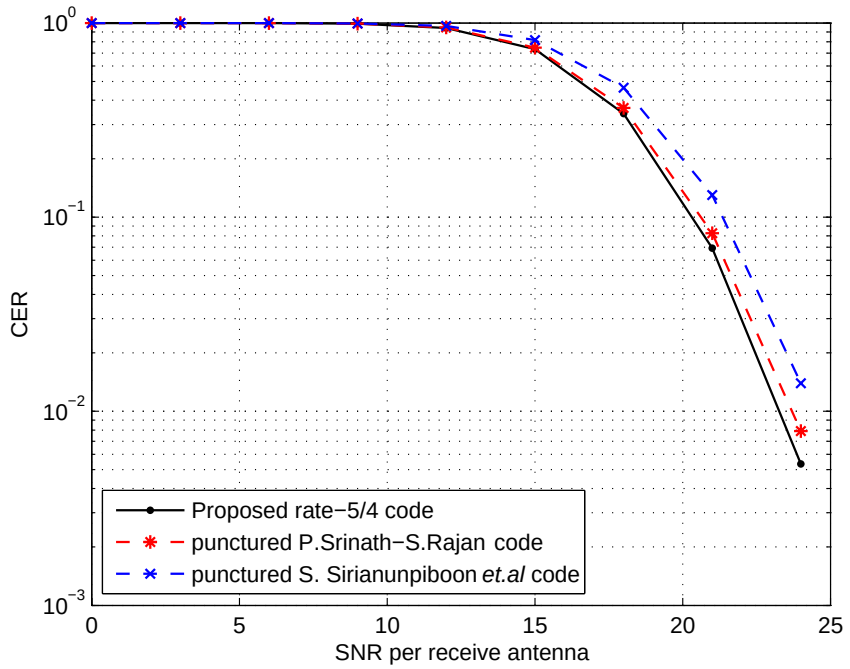

Figure 5.11: CER performance for 4×2 configuration and 64-QAM

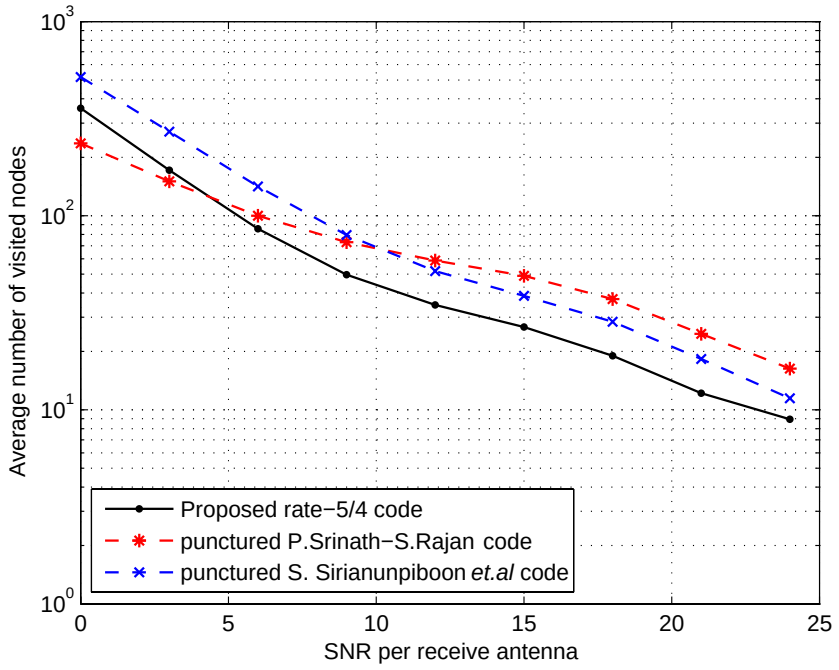

Figure 5.12: Average complexity for 4×2 configuration and 64-QAM

5.4 Conclusions

In this chapter, we focused on the multiplexing of two orthogonal codes by means of a unitary matrix $\mathbf{U}$ and a complex exponential $e^{j\phi}$, where $\mathbf{U}$ guarantees the cubic shaping property while ϕ is optimized to guarantee a large coding gain. We first derived an upper limit on the achievable rate (which is 5/4 complex symbol per channel use) of the proposed structure in order to achieve the cubic shaping property regardless of the phase angle ϕ. We then numerically found that taking $\phi = \frac{1}{2}\cos^{-1}(1/5)$ maximizes the coding gain and that it remains constant up to 64-QAM unnormalized constellations. This result was strengthen with an analytical proof that this choice of ϕ indeed guarantee the NVD property of the proposed code.

The proposed code is compared to the rate-5/4 punctured version of the low-complexity decodable 4×4 STBC in [46] and [59]. The proposed code showed better CER performance, and lower PAPR, lower average complexity at the expense of a slight increase in worst-case detection complexity that affects our code only for high-order QAM constellations.

Chapter 6

A New Family of Low-Complexity Decodable STBCs for Four Transmit Antennas

In this chapter we first propose a novel construction scheme for rate-1 FGD codes for 2^a transmit antennas. The resulting rate-1 code corresponding to a number of antennas that is not a power of two is easily obtained by removing the appropriate number of columns from the code matrix of the nearest greater number of antennas that is a power of two, for instance the rate-1 code for the case of three transmit antennas is obtained by removing one column from the rate-1 code matrix for four transmit antennas. We focus on the case of four transmit antennas and prove that the resultant code has the lowest worst-case decoding complexity order among state-of-the-art rate-1 low complexity codes. The coding gain of the proposed code is optimized through constellation stretching while keeping the PAPR at its minimum which is that of the underlying constellation. The coding gain is proved to be constant irrespectively to the underlying QAM constellation prior to normalization, thus the proposed code achieved the NVD property.

In a second step we propose two higher rate FD codes through multiplexing and numerical optimization giving rise to two new FD codes with rates 3/2 and 2 complex symbols per channel use. The proposed codes are compared to rivals codes in the literature. The worst-case decoding complexity analysis show that the proposed codes have the smallest worst-case decoding complexity among similar codes in the literature. Simulation results that our rate-1 and rate-3/2 codes have

lower average decoding complexity while our rate-2 code maintains its lower average decoding complexity in the low SNR regime.

6.1 A systematic approach to the construction of FGD codes

From the properties of the matrix representations of the Clifford algebra generators over $\mathbb{R}$ (2.58), it is straightforward to prove that if $\mathbf{A} = \prod_{i=1}^{m} \mathbf{R}_{k_i} | k_1 < k_2 \ldots < k_m$, we have:

$$\mathbf{A}^H = (-1)^{m(m+1)/2} \mathbf{A} \tag{6.1}$$

Proposition 6.1 *For 2^a transmit antennas, the two sets of matrices, namely $\mathcal{G}_1 = \{\mathbf{I}, \mathbf{R}_1, \ldots, \mathbf{R}_a\} \cup \mathcal{A}$ and $\mathcal{G}_2 = \{\mathbf{R}_{a+1}, \ldots, \mathbf{R}_{2a+1}\} \cup \mathcal{B}$ satisfy* (3.5) *where $\mathcal{A}$ and $\mathcal{B}$ are given in Table 6.1, Table 6.2, respectively, [24].*

Table 6.1: Different cases for $\mathcal{A}$

a	$\mathcal{A}$
$4n$	$\left\{ j \prod_{i=a+1}^{2a+1} \mathbf{R}_i \right\} \bigcup_{m=1}^{a-2} \left\{ j^{\delta_{\mathcal{A}}(m)} \prod_{i=a+1}^{2a+1} \mathbf{R}_i \prod_{i=1}^{m} \mathbf{R}_{k_i} : 1 \le k_1 < \ldots < k_m \le a \right\}$
$4n+1$	$\left\{ \prod_{i=a+1}^{2a+1} \mathbf{R}_i \right\} \bigcup_{m=1}^{a-2} \left\{ j^{\delta_{\mathcal{A}}(m)} \prod_{i=a+1}^{2a+1} \mathbf{R}_i \prod_{i=1}^{m} \mathbf{R}_{k_i} : 1 \le k_1 < \ldots < k_m \le a \right\}$
$4n+2$	$\left\{ \prod_{i=a+1}^{2a+1} \mathbf{R}_i \right\} \bigcup_{m=1}^{a-2} \left\{ j^{\delta_{\mathcal{A}}(m)} \prod_{i=a+1}^{2a+1} \mathbf{R}_i \prod_{i=1}^{m} \mathbf{R}_{k_i} : 1 \le k_1 < \ldots < k_m \le a \right\}$
$4n+3$	$\left\{ j \prod_{i=a+1}^{2a+1} \mathbf{R}_i \right\} \bigcup_{m=1}^{a-2} \left\{ j^{\delta_{\mathcal{A}}(m)} \prod_{i=a+1}^{2a+1} \mathbf{R}_i \prod_{i=1}^{m} \mathbf{R}_{k_i} : 1 \le k_1 < \ldots < k_m \le a \right\}$

Table 6.2: Different cases for $\mathcal{B}$

a	$\mathcal{B}$
$4n$	$\left\{ j \prod_{i=1}^{a} \mathbf{R}_i \right\} \bigcup_{m=2,4}^{a-2} \left\{ j^{\delta_{\mathcal{B}}(m)} \prod_{i=1}^{a} \mathbf{R}_i \prod_{i=1}^{m} \mathbf{R}_{k_i} : a+1 \le k_1 < \ldots < k_m \le 2a+1 \right\}$
$4n+1$	$\bigcup_{m=1,3}^{a-2} \left\{ j^{\delta_{\mathcal{B}}(m)} \prod_{i=1}^{a} \mathbf{R}_i \prod_{i=1}^{m} \mathbf{R}_{k_i} : a+1 \le k_1 < \ldots < k_m \le 2a+1 \right\}$
$4n+2$	$\left\{ \prod_{i=1}^{a} \mathbf{R}_i \right\} \bigcup_{m=2,4}^{a-2} \left\{ j^{\delta_{\mathcal{B}}(m)} \prod_{i=1}^{a} \mathbf{R}_i \prod_{i=1}^{m} \mathbf{R}_{k_i} : a+1 \le k_1 < \ldots < k_m \le 2a+1 \right\}$
$4n+3$	$\bigcup_{m=1,3}^{a-2} \left\{ j^{\delta_{\mathcal{B}}(m)} \prod_{i=1}^{a} \mathbf{R}_i \prod_{i=1}^{m} \mathbf{R}_{k_i} : a+1 \le k_1 < \ldots < k_m \le 2a+1 \right\}$

where $\delta_{\mathcal{A}}(m), \delta_{\mathcal{B}}(m)$ are given in Table 6.3:

Proof. It is easy to see that $\mathcal{G}_1 \backslash \mathcal{A} \cup \mathcal{G}_2 \backslash \mathcal{B}$ is the set of weight matrices for the COD for 2^a transmit antennas. Thus we need only to prove that the $\mathcal{A}, \mathcal{G}_2$, and $\mathcal{B}, \mathcal{G}_1$ satisfy

Table 6.3: Different cases for δ

a	$\delta_{\mathcal{A}}(m)$	$\delta_{\mathcal{B}}(m)$
$4n$	$\frac{\left((m)_4-1\right)\left((m)_4-2\right)}{2}$	$\frac{2-(m)_4}{2}$
$4n+1$	$\frac{\left(\left((m)_4\right)\left((m)_4-1\right)\right)_4}{2}$	$\frac{(m)_4-1}{2}$
$4n+2$	$\frac{\left(\left((m)_4\right)\left((m)_4-3\right)\right)_4}{2}$	$\frac{(m)_4}{2}$
$4n+3$	$\frac{\left((m)_4-2\right)\left((m)_4-3\right)}{2}$	$\frac{3-(m)_4}{2}$

(3.5). Towards this end let $\mathbf{A}_k \in \mathcal{A}$, $\mathbf{B}_l \in \mathcal{B}$, $\mathbf{C} \in \mathcal{G}_1 \setminus \mathcal{A}$, and $\mathbf{D} \in \mathcal{G}_2 \setminus \mathcal{B}$. Let $a = 4n$, we have according to Table 6.2:

$$\mathbf{B}_1 = j \prod_{i=1}^{4n} \mathbf{R}_i \tag{6.2}$$

and

$$\mathbf{B}_{m/2+1} = \begin{cases} j \prod_{i=1}^{4n} \mathbf{R}_i \prod_{i=1}^{m} \mathbf{R}_{k_i} & 4n+1 \leq k_1 < \ldots < k_m \leq 8n+1, m = 4n' \\ \prod_{i=1}^{4n} \mathbf{R}_i \prod_{i=1}^{m} \mathbf{R}_{k_i} & 4n+1 \leq k_1 < \ldots < k_m \leq 8n+1, m = 4n'+2 \end{cases} \tag{6.3}$$

Recall that the matrices $\mathbf{R}_i,\ i = 1, \ldots, 2a+1$ have the following properties:

$$\mathbf{R}_i^H = -\mathbf{R}_i,\ \mathbf{R}_i^2 = -\mathbf{I},\ \forall 1 \leq i \leq 2a+1, \text{ and } \mathbf{R}_i\mathbf{R}_j + \mathbf{R}_j\mathbf{R}_i = \mathbf{0},\ \forall 1 \leq i \neq j \leq 2a+1. \tag{6.4}$$

Consequently, from (6.1) and (6.4) we can write:

$$\mathbf{B}^H = -\mathbf{B},\ \forall \mathbf{B} \in \mathcal{B} \tag{6.5}$$

$$\mathbf{B}^H\mathbf{C} + \mathbf{C}^H\mathbf{B} = \mathbf{0},\ \forall \mathbf{B} \in \mathcal{B} \tag{6.6}$$

On the other hand from Table 6.1 we have:

$$\mathbf{A}_1 = j \prod_{i=4n+1}^{8n+1} \mathbf{R}_i \tag{6.7}$$

and

$$\mathbf{A}_m = \begin{cases} j \prod_{i=4n+1}^{8n+1} \mathbf{R}_i \prod_{i=1}^{m} \mathbf{R}_{k_i} & 1 \leq k_1 < \ldots < k_m \leq 4n,\ m = 4n', n' \neq 0 \\ \prod_{i=4n+1}^{8n+1} \mathbf{R}_i \prod_{i=1}^{m} \mathbf{R}_{k_i} & 1 \leq k_1 < \ldots < k_m \leq 4n,\ m = 4n'+1, n' \neq 0 \\ \prod_{i=4n+1}^{8n+1} \mathbf{R}_i \prod_{i=1}^{m} \mathbf{R}_{k_i} & 1 \leq k_1 < \ldots < k_m \leq 4n,\ m = 4n'+2 \\ j \prod_{i=4n+1}^{8n+1} \mathbf{R}_i \prod_{i=1}^{m} \mathbf{R}_{k_i} & 1 \leq k_1 < \ldots < k_m \leq 4n,\ m = 4n'+3 \end{cases} \tag{6.8}$$

Again (6.1) and (6.4), it follows that:

$$\mathbf{A}_1^H = \mathbf{A}_1 \tag{6.9}$$

$$\mathbf{A}_m^H = \begin{cases} \mathbf{A}_m & m \text{ even} \\ -\mathbf{A}_m & m \text{ odd} \end{cases} \tag{6.10}$$

$$\mathbf{A}^H\mathbf{D} + \mathbf{D}^H\mathbf{A} = \mathbf{0}, \forall \mathbf{A} \in \mathcal{A} \tag{6.11}$$

Finally, from Eqs (6.2), (6.3), (6.7), (6.8), and (6.4) we get:

$$\mathbf{A}^H\mathbf{B} + \mathbf{B}^H\mathbf{A} = \mathbf{0}, \ \forall \mathbf{A} \in \mathcal{A}, \mathbf{B} \in \mathcal{B} \tag{6.12}$$

The proofs for other cases of a follow similarly and are therefore omitted. □

Proposition 6.2 *The rate of the proposed FGD codes is equal to one complex symbol per channel use regardless of the number of transmit antennas [24].*

Proof. The rate of the proposed FGD codes for the case of 2^a transmit antennas may be expressed as:

$$R = \frac{2a + 2 + |\mathcal{A}| + |\mathcal{B}|}{2^{a+1}} \tag{6.13}$$

However form Table 6.1, regardless of a we have:

$$|\mathcal{A}| = 1 + \sum_{i=1}^{a-2} \binom{a}{i} = \sum_{i=0}^{a-2} \binom{a}{i} = 2^a - (a+1) \tag{6.14}$$

On the other hand, from Table 6.2, we have for a even:

$$\begin{aligned} |\mathcal{B}| &= 1 + \sum_{i=2,4,6,\ldots}^{a-2} \binom{a+1}{i} = 1 + \sum_{i=2,4,6\ldots}^{a-2} \binom{a}{i-1} + \binom{a}{i} \\ &= 1 + \sum_{j=1,3,5\ldots}^{a-3} \binom{a}{j} + \sum_{i=2,4,6\ldots}^{a-2} \binom{a}{i} = 1 + \sum_{l=1}^{a-2} \binom{a}{l} = \sum_{l=0}^{a-2} \binom{a}{l} = 2^a - (a+1) \end{aligned} \tag{6.15}$$

where we used the recursion identity:

$$\binom{n}{k} = \binom{n-1}{k-1} + \binom{n-1}{k} \tag{6.16}$$

Similarly, for a odd, we have:

$$\begin{aligned} |\mathcal{B}| &= \sum_{i=1,3,5,\ldots}^{a-2} \binom{a+1}{i} = \sum_{i=1,3,5\ldots}^{a-2} \binom{a}{i-1} + \binom{a}{i} \\ &= \sum_{j=0,2,4\ldots}^{a-3} \binom{a}{j} + \sum_{i=1,3,5\ldots}^{a-2} \binom{a}{i} = \sum_{l=0}^{a-2} \binom{a}{l} = \sum_{l=0}^{a-2} \binom{a}{l} = 2^a - (a+1). \end{aligned} \tag{6.17}$$

Finally, using these relations, we get:

$$R = 1 \tag{6.18}$$

□

Examples of the rate-1 FGD codes for 4,8 and 16 transmit antennas are given in Table 6.4.

Table 6.4: Examples of rate-1 FGD codes

Tx	$\mathcal{G}_1$	$\mathcal{G}_2$
4	$\mathbf{I}, \mathbf{R}_2, \mathbf{R}_4, \mathbf{R}_1\mathbf{R}_3\mathbf{R}_5$	$\mathbf{R}_1, \mathbf{R}_3, \mathbf{R}_5, \mathbf{R}_2\mathbf{R}_4$
8	$\mathbf{I}, \mathbf{R}_2, \mathbf{R}_4, \mathbf{R}_6$	$\mathbf{R}_1, \mathbf{R}_3, \mathbf{R}_5, \mathbf{R}_7$
	$j\mathbf{R}_1\mathbf{R}_3\mathbf{R}_5\mathbf{R}_7$	$j\mathbf{R}_2\mathbf{R}_4\mathbf{R}_6\mathbf{R}_1$
	$j\mathbf{R}_1\mathbf{R}_3\mathbf{R}_5\mathbf{R}_7\mathbf{R}_2$	$j\mathbf{R}_2\mathbf{R}_4\mathbf{R}_6\mathbf{R}_3$
	$j\mathbf{R}_1\mathbf{R}_3\mathbf{R}_5\mathbf{R}_7\mathbf{R}_4$	$j\mathbf{R}_2\mathbf{R}_4\mathbf{R}_6\mathbf{R}_5$
	$j\mathbf{R}_1\mathbf{R}_3\mathbf{R}_5\mathbf{R}_7\mathbf{R}_6$	$j\mathbf{R}_2\mathbf{R}_4\mathbf{R}_6\mathbf{R}_7$
16	$\mathbf{I}, \mathbf{R}_2, \mathbf{R}_4, \mathbf{R}_6, \mathbf{R}_8$	$\mathbf{R}_1, \mathbf{R}_3, \mathbf{R}_5, \mathbf{R}_7, \mathbf{R}_9$
	$j\mathbf{R}_1\mathbf{R}_3\mathbf{R}_5\mathbf{R}_7\mathbf{R}_9$	$j\mathbf{R}_2\mathbf{R}_4\mathbf{R}_6\mathbf{R}_8$
	$\mathbf{R}_1\mathbf{R}_3\mathbf{R}_5\mathbf{R}_7\mathbf{R}_9\mathbf{R}_2$	$\mathbf{R}_2\mathbf{R}_4\mathbf{R}_6\mathbf{R}_8\mathbf{R}_1\mathbf{R}_3$
	$\mathbf{R}_1\mathbf{R}_3\mathbf{R}_5\mathbf{R}_7\mathbf{R}_9\mathbf{R}_4$	$\mathbf{R}_2\mathbf{R}_4\mathbf{R}_6\mathbf{R}_8\mathbf{R}_1\mathbf{R}_5$
	$\mathbf{R}_1\mathbf{R}_3\mathbf{R}_5\mathbf{R}_7\mathbf{R}_9\mathbf{R}_6$	$\mathbf{R}_2\mathbf{R}_4\mathbf{R}_6\mathbf{R}_8\mathbf{R}_1\mathbf{R}_7$
	$\mathbf{R}_1\mathbf{R}_3\mathbf{R}_5\mathbf{R}_7\mathbf{R}_9\mathbf{R}_8$	$\mathbf{R}_2\mathbf{R}_4\mathbf{R}_6\mathbf{R}_8\mathbf{R}_1\mathbf{R}_9$
	$\mathbf{R}_1\mathbf{R}_3\mathbf{R}_5\mathbf{R}_7\mathbf{R}_9\mathbf{R}_2\mathbf{R}_4$	$\mathbf{R}_2\mathbf{R}_4\mathbf{R}_6\mathbf{R}_8\mathbf{R}_3\mathbf{R}_5$
	$\mathbf{R}_1\mathbf{R}_3\mathbf{R}_5\mathbf{R}_7\mathbf{R}_9\mathbf{R}_2\mathbf{R}_6,$	$\mathbf{R}_2\mathbf{R}_4\mathbf{R}_6\mathbf{R}_8\mathbf{R}_3\mathbf{R}_7$
	$\mathbf{R}_1\mathbf{R}_3\mathbf{R}_5\mathbf{R}_7\mathbf{R}_9\mathbf{R}_2\mathbf{R}_8$	$\mathbf{R}_2\mathbf{R}_4\mathbf{R}_6\mathbf{R}_8\mathbf{R}_3\mathbf{R}_9$
	$\mathbf{R}_1\mathbf{R}_3\mathbf{R}_5\mathbf{R}_7\mathbf{R}_9\mathbf{R}_4\mathbf{R}_6,$	$\mathbf{R}_2\mathbf{R}_4\mathbf{R}_6\mathbf{R}_8\mathbf{R}_5\mathbf{R}_7$
	$\mathbf{R}_1\mathbf{R}_3\mathbf{R}_5\mathbf{R}_7\mathbf{R}_9\mathbf{R}_4\mathbf{R}_8$	$\mathbf{R}_2\mathbf{R}_4\mathbf{R}_6\mathbf{R}_8\mathbf{R}_5\mathbf{R}_9$
	$\mathbf{R}_1\mathbf{R}_3\mathbf{R}_5\mathbf{R}_7\mathbf{R}_9\mathbf{R}_6\mathbf{R}_8$	$\mathbf{R}_2\mathbf{R}_4\mathbf{R}_6\mathbf{R}_8\mathbf{R}_7\mathbf{R}_9$

6.2 The four transmit antennas case

In this section, a special attention is given to the case of four transmit antennas. The proposed rate-1 FGD code arises as the direct application of **Proposition 6.1** in the case of four transmit antennas. Setting $a = 2$, we have $\mathcal{G}_1 = \{\mathbf{I}, \mathbf{R}_2, \mathbf{R}_4, \mathbf{R}_1\mathbf{R}_3\mathbf{R}_5\}$ and $\mathcal{G}_2 = \{\mathbf{R}_1, \mathbf{R}_3, \mathbf{R}_5, \mathbf{R}_2\mathbf{R}_4\}$. It is worth noting that the above choice of weight matrices guarantees an equal average transmitted power per transmit antenna per time slot.

6.2.1 A new rate-1 FGD STBC for four transmit antennas

The Proposed rate-1 STBC denoted $\mathbf{X}_1$ is then expressed as:

$$\mathbf{X}_1(\mathbf{s}) = \mathbf{I}x_1 + \mathbf{R}_2x_2 + \mathbf{R}_4x_3 + \mathbf{R}_1\mathbf{R}_3\mathbf{R}_5x_4 + \mathbf{R}_1x_5 + \mathbf{R}_3x_6 + \mathbf{R}_5x_7 + \mathbf{R}_2\mathbf{R}_4x_8. \quad (6.19)$$

The proposed code $\mathbf{X}_1$ is a FGD STBC with $g = 2, n_1 = n_2 = 4$ and $g_1 = g_2 = 3$ such as $n_{i,j} = 1,\ i = 1, 2,\ j = 1, 2, 3 \Rightarrow \kappa_1 = \kappa_2 = 3$. Therefore, the decoding complexity order is equal to $\sum_{i=1}^{g} \sqrt{M}^{n_i - \kappa_i} = 2\sqrt{M}$. However, the coding gain $\mathbf{X}_1$ is equal to zero. In order to achieve full-diversity, we resort to the constellation stretching [63], [61] rather than the constellation rotation technique. Otherwise the orthogonal symbols inside each group will be entangled together which in turns will destroy the FGD structure of the proposed code and causes a significant increase in the decoding complexity.

The full-diversity code matrix takes the form of (6.20) where $\mathbf{s} = [x_1, \ldots, x_8]$ and k is chosen to provide a high coding gain. The term $\sqrt{\frac{2}{1+k^2}}$ is added to normalize the average transmitted power per antenna per time slot.

$$\mathbf{X}_1(\mathbf{s}) = \sqrt{\frac{2}{1+k^2}} \begin{bmatrix} x_1 + ikx_5 & x_2 + ikx_6 & x_3 + ikx_7 & -ikx_4 - x_8 \\ -x_2 + ikx_6 & x_1 - ikx_5 & -ikx_4 - x_8 & -x_3 - ikx_7 \\ -x_3 + ikx_7 & ikx_4 + x_8 & x_1 - ikx_5 & x_2 + ikx_6 \\ ikx_4 + x_8 & x_3 - ikx_7 & -x_2 + ikx_6 & x_1 + ikx_5 \end{bmatrix} \quad (6.20)$$

Proposition 6.3 *Taking $k = \sqrt{\frac{3}{5}}$, ensures the NVD property for the proposed code with a coding gain equal to 1 [24].*

Proof. The proposed code is 2-group decodable and the corresponding two sub-codes will be denoted by $\mathbf{X}_{\mathrm{I}} = \mathbf{X}(x_1, x_2, x_3, x_4, 0, 0, 0, 0)$ and $\mathbf{X}_{\mathrm{II}} = \mathbf{X}(0, 0, 0, 0, x_5, x_6, x_7, x_8)$ to avoid any ambiguity. The coding gain $\delta_{\mathbf{X}}$ is equal to the minimum Coding Gain Distance (CGD) [2], or mathematically:

$$\begin{aligned} \delta_{\mathbf{X}} &= \min_{\substack{\mathbf{s}\neq\mathbf{s}' \\ \mathbf{s},\mathbf{s}'\in\mathcal{C}}} \underbrace{\det\left((\mathbf{X}(\mathbf{s}) - \mathbf{X}(\mathbf{s}'))^H (\mathbf{X}(\mathbf{s}) - \mathbf{X}(\mathbf{s}'))\right)}_{\mathrm{CGD}(\mathbf{X}(\mathbf{s}),\mathbf{X}(\mathbf{s}'))} \\ &= \min_{\Delta\mathbf{s}\in\Delta\mathcal{C}\setminus\{\mathbf{0}\}} |\det\left((\mathbf{X}(\Delta\mathbf{s}))\right)|^2 \end{aligned} \quad (6.21)$$

where $\Delta\mathbf{s} = \mathbf{s} - \mathbf{s}'$, $\Delta\mathcal{C}$ is the vector space spanned by $\Delta\mathbf{s}$.
Thanks to **Proposition 3.1**, the quasi-orthogonality structure implies that:

$$\delta_{\mathbf{X}} = \min\left\{\delta_{\mathbf{X}_{\mathrm{I}}}, \delta_{\mathbf{X}_{\mathrm{II}}}\right\}. \quad (6.22)$$

The coding gain of the first sub-code is expressed as:

$$\delta_{\mathbf{X}_{\mathrm{I}}} = \left[\left(\Delta x_1^2 + \Delta x_2^2 + \Delta x_3^2 - k^2\Delta x_4^2\right)\left(\frac{2}{1+k^2}\right)\right]^4 \tag{6.23}$$

Choosing $k = \sqrt{\frac{3}{5}}$, the above expression becomes:

$$\delta_{\mathbf{X}_{\mathrm{I}}} = \left[\frac{(5\Delta x_1^2 + 5\Delta x_2^2 + 5\Delta x_3^2 - 3\Delta x_4^2)}{5}\left(\frac{2}{1+k^2}\right)\right]^4 \tag{6.24}$$

where $\Delta x_i = 2n_i,\ n_i \in \mathbb{Z}$. Consider the Diophantine quadratic equation below:

$$5(X_1^2 + X_2^2 + X_3^2) - 3X_4^2,\ X_1, X_2, X_3, X_4 \in \mathbb{Z} \tag{6.25}$$

The above equation equals 0 iff $X_1 = X_2 = X_3 = X_4 = 0$, this follows directly from Theorem 6, Chapter 7 of [74] as $-3 \times 5 \times 5 \times 5 \equiv 1 \pmod 8$ with $5 + 5 + 5 - 3 = 12 \equiv \pm 4 \pmod 8$. Moreover, one has:

$$5(X_1^2 + X_2^2 + X_3^2) - 3X_4^2 \neq \pm 1. \tag{6.26}$$

Otherwise, we must have:

$$3X_4^2 \equiv \pm 1 \pmod 5 \tag{6.27}$$

which cannot be true, since the quadratic residues modulo 5 are 0,1 and 4 [75], thus $3X_1^2 \equiv 0, \pm 3$ or $\pm\, 2 \pmod 5$. Therefore, we can write:

$$\left|5(X_1^2 + X_2^2 + X_3^2) - 3X_4^2\right| \geq 2,\ \forall\, (X_1, X_2, X_3, X_4) \neq \mathbf{0} \tag{6.28}$$

The above equality holds for many cases, take for instance $X_1 = X_2 = 1, X_3 = X_4 = 0$.

It is worth noting that the numerator of the expression (6.24) is a special case of the Diophantine equation in (6.25) as $\Delta x_i = 2n_i,\ n_i \in \mathbb{Z}, ß = 1, 2, 3, 4$. Therefore thanks to the above inequality one has:

$$\delta_{\mathbf{X}_{\mathrm{I}}} = (8/5)^4 \frac{2^4}{(8/5)^4} = 16. \tag{6.29}$$

The coding gain of the second sub-code is expressed as:

$$\delta_{\mathbf{X}_{\mathrm{II}}} = \left[\left(k^2\Delta x_5^2 + k^2\Delta x_6^2 + k^2\Delta x_7^2 - \Delta x_8^2\right)\left(\frac{2}{1+k^2}\right)\right]^4 \tag{6.30}$$

For $k = \sqrt{\frac{3}{5}}$, the above expression becomes:

$$\delta_{\mathbf{X}_{\text{II}}} = \left[\frac{(3\Delta x_5^2 + 3\Delta x_6^2 + 3\Delta x_7^2 - 5\Delta x_8^2)}{5} \left(\frac{2}{1+k^2} \right) \right]^4. \tag{6.31}$$

Consider the Diophantine quadratic equation below:

$$3(X_5^2 + X_6^2 + X_7^2) - 5X_8^2,\ X_5, X_6, X_7, X_8 \in \mathbb{Z} \tag{6.32}$$

It is easy to verify from Theorem 6, Chapter 7 of [74] that the above equation equals 0 iff $X_5 = X_6 = X_7 = X_8 = 0$ as $-3 \times 3 \times 3 \times 5 \equiv 1 \pmod 8$ with $3 + 3 + 3 - 5 = 4 \equiv \pm 4 \pmod 8$.
However, we have:

$$\left| 3(X_5^2 + X_6^2 + X_7^2) - 5X_8^2 \right| \geq 1,\ \forall (X_5, X_6, X_7, X_8) \neq \mathbf{0} \tag{6.33}$$

The above inequality holds for instance by taking $X_5 = 0,\ X_6 = X_7 = X_8 = 1$. By noting that the nominator in expression (6.31) is a special case of the Diophantine equation (6.32) as $\Delta x_i = 2n_i,\ n_i \in \mathbb{Z},\ i = 5, 6, 7, 8$, then thanks to the above inequality we have:

$$\delta_{\mathbf{X}_2} = (4/5)^4 \frac{2^4}{(8/5)^4} = 1 \tag{6.34}$$

and thus $\delta_{\mathbf{X}} = 1$. □

For illustration purpose, a comparison between regular and stretched 16-QAM constellation points is depicted in Fig 6.1 where the dark dots denote the regular 16-QAM constellation points whereas the red dots denote the stretched 16-QAM constellation points with stretching factor $k = \sqrt{\frac{3}{5}}$.

6.2.2 The proposed rate-2 code

The proposed rate-2 code denoted $\mathbf{X}_2$ is simply obtained by multiplexing two rate-1 codes by means of a unitary matrix. Mathematically speaking, the rate-2 STBC is expressed as:

$$\mathbf{X}_2 (x_1, \ldots, x_{16}) = \mathbf{X}_1 (x_1, \ldots, x_8) + e^{j\phi} \mathbf{X}_1 (x_9, \ldots, x_{16})\, \mathbf{U} \tag{6.35}$$

where $\mathbf{U}$ and ϕ are chosen in order to maximize the coding gain. It was numerically verified for QPSK constellation that taking $\mathbf{U} = j\mathbf{R}_1$ and $\phi = \tan^{-1}\left(\frac{1}{2}\right)$ maximizes the coding gain which is equal to 1.

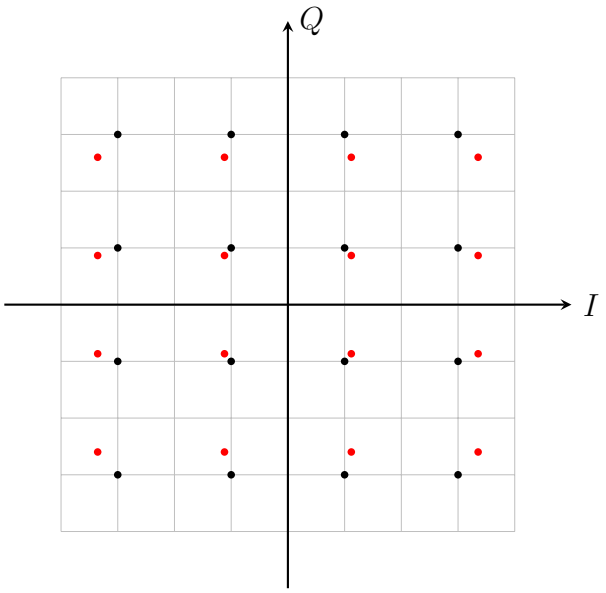

Figure 6.1: regular versus stretched 16-QAM constellation points

6.3 Decoding

To decode the proposed code, the receiver evaluates the QR decomposition of the real equivalent channel matrix $\tilde{\mathcal{H}}$ (2.7). Thanks to the FD structure (refer to Section 3.2) of the proposed rate-2 code with $K = 8, \kappa = 8, n_1 = n_2 = 4$, the corresponding upper-triangular matrix $\mathbf{R}$ takes the form below:

$$\mathbf{R} = \begin{bmatrix} \mathbf{A} & \mathbf{B} \\ \mathbf{0} & \mathbf{C} \end{bmatrix} \tag{6.36}$$

where $\mathbf{B} \in \mathbb{R}^{8\times 8}$ has no special structure, $\mathbf{C} \in \mathbb{R}^{8\times 8}$ is an upper triangular matrix and $\mathbf{A} \in \mathbb{R}^{8\times 8}$ takes the form below:

$$\mathbf{A} = \begin{bmatrix} x & 0 & 0 & x & 0 & 0 & 0 & 0 \\ 0 & x & 0 & x & 0 & 0 & 0 & 0 \\ 0 & 0 & x & x & 0 & 0 & 0 & 0 \\ 0 & 0 & 0 & x & 0 & 0 & 0 & 0 \\ 0 & 0 & 0 & 0 & x & 0 & 0 & x \\ 0 & 0 & 0 & 0 & 0 & x & 0 & x \\ 0 & 0 & 0 & 0 & 0 & 0 & x & x \\ 0 & 0 & 0 & 0 & 0 & 0 & 0 & x \end{bmatrix} \tag{6.37}$$

where x indicates a possible non-zero position. For each value of $(x_9, \ldots, x_{16})$, the decoder scans independently all possible values of x_4 and x_8, and assigns to them

the corresponding 6 ML estimates of the rest of symbols via hard slicers according to the following equations:

$$\begin{aligned} x_i^{\text{ML}}|\left(\hat{x}_4, \hat{x}_9, \ldots, \hat{x}_{16}\right) &= \text{sign}\left(z_i\right) \times \min\Big[\Big|2\,\text{round}\Big(\left(z_i-1\right)/2\Big)+1\Big|, \sqrt{M}-1\Big], \\ i &= 1,2,3 \\ x_j^{\text{ML}}|\left(\hat{x}_8, \hat{x}_9, \ldots, \hat{x}_{16}\right) &= \text{sign}\left(z_j\right) \times \min\Big[\Big|2\,\text{round}\Big(\left(z_j-1\right)/2\Big)+1\Big|, \sqrt{M}-1\Big], \\ j &= 5,6,7 \end{aligned}$$

where:

$$\begin{aligned} z_i &= \left(y_i' - r_{i,4}\hat{x}_4 - \sum_{k=9}^{16} r_{i,k}\hat{x}_k\right)/r_{i,i},\ i=1,2,3 \\ z_j &= \left(y_j' - r_{j,8}\hat{x}_8 - \sum_{k=9}^{16} r_{j,k}\hat{x}_k\right)/r_{j,j},\ j=5,6,7 \end{aligned}$$

A rate-3/2 code that will be denoted $\mathbf{X}_{3/2}$ may be easily obtained by puncturing the rate-2 proposed code in (6.35), and may be expressed as:

$$\mathbf{X}_{3/2}\left(x_1,\ldots,x_{12}\right) = \mathbf{X}_1\left(x_1,\ldots,x_8\right) + e^{j\phi_{\text{opt}}}\mathbf{X}_1\left(x_9,\ldots,x_{12}\right)\mathbf{U}_{\text{opt}} \tag{6.38}$$

A pseudo code for sphere decoder of $\mathbf{X}_2$ is illustrated on the next page where the $\texttt{SD}\left(\mathbf{y}', \mathbf{R}\right)$ function returns the ML estimates of the $(x_1,\ldots,x_8,)$ conditioned on a given value for $(x_9,\ldots,x_{16})$ as well as the corresponding ML metrics namely c_1 and c_2.

6.4 Numerical and simulation results

In this section, we compare our proposed codes to comparable low-complexity STBCs existing in the literature in terms of decoding complexity, PAPR, average decoding complexity and Codeword Error Rate (CER) performance over quasi-static Rayleigh fading channels. One can notice from Table 6.5 that the worst-case decoding complexity of the proposed rate-1 code is half that of [62] and [61]. The worst-case decoding complexity of the proposed rate-3/2 code is half that of the punctured rate-3/2 code in [46] and is smaller by a factor of $\sqrt{M}/2$ than the rate-3/2 code in [59].

Simulations are carried out on a quasi-static Rayleigh fading channel in the presence of AWGN for 1 receive antenna for our rate-1 code and 2 receive antennas

Algorithm III: The SD for $\mathbf{X}_2$ and square QAM of size M

$C = \infty$
$z_{16} = y'_{16}/r_{16,16}$
$x_{16}^{\mathsf{nc}} = \mathtt{sign}\left(z_{10}\right) \times \mathtt{min}\Big[\left|2\ \mathtt{round}(\left(z_{10}-1\right)/2)+1\right|, \sqrt{M}-1\Big]$
$\Xi_{16} = \mathtt{sort}(z_{16}, x_{16}^{\mathsf{nc}})$
$k_{16} = 1$
while $k_{16} \leq \sqrt{M}$ **and** $\left(y'_{16} - r_{16,16}\mathcal{A}\left(\Xi_{16}\left(k_{16}\right)\right)\right)^2 < C$ **do**
  $x_{16} = \mathcal{A}\left(\Xi_{16}\left(k_{16}\right)\right)$
  $W_{16} = \left(y'_{16} - r_{16,16}x_{16}\right)^2$
  $\ddots$
  $z_i = \left(y'_i - \sum_{j=9}^{16} r_{i,j}x_j\right)/r_{i,i},\ i = 4, 8$
  $x_i^{\mathsf{nc}} = \mathtt{sign}\left(z_i\right) \times \mathtt{min}\Big[\left|2\ \mathtt{round}(\left(z_i-1\right)/2)+1\right|, \sqrt{M}-1\Big],\ i = 4, 8$
  $\Xi_i = \mathtt{sort}(z_i, x_i^{\mathsf{nc}}),\ i = 4, 8$
  $k_i = 1,\ i = 4, 8$
  $c_l = \infty,\ l = 1, 2$
  $(x_1, \ldots, x_8, c_1, c_2) = \mathtt{SD}\left(\mathbf{y}', \mathbf{R}\right)$
  $P = \sum_{i=9}^{16} W_i + c_1 + c_2$
  if $P < C$ **then**
    $C = P$
    $\hat{\mathbf{s}} = \mathbf{x}$
  end
  $\ddots$
  $k_{16} = k_{16} + 1$
end

Algorithm IV: $(x_1, \ldots, x_8, c_1, c_2) = \mathtt{SD}\left(\mathbf{y}', \mathbf{R}\right)$

while $k_8 \leq \sqrt{M}$ **and** $\left(y'_8 - r_{8,8}\mathcal{A}\left(\Xi\left(k_8\right)\right) - \sum_{j=9}^{16} r_{8,j}x_j\right)^2 < c_1$ **do**

$t_8 = \mathcal{A}\left(\Xi_8\left(k_8\right)\right)$

$W_8 = \left(y'_8 - \sum_{j=8}^{16} r_{8,i}t_j\right)^2$

$z_i = \left(y'_i - \sum_{j=8}^{16} r_{i,j}t_j\right)/r_{i,i},\ i = 5, 6, 7$

$t_i = \mathtt{sign}\left(z_i\right) \times \mathtt{min}\left[\left|2\ \mathtt{round}(\left(z_i - 1\right)/2) + 1\right|, \sqrt{M} - 1\right],\ i = 5, 6, 7$

$W_i = \left(\left(z_i - t_i\right) r_{i,i}\right)^2,\ i = 5, 6, 7$

if $\sum_{i=5}^{8} W_i < c_1$ **then**

$c_1 = \sum_{i=5}^{8} W_i$

$x_i = t_i,\ i = 5, \ldots 8$

end

$k_8 = k_8 + 1$

end

while $k_4 \leq \sqrt{M}$ **and** $\left(y'_4 - r_{4,4}\mathcal{A}\left(\Xi\left(k_4\right)\right) - \sum_{j=9}^{16} r_{4,j}x_j\right)^2 < c_2$ **do**

$t_4 = \mathcal{A}\left(\Xi_4\left(k_4\right)\right)$

$W_4 = \left(y'_4 - r_{4,4}t_4 - \sum_{i=9}^{16} r_{4,i}t_i\right)^2$

$z_i = \left(y'_i - r_{i,4}t_4 \sum_{i=9}^{16} r_{i,j}t_j\right)/r_{i,i},\ i = 1, 2, 3$

$t_i = \mathtt{sign}\left(z_i\right) \times \mathtt{min}\left[\left|2\ \mathtt{round}(\left(z_i - 1\right)/2) + 1\right|, \sqrt{M} - 1\right],\ i = 1, 2, 3$

$W_i = \left(\left(z_i - t_i\right) r_{i,i}\right)^2,\ i = 1, 2, 3$

if $\sum_{i=1}^{4} W_i < c_2$ **then**

$c_2 = \sum_{i=1}^{4} W_i$

$x_i = t_i\ i = 1, \ldots 4$

end

$k_4 = k_4 + 1$

end

Table 6.5: Summary of comparisons in terms of decoding complexity and PAPR

Code	Square QAM decoding complexity	PAPR (dB)		
		QPSK	16QAM	64QAM
The proposed rate-1 code	$2\sqrt{M}$	0	2.5	3.7
M.Sinnokrot-J.Barry code [61]	$4\sqrt{M}$	0	2.5	3.7
Md.Khan-S.Rajan code [62]	$4\sqrt{M}$	5.8	8.3	9.5
The proposed rate-3/2 code	$2M^{2.5}$	3	5.6	6.7
S.Sirianunpiboon *et al.* code [59]	M^3	5.4	8	8.4
P.Srinath-S.Rajan rate-3/2 code [46]	$4M^{2.5}$	4	6.5	7.7
The proposed rate-2 code	$2M^{4.5}$	2.8	5.3	6.5
P.Srinath-S.Rajan code [46]	$4M^{4.5}$	2.8	5.3	6.5

for our punctured rate-3/2 and rate-2 codes with QPSK constellation. The ML detection is performed via a depth-first tree traversal with infinite initial radius SD. The radius is updated whenever a leaf node is reached and sibling nodes are visited according to the simplified Schnorr-Euchner enumeration [32].

Fig. 6.2 illustrates the performance comparison in terms of Codeword Error Rate (CER) of the proposed rate-1 code, the CIOD code in [62] and the M.Sinnokrot-J.Barry code in [61]. The performance loss of the proposed code is 1 dB w.r.t to the code in [62] and 0.4 dB w.r.t the code in [61] at 10^{-3} CER. It is worth noting that the proposed rate-1 code and the M.Sinnokrot-J.Barry code [61] are designed such that the PAPR is kept at its minimum which is that of the underlying constellation contrary to the case of the Coordinate Interleaved Orthogonal Design (CIOD) code [62]. Fig. 6.3 illustrates the comparison in terms of average complexity. The results show that proposed rate-1 code has the least average decoding complexity.

From Fig. 6.4, one can notice that the proposed rate-3/2 code gains about 0.2 dB w.r.t to S.Sirianunpiboon *et al.* code [59] while it loses only about 0.6 dB w.r.t to the punctured P.Srinath-S.Rajan code [46] at 10^{-3} CER. Again from Fig. 6.5, it can be noticed that the average complexity of our rate-3/2 code is significantly smaller than that of the punctured P.Srinath-S.Rajan code [46] and roughly equal to that of S.Sirianunpiboon *et al.* code [59] for the case of QPSK modulation.

From Fig. 6.6, one can notice that the proposed rate-2 code loses about 1 dB w.r.t the P.Srinath-S.Rajan code [46] at 10^{-3} CER. However, from Fig. 6.7 one can notice that our proposed code maintains its lower average decoding complexity in

the low SNR region.

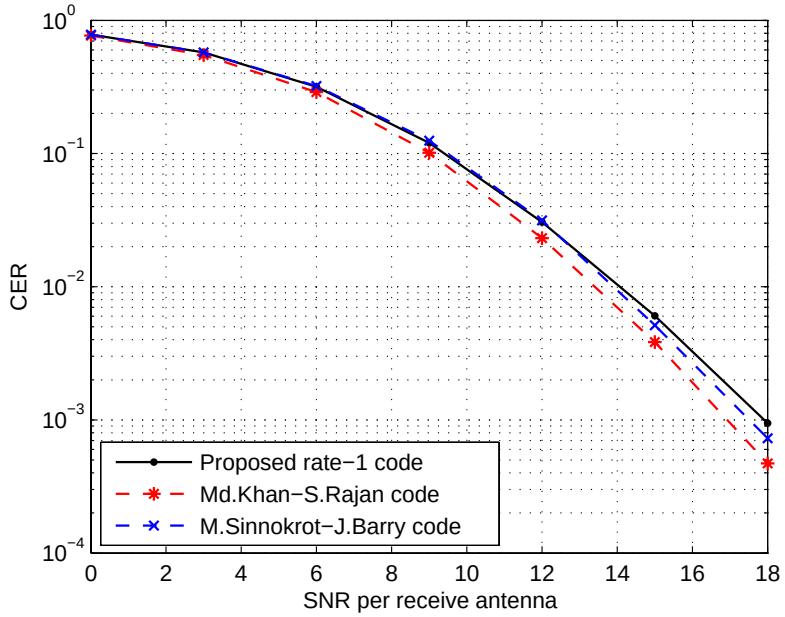

Figure 6.2: CER performance for 4×1 configuration and QPSK modulation

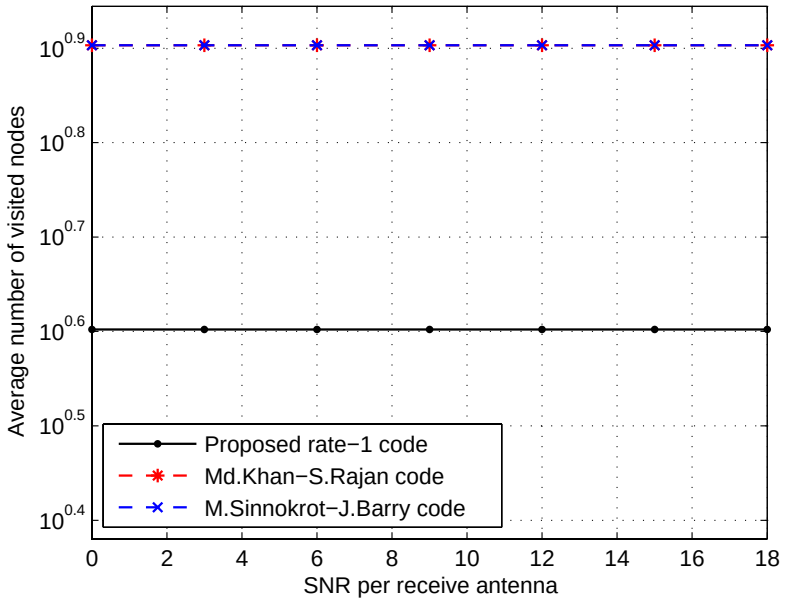

Figure 6.3: Average complexity for 4×1 configuration and QPSK modulation

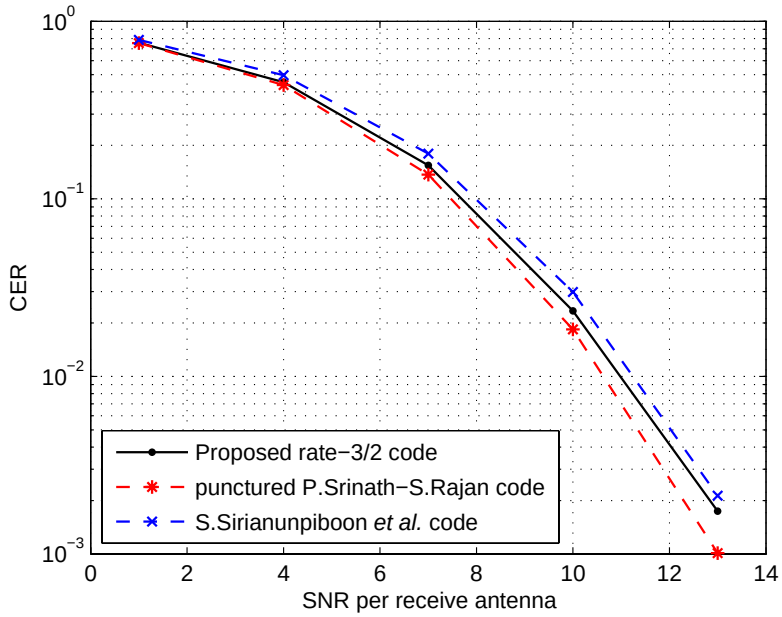

Figure 6.4: CER performance for 4×2 configuration and QPSK modulation

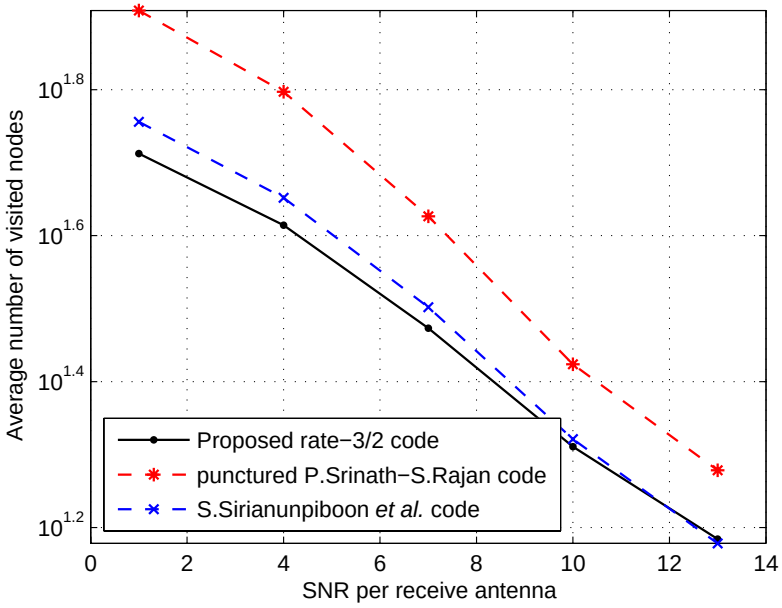

Figure 6.5: Average complexity for 4×2 configuration and QPSK modulation

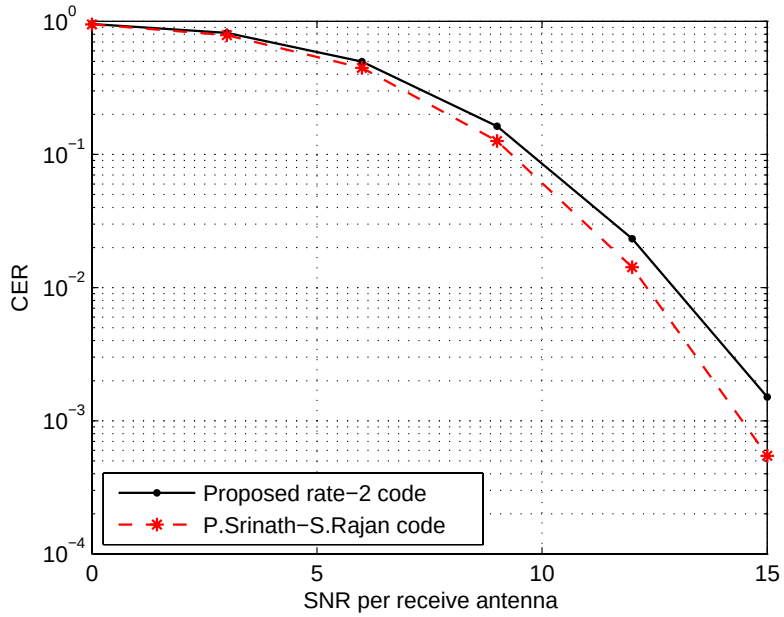

Figure 6.6: CER performance for 4×2 configuration and QPSK modulation

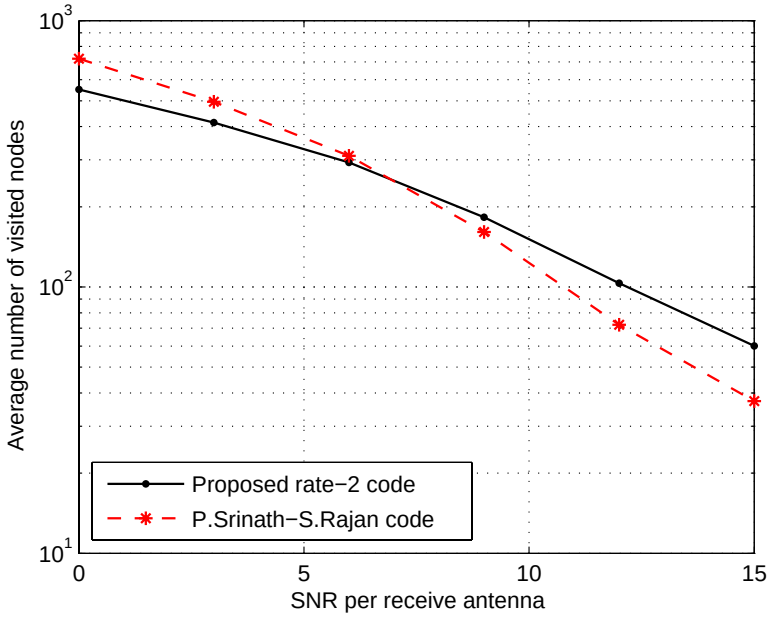

Figure 6.7: Average Complexity for 4×2 configuration and QPSK modulation

6.5 Conclusions

In this chapter we have proposed a systematic approach for the construction of rate-1 FGD codes for an arbitrary number of transmit antennas. This approach when applied to the special case of four transmit antennas results in a new rate-1 FGD STBC that has the smallest decoding complexity among existing comparable low-complexity STBCs. The coding gain of the proposed FGD rate-1 code is then optimized through constellation stretching and proved to be constant regardless of the underlying QAM constellation prior to normalization. In a second step, we managed to increase the rate to 2 through multiplexing two rate-1 codes through a unitary matrix. A compromise between complexity and throughput may be achieved through puncturing the proposed rate-2 code which results in a new low-complexity rate-3/2 code. The worst-case decoding complexity of proposed codes is lower than their counterparts in literature.

Simulations results show that the rate-1 code and the M.Sinnokrot-J.Barry code [61] offer similar performance while our rate-1 code loses about 1 dB in favor of the CIOD code [62] at 10^{-3} CER. The proposed rate-3/2 code offers better performance than the S.Sirianunpiboon *et al.* code [59], but loses about 0.6 dB w.r.t the punctured P.Srinath-S.Rajan code [46] at 10^{-3} CER. The proposed rate-2 code loses about 1 dB w.r.t the P.Srinath-S.Rajan code [46] at 10^{-3} CER. In terms of average decoding complexity, we found that the proposed rate-1 and rate-3/2 codes have a lower average decoding complexity while the proposed rate-2 code maintains its lower average decoding complexity in the low SNR region.

Chapter 7

Conclusions and Prospective Work

In this thesis, we addressed the construction of low-complexity STBCs with an emphasis on the case of four transmit antennas due its practical importance in current and upcoming communications standards. In the following, the contributions of the thesis are summarized and finally we give potential future research directions

7.1 Contributions

We addressed the issue of finding the maximal achievable rates of g-group-decodable STBCs for a specific type of code matrices that subsume the majority of the proposed STBCs in the literature. In this context, we proposed an exhaustive search construction method based on necessary and sufficient conditions for g-group-decodable codes and proved that for the considered special type of code matrices, the proposed method is considerably simplified. We focus on the case of four transmit antennas and provide the maximal-rate of symmetric 2-group decodable code 3-group decodable code.

Subsequently, we proposed a new 4×4 FD code structure that consists of multiplexing two orthogonal STBCs by the means of a unitary matrix. We demonstrated that in order to preserve the cubic shaping property, the rate of the new code cannot exceed $5/4$ complex symbols per channel use. The coding gain of the proposed code was maximized and proved to be independent of the underlying QAM constellation prior to normalization. Simulation results showed that not only the proposed code outperforms existent STBCs in the literature, but also it can be decoded at a lower average decoding complexity and provides a better PAPR.

We proposed a systematic approach for the construction of rate-1 FGD STBCs for an arbitrary number of transmit antennas. In the case of four transmit antennas, the new rate-1 FGD STBC has to the best of our knowledge the smallest worst-case decoding complexity among comparable STBCs in the literature. The coding gain of the proposed code was then optimized through constellation stretching rather than the constellation rotation to preserve the FGD structure and to minimize the PAPR which is that of the underlying constellation. We provided an analytical proof that the NVD property is indeed achievable by properly choosing the constellation stretching factor. Subsequently, the rate was increased through multiplexing two rate-1 codes by means of a unitary matrix giving rise to a new fast-decodable rate-2 STBC that has the least worst-case decoding complexity. The unitary matrix was numerically optimized for the case of QPSK constellation. A new rate-3/2 STBC was obtained through puncturing the rate-2 code. Simulation results showed that the proposed rate-1 and rate-3/2 codes have a lower average decoding complexity while the rate-2 code has a lower decoding complexity in the low SNR region.

We also considered the case where a limited feedback is available at the transmitter and proposed a new near-optimum equal-power transmit diversity scheme.

7.2 Prospective work

An interesting problem to pursue is to increase the rate of low-complexity STBCs through the relaxation of some of the constraints imposed in this thesis and generally in the literature. In that context, it would be interesting to investigate the maximum rates of rectangular g-group decodable STBCs (i.e. $T > N_t$). In [47], the authors addressed the construction of 2-group decodable codes for both the rectangular code matrix and the square code matrix and proved that for the rectangular case, the resulting 2-group decodable codes are asymptotically of full-rate, that is for $T \gg N_t$, the code rate approaches N_t. Obviously, this increase of the code rate comes at the expense of an increased delay, and therefore one has to find a compromise between this rate-delay trade-off that takes the system delay tolerance into consideration. A possible way would be to extend the work in [47] to the more general framework of g-group decodable STBCs.

Another point is that, the weight matrices in this thesis were restricted to unitary matrices. It would be also useful to address the problem of finding g-group decodable codes with Non-Unitary Weight (NUW) matrices with maximal rates. Only few examples of NUW-g-group decodable STBCs were proposed in the literature. For example, in [64] the authors focused on Single-Symbol Decodable (SSD) STBCs with non-unitary weight matrices that subsume the Coordinate Interleaved Orthogonal Design (CIOD) [62]. But, the construction of NUW-g-group-decodable STBCs in the general framework has not been addressed in a thorough way leaving the question about achievable rates of NUW-g-group-decodable codes still open.

Appendix A

Proof of Proposition 4.5

In the following, we will prove **Proposition 4.5**. We have:

$$\text{tr}\left(\mathbf{A}\right) = 0,\ \forall \mathbf{A} \in \mathcal{B}_{2a} \setminus \{j\mathbf{I}\}. \tag{A.1}$$

This can be easily verified from (2.56) by noting that:

$$\sigma_1\sigma_2 = j\sigma_3;\ \sigma_1\sigma_3 = -j\sigma_2;\ \sigma_2\sigma_3 = j\sigma_1 \text{ and } \text{tr}\left(\sigma_i\right) = 0;\ \forall\, i \in \{1,2,3\}\,. \tag{A.2}$$

And from (2.55) we have $\mathbf{A} \in \mathcal{B}_{2a} \setminus \{j\mathbf{I}\}$ may be expressed as:

$$\mathbf{A} = \lambda\Xi_1 \otimes \Xi_2 \ldots \otimes \Xi_a \tag{A.3}$$

where $\lambda \in \{\pm 1, \pm j\}$, $\Xi_i \in \{\sigma_1, \sigma_2, \sigma_3, \mathbf{I}\}$ but $\{\Xi_i : i = 1, \ldots, a\}$ cannot be equal simultaneously to $\mathbf{I}$ as the set $\mathcal{B}_{2^a}$ is linearly independent over $\mathbb{C}$. Consequently, one has:

$$\text{tr}\left(\mathbf{A}\right) = \lambda\text{tr}\left(\Xi_1 \otimes \Xi_2 \ldots \otimes \Xi_a\right) = \lambda \prod_{i=1}^{a} \text{tr}\left(\Xi_i\right) = 0 \tag{A.4}$$

as at least we have $\Xi_k \in \{\sigma_1, \sigma_2, \sigma_3\}\,, k \in \{1, \ldots, a\}$. Therefore, thanks to **Proposition 4.3** we may write:

$$\text{tr}\left(\boldsymbol{\alpha}_m^H \boldsymbol{\alpha}_n\right)\Big|_{m\neq n} = \text{tr}\left(\boldsymbol{\alpha}_k\right)\Big|_{k\neq 1} = 0 \tag{A.5}$$

Eq (A.5) may be used to find the coefficients $a_{i=1,2,\ldots,2^{2a}}$ in Eq 4.21 as below:

$$\text{tr}\left(\boldsymbol{\alpha}_k^H \boldsymbol{\Lambda}\right) = na_k + \underbrace{\sum_{\substack{i=1 \\ i\neq k}}^{n^2} a_i \boldsymbol{\alpha}_k^H \boldsymbol{\alpha}_i}_{0} = na_k. \tag{A.6}$$

where $n = 2^a$. On the other hand, it can be verified that any element of the basis over $\mathbb{C}$ in (4.18) may be expressed as:

$$\boldsymbol{\alpha}_k = \mathbf{T}_i \mathbf{D}_k,\ i \in \{1, 2, \dots n\}, k \in \left\{1, 2, \dots, n^2\right\} \tag{A.7}$$

where $\mathbf{T}_i$ is one of the disjoint permutation matrices that indicate the threads occupied by the basis elements (4.18) and $\mathbf{D}_k$ is a diagonal matrix with entries $\in \{\pm 1, \pm j\}$. For instance, the four permutation matrices for the case of four transmit antennas denoted $\mathbf{T}_1, \mathbf{T}_2, \mathbf{T}_3, \mathbf{T}_4$ are shown in Table A.1.

Table A.1: The four permutation matrices for the case of 4×4 matrices

$\mathbf{T}_1 = \begin{bmatrix} 1 & 0 & 0 & 0 \\ 0 & 1 & 0 & 0 \\ 0 & 0 & 1 & 0 \\ 0 & 0 & 0 & 1 \end{bmatrix}$	$\mathbf{T}_2 = \begin{bmatrix} 0 & 1 & 0 & 0 \\ 1 & 0 & 0 & 0 \\ 0 & 0 & 0 & 1 \\ 0 & 0 & 1 & 0 \end{bmatrix}$	$\mathbf{T}_3 = \begin{bmatrix} 0 & 0 & 1 & 0 \\ 0 & 0 & 0 & 1 \\ 1 & 0 & 0 & 0 \\ 0 & 1 & 0 & 0 \end{bmatrix}$	$\mathbf{T}_4 = \begin{bmatrix} 0 & 0 & 0 & 1 \\ 0 & 0 & 1 & 0 \\ 0 & 1 & 0 & 0 \\ 1 & 0 & 0 & 0 \end{bmatrix}$

It follows directly from the properties of basis elements (4.18) that the matrices $\mathbf{T}_i,\ i \in \{1, 2, \dots n\}$ have the following properties:

$$\mathbf{T}_k^T = \mathbf{T}_k \tag{A.8}$$

$$\mathbf{T}_{k_1}\mathbf{T}_{k_2} = \begin{cases} \mathbf{T}_{k_3} & k_1 \neq k_2 \neq k_3 \in \{2, 3, \dots n\} \\ \mathbf{I} & k_1 = k_2 \end{cases} \tag{A.9}$$

From the definition of the matrix $\mathbf{\Lambda}$ in Eq 4.2, it can be verified that restricting the weight matrices $\mathbf{A}$ and $\mathbf{B}$ to single-thread matrices with entries $\in \{\pm 1, \pm j\}$ turns out that the corresponding matrix $\mathbf{\Lambda}$ is evenly a single-thread matrix with entries $\in \{\pm 1, \pm j\}$, and thus may expressed as:

$$\mathbf{\Lambda} = \begin{cases} \mathbf{T}_{k_1}\mathbf{D}_{k_1} & k_1 \in \{1, 2, \dots, n\} \\ \mathbf{T}_{k_1}\mathbf{D}_{k_1} + \mathbf{T}_{k_2}\mathbf{D}_{k_2} & k_1, k_2 \in \{1, 2, \dots, n\},\ k_1 \neq k_2 \\ \mathbf{T}_{k_1}\mathbf{D}_{k_1} + \mathbf{T}_{k_2}\mathbf{D}_{k_2} + \mathbf{T}_{k_3}\mathbf{D}_{k_3} & k_1, k_2, k_3 \in \{1, 2, \dots, n\},\ k_1 \neq k_2 \neq k_3 \\ \vdots & \vdots \\ \sum_{i=1}^{n/2} \mathbf{T}_{k_i}\mathbf{D}_{k_i} & k_1, k_2, \dots k_{n/2} \in \{1, 2, \dots, n\},\ k_1 \neq k_2 \neq \dots k_{n/2} \end{cases} \tag{A.10}$$

where $\mathbf{D}_{k_i},\ k_i \in \{1, 2, \dots, n\}$ are diagonal matrices with entries $\in \{0, \pm 1, \pm j\}$ such that $\mathbf{D}_{k_m}\mathbf{D}_{k_n} = \mathbf{0},\ \forall\ k_m \neq k_n$. This is because the matrix $\mathbf{\Lambda}$ is required to be anti-hermitian (see **Proposition 4.1**), then it cannot have an odd number of common positions with threads $\mathbf{T}_1, \mathbf{T}_2, \dots, \mathbf{T}_n$. By common positions with $\mathbf{T}_k$, we mean the

number entries in the matrix $\mathbf{\Lambda}$ that corresponds to a non-zero entry in $\mathbf{T}_k$. This can be verified by noting that the matrices $\mathbf{T}_1, \mathbf{T}_2, \ldots, \mathbf{T}_n$ are symmetric and disjoint. Moreover, the matrix $\mathbf{\Lambda}$ is required to be a single-thread matrix. For the case of four transmit antennas, the above reduces to:

$$\mathbf{\Lambda} = \begin{cases} \mathbf{T}_{k_1}\mathbf{D}_{k_1} & k_1 \in \{1,2,3,4\} \\ \mathbf{T}_{k_1}\mathbf{D}_{k_1} + \mathbf{T}_{k_2}\mathbf{D}_{k_2} & k_1, k_2 \in \{1,2,3,4\}\,,\ k_1 \neq k_2 \end{cases} \tag{A.11}$$

It is worth noting that the matrix $\mathbf{\Lambda}$ being single-thread implies that in the first case all of the diagonal elements of the matrix $\mathbf{D}_{k1}$ are strictly non-zero and in the second case each of the diagonal matrices $\mathbf{D}_{k_1}$ and $\mathbf{D}_{k_2}$ has strictly two non-zero elements such that $\mathbf{D}_{k_1}\mathbf{D}_{k_2} = \mathbf{0}$. Let $\boldsymbol{\alpha}_k = \mathbf{T}_m\mathbf{D}_m$, thus one has:

$$\text{tr}\left(\boldsymbol{\alpha}_k^H \mathbf{\Lambda}\right) = \sum_{i=1}^{n/2} \text{tr}\left(\mathbf{T}_m \mathbf{T}_{k_i} \mathbf{D}_{k_i} \mathbf{D}_m^H\right) = \begin{cases} 0 & m \neq k_1 \neq k_2 \neq \ldots k_{n/2} \\ \text{tr}\left(\mathbf{D}_{k_i}\mathbf{D}_m^H\right) & k_i = m \end{cases} \tag{A.12}$$

Recalling that a_k is restricted to be real (see **Proposition 4.4**) and equating (A.6) and (A.12) one easily obtains:

$$a_k \in \left\{ \frac{n - 2\kappa}{n} \,:\, \kappa \in \mathbb{N} \right\} \tag{A.13}$$

On the other hand, according to **Proposition 4.4** one has $\sum_{k=1}^{n^2} a_k^2 = 1$ thus completing the proof.

Appendix B

Proof of Proposition 5.2

In the following we will prove that choosing $\phi = \frac{1}{2}\cos^{-1}(1/5)$ indeed maximizes the coding gain $\delta_{\mathbf{X}}$ (which is equal to 16^2) for unnormalized QAM constellations and guarantees the NVD property for the proposed code. The coding gain δ is equal to the minimum Coding Gain Distance (CGD) [2], or mathematically:

$$\begin{aligned}\delta_{\mathbf{X}} &= \min_{\substack{\mathbf{s}\neq\mathbf{s}'\\ \mathbf{s},\mathbf{s}'\in\mathcal{C}}} \underbrace{\det\left(\left(\mathbf{X}(\mathbf{s})-\mathbf{X}(\mathbf{s}')\right)^H\left(\mathbf{X}(\mathbf{s})-\mathbf{X}(\mathbf{s}')\right)\right)}_{\mathrm{CGD}(\mathbf{X}(\mathbf{s}),\mathbf{X}(\mathbf{s}'))} \\ &= \min_{\Delta\mathbf{s}\in\Delta\mathcal{C}\setminus\{\mathbf{0}\}} |\det\left(\left(\mathbf{X}(\Delta\mathbf{s})\right)\right)|^2 \end{aligned} \tag{B.1}$$

where $\Delta\mathrm{s} = \mathrm{s} - \mathrm{s}'$, $\Delta\mathcal{C}$ is the vector space spanned by $\Delta\mathrm{s}$. The code structure in Eq (5.18) imposes:

$$\min_{\Delta\mathbf{s}\in\Delta\mathcal{C}\setminus\{0\}} |\det\left(\left(\mathbf{X}(\Delta\mathbf{s})\right)\right)| \leq |\det\left(\mathbf{X}_{3/4}(2,0,0,0,0,0\right)| = 16$$

As a result, the angle ϕ that maximizes the coding gain has to satisfy:

$$|\det\left(\left(\mathbf{X}(\Delta\mathbf{s})\right)\right)| \geq 16, \forall\ \Delta\mathbf{s}\neq\mathbf{0} \tag{B.2}$$

For the proposed code we have:

$$|\det\left(\left(\mathbf{X}(\Delta\mathbf{s})\right)\right)| = \left|\left(\sum_{i=1}^{6}\Delta x_i^2\right)^2 + e^{j2\phi}b + e^{j4\phi}\left(\sum_{i=7}^{10}\Delta x_i^2\right)^2\right| \tag{B.3}$$

where $\Delta x_i = 2n_i,\ n_i \in \mathbb{Z}\ i = 1,\ldots,10$, and

$$\begin{aligned} b = 2\left(\sum_{i=1}^{6}\Delta x_i^2\right)\left(\sum_{j=7}^{10}\Delta x_j^2\right) - 4\Big[&(\Delta x_7\Delta x_4 - \Delta x_8\Delta x_3 + \Delta x_9\Delta x_6 - \Delta x_{10}\Delta x_2)^2 \\ &+(\Delta x_7\Delta x_6 + \Delta x_8\Delta x_2 - \Delta x_9\Delta x_4 - \Delta x_{10}\Delta x_3)^2 \\ &+(\Delta x_7\Delta x_2 - \Delta x_8\Delta x_6 - \Delta x_9\Delta x_3 + \Delta x_{10}\Delta x_4)^2\Big]. \end{aligned}$$

A simplification of the expression of b is possible by noting that:

$$\left(\sum_{i=1}^{6}\Delta x_i^2\right)\left(\sum_{j=7}^{10}\Delta x_j^2\right) = \left(\Delta x_2^2+\Delta x_3^2+\Delta x_4^2+\Delta x_6^2\right)\left(\Delta x_7^2+\Delta x_8^2+\Delta x_9^2+\Delta x_{10}^2\right)+ \left(\Delta x_1^2+\Delta x_5^2\right)\left(\Delta x_7^2+\Delta x_8^2\right)+\left(\Delta x_1^2+\Delta x_5^2\right)\left(\Delta x_9^2+\Delta x_{10}^2\right) \tag{B.4}$$

Recall Fibonacci's two square identity:

$$\left(a^2+b^2\right)\left(c^2+d^2\right) = (ac+bd)^2+(ad-bc)^2$$

and Euler's four square identity:

$$\begin{aligned}\left(a_1^2+a_2^2+a_3^2+a_4^2\right)\left(b_1^2+b_2^2+b_3^2+b_4^2\right) &= (b_1a_3-b_2a_2+b_3a_4-b_4a_1)^2\\ &+(b_1a_4+b_2a_1-b_3a_3-b_4a_2)^2\\ &+(b_1a_1-b_2a_4-b_3a_2+b_4a_3)^2\\ &+(b_1a_2+b_2a_3+b_3a_1+b_4a_4)^2\,.\end{aligned}$$

Applying the Euler's four square identity on the first term and the Fibonacci's two square identity on the rest of terms of Eq (B.4) we obtain:

$$\begin{aligned}\left(\sum_{i=1}^{6}\Delta x_i^2\right)\left(\sum_{j=7}^{10}\Delta x_j^2\right) &= (\Delta x_7\Delta x_4-\Delta x_8\Delta x_3+\Delta x_9\Delta x_6-\Delta x_{10}\Delta x_2)^2\\ &+(\Delta x_7\Delta x_6+\Delta x_8\Delta x_2-\Delta x_9\Delta x_4-\Delta x_{10}\Delta x_3)^2\\ &+(\Delta x_7\Delta x_2-\Delta x_8\Delta x_6-\Delta x_9\Delta x_3+\Delta x_{10}\Delta x_4)^2\\ &+(\Delta x_7\Delta x_3+\Delta x_8\Delta x_4+\Delta x_9\Delta x_2+\Delta x_{10}\Delta x_6)^2\\ &+(\Delta x_7\Delta x_1+\Delta x_8\Delta x_5)^2+(\Delta x_8\Delta x_1-\Delta x_7\Delta x_5)^2\\ &+(\Delta x_9\Delta x_1+\Delta x_{10}\Delta x_5)^2+(\Delta x_{10}\Delta x_1-\Delta x_9\Delta x_5)^2\\ &=\sum_{i=1}^{8}a_i^2,\ a_i\in\mathbb{Z}.\end{aligned} \tag{B.5}$$

Therefore, one may write b in more compact form as below:

$$b = 2\left(\sum_{i=1}^{8}a_i^2-2(a_1^2+a_2^2+a_3^2)\right) \tag{B.6}$$

Setting $x = e^{j2\phi}$, the discriminant Δ of the second degree equation (B.3) is expressed as:

$$\Delta = 4\left(\sum_{i=1}^{8}a_i^2-2\left(a_1^2+a_2^2+a_3^2\right)\right)^2-4\left(\sum_{i=1}^{8}a_i^2\right)^2\leq 0 \tag{B.7}$$

Consequently, the roots of Eq (B.3) are:

$$\begin{aligned}\lambda_{1,2} =& \frac{-b \pm j\sqrt{4\left(\sum_{i=1}^{6}\Delta x_i^2\right)^2\left(\sum_{j=7}^{10}\Delta x_j^2\right)^2 - b^2}}{2\left(\sum_{j=7}^{10}\Delta x_j^2\right)^2}, \\ \lambda_2 = \lambda_1^*,\ |\lambda_1| = |\lambda_2| =& \frac{\sum_{i=1}^{6}\Delta x_i^2}{\sum_{j=7}^{10}\Delta x_j^2}.\end{aligned} \tag{B.8}$$

For the sake of simplicity, we will denote hereafter $\sum_{i=1}^{6}\Delta x_i^2 = \sigma_1$ and $\sum_{j=7}^{10}\Delta x_j^2 = \sigma_2$. In the case of $\sigma_1 \neq \sigma_2$, Eq. (B.3) can be lower bounded as below:

$$\begin{aligned}\left|\det\left((\mathbf{X}(\Delta\mathbf{s}))\right)\right|\Big|_{\substack{\Delta\mathbf{s}\neq\mathbf{0}\\ \sigma_1\neq\sigma_2}} &= \sigma_2^2\Big|\left(x-\lambda_1\right)\left(x-\lambda_2\right)\Big| \\ &\geq \sigma_2^2\Big|\left(|x|-|\lambda_1|\right)\left(|x|-|\lambda_2|\right)\Big| \\ &= \sigma_2^2\left(1-\frac{\sigma_1}{\sigma_2}\right)^2 \\ &= \left(\sigma_2-\sigma_1\right)^2 \geq 16\end{aligned} \tag{B.9}$$

where the latter inequality follows by substituting $\Delta x_i = 2n_i,\ n_i \in \mathbb{Z}$ as we are dealing with unnormalized QAM constellations. If $\sigma_1 = \sigma_2 = \sigma$, Eq (B.3) can be written as

$$\left|\det\left((\mathbf{X}(\Delta\mathbf{s}))\right)\right|\Big|_{\substack{\Delta\mathbf{s}\neq\mathbf{0}\\ \sigma_1=\sigma_2}} = \left|2\sigma^4\cos(2\phi)+b\right| \tag{B.10}$$

where $b = 2\left(\sigma^2 - 2(a_1^2+a_2^2+a_3^2)\right)$. It is worth noting that setting $\sigma_1 = \sigma_2$ implies that $(a_1,\ldots,a_8)$ cannot be equal to $\mathbf{0}$, otherwise from Eq (B.5) we will have $\Delta x_i = 0,\ \forall i \in \{1,\ldots 10\}$. Taking $\cos(2\phi) = 1/5$, we have to prove that:

$$\left|\frac{2\sigma^2}{5}+b\right| \geq 16\ \forall\ \sigma_1=\sigma_2=\sigma\neq 0. \tag{B.11}$$

Multiplying both sides by 5 and using (B.6), the above inequality becomes:

$$\left|12\sigma^2 - 20(a_1^2+a_2^2+a_3^2)\right|\Big|_{(a_1,\ldots,a_8)\neq\mathbf{0}} \geq 5\times 16 \tag{B.12}$$

Denoting $\tilde{a}_i = \frac{a_i}{4}$ and $\tilde{\sigma} = \frac{\sigma}{4}$ we may have:

$$\left|12\tilde{\sigma}^2 - 20(\tilde{a}_1^2+\tilde{a}_2^2+\tilde{a}_3^2)\right|\Big|_{(\tilde{a}_1,\ldots,\tilde{a}_8)\neq\mathbf{0}} \geq 5. \tag{B.13}$$

The above inequality is satisfied iff:

$$\left|3\tilde{\sigma}^2 - 5(\tilde{a}_1^2+\tilde{a}_2^2+\tilde{a}_3^2)\right|\Big|_{(\tilde{a}_1,\ldots,\tilde{a}_8)\neq\mathbf{0}} \geq 2. \tag{B.14}$$

However, the L.H.S of the above inequality can be considered as a special case of:

$$3X_1^2 - 5(X_2^2 + X_3^2 + X_4^2)\Big|_{(X_1,X_2,X_3,X_4)\neq\mathbf{0}} \tag{B.15}$$

where $X_i \in \mathbb{Z}$. This type of equations have been extensively studied in the mathematical literature dealing with the solvability of quadratic Diophantine equations (see [74]). Applying Theorem 6, Chapter 7 of [74] we have:

$$3X_1^2 - 5(X_2^2 + X_3^2 + X_4^2) \neq 0 \,\forall\, (X_1, X_2, X_3, X_4) \neq \mathbf{0} \tag{B.16}$$

as $-3 \times 5 \times 5 \times 5 \equiv 1 \pmod 8$ with $3 - 5 - 5 - 5 \equiv 4 \pmod 8$.
Moreover,

$$3X_1^2 - 5(X_2^2 + X_3^2 + X_4^2) \neq \pm 1. \tag{B.17}$$

Otherwise, we must have:

$$3X_1^2 \equiv \pm 1 \pmod 5 \tag{B.18}$$

which cannot be true, since the quadratic residues modulo 5 are 0,1 and 4 [75], thus $3X_1^2 \equiv 0, \pm 3$ or $\pm\, 2 \pmod 5$. Therefore, we can write:

$$\left|3X_1^2 - 5(X_2^2 + X_3^2 + X_4^2)\right| \geq 2, \forall\, (X_1, X_2, X_3, X_4) \neq \mathbf{0} \tag{B.19}$$

which in turns implies:

$$\left|\det\left(\left(\mathbf{X}\left(\Delta\mathbf{s}\right)\right)\right)\right|\Big|_{\substack{\Delta\mathbf{s}\neq\mathbf{0}\\ \sigma_1=\sigma_2}} > 16 \tag{B.20}$$

thus completing the proof.

Appendix C

Additional Optimal Rotation Angles for the QOD

In this Appendix, we prove that taking the rotation angle ϕ of the QOD in [37] equal to $\pi/6$ ensures that the coding gain is maximized and is independent of the used constellation. The coding gain δ may be expressed as:

$$\delta = \min_{\Delta\mathbf{s}\in\Delta\mathcal{C}\setminus\{\mathbf{0}\}} |\det\left((\mathbf{X}(\Delta\mathbf{s}))\right)|^2 \tag{C.1}$$

The quasi-orthogonal structure enables separate optimization of the coding gain for each sub-code matrix $\mathbf{X}(s_1, 0, s_3, 0)$ and $\mathbf{X}(0, s_2, 0, s_4)$ denoted by $\mathbf{X}_1(s_1, s_3)$ and $\mathbf{X}_2(s_2, s_4)$ respectively.

$$\begin{aligned} |\det\left(\mathbf{X}_1\left(\Delta s_1, \Delta s_3\right)\right)| &= |\Delta s_1^2 + \Delta s_3^2|^2 \\ &= |\Delta s_1|^4 + |\Delta s_3|^4 + 2\Re\{\Delta s_1^{*2}\Delta s_3^2\} \\ &= |\Delta s_1|^4 + |\Delta s_3|^4 + 2|\Delta s_1|^2|\Delta s_3|^2\cos(2\theta_3 - 2\theta_1 + 2\phi) \\ &= \left(|\Delta s_1|^2 - |\Delta s_3|^2\right)^2 + 4|\Delta s_1|^2|\Delta s_3|^2\cos^2(\theta_3 - \theta_1 + \phi) \end{aligned} \tag{C.2}$$

where $\Delta s_1 = 2(n_1 + jn_2)$ and $\Delta s_3 = 2(n_5 + jn_6)e^{j\phi}$, $n_1, n_2, n_5, n_6 \in \mathbb{Z}$. From the QOD code matrix we may write:

$$\min_{\Delta s_1\in\Delta\mathcal{A}\setminus\{0\}} |\det\left((\mathbf{X}_1(\Delta s_1, 0))\right)| = \min_{\Delta s_1\in\Delta\mathcal{A}\setminus\{0\}} |\Delta s_1|^4 = 16$$

thus,

$$\min_{\substack{(\Delta s_1,\Delta s_3)\in\Delta\mathcal{A}\times\Delta\mathcal{A}' \\ (\Delta s_1,\Delta s_3)\neq(0,0)}} |\det\left((\mathbf{X}_1(\Delta s_1, \Delta s_3))\right)| \leq 16. \tag{C.3}$$

In the case where $|\Delta s_1| \neq |\Delta s_3|$, it can be easily seen that:

$$|\det\left((\mathbf{X}_1(\Delta s_1, \Delta s_3))\right)| \geq 16 \tag{C.4}$$

Thus for maximizing the coding gain, it suffices to prove that there exists a rotation ϕ such that:

$$|\det\left((\mathbf{X}_1(\Delta s_1, \Delta s_3))\right)| \geq 16;\ \forall\ |\Delta s_1| = |\Delta s_3| = |\Delta s| \neq 0 \tag{C.5}$$

or equivalently:

$$\begin{aligned} &4|\Delta s|^4 \cos^2(\theta_3 - \theta_1 + \phi) \geq 16 \\ &|\Delta s|^4 \left[\cos(\theta_3 - \theta_1)\cos(\phi) - \sin(\theta_3 - \theta_1)\sin(\phi)\right]^2 \geq 4 \\ &\left[(n_5 n_1 + n_6 n_2)\cos(\phi) - (n_6 n_1 - n_5 n_2)\sin(\phi)\right]^2 \geq \frac{1}{4} \end{aligned} \tag{C.6}$$

The L.H.S of the above expression can be bounded as:

$$\begin{aligned} |(n_5 n_1 + n_6 n_2)\cos(\phi) + (n_5 n_2 - n_6 n_1)\sin(\phi)| \geq \\ \Big||(n_5 n_1 + n_6 n_2)\cos(\phi)| - |(n_5 n_2 - n_6 n_1)\sin(\phi)|\Big|. \end{aligned} \tag{C.7}$$

Consequently, it is sufficient to find an angle ϕ such that:

$$\Big||(n_5 n_1 + n_6 n_2)\cos(\phi)| - |(n_5 n_2 - n_6 n_1)\sin(\phi)|\Big|^2 \geq \frac{1}{4} \tag{C.8}$$

with $n_5^2 + n_6^2 = n_1^2 + n_2^2 = |\Delta s|^2$.
Taking $\phi = \pi/6$, we have to prove that:

$$\left|\sqrt{3}|n_5 n_1 + n_6 n_2| - |n_5 n_2 - n_6 n_1|\right|^2 \geq 1. \tag{C.9}$$

But from the triangle inequality we have:

$$\left|\sqrt{3}|n_5 n_1 + n_6 n_2| - |n_5 n_2 - n_6 n_1|\right|^2 > \left(|\Delta s|^2 - 2|n_5 n_1 + n_6 n_2|\right)^2. \tag{C.10}$$

The R.H.S of the above inequality cannot be zero. This can be verified by noting that setting $|\Delta s|^2 = 2|n_5 n_1 + n_6 n_2|$ implies:

$$(n_5 n_2 - n_6 n_1)^2 = 3(n_5 n_1 + n_6 n_2)^2 \tag{C.11}$$

which cannot be true, since $\sqrt{3}$ is irrational. By noting that the R.H.S of (C.10) is an integer quantity, inequality (C.9) is proved and we have:

$$|\det\left((\mathbf{X}_1(\Delta s_1, \Delta s_3))\right)|\Big|_{\Delta s_1 = \Delta s_3} > 16 \tag{C.12}$$

The same procedure can be adopted for the other sub-code matrix $\mathbf{X}_2(s_2, s_4)$ as $|\det\left[\mathbf{X}_2(\Delta s_2, \Delta s_4)\right]| = |\Delta s_2^2 + \Delta s_4^2|^2$, which concludes the proof.

Appendix D

A Near-Optimum Equal-Power Transmit Diversity Scheme

For several decades, point-to-point wireless communications systems employed receive diversity based on antenna switching, Equal-Gain Combining (EGC), or Maximal-Ratio Combining (MRC) [76]. But with the development of cellular systems in the 1990s, attention was turned to transmit diversity, which is more appropriate for the downlink. The user terminal cost and power consumption considerations indeed favor transmit diversity with respect to receive diversity on the downlink, because this technique does not require the use of multiple antennas at user terminals.

The most well-known transmit diversity technique is the one introduced by Alamouti [27]. This technique, which does not require any CSI at the transmitter, has been included in most of the recently developed wireless communications systems standards including the IEEE 802.11n-2009 standard [5] for Local Area Networks and the IEEE 802.16e-2005 standard [6], on which mobile WiMAX systems are based. Alamouti's transmit diversity leads to the same diversity order as the receive diversity based on MRC, but it loses 3 dB in terms of received signal-to-noise ratio (SNR) for the same total transmit power.

There are other transmit diversity options when the channel state information is known either partially or fully at the transmitter side. One of these is the switching transmit diversity (STD) (see, e.g., [77] and references therein). In such a scheme, the channel is monitored through power measurements for the two transmit antennas and the best antenna is selected for transmission. STD loses some diversity

gain with respect to MRC and Alamouti's transmit diversity, but it avoids the 3 dB transmit power loss of Alamouti's technique. On the other hand, optimum transmit diversity (OTD) achieves the performance of MRC, but it requires the use of two transmit amplifiers each of which is capable of transmitting as much power as the transmit power in receive diversity based on MRC. This leads to costly transmitters.

Here, we focus on Equal-Power Transmit Diversity (EPTD), which transmits the same power from each antenna as Alamouti's technique. We describe a simple scheme which achieves near-optimum performance, thus significantly outperforming Alamouti's transmit diversity and STD. More specifically, each transmit antenna in this technique is fed by a high-power amplifier (HPA) of transmit power $P/2$, where P is the total transmitted power. Note that in OTD, each of the two amplifiers must be capable of transmitting at power P. In the proposed technique, each symbol is transmitted from the two transmit antennas such that it arrives in almost the same phase at the receive antenna. We first describe the *ideal* EPTD, and then we describe our proposed suboptimum technique which is more suitable for practical applications.

The Appendix is organized as follows: In the next section, we briefly recall conventional transmit and receive diversity techniques including MRC, switched diversity, and Alamouti's space-time coding (STC). In Section 2, we describe the ideal equal-power transmit diversity technique and introduce our proposed scheme. Next, in Section 3, we evaluate the performance of these techniques by means of computer simulations. This includes performance on narrowband fading channels as well as performance in OFDM systems operating on frequency-selective channels. Finally, we give our conclusions in Section 4.

D.1 Conventional Diversity Techniques

A single-input single-output (SISO) system, which employs a single antenna on each side of the transmission, can be described by a simple equation:

$$r_k = h_k s_k + n_k \tag{D.1}$$

where r_k is the received signal at time k, s_k is the transmitted symbol, h_k is the complex channel gain, and n_k is the additive noise. The SNR at the receiver at time k is given by:

$$\text{SNR}_k = |h_k|^2 \, \text{SNR}_0 \tag{D.2}$$

where SNR_0 designates the SNR in the absence of fading.

The optimum spatial diversity technique at the receiver side is MRC, which can be described as follows for 2 receive antennas: Let h_{k1} and h_{k2} be the channel responses between the transmit antenna and the first and the second receive antenna, respectively. The signals received by the two receive antennas can be written as:

$$r_{k1} = h_{k1}s_k + n_{k1} \tag{D.3}$$

$$r_{k2} = h_{k2}s_k + n_{k2} \tag{D.4}$$

where n_{k1} and n_{k2} are the additive noise terms. In MRC, the receiver computes:

$$x_k = h_{k1}^* r_{k1} + h_{k2}^* r_{k2} = \left(|h_{k1}|^2 + |h_{k2}|^2 \right) \, s_k + h_{k1}^* n_{k1} + h_{k2}^* n_{k2} \tag{D.5}$$

Symbol s_k is detected by sending x_k to a threshold detector. The SNR at the threshold detector input can be expressed as:

$$\text{SNR}_k = \left(|h_{k1}|^2 + |h_{k2}|^2 \right) \text{SNR}_0 \tag{D.6}$$

Note that OTD achieves the same performance as MRC. It consists of transmitting the data symbols such that the signals from the two transmit antennas arrive at the receiver in strictly identical phase and using optimum power loading. More specifically, with $h_{k1} = |h_{k1}| \exp(j\theta_{k1})$ denoting the channel response between the first transmit antenna and the receive antenna, and $h_{k2} = |h_{k2}| \exp(j\theta_{k2})$ denoting the response between the second transmit antenna and the receive antenna, the signals transmitted by the two antennas are of the form:

$$x_{k1} = \frac{|h_{k1}|}{\sqrt{|h_{k1}|^2 + |h_{k2}|^2}} s_k, \; x_{k2} = \frac{|h_{k2}| \, e^{j(\theta_{k1} - \theta_{k2})}}{\sqrt{|h_{k1}|^2 + |h_{k2}|^2}} s_k \tag{D.7}$$

respectively. It can be easily verified that the SNR at the receiver is identical to that of MRC given by (D.6).

A diversity technique which comes close to OTD in terms of performance while avoiding the simultaneous use of multiple transmitters is STD. The performance

of STD is the same whether switching is used at the transmitter or at the receiver. Focusing on STD at the transmit side, in two transmit antenna case, the signal is transmitted from the first antenna if $|h_{k1}| \geq |h_{k2}|$ and it is transmitted from the second antenna otherwise. Then, the received signal can be written in the form:

$$r_k = \begin{cases} h_{k1}s_k + n_{k1}, & \text{if } |h_{k1}| \geq |h_{k2}| \\ h_{k2}s_k + n_{k2}, & \text{if } |h_{k1}| < |h_{k2}| \end{cases} \tag{D.8}$$

and the SNR at the threshold detector input becomes:

$$\text{SNR}_k = \begin{cases} |h_{k1}|^2 \text{SNR}_0 & \text{if } |h_{k1}| \geq |h_{k2}| \\ |h_{k2}|^2 \text{SNR}_0 & \text{if } |h_{k1}| < |h_{k2}| \end{cases} . \tag{D.9}$$

It can be easily shown that, in terms of mean SNR, STD loses about 1.25 dB with respect to OTD.

When no CSI is available at the transmitter side, OTD and STD cannot be implemented. In that case, one may resort to Alamouti's transmit diversity [27]. This technique leads to the same diversity performance as MRC and OTD, but it loses 3 dB in terms of total transmit power. This can be deduced by comparing (D.6) to the receiver SNR in Alamouti's transmit diversity which is given by:

$$\text{SNR}_k = \left(|h_{k1}|^2 + |h_{k2}|^2\right) \text{SNR}_0/2 \tag{D.10}$$

D.2 Equal-Power Transmit Diversity

As given by (D.7), the instantaneous power transmitted from each antenna in OTD is a function of the two channel responses. If the magnitude of h_{k1} is close to 0, virtually all of the power is transmitted from the second antenna, and, conversely, if the magnitude of h_{k2} is close to 0, virtually all of the power is transmitted from the first antenna. Therefore, an OTD system must use two transmitters each having a high-power amplifier with the same characteristics as that of a transmitter used in an MRC-based system to achieve the same performance. On the other hand, the transmit power in Alamouti's transmit diversity is equally divided between the two transmitters, but as indicated earlier this technique loses 3 dB with respect to OTD.

We now focus on equal-power transmit diversity (EPTD), which transmits from each antenna the same power as Alamouti's transmit diversity, while avoiding

most of the 3 dB loss of the latter technique. The signals transmitted from the two antennas in ideal EPTD are given by:

$$x_{k1} = \frac{s_k}{\sqrt{2}},\ x_{k2} = \frac{e^{j(\theta_{k1}-\theta_{k2})}s_k}{\sqrt{2}} \tag{D.11}$$

The signals received from the two antennas are perfectly phase aligned, and the SNR at the receiver is:

$$\text{SNR}_k = \left(|h_{k1}| + |h_{k2}|\right)^2 \text{SNR}_0/2, \tag{D.12}$$

If the total transmit power is denoted by P, $P/2$ is transmitted from the first antenna and $P/2$ is transmitted from the second antenna. Therefore, compared to OTD, this technique reduces by 3 dB the required power characteristics of the transmit amplifiers. But, implementation of this technique remains very complex, because it requires an accurate estimation of the phase response of the two channels. To avoid an explicit estimation of the phase responses, we describe a simple suboptimum technique, which achieves performance close to the ideal EPTD.

The proposed technique consists of phase aligning the received signals to within π/N, where N is design parameter. Increasing the value of parameter N will improve the performance at the expense of increased complexity. In the preferred embodiment of this technique, we take $N = 4$. This value highly simplifies the implementation while keeping the performance loss negligible as it can be confirmed by the simulation results and the analytical derivation provided below.

Proof. we prove analytically (by evaluating the mean SNR) that the proposed technique performs better that the Alamouti technique and that it compensates most the 3dB loss towards the performance of the OTD. We also show that the number of sectors N chosen as small as 4 is sufficient to approach the ideal EPTD.
The instantaneous SNR in the proposed technique is expressed as:

$$\text{SNR}_k = \frac{\left|h_{k1} + e^{jn\pi/2}h_{k2}\right|^2}{2}\text{SNR}_0. \tag{D.13}$$

Taking the expectation of both sides w.r.t. the channel coefficients of the above equation we obtain:

$$\overline{\text{SNR}} = \mathbb{E}\left\{\frac{|h_{k1}|^2 + |h_{k2}|^2 + 2\Re\left\{h_{k1}^* h_{k2} e^{jn\pi/2}\right\}}{2}\right\}\text{SNR}_0 \tag{D.14}$$

which can be written as:

$$\overline{\text{SNR}} = \left[\frac{\mathbb{E}\left|h_{k1}\right|^2 + \mathbb{E}\left|h_{k2}\right|^2}{2} + \mathbb{E}\left\{ \left|h_{k1}\right| \left|h_{k2}\right| \cos(\phi) \right\} \right] \text{SNR}_0 \tag{D.15}$$

with $\phi = \theta_{k2} + n\pi/2 - \theta_{k1}$ where θ_{ki} is the phase associated to the i'th antenna at the k'th instant.

If we consider the flat fading scenario, the channel coefficients are simulated as standard circularly symmetric complex Gaussian random numbers ($h_{ki} \sim \mathcal{CN}(0,1)$) that are i.i.d in both space and time. Consequently, the magnitude of the channel coefficient is Rayleigh distributed and is independent of its corresponding phase which is uniformly distributed over the range $[0, 2\pi]$ [78].
Thus, the above equation can be written as:

$$\overline{\text{SNR}} = \left[1 + \mathbb{E}\left|h_{k1}\right| \mathbb{E}\left|h_{k2}\right| \mathbb{E}\left\{ \cos(\phi) \right\} \right] \text{SNR}_0 \tag{D.16}$$

It is worth noting that, for N=4, the angle ϕ is uniformly distributed over the range$[-\pi/4, \pi/4]$. This can be verified by noting that the phase difference $\widetilde{\Delta\theta} = \theta_{k2} - \theta_{k1}$ follows a symmetric triangular distribution between $[-2\pi, 2\pi]$ with zero mean. Thus, $\Delta\theta$ defined as:

$$\Delta\theta = \begin{cases} \widetilde{\Delta\theta}, \text{ if } \widetilde{\Delta\theta} \geq 0 \\ \widetilde{\Delta\theta} + 2\pi, \text{ otherwise} \end{cases} \tag{D.17}$$

is uniformly distributed over$[0, 2\pi]$. As a result, from its definition, n is uniformly distributed over the set $\{0, 1, 2, 3\}$. The probability distribution of ϕ can be expressed as:

$$\begin{aligned} P(\phi) &= \sum_{n=0}^{3} P(\phi|n) P(n) \\ &= \sum_{n=0}^{3} P\left(\Delta\theta | n + n\pi/2\right) P(n) \\ &= \sum_{n=0}^{3} \mathcal{U}\left[-\frac{\pi}{4}, \frac{\pi}{4}\right] P(n) \\ &= \mathcal{U}\left[-\frac{\pi}{4}, \frac{\pi}{4}\right] \end{aligned} \tag{D.18}$$

where $\mathcal{U}\left[a, b\right]$ denotes the uniform distribution over $[a, b]$. From the above discus-

sion, equation (D.16) can be expressed as:

$$\overline{\text{SNR}} = \left[1 + \frac{\sqrt{\pi}}{2}\frac{\sqrt{\pi}}{2}\frac{2}{\pi}\int_{-\pi/4}^{\pi/4}\cos(\phi)d\phi\right]\text{SNR}_0 \quad \text{(D.19)}$$

$$= \left[1 + \frac{\pi}{4}\frac{2}{\pi}\sin(\phi)\Big|_{-\pi/4}^{\pi/4}\right]\text{SNR}_0 \quad \text{(D.20)}$$

$$= \left[1 + \frac{1}{\sqrt{2}}\right]\text{SNR}_0 \approx 1.7\,\text{SNR}_0 \quad \text{(D.21)}$$

whereas, in the OTD, the STD and the Alamouti schemes, the mean SNR is equal to 2 SNR_0, 1.5 SNR_0 and SNR_0 respectively.

In the same way, if we look at the averaged SNR with the ideal EPTD ($\phi = 0$), we have:

$$\overline{\text{SNR}} = \left[1 + \mathbb{E}\left|h_{k1}\right|\mathbb{E}\left|h_{k2}\right|\right]\text{SNR}_0 \quad \text{(D.22)}$$

$$= \left[1 + \frac{\pi}{4}\right]\text{SNR}_0 \approx 1.79\,\text{SNR}_0 \quad \text{(D.23)}$$

We can see that the difference with the suboptimum EPTD with $N = 4$ is very small. Thus, we can implement a highly simplified suboptimum EPTD without having to take a high number of sectors N. Results from Figure 2 also confirm this claim. □

At time k, the transmitter evaluates $\left|h_{k1} + e^{jn\pi/2}h_{k2}\right|$ for $n = 0, 1, 2,$ and 3 and transmits

$$x_{k1} = \frac{s_k}{\sqrt{2}} \quad \text{(D.24)}$$

from the first antenna, and

$$x_{k2} = \frac{e^{jn\pi/2}s_k}{\sqrt{2}} \quad \text{(D.25)}$$

from the second antenna, where n maximizes the quantity $H_k\left(n\right) = \left|h_{k1} + e^{jn\pi/2}h_{k2}\right|$ over $n = 0, 1, 2, 3$. This process ensures that the signals received from the two antennas will not have an angle of magnitude higher than $\pi/4$. Indeed, if h_{k1} and h_{k2} have a phase difference less than $\pi/4$, then $n = 0$ maximizes $H_k(n)$, and $s_k/\sqrt{2}$ is transmitted from the second antenna. If the two channel responses have a phase difference comprised between $\pi/4$ and $3\pi/4$, $H_k(n)$ is maximized with $n = 3$ and $-js_k/\sqrt{2}$ is transmitted from the second antenna. Similarly, if the two channel responses have a phase difference comprised between $3\pi/4$ and $5\pi/4$, $H_k(n)$ is

maximized with $n = 2$ and $-s_k/\sqrt{2}$ is transmitted from the second antenna. Finally, if the two channel responses have a phase difference between $5\pi/4$ and $7\pi/4$, $H_k(n)$ is maximized with $n = 1$ and $js_k/\sqrt{2}$ is transmitted from the second antenna. This technique is illustrated in Fig D.1, which shows 4 regions separated by dotted diagonal lines and denoted A, B, C, and D, respectively. In region A, the phase difference between the two channel responses is $\Delta\theta \in [-\pi/4, \pi/4]$. Similarly, we have $\Delta\theta \in [\pi/4, 3\pi/4]$ in region D, $\Delta\theta \in [3\pi/4, 5\pi/4]$ in region C, and $\Delta\theta \in [5\pi/4, 7\pi/4]$ in region B. The figure shows a vector h_{k2} located in region D for which the optimal rotation angle is $3\pi/2$, because $H_k(3) \geq H_k(n)$, $n = 0, 1, 2$. As explained above, the proposed method requires the CSI at the transmitter side.

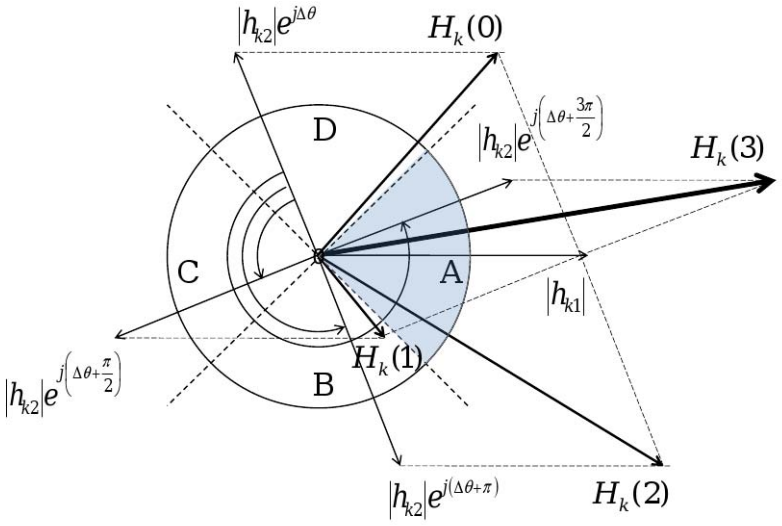

Figure D.1: Graphical illustration of the proposed technique for N=4

In time-division duplex (TDD) systems defined in WiMAX [79] and LTE [80] systems, the CSI is readily available at the transmitter side. In these systems the trivial way for getting this information is to benefit from the channel reciprocity, i.e., the symmetry of the downlink and uplink channels. But in frequency-division duplex (FDD) systems, implementation of this technique requires the transmission of CSI from the receiver to the transmitter. Note however that this requirement holds

also for all transmit diversity techniques mentioned above with the exception of Alamouti's space-time coding.

D.3 Performance Analysis

In this section, performance of the proposed transmit diversity technique is analyzed by means of computer simulations, and it is compared to those of the above mentioned schemes, namely, OTD, Alamouti scheme, and STD.

In the first set of simulations, the considered channel is a simple flat fading channel with the channel coefficients modeled as independent identically distributed (i.i.d) circularly symmetric complex Gaussian variables. Conventional single-carrier transmission with uncoded QPSK modulation is used. Fig D.2 shows the corresponding performance comparison of the above mentioned schemes. We can see that the SNR loss of the proposed scheme with respect to OTD is only 0.7 dB, and the loss w.r.t ideal EPTD is negligible. This means that it recovers most of the 3 dB loss of the Alamouti scheme while maintaining the same power amplifier characteristics. Next, we considered an OFDM transmission system and a frequency

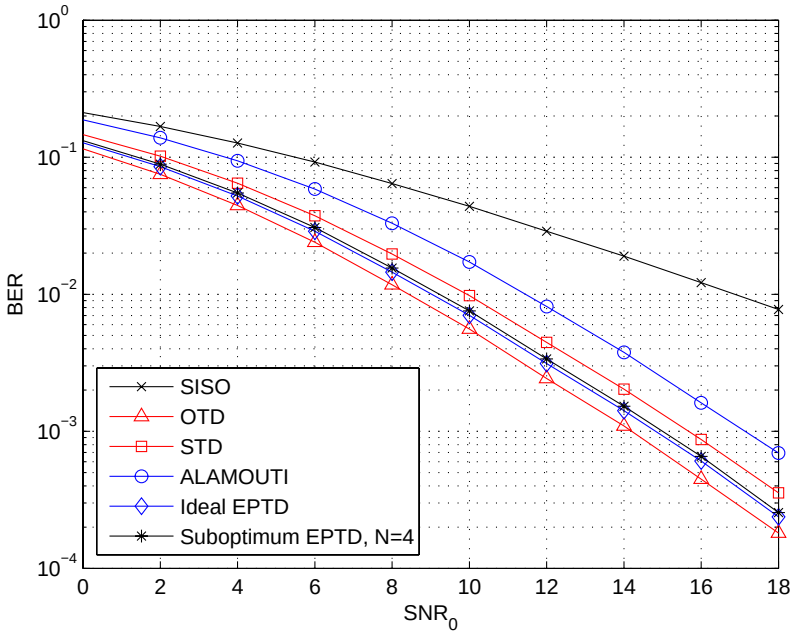

Figure D.2: Performance of the proposed scheme on flat fading channels (single-carrier transmission, QPSK, no coding)

selective channel model, namely, vehicular-A channel with a velocity of 30 km/h whose power delay profile is described in [1]. The carrier frequency is 2.5 GHz and the system bandwidth is 10 MHz corresponding to an FFT size of 1024 as specified in [1]. In addition to the schemes described above, we also simulated a subcarrier-based STD, where for each subcarrier, the corresponding symbol is sent over the channel having the maximum absolute gain. In the conventional STD, the first transmit antenna is used if $\sum_k |h_{k1}|^2 \geq \sum_k |h_{k2}|^2$, where h_{ki} is the channel coefficient for the i-th transmit antenna at the k-th sub-carrier and the summation is held over all the sub-carriers. Otherwise, the second transmit antenna is used. This decision is made for every OFDM block. The results in the absence of coding are shown in Fig D.3. It can be seen that the SNR loss of the proposed scheme

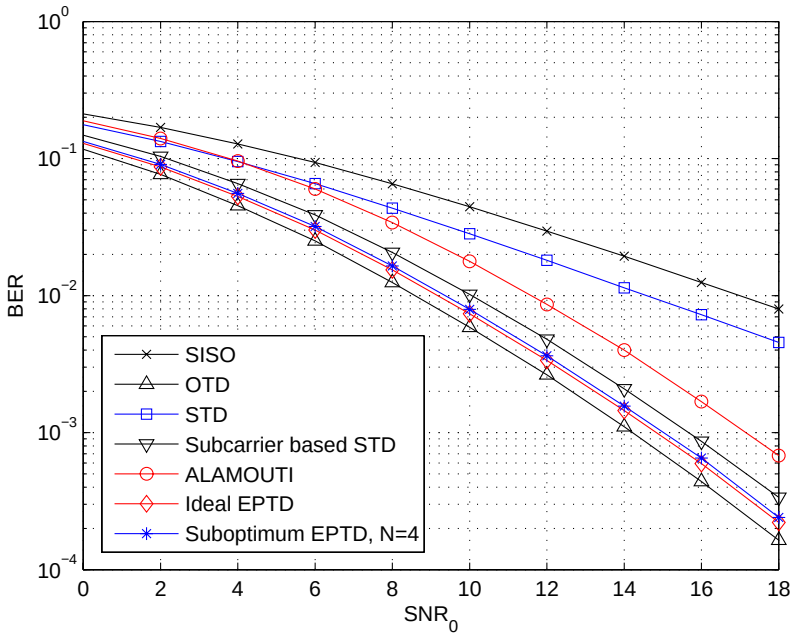

Figure D.3: Performance of the proposed scheme on frequency-selective vehicular channel model [1] with velocity 30 km/h (OFDM, QPSK, no coding)

compared to OTD is around 0.7 dB as in the flat fading case. Here too, it virtually achieves the same performance as that of ideal EPTD.

In the third set of simulations, again the vehicular-A channel model of [1] and OFDM were used, but channel coding was introduced. Fig D.4 shows the performance. Here, the introduction of Convolutional Turbo Code (CTC) slightly de-

creases the SNR loss between the proposed scheme and the OTD to nearly 0.5 dB.

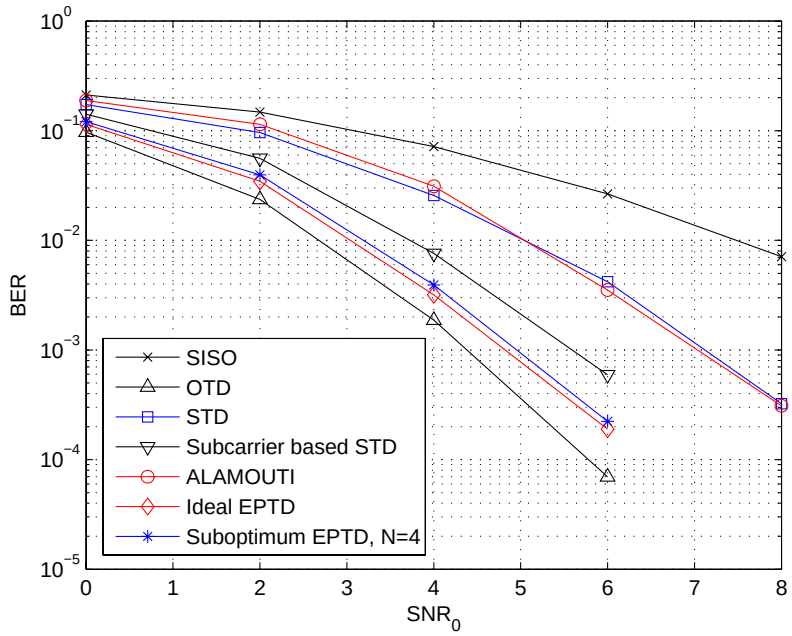

Figure D.4: Performance of the proposed scheme on frequency-selective vehicular channel model [1] with velocity 30 km/h (OFDM, QPSK, Convolutional Turbo Code (CTC) of rate 1/2)

D.4 Conclusions

we have introduced a simple equal power transmit diversity scheme which offers better performance than the STD and Alamouti schemes and closely approaches the performance of optimum transmit diversity. Compared to the optimum transmit diversity, the proposed scheme relaxes the power amplifier requirements by 3 dB for a given total transmit power. The simulation results show that in all of the cases investigated, we achieve a performance gain of 0.7 dB over STD and of 2.25 dB over the Alamouti scheme.

Bibliography

[1] "802.16m Evaluation Methodology."

[2] H. Jafarkhani, *Space-Time coding, theory and practice*. Cambridge university press, 2005.

[3] R. Nabar, H. Bolcskei, V. Erceg, D. Gesbert, and A. Paulraj, "Performance of multiantenna signaling techniques in the presence of polarization diversity," *IEEE Transactions on Signal Processing*, vol. 50, pp. 2553 – 2562, 2002.

[4] L. Zheng and D. Tse, "Diversity and multiplexing: a fundamental tradeoff in multiple-antenna channels," *IEEE Transactions on Information Theory*, vol. 49, pp. 1073 – 1096, 2003.

[5] "IEEE Standard for Information Technology,Telecommunications and Information Exchange between Systems – Local and Metropolitan Area Networks - Specific Requirements - Part 11: Wireless LAN Medium Access Control (MAC) & Physical Layer specifications Enhancements for Higher Throughput."

[6] "IEEE Standard for Local and metropolitan area networks Part 16: Air Interface for Broadband Wireless Access Systems."

[7] V. Tarokh, N. Seshadri, and A. Calderbank, "Space-time codes for high data rate wireless communication: performance criterion and code construction," *IEEE Transactions on Information Theory*, vol. 44, pp. 744 –765, 1998.

[8] B. Hassibi and B. Hochwald, "High-rate codes that are linear in space and time," *IEEE Transactions on Information Theory,*, vol. 48, pp. 1804 –1824, 2002.

[9] E. Viterbo and J. Boutros, "A universal lattice code decoder for fading channels," *IEEE Transactions on Information Theory*, vol. 45, pp. 1639 –1642, 1999.

[10] M. Damen, H. El Gamal, and G. Caire, "On maximum-likelihood detection and the search for the closest lattice point," *IEEE Transactions on Information Theory*, vol. 49, pp. 2389 – 2402, 2003.

[11] G. Foschini, G. Golden, R. Valenzuela, and P. Wolniansky, "Simplified processing for high spectral efficiency wireless communication employing multi-element arrays," *IEEE Journal on Selected Areas in Communications,*, vol. 17, pp. 1841 –1852, 1999.

[12] L. Luzzi, G. Othman, and J. Belfiore, "Augmented Lattice Reduction for MIMO Decoding," *IEEE Transactions on Wireless Communications*, vol. 9, pp. 2853 –2859, 2010.

[13] A. Burg, M. Borgmann, M. Wenk, M. Zellweger, W. Fichtner, and H. Bolcskei, "VLSI implementation of MIMO detection using the sphere decoding algorithm," *IEEE Journal of Solid-State Circuits*, vol. 40, pp. 1566 – 1577, 2005.

[14] E. Biglieri, Y. Hong, and E. Viterbo, "On Fast-Decodable Space-Time Block Codes," *IEEE Transactions on Information Theory*, vol. 55, pp. 524 –530, 2009.

[15] A. Ismail, J. Fiorina, and H. Sari, "A Novel Construction of 2-Group Decodable 4×4 Space-Time Block Codes," in *Proceedings. IEEE Global Telecommunications Conference 2010, (GLOBECOM'10)*.

[16] S. Karmakar and B. Rajan, "Multigroup Decodable STBCs From Clifford Algebras," *IEEE Transactions on Information Theory*, vol. 55, pp. 223 –231, 2009.

[17] K. Srinath and B. Rajan, "Generalized Silver Codes," *IEEE Transactions on Information Theory*, 2011.

[18] T. P. Ren, Y. L. Guan, C. Yuen, and R. J. Shen, "Fast-group-decodable space-time block code," in *2010 IEEE Information Theory Workshop (ITW'10)*, 2010.

[19] S. Karmakar and B. Rajan, "High-Rate, Multisymbol-Decodable STBCs From Clifford Algebras," *IEEE Transactions on Information Theory*, vol. 55, pp. 2682 –2695, 2009.

[20] F. Oggier, J.-C. Belfiore, and E. Viterbo, *Cyclic Division Algebras: A Tool for Space-Time Coding*. Foundations and Trends in Communications and Information Theory, 2007.

[21] A. Ismail, J. Fiorina, and H. Sari, "A New Low-Complexity Decodable Rate-1 Full-Diversity 4×4 STBC with Nonvanishing Determinants," *IEEE Transactions on Wireless Communications*, vol. 10, pp. 2456 –2460, August 2011.

[22] A. Ismail, J. Fiorina, and H. Sari, "A New Low-Complexity Decodable Rate-5/4 STBC for Four Transmit Antennas with Nonvanishing Determinants," in *Proceedings. IEEE Global Telecommunications Conference GLOBECOM 2011, (GLOBECOM'11)*.

[23] A. Ismail, J. Fiorina, and H. Sari, "A New Family of Low-Complexity Decodable STBCs for Four Transmit Antennas," in *Proceedings. IEEE International Conference on Communications 2012, (ICC'12)*.

[24] A. Ismail, J. Fiorina, and H. Sari, " New Low-Complexity STBCs for Four Transmit Antennas," *submitted to IEEE Transactions on Wireless Communications,*.

[25] A. Ismail, S. Sezginer, J. Fiorina, and H. Sari, "A Near-Optimum Equal-Power Transmit Diversity Scheme," in *Proceedings. IEEE 21st International Symposium on Personal Indoor and Mobile Radio Communications 2010, (PIMRC'10)*.

[26] A. Ismail, S. Sezginer, J. Fiorina, and H. Sari, "A Simple and Robust Equal-Power Transmit Diversity Scheme," *IEEE Communications Letters*, vol. 15, pp. 37 –39, January 2011.

[27] S. Alamouti, "A simple transmit diversity technique for wireless communications," *IEEE Journal on Selected Areas in Communications*, vol. 16, pp. 1451 –1458, 1998.

[28] M. Damen, K. Abed-Meraim, and J.-C. Belfiore, "Diagonal algebraic space-time block codes," *IEEE Transactions on Information Theory*, vol. 48, pp. 628 –636, 2002.

[29] H. El Gamal and M. Damen, "Universal space-time coding," *IEEE Transactions on Information Theory*, vol. 49, pp. 1097 – 1119, 2003.

[30] F. Oggier, G. Rekaya, J.-C. Belfiore, and E. Viterbo, "Perfect Space-Time Block Codes," *IEEE Transactions on Information Theory*, vol. 52, pp. 3885 –3902, 2006.

[31] Z. Liu, Y. Xin, and G. Giannakis, "Space-time-frequency coded OFDM over frequency-selective fading channels," *IEEE Transactions on Signal Processing*, vol. 50, pp. 2465 – 2476, 2002.

[32] C. P. Schnorr and M. Euchner, "Lattice basis reduction: Improved practical algorithms and solving subset sum problems," *Mathematical Programming*, vol. 66, pp. 181–199, 1994.

[33] P. Elia, K. Kumar, S. Pawar, P. Kumar, and H.-F. Lu, "Explicit space-time codes achieving the diversity-multiplexing gain tradeoff," *IEEE Transactions on Information Theory*, vol. 52, pp. 3869 –3884, sept. 2006.

[34] E. Telatar, "Capacity of Multi-antenna Gaussian Channels," *European Transactions on Telecommunications*, vol. 10, no. 6, pp. 585–595, 1999.

[35] J. Forney, G.D. and L.-F. Wei, "Multidimensional constellations. I. Introduction, figures of merit, and generalized cross constellations," *IEEE Journal on Selected Areas in Communications*, vol. 7, pp. 877 –892, aug 1989.

[36] H. Jafarkhani, "A Quasi-Orthogonal Space-Time Block Code," *IEEE Transactions on Communications*, vol. 49, pp. 1 –4, 2001.

[37] N. Sharma and C. Papadias, "Improved Quasi-Orthogonal Codes Through Constellation Rotation," *IEEE Transactions on Communications*, vol. 51, pp. 332 – 335, 2003.

[38] W. Su and X.-G. Xia, "Signal constellations for quasi-orthogonal space-time block codes with full diversity," *IEEE Transactions on Information Theory*, vol. 50, pp. 2331 – 2347, 2004.

[39] N. Sharma and C. B. Papadias, "Full-Rate Full-Diversity Linear Quasi-Orthogonal Space-Time Codes for Any Number of Transmit Antennas," *EURASIP Journal on Applied Signal Processing*, vol. 2004, pp. 1246–1256, 2004.

[40] D. N. Dao, C. Yuen, C. Tellambura, Y. L. Guan, T. T. Tjhung, C. Yuen, Y. L. Guan, and T. T. Tjhung, "Four-Group Decodable Space-Time Block Codes," *IEEE Transactions on Signal Processing*, vol. 56, pp. 424 –430, 2008.

[41] S. Sezginer and H. Sari, "Full-rate full-diversity 2×2 space-time codes of reduced decoder complexity," *IEEE Communications Letters*, vol. 11, pp. 973 – 975, 2007.

[42] R. A. Horn and C. R. Johnson, *Matrix Analysis*. Cambridge University Press, 1990.

[43] S. Sezginer, H. Sari, and E. Biglieri, "On High-Rate Full-Diversity 2×2 Space-Time Codes with Low-Complexity Optimum Detection," *IEEE Transactions on Communications*, vol. 57, pp. 1532 –1541, 2009.

[44] J. Paredes, A. Gershman, and M. Gharavi-Alkhansari, "A New Full-Rate Full-Diversity Space-Time Block Code With Nonvanishing Determinants and Simplified Maximum-Likelihood Decoding," *IEEE Transactions on Signal Processing*, vol. 56, pp. 2461 –2469, 2008.

[45] C. Hollanti, J. Lahtonen, K. Ranto, R. Vehkalahti, and E. Viterbo, "On the algebraic structure of the Silver code: A 2×2 perfect space-time block code," in *Proceedings. IEEE Information Theory Workshop, 2008. ITW '08.*, 2008.

[46] K. Srinath and B. Rajan, "Low ML-Decoding Complexity, Large Coding Gain, Full-Rate, Full-Diversity STBCs for 2×2 and 4×2 MIMO Systems," *IEEE Journal of Selected Topics in Signal Processing*, vol. 3, pp. 916 –927, 2009.

[47] T. P. Ren, Y. L. Guan, C. Yuen, E. Gunawan, and E. Y. Zhang, "Group-Decodable Space-Time Block Codes with Code Rate > 1," *IEEE Transactions on Communications*, vol. 59, pp. 987 –997, april 2011.

[48] G. Rajan and B. Rajan, "Multigroup ML Decodable Collocated and Distributed Space-Time Block Codes," *IEEE Transactions on Information Theory*, vol. 56, pp. 3221 –3247, july 2010.

[49] S. Karmakar and B. Rajan, "Minimum-Decoding-Complexity, Maximum-rate Space-Time Block Codes from Clifford Algebras," in *Proceedings. IEEE International Symposium on Information Theory 2006, (ISIT'06)*, pp. 788 –792, july 2006.

[50] O. Tirkkonen, "Maximal symbolwise diversity in non-orthogonal space-time block codes," in *Proceedings. IEEE International Symposium on Information Theory 2001,(ISIT'01)*, 2001.

[51] K. Srinath and B. Rajan, "High-rate, 2-group ML-decodable STBCs for 2^m transmit antennas," in *Proceedings. IEEE International Symposium on Information Theory 2009, (ISIT'09)*, 2009.

[52] C. Yuen, Y. Guan, and T. Tjhung, "On the Search for High-Rate Quasi-Orthogonal Space-Time Block Code," *International Journal of Wireless Information Networks*, vol. 13, pp. 329–340, 2006.

[53] C. Yuen, Y. L. Guan, and T. T. Tjhung, "Quasi-orthogonal stbc with minimum decoding complexity," *Wireless Communications, IEEE Transactions on*, vol. 4, pp. 2089–2094, sept. 2005.

[54] K. Srinath and B. Rajan, "Reduced ML-Decoding Complexity, Full-Rate STBCs for 2^a Transmit Antenna Systems," in *Proceedings. IEEE Global Telecommunications Conference 2010, (GLOBECOM'10)*, 2010.

[55] K. Srinath and B. Rajan, "Reduced ML-decoding complexity, full-rate STBCs for 4 transmit antenna systems," in *Proceedings. IEEE International Symposium on Information Theory Proceedings 2010, (ISIT'10)*, 2010.

[56] M. Sinnokrot, J. Barry, and V. Madisetti, "Embedded Orthogonal Space-Time Codes for High Rate and Low Decoding Complexity," in *Proceedings. IEEE Global Telecommunications Conference 2009, (GLOBECOM'09)*, 2009.

[57] M. Sinnokrot, J. Barry, and V. Madisetti, "Embedded Alamouti space-time codes for high rate and low decoding complexity," in *Proceedings. 42nd Asilomar Conference on Signals, Systems and Computers 2008, (Asilomar'08)*, 2008.

[58] A. Ismail, J. Fiorina, H. Sari, and M. Damen, "A Low-PAPR High-Rate Full-Diversity 4×4 Space-Time Code with Fast Maximum-Likelihood Decoding," in *Proceedings. IEEE Wireless Communications and Networking Conference 2010, (WCNC'10)*.

[59] S. Sirianunpiboon, Y. Wu, A. Calderbank, and S. Howard, "Fast Optimal Decoding of Multiplexed Orthogonal Designs by Conditional Optimization," *IEEE Transactions on Information Theory*, vol. 56, pp. 1106 –1113, 2010.

[60] O. Tirkkonen and A. Hottinen, "Square-matrix embeddable space-time block codes for complex signal constellations," *IEEE Transactions on Information Theory*, vol. 2002, pp. 384 –395, 2002.

[61] M. Sinnokrot and J. Barry, "A Single-Symbol-Decodable Space-Time Block Code with Full rate and Low Peak-to-Average Power Ratio," *IEEE Transactions on Wireless Communications*, vol. 8, pp. 2242 –2246, 2009.

[62] M. Khan and B. Rajan, "Single-symbol maximum likelihood decodable linear STBCs," *IEEE Transactions on Information Theory*, vol. 52, pp. 2062 – 2091, 2006.

[63] P. Marsch, W. Rave, and G. Fettweis, "Quasi-Orthogonal STBC Using Stretched Constellations for Low Detection Complexity," in *Proceedings. IEEE Wireless Communications and Networking Conference 2007, (WCNC'07)*, pp. 757 –761, march 2007.

[64] S. Karmakar and B. Rajan, "Non-Unitary-Weight Space-Time Block codes with Minimum Decoding Complexity," in *Information Theory, 2006 IEEE International Symposium on*, july 2006.

[65] G. Bauch, "Concatenation of space-time block codes and "turbo"-TCM," in *Proceedings. IEEE International Conference on Communications 1999, (ICC'99)*, 1999.

[66] V. Tarokh, H. Jafarkhani, and A. Calderbank, "Space-time block codes from orthogonal designs," *IEEE Transactions on Information Theory*, vol. 45, pp. 1456 –1467, 1999.

[67] X.-B. Liang, "Orthogonal designs with maximal rates," *IEEE Transactions on Information Theory*, vol. 49, pp. 2468 – 2503, 2003.

[68] "http://www1.tlc.polito.it/ viterbo/rotations/rotations.html,"

[69] P. Dayal and M. Varanasi, "An optimal two transmit antenna space-time code and its stacked extensions," in *Conference Record of the Thirty-Seventh Asilomar Conference on Signals, Systems and Computers 2003, (Asilomar'03)*, vol. 1, pp. 987 – 991 Vol.1, nov. 2003.

[70] H. Yao and G. W. Wornell, "Achieving the full MIMO diversity-multiplexing frontier with rotation-based space-time codes," in *Proceedings. Allerton Conference on Communication, Control, and Computing, 2003, (Allerton'03)*, 2003.

[71] J.-C. Belfiore, G. Rekaya, and E. Viterbo, "The golden code: a 2×2 full-rate space-time code with nonvanishing determinants," *IEEE Transactions on Information Theory*, vol. 51, pp. 1432 – 1436, 2005.

[72] P. Elia, B. Sethuraman, and P. Vijay Kumar, "Perfect Space -Time Codes for Any Number of Antenna," *IEEE Transactions on Information Theory*, vol. 53, pp. 3853 –3868, 2007.

[73] D. B. Shapiro and R. Martin, "Anticommuting Matrices," *The American Mathematical Monthly*, vol. 105, no. 6, pp. pp. 565–566, 1998.

[74] L. J. Mordell, *Diophantine Equations*. Academic Press, 1969.

[75] T. P. Dence and J. B. Dence, *Elements of the Theory of Numbers*. Academic Press, 1999.

[76] A. Goldsmith, *Wireless Communications*. Cambridge University Press, 2005.

[77] Z. Chen, J. Yuan, and B. Vucetic, "Analysis of Transmit Antenna Selection/Maximal-Ratio Combining in Rayleigh Fading Channels," *IEEE Transactions on Vehicular Technology*, vol. 54, pp. 1312 – 1321, july 2005.

[78] P. V. D. Tse, *Fundamentals of wireless communications*. Cambridge university press, 2005.

[79] "WiMAX ForumTM Mobile System Profile, Release 1.0 Approved Specification, Revision 1.7.1, Nov. 2008."

[80] "3GPP TS 36.213, Physical layer procedures, V8.8.0, Sept. 2009."

Author's publications

Journal articles

J1 Ismail, A.; Fiorina, J.; Sari, H.; , "A Novel Construction of Multigroup-Decodable Space-Time Block Codes," submitted to *IEEE Trans. Communications* (accepted for publication).

J2 Ismail, A.; Fiorina, J.; Sari, H.; , "A New Low-Complexity Decodable Rate-1 Full-Diversity 4×4 STBC with Nonvanishing Determinants," *IEEE Trans. Wireless Communications*, vol. 10, no. 8, pp. 2456-2460, August 2011.

J3 Ismail, A.; Sezginer, S.; Fiorina, J.; Sari, H.; ,"A Simple and Robust Equal-Power Transmit Diversity Scheme," *IEEE Communications Letters*, vol. 15, no. 1, pp. 37-39, January 2011.

J4 Ismail, A.; Sari, H.; Fiorina, J.; , "A Pragmatic Approach Space-Time Code Design," *IEEE Vehicular Technology Magazine*, vol. 5, no. 1, pp. 91-96, March 2010.

J5 Ismail, A.; Fiorina, J.; Sari, H.; , "New Low-Complexity STBCs for Four Transmit Antennas," submitted to *IEEE Trans. Wireless Communications*.

Conference proceedings

C1 Ismail, A.; Fiorina, J.; Sari, H.; ,"A New Family of Low-Complexity Decodable STBCs for Four Transmit Antennas," *in Proceedings. IEEE International Conference on Communications 2012, (ICC'12)*.

C2 Ismail, A.; Fiorina, J.; Sari, H.; ,"A New Low-Complexity Decodable Rate-5/4 STBC for Four Transmit Antennas with Nonvanishing Determinants," *in Proceedings. IEEE Global Telecommunications Conference 2011, (GLOBECOM'11)*.

C3 Ismail, A.; Fiorina, J.; Sari, H.; ,"A Novel Construction of 2-Group Decodable 4×4 Space-Time Block Codes," *in Proceedings. IEEE Global Telecommunications Conference 2010, (GLOBECOM'10)*.

C4 Ismail, A.; Sezginer, S.; Fiorina, J.; Sari, H.; ,"A Near-Optimum Equal-Power Transmit Diversity Scheme," *in Proceedings. IEEE International Symposium on Personal, Indoor and Mobile Radio Communications 2010, (PIMRC'10)*.

C5 Ismail, A.; Fiorina, J.; Sari, H.; Damen, M.O.; ,"A Low-PAPR High-Rate Full-Diversity 4×4 Space-Time Code with Fast Maximum-Likelihood Decoding," *in Proceedings. IEEE Wireless Communications and Networking Conference 2010, (WCNC'10)*.

C6 Ismail, A.; Fiorina, J.; Sari, H.; Damen, M.O.; , "A Rate-3/2 Full-Diversity 4×4 Space-Time Code with Fast Maximum-Likelihood Decoding," *in Proceedings. IEEE International Symposium on Personal, Indoor and Mobile Radio Communications 2009, (PIMRC'09)*.